Investigating the role of the imprinted Grb10 gene in the regulation of maternal nutrient transfer

Cowley, Michael

Award date:
2009

Awarding institution:
University of Bath

Investigating the role of the imprinted *Grb10* gene in the regulation of maternal nutrient transfer

Michael Anthony Cowley

A thesis submitted for the degree of Doctor of Philosophy

University of Bath

Department of Biology and Biochemistry

September 2009

To Mum and Dad.

Thank you.

And to Catherine,

for believing.

"A smooth sea never made a skilful mariner,

neither do uninterrupted prosperity and success qualify for usefulness and happiness.

The storms of adversity, like those of the ocean, rouse the faculties,

and excite the invention, prudence, skill and fortitude of the voyager.

The martyrs of ancient times, in bracing their minds to outward calamities,

acquired a loftiness of purpose and a moral heroism

worth a lifetime of softness and security."

– *English proverb*

Acknowledgements

Perhaps the most valuable lesson I have learned in the past four years is that collaboration and discussion are critical for the development and progression of ideas, and that conversations with researchers in even the most distant of disciplines can encourage one to address old problems with new approaches. As such, I cannot thank all of those who have indirectly contributed to the work in this study.

Others have had a more direct role. At the very top of the list must come my supervisor Dr Andrew Ward, without whom this work would not have been possible. In particular, I am grateful for our stimulating discussions, which, even in those 'results deserts', have had the ability to promote optimism and to motivate. The freedom to pursue my own ideas and hypotheses has been an invaluable learning experience, and I hope you feel it was fruitful in the end.

Next must come Dr Al Garfield and Marta Madon, with whom I have worked closely on several projects. Dr Garfield was particularly instrumental during my first two years, showing me 'the ropes' and guiding my development. Marta: our '*Grb10* team' approach, helping with each others' projects wherever possible, has been great and I wish you the best of luck for the future. Thanks for listening intently to my frequently wild ideas. Dr Kim Moorwood and Dr Joanne Stewart-Cox have offered valuable technical expertise in various aspects of the work. Mrs Iryna Withington is a most talented histologist, not only with an extensive knowledge of useful techniques, but an ability to devise novel and ingenious solutions to the range of technical challenges with which I have presented her. The animal technicians, who prefer to remain anonymous, are of fundamental importance in our work, and their contributions can often be undervalued.

I have been lucky enough to have supervised an army of project students during my PhD, some of whom have been very talented and have been partly involved with the projects presented here. These include Dr Jayant Rane, Emma Roberts, Sam Carter and Alison Galloway. Other members of the department whose advice have enabled successful execution of a range of experiments include, in no particular order, Giusi Manfredi, Kathy O'Neill and Emily-jane Myatt (*in vitro* work), Toby Warnecke (bioinformatics), Sarah Fontaine and Dr Paul Davies (Western blot troubleshooting), Dr Zoe Burke (e8.0 embryo manipulation), Dr Julia Mackay (milk protein gels) and Dr Monique Welten (OPT scanning). Dr Marika Charalambous (University of Cambridge) is a talented collaborator and good friend, and I hope this relationship will continue into the future.

My PhD was funded by the Department of Biology and Biochemistry at the University of Bath.

List of abbreviations

2D	Two dimensions
3D	Three dimensions
Ag	Androgenetic
AHO	Albright's hereditary osteodystrophy
ALL	Acute lymphoblastic leukaemia
AMPS	2-acrylamido-2-methylpropane sulfonic acid
ANOVA	Analysis of variance
APTS	(3-aminopropyl)trimethoxysilane
AS	Angelman syndrome
ATP	Adenosine triphosphate
AVE	Anterior visceral endoderm
bp	Base pairs
BPS domain	Between PH and SH2 domain
BSA	Bovine serum albumin
BWS	Beckwith-Wiedemann syndrome
$CaCl_2$	Calcium chloride
cAMP	Cyclic adenosine monophosphate
CDK	Cyclin dependent kinase
cDNA	Complimentary deoxyribonucleic acid
cfu	Colony forming units
ChIP	Chromatin immunoprecipitation
CHO/IR	Chinese hamster ovary cells over-expressing insulin receptor
cm	Centimetre
CML	Chronic myelogenous leukaemia
CO_2	Carbon dioxide
CNS	Central nervous system
CRM	*Cis*-regulatory module

DAB	3,3’-diaminobenzidine
dCTP	Deoxycytidine triphosphate
DEPC	Diethylpyrocarbonate
DMD	Differentially methylated domain
DMEM	Dulbecco’s modified Eagle’s medium
DMF	N,N-dimethylformamide
DMR	Differentially methylated region
DMSO	Dimethyl sulfoxide
DNA	Deoxyribonucleic acid
DNase	Deoxyribonuclease
dsRNA	Double stranded ribonucleic acid
DTT	Dithiothreitol
ECM	Extracellular matrix
EDTA	Ethylenediaminetetraacetic acid
EG cells	Embryonic germ cells
EGTA	Ethylene glycol tetraacetic acid
ES cells	Embryonic stem cells
eX	Embryonic day X
FISH	Fluorescence *in situ* hybridisation
g	Gram
g	Gravity
G(X)	Gestational day X
GDP	Guanosine diphosphate
GEF	Guanine nucleotide exchange factor
GFP	Green fluorescent protein
GM	Grb10 and Mig
GPCR	G-protein coupled receptor
GTP	Guanosine triphosphate
GYF domain	Glycine-tyrosine-phenylalanine domain
H_2O	Water

HCl	Hydrogen chloride
ICR	Imprinting control region
IGF	Insulin-like growth factor
IHC	Immunohistochemistry
IPTG	Isopropyl-β-D-thiogalactopyranoside
IU	International unit
JAK	Janus kinase
$K_3Fe(CN)_6$	Potassium ferricyanide
$K_4Fe(CN)_6$	Potassium ferrocyanide
kb	Kilobase pairs
KCl	Potassium chloride
kDa	Kilo-Dalton
LB	Luria broth
LOI	Loss of imprinting
M	Molar
MAP	Mitogen-activated protein
Me-AIB	α-methylamino-isobutyric acid
Me-RDA	Methylation representational difference analysis
mg	Milligram
$MgCl_2$	Magnesium chloride
ml	Millilitre
mM	Millimolar
MMP	Matrix metalloprotease
$MnCl_2$	Manganese chloride
MOPS	3-(N-morpholino)propanesulfonic acid
mRNA	Messenger ribonucleic acid
mUPD	Maternal uniparental disomy
mUpDp	Maternal uniparental duplication
MYA	Million years ago
Na_2HPO_4	Disodium hydrogen phosphate

NaCl	Sodium chloride
NaOH	Sodium hydroxide
ng	Nanogram
NH_3	Ammonia
OCT	Optimal cutting temperature (compound)
OPT	Optical projection tomography
P(X)	Postnatal day X
pA *or* poly-(A)	Poly-adenylation
PAGE	Polyacrylamide gel electrophoresis
PBS	Phosphate buffered saline
PcG	Polycomb group
PCR	Polymerase chain reaction
PD	Parkinson disease
P domain	Proline-rich domain
PEV	Position-effect variegation
Pg	Parthenogenetic
PH domain	Pleckstrin homology domain
PIF	Prolactin-inhibiting factor
PIPES	Piperazine-N,N′-bis(2-ethanesulfonic acid)
PMSF	Phenylmethanesulphonylfluoride
PRC2	Polycomb repressor complex 2
PFA	Paraformaldehyde
pUPD	Paternal uniparental disomy
pUpDp	Paternal uniparental duplication
PVDF	Polyvinylidene fluoride
PWS	Prader-Willi syndrome
pY	Phosphotyrosine
qPCR	Quantitative (real time) polymerase chain reaction
RACE	Rapid amplification of complimentary deoxyribonucleic acid ends
RA domain	Ras-associating domain

RNA	Ribonucleic acid
RNAi	Ribonucleic acid interference
RNA IP	Ribonucleic acid immunoprecipitation
RNase	Ribonuclease
rpm	Revolutions per minute
RT-PCR	Reverse transcription polymerase chain reaction
RTK	Receptor tyrosine kinase
SA	Splice acceptor
SDS	Sodium dodecyl sulphate
SH2 domain	Src-homology 2 domain
SH3 domain	Src-homology 3 domain
snoRNA	Small nucleolar RNA
SNP	Single nucleotide polymorphism
Socs	Suppressors of cytokine signalling
SRS	Silver-Russell syndrome
STAT	Signal transducer and activator of transcription
TAF	TATA-binding protein-associated factor
TE	Tris-ethylenediaminetetraacetic acid
TEB	Terminal end bud
TEMED	Tetramethylethylenediamine
TIDA	Tuberoinfundibular
TNDM	Transient neonatal diabetes mellitus
TUNEL	Terminal deoxynucleotidyl transferase mediated dUTP nick end labelling
UCSC	University of California, Santa Cruz
U	Unit
UPD	Uniparental disomy
UpDp	Uniparental duplication
UTR	Untranslated region
UV	Ultraviolet

V	Volts
v/v	Volume/volume
WW domain	Tryptophan-rich domain
w/v	Weight/volume
X-gal	5-bromo-4-chloro-3-indolyl-β-D-galactopyranoside
µCi	MicroCurie
µg	Microgram
µJ	MicroJoule
µl	Microlitre
µm	Micrometer (micron)
µM	Micromolar

Genotype abbreviations

+/+	Wild type
+/p	Paternal transmission heterozygote
m/+	Maternal transmission heterozygote
m/p	Homozygote

Contents

List of figures

List of tables

Abstract

Imprinted genes are a subset of loci, positioned on autosomes and the X-chromosome, which are expressed monoallelically in a parent-of-origin specific manner. The influence of such genes on the regulation of embryonic growth and postnatal energy homeostasis is well established. The parental conflict hypothesis predicts that, *in utero*, paternally-expressed genes will promote maternal resource acquisition and thus growth, whereas maternally-expressed genes will oppose this action, restricting resource investment in a single brood in the interests of the lifetime reproductive success of the mother. *Grb10* is an imprinted gene which encodes the cytoplasmic adaptor protein Growth factor receptor bound protein 10. In the majority of tissues, *Grb10* is expressed from the maternally-derived chromosome. Consistent with conflict theory, transgenic mice inheriting a disrupted *Grb10* allele through the maternal line (*Grb10Δ2-4*$^{m/+}$) exhibit embryonic overgrowth, although the mechanisms and signalling pathways responsible for this effect are unclear. *Grb10Δ2-4*$^{m/+}$ mice also demonstrate enhanced insulin signalling and improved whole body glucose clearance, consistent with the established role of imprinted genes in the regulation of postnatal metabolism. An integrated *LacZ* gene-trap in the *Grb10Δ2-4* allele failed to fully recapitulate endogenous *Grb10* expression, notably within the central nervous system. To address this issue, a second transgenic mouse line, *Grb10KO*, was created. This allele produced strong *LacZ* reporter expression in the central nervous system, but only when transmitted through the paternal line (*Grb10KO*$^{+/p}$), establishing *Grb10* as the only known imprinted gene with a reciprocal imprinting profile between the central nervous system and peripheral tissues. *Grb10KO*$^{+/p}$ mice exhibit a social dominance phenotype, suggesting distinct roles for maternally- and paternally-expressed *Grb10*, consistent with their respective sites of expression. The current study characterised the *Grb10KO* allele at the genetic level, and in doing so, revealed a phenotypic difference between *Grb10KO*$^{m/p}$ and *Grb10Δ2-4*$^{m/p}$ mice for which a possible explanation was provided. Importantly, with this knowledge, the current study elucidated the genetic and molecular basis for inconsistencies in reporter expression between the two transgenic lines, identifying a novel tissue-specific enhancer element at the locus. In addition to the central nervous system, this enhancer appeared to be active in the mammary epithelium, identifying a novel site of *Grb10* expression, which was pregnancy-dependent and specifically from the maternally-inherited chromosome. Characterisation of the functional significance of expression in this tissue revealed that maternally-expressed *Grb10* mediates a supply/demand system between lactating mother and suckling pup, acting as a supply promoter and demand suppressor. This role is inconsistent with conflict theory, but suggests the maintenance of the *Grb10* imprint in the mammary epithelium might be associated with improved coadaptiveness between mother and offspring. Intriguingly, *in utero*, *Grb10* is both a demand and supply suppressor. When considered together, these findings suggest a wider role for maternally-expressed *Grb10* in the homeostatic control of growth and achievement of optimal fitness.

Chapter One

Introduction

1.1 Genomic Imprinting

1.1.1 Introduction

The concept and basic behaviour of 'the gene' was defined in 1865 by the Augustinian priest Gregor Mendel, whose experimental work on the inherited traits of pea plants remains a historic milestone in our understanding of biology. The importance of his work was not widely recognised until the twentieth century, when eminent names such as William Bateson and R.A. Fisher applied Mendel's theories to explain other examples of phenotypic variation.

Although the terminology we use today to describe genes and heredity did not exist at the time of Mendel's discovery, he postulated that 'particulate factors' (genes) may pass unchanged from parent to progeny and that these factors may exist in alternative forms (alleles). Diploid organisms with two sets of chromosomes would inherit one copy from each parent, implying equal parental contribution to progeny characteristics. Whilst this holds true in the majority of cases, some genes appear to be 'exempt' from Mendel's laws of inheritance, such that the parental contribution to a given trait is not equal.

One of the most striking demonstrations of the non-equivalence of parental genomes comes from the study of mice with uniparental disomies (UPD), in which zygotes possess two paternal or two maternal copies of a specific chromosome. This can be achieved through Robertsonian translocations, a type of balanced translocation in which the long arms of two chromosomes join. Whilst a carrier of such a translocation possesses the normal complement of genetic information, progeny can inherit an extra dose. Studies in the 1970s demonstrated that, whilst zygotes with maternal or paternal disomy (mUPD or pUPD, respectively) for chromosomes 1, 4, 5, 9, 13, 14 and 15 appeared to develop normally (Cattanach, 1986), mice disomic for chromosome 11, for example, exhibited opposite growth phenotypes depending on the parental origin of the disomy. When both chromosome 11 copies were of maternal origin, neonates exhibited growth retardation, whilst neonatal overgrowth was apparent in mice inheriting two copies of chromosome 11 through the paternal line (Cattanach and Moseley, 1973; Cattanach and Kirk, 1985).

Functional non-equivalence was further illustrated using pronuclear transplantation experiments, which convincingly demonstrated a requirement for both parental genomes for successful embryonic development (McGrath and Solter, 1983). The technique was employed to generate parthenogenetic zygotes (possessing two maternal genome copies; also called gynogenetic; Pg) and androgenetic zygotes (possessing two paternal genome copies; Ag), which failed to develop beyond implantation, despite possessing the full complement of genes (McGrath and Solter, 1984; Surani *et al*, 1984). Further, the resulting embryos exhibited somewhat opposing characteristics; parthenogenotes predominantly consisted of embryonic material, whilst androgenotes displayed a much greater development of extra-embryonic tissue (Barton *et al*, 1984). The phrase 'imprinting of the genome' in reference to this observation was first coined by Surani *et al* (1984), who

suggested that the presence of both a male and female pronucleus is essential for a zygote to develop to term.

The observation that mice with UPD for certain chromosomes essentially developed normally suggested that, rather than the entire gene complement of the genome, individual genes or chromosomal regions might be responsible for these parent-of-origin specific effects. The *Insulin-like growth factor 2* (*Igf2*) gene was the first such imprinted gene to be identified (DeChiara *et al*, 1991). Whilst the growth effects of *Igf2* had been studied for some years previously, its imprinted status was not realised until mice with a targeted disruption of the gene were engineered. Inheritance of this mutation engendered a dwarfing phenotype, but only when the disrupted allele was transmitted through the paternal line. RNase protection assays and *in situ* hybridisation confirmed that the paternally-derived copy was transcriptionally active in embryo and placenta, whereas transcripts arising from the maternally-inherited copy could not be detected, except in the choroid plexus.

To date, 131 imprinted genes have been identified in mouse (MouseBook, UK Medical Research Council, www.mousebook.org), although estimates of how many exist are wide-ranging; up to 600 have been predicted (Luedi *et al*, 2005). Genomic imprinting is also evident in flowering plants (angiosperms) and coccid insects, as well as sciarid flies; 12 imprinted genes have been found in flowering plants, all of which are imprinted in the endosperm (Feil and Berger, 2007). Indeed, the phenomenon of parent-of-origin specific effects was first revealed in maize (Kermicle, 1970), although the term 'genomic imprinting' was not applied to this effect until later. Originally, 'genomic imprinting' referred to the process of whole chromosome inactivation in sciarid flies (Crouse, 1971), which is responsible for sex determination (reviewed in Goday and Esteban, 2001). Both the functions and mechanisms of imprinting exhibit some commonalities between mammals and plants (discussed later), suggestive of convergent evolution (Feil and Berger, 2007), but the system in insects appears to have evolved for entirely different reasons, and is not discussed further in this review.

Early attempts to identify murine imprinted genes focussed on mapping candidates within chromosomal regions which displayed opposite phenotypes when inherited as uniparental disomies or following uniparental transmission of a deletion. This approach led to the identification of *Insulin-like growth factor 2 receptor* (*Igf2r*) as an imprinted gene, which was found to be the gene responsible for the maternal-effect mutation in mouse called *Tme* (Barlow *et al*, 1991). Later, more high-throughput screens were performed using subtractive hybridisation or microarray experiments. Schulz *et al* (2006), for example, describe a microarray-based screen for imprinted genes using mice with uniparental duplication (UpDp) of chromosomes 7 and 11. Because imprinted genes are monoallelically expressed, UpDp might be expected to double their expression levels or ablate them altogether, depending on the directions of the imprint and the duplication. Transcript levels of biallelically-expressed genes would not be expected to differ. Microarray analysis was used to compare the transcriptomes of maternal UpDp (mUpDp) and paternal UpDp (pUpDp) tissues, to identify imprinted candidates. The technique provided an inbuilt filter

to eliminate false positives; many candidates could be excluded because they were positioned outside of the chromosomal duplication. This study led to the identification of seven novel imprinted genes, whose imprinted status was validated by single nucleotide polymorphism (SNP) analysis. One disadvantage of this microarray-based approach is that the outcome is limited by the transcripts represented on the DNA-chip.

Subtractive hybridisation circumvents this problem, and has been used to identify *Peg3*, *Peg1/Mest* and *Neuronatin* (Kuroiwa *et al*, 1996; Kaneko-Ishino *et al*, 1995; Kagitani *et al*, 1997). In the case of *Peg1/Mest*, cDNA from Pg embryos was biotinylated. This was pooled with cDNA from normal embryos, which had been ligated to oligonucleotide linkers. Upon denaturation and reassociation, cDNA from the two sources cross-hybridised, and these products were subsequently purified out using beads conjugated to streptavidin. The absence of paternally-expressed genes in the Pg embryos prevented the corresponding cDNA from the normal embryos hybridising to biotinylated-cDNA. Any products not pulled out using streptavidin could thus be identified by the polymerase chain reaction (PCR), using primers recognising the oligonucleotide linkers. Although this technique has proved successful in identifying novel imprinted genes, its scope is limited as Pg embryos die early, preventing the assessment of imprinting at later developmental stages or in specific tissues (Oakey and Beechey, 2002).

One property common to most imprinted genes is differential DNA methylation. This is discussed in more detail in Section 1.1.3, but, briefly, imprinted genes can exhibit different patterns of methylation dependent on their parent-of-origin, thereby enabling the maternally- and paternally-derived alleles to be distinguished. This property can be exploited in the search for novel imprinted genes, using a technique called methylation representational difference analysis (Me-RDA). Again, the approach compares UpD or UpDp embryos with normal controls. Genomic DNA is digested by a methylation-sensitive restriction enzyme, such as *Hpa*II, and digestion products are ligated to oligonucleotides to drive PCR amplification. Any DNA species in common between the two samples are removed by successive rounds of subtractive hybridisation, leaving sequences enriched for differential DNA methylation. *Nesp*, *Gnasxl* and *Nespas* have all been identified using this technique (Peters *et al*, 1999; Kelsey *et al*, 1999; Wroe *et al*, 2000). Although the approach again relies on Pg/Ag embryos, it can be used to identify imprinted genes which are differentially methylated but might not be expressed at early embryonic stages.

1.1.2 Evolutionary theories of genomic imprinting

The advantages of diploidy are manifested at two levels. For the individual, possessing two copies of a gene is beneficial if one copy is damaged, as the other can often compensate. For the population, diploidy promotes the diffusion of genetic variance, increasing the ability to respond to new environmental stresses, such as disease. Genes subject to genomic imprinting are functionally haploid. This means that two copies are inherited, but only one is transcriptionally active, thereby effectively eliminating the benefits to the individual of diploidy. Thus, imprinting must confer an advantage which outweighs the cost

of functional haploidy. Theories to explain the evolution of imprinting are plentiful, and the matter is hotly-contested.

The most widely-accepted theory is the parental conflict hypothesis, otherwise referred to as the parental tug-of-war, or simply conflict theory (Haig and Westoby, 1989; Moore and Haig, 1991). The model describes how paternally-expressed genes in an embryo or placenta (or indeed, in an endosperm) will promote maternal resource acquisition, whilst maternally-expressed genes will antagonise such an activity. A pregnant female mouse, for example, would be expected to limit resource transfer to developing embryos in the interests of her lifetime reproductive success, whereas males, who may not father subsequent offspring from the same female, and whose energy investment in raising a brood is relatively small, might promote nutrient transfer to provide his offspring with the best chance of survival. At the time of its conception, this model was supported by the gross phenotype of Ag embryos, which exhibit enlarged trophoblasts, a structure involved in nutrient transfer from mother to offspring. The growth retardation associated with mUPD for chromosome 11, and the overgrowth associated with pUPD for the same chromosome, also provided support for this model.

Advances in mouse genetics have enabled the functions of many imprinted genes to be elucidated, no longer relying on the study of large-scale modifications such as chromosomal translocations. For many imprinted genes, such studies have revealed functions consistent with the parental conflict hypothesis. Indeed, the discovery of the growth retardation phenotype of mice inheriting a dysfunctional *Igf2* allele through the paternal line (DeChiara *et al*, 1991) could be explained by the model. Further, a prediction of the model is that some imprinted genes might be in an 'arms race' with others, suggesting that maternally- and paternally-expressed genes might act antagonistically in the same molecular or genetic pathways. This also sits comfortably with some imprinted gene examples. *Igf2r* is maternally-expressed and opposes the actions of paternally-expressed *Igf2* in the same signalling pathway (Barlow *et al*, 1991). The non-coding maternally-expressed *H19* gene also regulates *Igf2* imprinting, such that a relaxation of *H19* expression causes *Igf2* to be transcribed from both parental alleles, an example of antagonism at the genetic level (Steenman *et al*, 1994).

A similar effect is observed for imprinted genes in the endosperm of flowering plants. An increased dosage of maternal genomes reduces endosperm size and restricts seed development, with the opposite effect resulting from multiple paternal genomes (Scott *et al*, 1998). *MEDEA* (*MEA*) is a maternally-expressed gene active in the endosperm (Kiyosue *et al*, 1999). Maternal inheritance of a loss-of-function *MEA* mutant results in endosperm overgrowth, suggesting the normal function is to restrict endosperm development (Kinoshita *et al*, 1999). Such observations are consistent with the conflict theory. The development of flowering plant seeds, like mammalian embryos, requires a much greater maternal than paternal investment, establishing the imbalance which is likely to favour the evolution of imprinting.

It is interesting to note that the authors of the original parental conflict hypothesis made some predictions about where and when murine imprinted genes might be expressed to

correlate with this proposed role of regulating maternal resource allocation; essentially any loci involved in the acquisition of maternal nutrients, including loci influencing placental growth, suckling, neonatal behaviour, appetite and hypothalamic function, nutrient metabolism and postnatal growth rate (Moore and Haig, 1991). At the time of publication, only the *Igf2* gene had been identified as being imprinted, yet subsequent studies have revealed imprinted genes involved in all of these processes. Indeed, the imprinted gene encoding the Growth factor receptor bound protein 10, *Grb10*, influences at least three of these processes in the mouse; placental growth, nutrient metabolism and postnatal growth (Charalambous *et al*, 2003; Smith *et al*, 2007; Charalambous *et al*, submitted).

An alternative proposal is derived from the observation that parthenogenetic mammals do not exist, and efforts to produce such lines in the laboratory have generated teratocarcinomas (Kaufman *et al*, 1983). Such a phenomenon does occur in other vertebrates, including some reptiles, fish and even birds (Lampert, 2008). As genomic imprinting is limited among vertebrates to mammals, it has been proposed that such a system developed to prevent parthenogenesis, requiring a contribution from both parental genomes. Imprinting would therefore be under maternal control. However, silencing an allele which terminates parthenogenetic embryos would also prevent asexual reproduction, thereby decreasing its frequency compared with an active allele which permitted this mode of reproduction. Thus, an allele with such properties would be selected against (Hurst, 1997). However, an argument in favour of preventing parthenogenesis has been presented by Varmuza and Mann (1994). Through their dramatically named 'ovarian time bomb' hypothesis, the authors argue that ovarian trophoblastic disease has sufficient cost to warrant the elimination of parthenogenotes. Trophoblastic disease could arise from an unfertilised egg developing in the ovaries, with potentially fatal consequences for the mother. Inactivation of maternal growth-promoting genes would guard against such a catastrophe, and the system would spread rapidly due to the increased fitness correlated with suppression of a deadly disease (Varmuza and Mann, 1994; Weisstein *et al*, 2002).

One strong counter-argument to the ovarian time bomb hypothesis is that the frequency of mammalian ovarian teratomas is very low, and the selection pressure for the evolution of imprinting to guard against this disease is not sufficiently strong (Solter, 1994). Weisstein *et al* (2002) demonstrate that even a low frequency of teratomas provides sufficient selection pressure to maintain genomic imprinting, but point out that the pressure must be higher initially for imprinting to evolve. A second objection to the model is that the silencing of a single maternal allele would be sufficient to prohibit parthenogenesis, and so the existence of multiple imprinted genes is inconsistent (Haig, 1994). Thirdly, the ovarian time bomb hypothesis fails to explain the silencing of paternally-inherited alleles. Finally, the reproductive strategies of angiosperms eliminate the possibility of ovarian cancer, and thus the hypothesis cannot explain imprinting in this system (Haig, 1994; Moore, 1994).

A host of models has been proposed to explain the evolution of imprinting, each with their merits and pitfalls (for a review, see Hurst, 1997), yet the most widely-accepted remains the parental conflict theory. However, despite its consistency with the elucidated functions

of many imprinted genes, the hypothesis is inadequate to explain other observations. An important limitation is that it cannot account for the persistence of imprinting in adult tissues (Hurst *et al*, 2000). It also offers no explanation for the predominance of maternally-expressed imprinted genes in the placenta, which would be expected to occur with equal frequency to paternally-expressed genes. These two arguments are addressed by the maternal-offspring coadaptation theory (Wolf and Hager, 2006). This model describes how genes which benefit both mother and offspring are under greater pressure to become imprinted. This could occur through pleiotropy, in which a single gene affects different traits in mother and offspring, or linkage disequilibrium, in which two genes on the same chromosome might become tightly linked because one influences a maternal trait, and the other, an offspring trait. In such situations, natural selection would favour genomic imprinting because it promotes the genetic integration of coadapted mother and offspring traits. Moreover, genes fulfilling this role are most likely to be maternally-expressed, explaining the predominance of maternally-expressed imprinted genes in the placenta. Further, the model would account for the persistence of imprinting in adult tissues if they influenced maternal behaviour or physiology to enhance fitness. However, this model cannot explain the apparent convergent evolution of imprinting in mammals and plants. The maternal-offspring coadaptation model is discussed further in Chapter Six.

Another provocative argument against the conflict theory is that imprinting persists in monogamous species. This was demonstrated by Vrana *et al* (1998) comparing the monogamous *Peromyscus polionotus* and the polyandrous *P. maniculatus*. *P. polionotus* is a rare example of a monogamous rodent species, which inhabits much of North America (Crossland and Lewandowski, 2006). Monogamy has been confirmed by genetic studies (Foltz, 1981), as well as being inferred from the absence of sexual dimorphism, which typically correlates with monogamy in wild populations (Vrana *et al*, 1998). The imprinted statuses of *H19*, *Igf2* and *Igf2r* observed in *P. maniculatus*, which are similar to those observed in the more common laboratory mouse species *Mus musculus*, also persisted in *P. polionotus*. On the surface, this observation cannot be explained by the conflict theory, which relies on multiple paternities. The authors argue that the theory might have predicted a relaxation of imprinting in the monogamous species. However, as highlighted by Moore and Mills (1999), the loss of imprinting (LOI) of a potent growth promoter, such as *Igf2*, would double gene dosage and by inference, increase resource demands. Such LOI would therefore be strongly counter-selected, and would be sufficient to maintain genomic imprinting even in the absence of multiple paternities. Additionally, even a low rate of partner exchange may be sufficient to exceed the negative effects of exposure to deleterious recessive alleles, maintaining imprinting (Hurst, 1998; Haig, 1999).

In conclusion, the conflict theory persists as the most widely-accepted model for the evolution of imprinting in mammals, accounting for the majority of imprinted gene expression patterns and functions. Further, this remains the only model accounting for the apparent convergent evolution of imprinting in mammals and plants. However, it is plausible that whilst parental conflict may have been the initial selective pressure for imprinting mechanisms to evolve, the system may have been subsequently adopted by

other loci in the mammalian genome for different reasons. Perhaps there is not a 'one size fits all' model.

1.1.3 Mechanisms and features of imprinted genes

As well as stimulating much debate on the fundamental reasons for its evolution, genomic imprinting raises another key question: how can such a system be regulated? If two alleles of a gene, one from each parent, are identical in sequence, how can they be distinguished to permit parent-of-origin specific expression?

Almost all imprinted genes identified in mammals and plants thus far are under the influence of differential DNA methylation. DNA can be methylated on CpG dinucleotides, such that the sequence of the DNA is unaffected. This is referred to as an epigenetic modification. Sequences rich in CpG dinucleotides are called CpG islands, and imprinted genes are typically rich in such regions; around 88 % of mouse imprinted genes include or overlap with a CpG island, compared with the genomic average of 47 % (Reik and Walter, 2001). CpG islands can be differentially methylated, such that one parental allele is relatively rich in methyl groups (hypermethylated) whilst the other is relatively poor (hypomethylated). This provides a mechanism for distinguishing parental alleles.

Differentially methylated regions (DMRs) vary in their properties. Whilst some are tissue specific (somatic DMRs) others are established in parental germ cells and persist at all developmental stages and tissue types (germline DMRs). Additionally, whilst promoter methylation at biallelically-expressed loci has traditionally been considered repressive for transcription, methylation at DMRs can be associated with the promotion or suppression of gene activity, depending on the locus in question.

If DNA methylation is to mark parental alleles, and so permit their discrimination, the mark must be reset every generation, such that the imprint in the gametes reflects the gender of the parent. To this end, there is a well-defined life cycle for imprints, involving erasure of the existing imprint early in germ cell development, establishment of a new imprint in the germ cells, and maintenance of the imprint as chromosomes segregate and cells multiply and differentiate (Figure 1.1). At around embryonic day 12.5 (e12.5), the germ cells of both sexes undergo a global demethylation event (Tada *et al*, 1998), although it is not certain if this is an active or passive process. The fusion of embryonic germ (EG) cells isolated at this stage with somatic cells causes demethylation of the somatic genome, suggesting the process is active and dominant (Tada *et al*, 1997). At later foetal stages, and persisting after birth, the germ cells undergo *de novo* methylation. For oocytes, which are held in meiotic arrest, *de novo* methylation occurs during their growth (Obata *et al*, 1998), whilst the nuclei of sperm are methylated prior to meiosis (Ueda *et al*, 2000). However, a mechanism must exist to permit specific targeting of DMRs in the male or female germ cells. This is made more challenging because the *de novo* methylation event is not specific to imprinted genes, but a global effect. Thus, the CpG islands of imprinted genes must exhibit other features which mark them out. One possible mechanism is the different timing of DNA replication

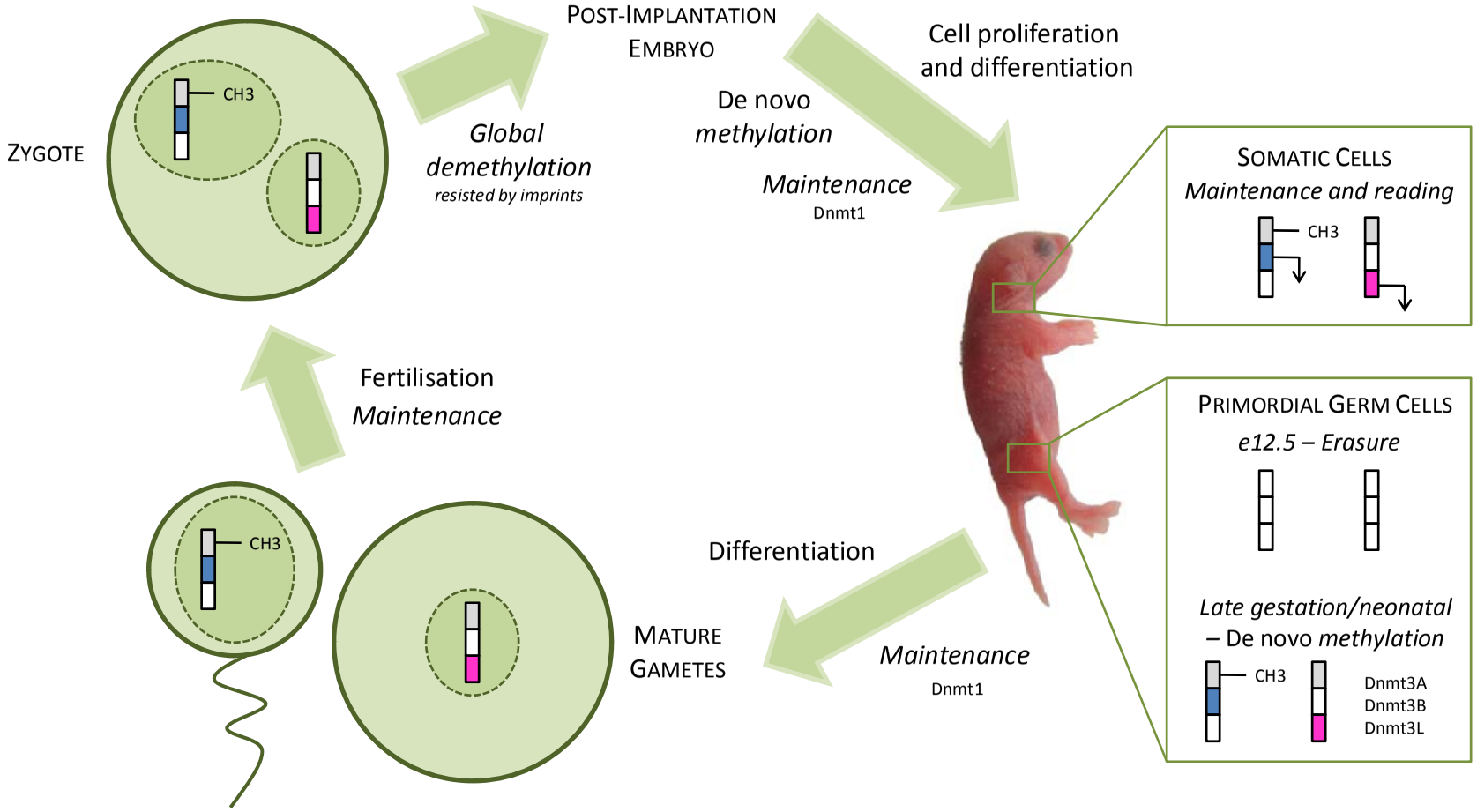
ZYGOTE
CH3
Global
demethylation
resisted by imprints
POST-IMPLANTATION
EMBRYO
De novo
methylation
Maintenance
Dnmt1
Cell proliferation
and differentiation
SOMATIC CELLS
Maintenance and reading
CH3
PRIMORDIAL GERM CELLS
e12.5 – Erasure
Late gestation/neonatal
– De novo methylation
CH3
Dnmt3A
Dnmt3B
Dnmt3L
Differentiation
Maintenance
Dnmt1
MATURE
GAMETES
Fertilisation
Maintenance
CH3

during S phase which is characteristic of imprinted genes (Kitsberg *et al*, 1993). Indeed, this feature arises early in germ cell development, and at least in oocytes, precedes *de novo* methylation (Simon *et al*, 1999). Such timing differences might alter the accessibility of DMRs to *de novo* methylation enzymes, marking them out from other genes. The key *de novo* methylation enzymes are DNA methyltransferase (Dnmt)3A and Dnmt3B, which methylate CpG dinucleotides on previously unmethylated DNA. Although very similar in tertiary structure, both proteins are essential for embryonic development, as deficiency for either protein is embryonic lethal, suggesting some non-redundant roles for each (Okano *et al*, 1999). Whilst Dnmt3A and Dnmt3B can catalyse *de novo* methylation, they are unable, alone, to establish sex-specific imprints in the germ line. Dnmt3L was identified as a potential candidate for this role based on sequence similarity to Dnmt3A and Dnmt3B (Aapola *et al*, 2000), but intriguingly, lacked some of the active sites necessary to catalyse CpG methylation itself (Bourc'his *et al*, 2001). Mice inheriting a disrupted *Dnmt3L* allele, although viable, were infertile (Bourc'his *et al*, 2001). Analysis of germ cells confirmed that *Dnmt3L* was expressed at the stages when imprints are established, utilising a *LacZ* gene trap knocked-in to the locus. Moreover, maternally-methylated imprinted genes, including *Snrpn* and *Peg1*, were heavily methylated in control oocytes, but hypomethylated in *Dnmt3L*-disrupted oocytes. Global DNA methylation was not notably affected by ablation of *Dnmt3L*, suggesting this formed part of the mechanism for establishing maternal methylation imprints during oogenesis, although the lack of a DNA methyltransferase domain implied that the protein did not perform *de novo* methylation itself (Bourc'his *et al*, 2001). Interestingly, in *Dnmt3L*$^{-/-}$ oocytes, some DMRs are methylated 'correctly', but this is a stochastic process (Arnaud *et al*, 2006). This suggests that other factors may also be involved in mediating this process, which can, alone, be sufficient to correctly methylate some DMRs.

The maintenance of differential methylation is mediated by a different enzyme, Dnmt1. Mice deficient for Dnmt1 die in mid-gestation, exhibiting delayed development, with a 3-fold reduction in DNA methylation (Li *et al*, 1992). Dnmt1 interacts with several cell cycle regulators, including proliferating cell nuclear antigen (PCNA) and p21WAF, a cyclin-dependent kinase (CDK) inhibitor (Chuang *et al*, 1997), suggesting it is tightly coupled to cell replication. Maintenance of methylation is achieved through the preference of Dnmt1 for hemi-methylated, rather than unmethylated, DNA (Zucker *et al*, 1985). However, there is a second wave of global demethylation which follows fertilisation, and subsequent *de novo* methylation post-implantation. Imprints must resist these, yet it is not known how this is achieved. The fertilisation-induced demethylation occurs in the pronuclei, before nuclear fusion. In the paternal pronucleus, the process is predominantly active (Oswald *et al*, 2000). The female pronucleus, however, fails to maintain methylation during DNA replication, thereby demethylating its genome in a passive manner (Rougier *et al*, 1998). This is associated with the exclusion of Dnmt1 from the nucleus (Carlson *et al*, 1992), so this enzyme cannot form part of the mechanism responsible for protecting imprints.

Polycomb group (PcG) proteins are also involved in the epigenetic regulation of imprinted genes. The imprinted paternal X chromosome is reactivated in embryos deficient for the PcG protein Eed (Wang *et al*, 2001). This was extended to examine autosomal imprinted

loci, for which LOI was apparent for four paternally-repressed genes: *Cdkn1c*, *Ascl2*, *Grb10* and *Meg3* (Mager *et al*, 2003). Other imprinted loci exhibited normal parent-of-origin specific expression, indicating that Eed regulates imprinting of a subset of genes. LOI correlated with aberrant DMR methylation in e7.5 *Eed*$^{-/-}$ embryos.

Eed is a component of Polycomb repressor complex 2 (PRC2), which mediates histone methylation. This is another example of an epigenetic modification, which can regulate the expression of genes. Histone modifications are discussed in more detail in Chapter Five, but in summary, are important for the regulation of imprinting at some loci, both in mammals and plants. For example, the imprinted expression of *Grb10* is partly regulated by histone methylation, which is lost in *Eed*$^{-/-}$ embryonic stem (ES) cells, resulting in relaxation of the imprint (Sanz *et al*, 2008). This suggests that Eed, through its role in PRC2, regulates histone methylation, and that this, in turn, may perturb DNA methylation at some DMRs. This illustrates the intimate relationship between various regulatory mechanisms to tightly control imprinted gene expression.

Non-coding antisense transcripts are also involved in regulating genomic imprinting, and in some cases, these have also been shown to tightly couple with histone modifications. Intriguingly, most of these transcripts identified to date are themselves subject to imprinting (Reik and Walter, 2001). The most extensively studied example is the *Air* transcript which is driven by a promoter located in intron 2 of the *Igf2r* gene (Lyle *et al*, 2000). *Air* is expressed exclusively from the paternally-inherited chromosome. In the embryo proper, *Air* suppresses *Igf2r* expression *in cis*. The mechanism for achieving this is not clear, but given the overlap between the two, it is conceivable that the *Air* transcript hybridises with the *Igf2r* transcript, resulting in dsRNA-induced degradation. However, this is disputed. Evidence against this mechanism comes from the observation that *Air* also suppresses the transcription of two other imprinted paternally-expressed genes, *Slc22a2* and *Slc22a3*, which are situated over 230 kb away from the *Air* promoter (Sleutels *et al*, 2002; 2003). Further, suppression of these two genes is tissue- and stage-specific, occurring only in the early- and mid-gestation placenta (Nagano *et al*, 2008). Imprinting of *Slc22a3* is relaxed between e11.5 and e15.5, although *Air* continues to be transcribed. Intriguingly, *Air* transcripts were found to overlap with the *Slc22a3* gene locus in the e11.5 placenta, as demonstrated by RNA-DNA fluorescence *in situ* hybridisation (FISH). A cover index was used to quantify the extent of the paternal *Slc22a3* locus 'clouded' by *Air in situ* signal. At e11.5, an analysis of z-stacked images suggested a high cover index, which was significantly reduced at e15.5, concomitant with a relaxation of the *Slc22a3* imprint. These results implied that *Air* transcripts coat the genomic locus to suppress transcription, in a mechanism reminiscent of that observed for X chromosome inactivation (reviewed in Chow and Heard, 2009). Whether this is also the mechanism for the regulation of *Igf2r* expression requires further attention.

As a further demonstration of the coupling of regulatory mechanisms, the *Slc22a3* promoter is subject to differential histone modifications at e11.5 versus e15.5. As discussed in Chapter Five, specific modifications are associated with transcriptionally active and inactive DNA. At e11.5, histone modifications at the paternal *Slc22a3* locus were

predominantly repressive, which were replaced by active marks at e15.5 (Nagano *et al*, 2008). This correlation between the enrichment of such marks and the changes in *Air* cover index suggested the two may be functionally linked. One possibility was that *Air* may recruit histone-modifying complexes, such as the G9a histone methyltransferase, which is involved in modifying histones at the *Kcnq1* imprinted domain in the placenta (Wagschal *et al*, 2008). RNA immunoprecipitation (RNA IP) demonstrated that *Air* and G9a were physically coupled, and chromatin immunoprecipitation (ChIP) confirmed G9a enrichment only at the paternally-inherited allele (Nagano *et al*, 2008). In mice with a truncated *Air* transcript, *Air-T* (Sleutels *et al*, 2002), inherited through the paternal line, FISH signal for *Air* was weak at the *Slc22a3* promoter. Moreover, ChIP suggested a considerable reduction in G9a at the site, suggesting that full-length *Air* is necessary for the correct targeting of G9a to the paternal promoter.

The complexities of understanding imprinted gene regulation are further obscured by the clustering of such genes. Clusters can include a range of maternally-, paternally- and biallelically-expressed genes, which share regulatory elements, such as DMRs. Germline DMRs which influence the expression of multiple genes in a cluster are called imprinting control regions (ICRs). Thus, despite the earlier statement that ~88 % of imprinted genes possess CpG islands, almost all others are probably influenced by DMRs shared with other genes. The *H19*/*Igf2* locus exemplifies several of the regulatory features of imprinted clusters, and is discussed further in Chapter Five.

The control of imprinted gene expression is complex, with multiple mechanisms interacting to achieve fine-tuned levels of transcription. As many imprinted genes encode potent regulators of growth, metabolism and behaviour (discussed in the next section), changes to their expression can have dramatic, and often catastrophic, consequences. Human disorders such as Beckwith-Weidemann syndrome, Angelman syndrome and Prader-Willi syndrome can all arise as a consequence of aberrant imprinting.

1.1.4 Imprinted genes in mammals – functions and disease

As mentioned earlier, the parental conflict hypothesis predicted that imprinted loci should be a subset of genes involved with the regulation of maternal resource allocation, and the authors proposed several physiological processes likely to be under the influence of genomic imprinting (Moore and Haig, 1991). It follows that the mutation of such genes, or their LOI, would perturb these processes, resulting in aberrant development and potentially disease. Here, we review the various physiological processes influenced by imprinted genes and relate them, where possible, to human disease states.

Perhaps most predictably, several imprinted genes influence the growth of the mammalian placenta, which is a transient organ largely responsible for regulating foetal development. Although the functions of many imprinted genes have been elucidated through gene knockout experiments, many are expressed in both the placenta and foetus, and it can therefore be difficult to determine the influence of gene ablation in the placenta alone on

foetal development. This problem can be conveniently circumvented in the case of *Igf2*, because the majority of transcripts expressed in the placenta arise from a tissue-specific promoter. Ablation of these so-called *Igf2P0* transcripts resulted in placental growth retardation similar to that observed for complete *Igf2* null embryos (DeChiara *et al*, 1991; Constância *et al*, 2002; Reik *et al*, 2003).

Igf2 encodes the ligand insulin-like growth factor 2, which forms part of the important growth regulatory IGF signalling system. Whilst ablation of either *Igf2* or the structurally-related *Igf1* engendered a 40 % growth reduction at birth relative to wild type controls (DeChiara *et al*, 1990; Liu *et al*, 1993), dual ablation resulted in a more dramatic growth restriction. Intriguingly, these double knockout mice were essentially indistinguishable from animals lacking the *Insulin-like growth factor 1 receptor* (*Igf1r*) gene, suggesting the growth effects of these two ligands are predominantly mediated through IGF1R (Liu *et al*, 1993). This signalling system is in part regulated by the actions of the insulin-like growth factor 2 receptor (IGF2R), also called the mannose-6-phosphate receptor (M-6-Pr), the genetic ablation of which results in embryonic overgrowth, when maternally transmitted (Lau *et al*, 1994). *Igf2r*$^{-/-}$ mice can be rescued from perinatal lethality on an *Igf2*$^{-/-}$ background, supporting earlier evidence that the lethality is associated with elevated IGF2 levels which are incompatible with life (Ludwig *et al*, 1996). As mentioned previously, this identified *Igf2r* as a negative regulator of *Igf2* activity. *Igf2r* is itself imprinted and expressed from maternally-inherited chromosome 17 in mouse (Barlow *et al*, 1991), providing a classic example of the antagonistic actions of maternally- and paternally-expressed genes in the regulation of foetal growth, consistent with conflict theory. Further, M-6-Pr orthologs in chicken, *Xenopus* and platypus, species which do not exhibit imprinting, lack the IGF2 binding domain, suggesting that this function correlates with the evolution of genomic imprinting (Killian *et al*, 2000).

IGF2 in the placenta signals through an as-yet unidentified receptor, and whilst IGF2 appears to control placental size, and by inference foetal growth, the mechanism by which this is achieved remains unclear. The actions of IGF2 in the placenta are further discussed in Chapter Four.

Although a large part of the growth effects of *Igf2* appear to be attributable to *Igf2P0* in the placenta, changes in the levels of *IGF2* expression in humans correlate with an imprinted gene disorder called Beckwith-Weidemann syndrome (BWS). BWS is characterised by intrauterine overgrowth of both embryonic and extra-embryonic tissues, which persists postnatally, as well macroglossia (hypertrophy of the tongue), anterior abdominal wall defects and a predisposition to childhood cancers (Maher and Reik, 2000). The molecular basis of the syndrome is complex, being associated with a cluster of at least fifteen genes on human chromosome 11p15.5, referred to as the BWS locus. At least nine of these are imprinted, and include *IGF2* and *H19*. The embryonic and postnatal overgrowth are often correlated with elevated *IGF2* expression. Indeed, a large proportion of patients which do not possess cytological abnormalities, such as duplication of 11p15.5, demonstrate increased *IGF2* expression (Weksberg *et al*, 1993). This is typically the result of aberrant

methylation at the *IGF2*/*H19* ICR, resulting in silencing of *H19* and biallelic expression (or LOI) of *IGF2*.

The maternally-expressed *p57KIP2* gene also forms part of the BWS locus. Point mutations in this gene are associated with 5-10 % of sporadic and 40 % of familial BWS cases (Smith *et al*, 2006). Whilst these patients do not exhibit altered levels of *IGF2*/*H19* expression, the disease presentation is similar to that for cases in which the primary genetic defect is disruption of *IGF2*/*H19*. This suggests that the protein product of the *p57KIP2* gene may negatively regulate the *IGF2* growth pathway. This hypothesis is supported by mouse genetics, in which *Igf2* over-expression suppresses the ortholog of *p57KIP2*, *Cdkn1c* (Grandjean *et al*, 2000). Additionally, mice exhibiting both loss of function of *Cdkn1c* and LOI of *Igf2* more closely recapitulate the aetiology of the human syndrome than mice with either mutation alone (Smith *et al*, 2006). Thus, perhaps *Igf2*/*IGF2* and *Cdkn1c*/*p57KIP2* act antagonistically in the same growth pathway, again consistent with conflict theory.

A further epigenetic cause of BWS is loss of methylation on the maternal allele at the ICR situated near the *KVLQT1* gene, referred to as KvDMR1. Patients with an inversion breakpoint at this DMR exhibited biallelic *IGF2* expression, whilst retaining imprinted *H19* expression and normal methylation patterns at the *IGF2*/*H19* locus (Brown *et al*, 1996). This suggests that *IGF2* expression can be regulated in a manner independent of *H19*, although the mechanism for this is not certain. Loss of methylation on the maternal KvDMR1 correlates with expression of an antisense transcript, *KCNQ1OT*, from the maternal gene copy, which might act to de-repress *IGF2* imprinting (Maher and Reik, 2000).

Like paternally-expressed *Igf2*, maternally-expressed *Grb10* is expressed in both the placenta and embryo proper, but the relative influence of these sites of expression on foetal growth have not been determined. Mice inheriting a disrupted *Grb10* allele through the maternal line are 30 % larger than wild type littermates at birth, and possess disproportionately enlarged livers, whilst the brain is spared (Charalambous *et al*, 2003). This correlates with sites of action of *Grb10* expressed from the maternally-inherited allele in the foetus, suggesting part of the overgrowth is attributable to *Grb10* expression in the embryo itself. However, the associated placentae are also overgrown, with disproportionately enlarged labyrinths (Charalambous *et al*, submitted), the cell layer involved in mediating maternal nutrient transfer. Thus, the direct and indirect influences of *Grb10* ablation on foetal development cannot be uncoupled, without further genetic or transplantation experiments.

An increased dosage of *GRB10* has been implicated with Silver-Russell syndrome (SRS), a disease characterised by intrauterine and postnatal growth restriction, as well as other features (for a review, see Preece, 2002). About 10 % of SRS cases correlate with maternal UPD of chromosome 7, and whilst three imprinted genes reside on this chromosome, most cases are associated with mUPD of 7p11.2-p12 at which *GRB10* is situated (Preece, 2002). Two other genes within this region influence foetal growth, *IGFBP1* and *EGFR*, but both are biallelically-expressed, leaving *GRB10* as the most likely SRS candidate gene. Indeed, *Grb10* over-expression in mice results in intrauterine growth restriction (Shiura *et al*, 2005), as does a maternal duplication of mouse proximal chromosome 11, which includes *Grb10*

(Cattanach *et al*, 1996). However, no methylation abnormalities at the *GRB10* locus have been identified in SRS patients, suggesting that, if *GRB10* expression is the molecular basis for SRS, it may be mediated by another regulatory mechanism. Recently, an imprinted antisense RNA was identified at the mouse *Grb10* locus (Babak *et al*, 2008), although its properties and functions are yet to be investigated.

Foetal growth and adult metabolism are closely linked, often involving the same genetic pathways or players. Impaired foetal development has long been correlated with adult disease states, and nutrition availability *in utero* can influence the epigenetic regulation of genes involved with metabolism (for a review, see Waterland and Jirtle, 2004), in the process of 'foetal programming'. Many of the imprinted genes implicated in growth therefore influence postnatal energy homeostasis. Murine *Grb10*, for example, also influences adult metabolism. *Grb10* ablation on the maternal chromosome enhances blood glucose clearance, in part by enhancing insulin signalling and also because *Grb10* ablation results in increased lean tissue, a sink for glucose (Smith *et al*, 2007).

The human *Zinc finger protein that regulates apoptosis and cell-cycle arrest* (*ZAC*) and *Hydatidiform-mole associated and imprinted transcript* (*HYMAI*) genes are also thought to influence both foetal growth and adult metabolism. Both genes are imprinted and expressed from paternally-inherited chromosome 6q24, situated at a region associated with transient neonatal diabetes mellitus (TNDM). This paternal-transmission disorder is characterised by intrauterine growth retardation, dehydration and hyperglycaemia, with associated hypoinsulinaemia (Hamilton-Shield, 2007). Following the neonatal period, most TNDM patients demonstrate normal glucose homeostasis until adolescence or early adulthood, when type 2 diabetes reappears (Temple *et al*, 2000). *ZAC* is pro-apoptotic and was independently discovered as a tumour suppressor gene (originally called *Pleomorphic adenoma gene-like 1*, *PLAGL1*; Kas *et al*, 1998). One of its transcriptional targets is the *Pituitary adenylate-cyclase activating polypeptide* (*PACAP*) *type 1 receptor* (*PAC1-R*) gene; PACAP regulates insulin secretion in response to elevated serum glucose and promotes pancreatic β-cell proliferation (Ciani *et al*, 1999; Rodríguez-Henche *et al*, 2002). Perturbation of β-cell proliferation or secretory function is thought to be the basis for TNDM; this was supported by the post-mortem histological assessment of a patient with TNDM, whose pancreas was lacking insulin-positive cells (Blum *et al*, 1993). Mice over-expressing the human TNDM locus also demonstrate a reduction in fully-differentiated β-cells, suggesting this is the likely pathological basis for the disorder (Ma *et al*, 2004).

The *Gnas* locus on mouse chromosome 2 is predominantly associated with the control of metabolic processes, rather than growth. The locus consists of a maternally-expressed gene, *Nesp*, three paternally-expressed genes, *Nespas*, *Gnasxl* and *Exon 1A*, as well as the *Gnas* gene itself, which is generally biallelically-expressed but imprinted (paternally-silenced) in some tissues, including the proximal renal tubules, anterior pituitary gland, thyroid gland and ovary (Yu *et al*, 1998; Hayward *et al*, 2001; Germain-Lee *et al*, 2002; Mantovani *et al*, 2002). *Gnas* and *Gnasxl* encode G-protein α subunits ($G\alpha_s$ and $XL\alpha_s$, respectively) which activate adenylyl cyclases in response to ligand-binding at G-protein

coupled receptors (GPCRs), promoting the synthesis of cyclic adenosine monophosphate (cAMP).

Gnas exon 2 is common to all transcripts arising at the *Gnas* locus identified to date, except for *Nespas* which produces a non-coding RNA (Plagge *et al*, 2008). Mice inheriting a dysfunctional exon 2 through the maternal line are hypometabolic, whereas paternal transmission results in mice which are lean and hypermetabolic, reflecting the imprinted status of the locus (Yu *et al*, 1998). Specific deletion of *Gnasxl* produces mice which are lean and exhibit reduced circulating insulin, glucagon and glucose levels, comparable with the hypometabolic state engendered by paternal deletion of *Gnas* exon 2 (Plagge *et al*, 2004). Conversely, paternal deletion of *Gnas* exon 1, which affects only *Gnas* transcripts, engenders obesity and insulin resistance, comparable to maternal *Gnas* exon 2 ablation (Chen *et al*, 2005). Together, these results imply that *Gnas* and *Gnasxl* have opposite effects on glucose and lipid metabolism (Plagge *et al*, 2004; Plagge *et al*, 2008). This is likely to be a consequence of their differential expression profiles in the central nervous system (CNS) which correlate with distinct functions in the regulation of homeostasis; for example, $XL\alpha_s$ is expressed in the orofacial motornuclei, which are required for the physical action of suckling, and is thus likely to be a contributory factor to the lean phenotype following *Gnasxl* ablation (Plagge *et al*, 2004).

GNAS mutations in humans are associated with Albright's hereditary osteodystrophy (AHO). Clinical features of this disorder include subcutaneous ectopic ossifications, obesity, cognitive defects and brachydactyly. However, AHO can also be associated with hormone resistance, but this is parent-of-origin specific (Davies and Hughes, 1993). Transmission of a mutation in the *GNAS* locus through the maternal line results in resistance to a range of hormones, including parathyroid hormone (PTH), thyroid-stimulating hormone (TSH) and growth hormone-releasing hormone (GHRH) in adulthood. An identical mutation which is paternal in origin produces no such hormone resistance, reflecting the importance of the imprinted (maternally-expressed) *Gnas* transcripts detected in some cell types (Weinstein *et al*, 2001). Such resistance is likely to arise as a direct consequence of impaired signal transduction in target cells, consistent with the role of maternally-expressed *GNAS* products as Gα subunits.

Other imprinted genes have been implicated in neuroendocrine disorders. Prader-Willi syndrome (PWS), for example, is characterised by hypotonia and failure to suckle at birth, which is overcompensated for by a voracious appetite in early childhood. Other features are more variable, and include behavioural abnormalities, such as obsessive-compulsive traits and tantrums (Cassidy and Driscoll, 2009). The physiological basis of the disease is perturbed hypothalamic/pituitary axis function, which causes low serum levels of testosterone and gonadotrophins, the latter most probably due to a resistance to gonadotropin releasing hormone (GnRH; Davies *et al*, 2008). Growth hormone (GH) levels are also low, resulting in reduced *Igf1* expression (Miller *et al*, 2007). Paradoxically, PWS patients also exhibit elevated obestatin levels, a hormone which suppresses appetite (Butler *et al*, 2007). The extreme hyperphagia observed in childhood is likely to be a consequence of developing resistance to high obestatin levels.

The genetic basis for PWS is the absence, or reduction, of expression from a locus on paternally-inherited chromosome 15q11-q13. This is most commonly caused by a genetic deletion at the locus, but can also occur as a consequence of mUPD for the region, or a mutation at the ICR. Several imprinted genes reside at this locus, and the variable phenotypes of the disorder are likely to be dependent on the number of genes affected by a particular mutation. For example, mice deficient for the paternally-expressed gene *Necdin* recapitulate some of the neuroanatomical features of PWS, including a reduction in oxytonergic and GnRH neurones (Muscatelli *et al*, 2000). This PWS model also results in early lethality, which is common to PWS patients, and exhibits several of the behavioural characteristics of the disorder, including improved spatial learning and memory. Deletions of the murine *Magel2* gene reproduce the excessive weight gain and increased adiposity observed in PWS patients post-weaning (Bischof *et al*, 2007). Perhaps the most comprehensive model of PWS is the PWS-IC deletion mouse, which ablates the ICR and results in suppression of paternally-expressed genes at the locus, with concomitant activation (and thus biallelic expression) of normally maternally-expressed genes (Chamberlain *et al*, 2004). This is strong evidence that PWS is an imprinting disorder which is caused by the LOI of several clustered genes. Recently, the importance of a non-coding small nucleolar RNA (snoRNA) species has been revealed in the aetiology of PWS. *mbii-52* (or *hbii-52* in humans), which is expressed from the paternal chromosome at the PWS locus, regulates the post-transcriptional editing of the *Serotonin 2C receptor* (*5htr2c*) pre-mRNA (Doe *et al*, 2009). Loss of editing is associated with the alteration of a number of 5HTR2C-mediated behaviours, which recapitulate some of the specific features of PWS patients.

The involvement of imprinted genes in the regulation of adult metabolism is not necessarily consistent with the predictions of the parental conflict hypothesis, which cannot account for the persistence of imprinting post-weaning, as previously discussed. Indeed, it is apparent from mouse genetics studies that imprinted genes expressed from both the maternally- and paternally-inherited chromosomes can influence energy homeostasis in a similar manner. For example, at the gross level, both the ablation of maternally-expressed *Grb10* and paternally-expressed *Gnasxl* reduce adult adiposity (Smith *et al*, 2007; Plagge *et al*, 2004). Whilst the molecular events responsible for this effect are very different, the phenotypic outcome is similar, although the models also exhibit other, disparate, phenotypes. It could be argued that the involvement of imprinted genes in adult metabolism is simply a result of their importance in foetal growth, two physiological processes which share many of the same signalling pathways and molecular players. As such, imprinting in adult tissues would be the result of a 'bystander effect'. However, the importance of imprinted genes, such as those at the *Gnas* locus, in regulating adult metabolism but having a negligible effect on embryonic development, argues against this suggestion. Additionally, it has become apparent in recent years that several imprinted genes are expressed in the adult brain and affect behaviour; for many, a function in foetal development has not been defined. Behaviour thus represents an additional physiological process under the influence of imprinting, which we briefly address here.

As highlighted already, some imprinted genes expressed in the brain influence neuroendocrine function and can thus be grouped with many other peripherally-expressed genes as regulators of metabolism. The brain expression of other imprinted genes is inconsistent with such a role. For example, *Ube3a* is maternally-expressed in neurons of the hippocampus and cerebellum, whilst being biallelically-expressed in glia (Yamasaki *et al*, 2003). Maternal ablation of this gene in mice results in motor dysfunction, seizures and learning deficits, recapitulating several of the features of Angelman syndrome (AS), a human disorder caused by silencing of the *UBE3A* gene (Jiang *et al*, 1998).

Grb10 is an intriguing example of an imprinted gene with reference to behaviour. Whilst maternally-expressed *Grb10* influences foetal development and postnatal metabolism (Charalambous *et al*, 2003; Shiura *et al*, 2005; Smith *et al*, 2007), it is the paternally-derived allele which is expressed in the brain (Garfield, 2007; Garfield *et al*, submitted). This reciprocal imprinting profile is apparently unique to *Grb10*. Transmission of a dysfunctional *Grb10* allele through the paternal line produced mice which were socially dominant over wild type controls, but otherwise indistinguishable when assayed for other behavioural characteristics. This was demonstrated by use of the 'tube-test' and the observation of increased allogrooming (barbering of other animals) in cages containing mutant mice. These results suggest that paternally-expressed *Grb10* mediates a specific behavioural trait, which does not influence foetal development or postnatal metabolism (Smith *et al*, 2004; Garfield, 2007; Garfield *et al*, submitted).

Why imprinted genes should be associated with modulating social behaviour is unclear. Indeed, *Grb10* does not appear to be alone; *Nesp55*, a maternally-expressed transcript arising from the *Gnas* cluster, promotes risk-tolerance (Plagge *et al*, 2005). This is of additional interest because *Nesp55* and *Grb10* expression exhibit considerable overlap in the brain, and the opposite phenotypes of knock-out mouse models suggest they may act antagonistically in the same neurological pathway (Garfield *et al*, submitted). It is intriguing that they are also expressed from opposing alleles, reminiscent of the antagonistic basis of conflict theory. As already discussed, the influences of some imprinted genes on maternal behaviour can be explained in the context of coadaptation between mother and offspring, exemplified by *Peg3*. However, the evolutionary basis for the control of social dominance, or indeed, for the reciprocal *Grb10* imprint, remains elusive, yet represents an evocative area for future studies.

1.2 Growth factor receptor bound protein 10

1.2.1 The Grb7 family

Growth factor receptor bound protein 10 (Grb10) is a member of the Grb7 superfamily of adapter proteins, which also includes Grb7 and Grb14. These proteins do not possess catalytic activity, but are characterised by several molecular interaction domains, permitting association with a range of intracellular signalling molecules. This includes a N-terminal proline-rich (P) domain, a pleckstrin homology (PH) domain, a C-terminal Src-homology 2 (SH2) domain and a unique region positioned between the PH and SH2 domains termed the BPS domain (for between PH and SH2; Figure 1.2; Lim *et al*, 2004). Additionally, a Ras-associating (RA) domain has been predicted based on sequence comparisons (Wojcik *et al*, 1999), but the significance of this to Grb7/10/14 function remains unclear. Certainly, biochemical studies have shown Grb14 has the capability of interacting with Ras, but this has not been extrapolated to an *in vivo* context (Depetris *et al*, 2009). The amino acid sequence of the SH2 domain is highly conserved between the three members, with Grb14 exhibiting 67 % and 74 % identity with Grb7 and Grb10, respectively, in this region (Daly *et al*, 1996). In general, the N-terminal P domain is poorly conserved between family members, with the exception of a single proline-rich motif P(S/A)IPNPFPEL (Daly *et al*, 1996). Members of the superfamily are also structurally related to the Mig-10 protein isolated from *Caenorhabditis elegans*, which possesses both P and PH domains; thus, this region has been termed the GM region, for Grb10 and Mig (Manser *et al*, 1997). The function of Mig-10 is comparable to that of Grb7, both of which transduce signals responsible for cell migration (Manser *et al*, 1997; Han *et al*, 1999).

Several murine *Grb10* transcripts have been described, which are tissue- and parent-of-origin specific (Figure 1.2; Arnaud *et al*, 2003; Hikichi *et al*, 2003; Sanz *et al*, 2008). As discussed previously, the majority of transcripts arise from the maternally-inherited chromosome. The two predominant maternally-expressed transcripts are *Grb10*α and *Grb10*δ, which initiate at exon 1A and differ by their inclusion and exclusion of exon 5, respectively. Interestingly, exon 5 encodes the RA domain, suggesting that this is not required for some of the functions of Grb10. Most *in situ* and Northern hybridisation experiments do not permit differentiation between these isoforms, and whether there are tissue-specific differences in their expression profiles thus remains unclear. An embryo-specific transcript has also been detected, which initiates at exon 1A and splices onto exon 1C, before continuing downstream (Sanz *et al*, 2008). It is not clear if this transcript includes or excludes exon 5. Transcripts originating from the paternally-inherited chromosome initiate at exons 1B1, 1B2 and 1C, and all splice onto exon 2. Paternal transcripts have been described which lack exons 5 and 6, but it is not clear if all combinations are possible (i.e. transcripts initiating at each of 1B1, 1B2 and 1C which incorporate or exclude exons 5 and 6; Arnaud *et al*, 2003). The translation initiation site for all variants is located in exon 3, and only the 3' extreme of exon 18 forms the 3' untranslated region (UTR).

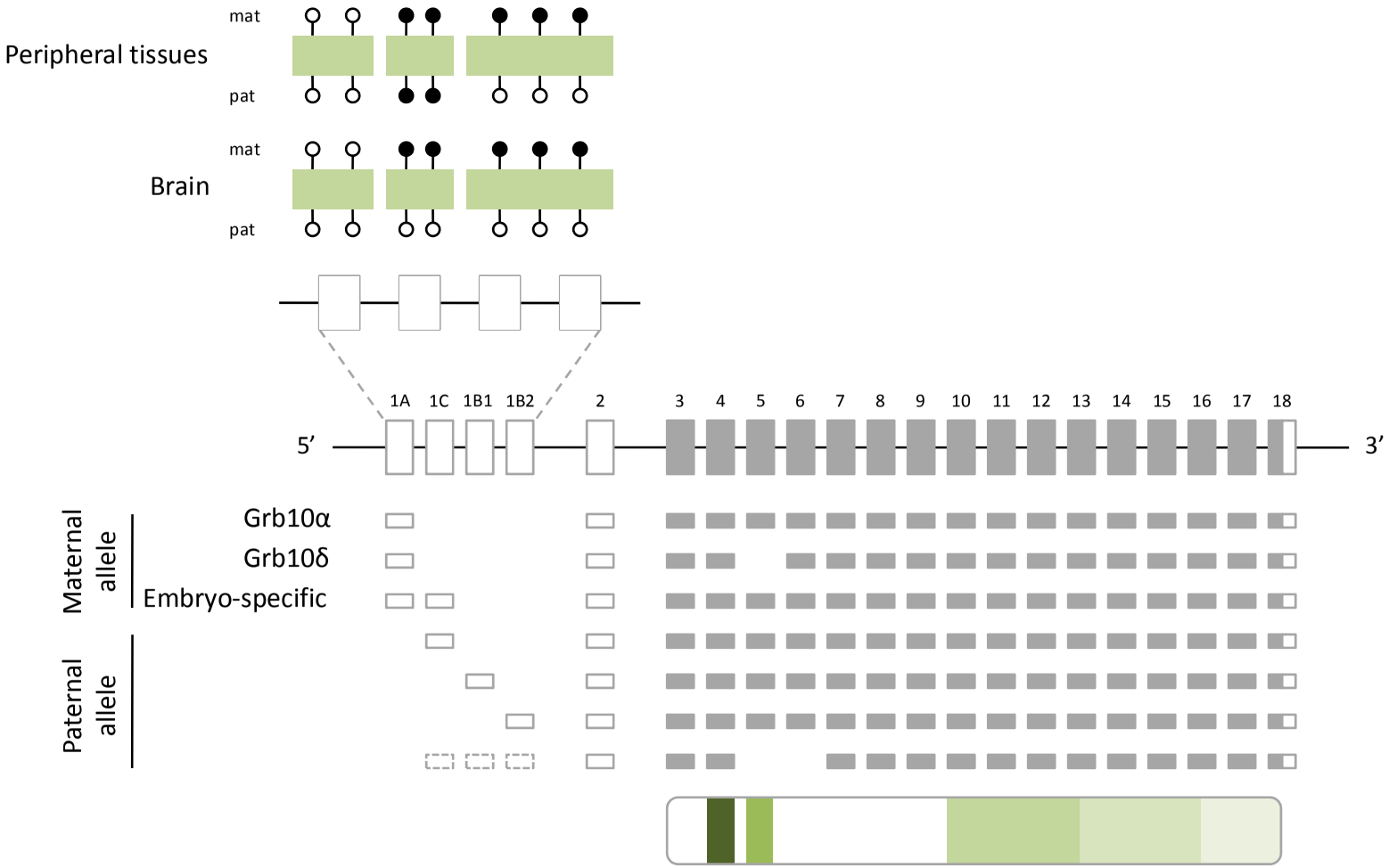
Peripheral tissues
mat
pat
Brain
mat
pat
1A
1C
1B1
1B2
2
3
4
5
6
7
8
9
10
11
12
13
14
15
16
17
18
5’
3’
Maternal allele
Paternal allele
Grb10α
Grb10δ
Embryo-specific

Three human GRB10 protein isoforms have been described to date: GRB10β, GRB10γ and GRB10ζ. GRB10ζ is the most similar to Grb10α, but lacks a 88 amino acid sequence close to the N-terminus of the protein, and a 46 amino acid sequence which forms part of the PH domain. The remaining functional domains show extensive sequence homology; the SH2 domain, for example, is 99 % identical at the amino acid level between Grb10α and GRB10ζ (Lim *et al*, 2004). GRB10β does not possess a PH domain due to the exclusion of exon 7 from the transcript. Transcripts encoding GRB10γ do not contain exon 1, resulting in the use of an alternative initiation codon and the loss of 55 amino acids at the N-terminus of the protein.

In addition to the proline-rich motif common to all Grb7 superfamily members, murine Grb10 also possesses two other such motifs, only one of which is conserved in human GRB10 isoforms, exhibiting 64 % amino acid sequence identity (Lim *et al*, 2004). Typically, sequences rich in proline interact with Src-homology 3 (SH3) and tryptophan-rich (WW) domains of other proteins. Rat Grb10 has been shown to interact with the non-tyrosine kinase c-Abl, which possesses a SH3 domain, and the interaction was outcompeted by a proline-rich peptide mimetic (Frantz *et al*, 1997), suggesting a likely interaction mediated by these two domains. Two novel binding partners of Grb10 were identified in a yeast two-hybrid screen using the Grb10 N-terminus as bait (Giovannone *et al*, 2003). These were termed Grb10 interacting GYF protein (GIGYF)1 and GIGYF2; GYF (glycine-tyrosine-phenylalanine) domains were first identified in the CD2 binding protein (CD2BP) and were shown to bind proline-rich peptide sequences in the CD2 tail (Nishizawa *et al*, 1998). At least two of the three proline-rich motifs in Grb10 are necessary to permit interaction with GIGYF1 and GIGYF2, and thus it would be interesting to establish if this interaction extrapolates to humans.

The novel GIGYF proteins are thought to mediate IGF1 signalling. Stimulation of fibroblasts with IGF1 promotes the association of both Grb10 and GIGYF1 with the IGF1R (Giovannone *et al*, 2003). This implicates the two proteins in cooperative modulation of IGF1 signalling.

Mutations in the human *GIGYF2* gene have been associated with some cases of familial Parkinson disease (PD). A screen of unrelated Central European PD patients and their families revealed a total of seven different missense mutations in the gene resulting in single amino acid substitutions (Lautier *et al*, 2008). Together, these were associated with 4.8 % of the PD patients screened but were not detected in controls, suggesting aberrant GIGYF2 activity may be associated with PD pathology, and that mutations in the gene might be a risk-factor for the disease. However, no such mutations were found amongst North American or Belgian populations of PD patients (Guo *et al*, 2009; Meeus *et al*, 2009).

The PH domain was first described in the cytoskeletal protein pleckstrin, and now represents the eleventh most common domain in the human proteome (Haslam *et al*, 1993; Lemmon, 2007). It is commonly associated with the binding of phosphoinositides. These signalling molecules are generated at the cell membrane in response to receptor activation, and recruit PH domain-containing proteins to the membrane. It is unclear if phosphoinositide binding is performed by Grb10, as the human GRB10β isoform lacks a functional PH domain and is still capable of translocating to the cell membrane (Dong *et al*,

1997a). Alternatively, the PH domain may promote the interaction of Grb10 with the insulin receptor (IR) and IGF1R, which is mediated by the SH2 and BPS domains, by providing a more favourable structural conformation (Dong *et al*, 1997b).

SH2 domains are associated with the binding of phosphotyrosine (pY) residues, representing another mechanism by which Grb10 may interact with cellular signalling partners. pY residues are commonly associated with activated proteins, and thus are widespread, but specificity of binding is achieved by the recognition of 3-6 amino acid residues C-terminal to the pY (Songyang *et al*, 1993). Intriguingly, the SH2 domain of GRB10 is dimeric in solution (Stein *et al*, 2003), unlike the more typical monomeric behaviour of this domain in other proteins. An α-helix situated in the C-terminal half of the domain is responsible for the dimerisation, and the amino acid sequence in this region is highly conserved with GRB7 and GRB14, suggesting these may also dimerise in solution (Lim *et al*, 2004). Resolving the GRB10 crystal structure has revealed that dimeric GRB10 is likely to favour the binding of dimeric, turn-containing pY sequences, which are found on both the IR and IGF1R (Stein *et al*, 2003).

The BPS domain is critical for the interaction of Grb10 with the IGF1R. The domain is relatively small, constituting 50 amino acids, and is unique to Grb7/10/14. A yeast two-hybrid screen of a mouse embryonic library also identified the ubiquitin protein ligase Nedd4 as a possible partner of Grb10, an association mediated by the BPS domain. Although Grb10 is not ubiquitinated by Nedd4 (Morrione *et al*, 1999), together the proteins have been shown to negatively regulate IGF1 signalling (Vechione *et al*, 2003). Ligand-activated receptor recruits the Grb10 and Nedd4 complex, which results in multi-ubiquitination of the receptor, triggering internalisation and degradation (Monami *et al*, 2008). The association of Grb10 and the IGF1R seems to be a role specific to this Grb7 superfamily member, although the IGF1R was sensitive to the inhibition of tyrosine kinase activity by Grb14 in an *in vitro* system, albeit much less so than the IR (Bérézіat *et al*, 2002).

1.2.2 Cellular signalling partners

Biochemical studies have identified a considerable number of cellular signalling cascades potentially mediated by the Grb7 superfamily, but their relevance to an *in vivo* context is variable. Indeed, Grb10 was first identified in a bacterial expression library screen in which the C-terminus of the epidermal growth factor receptor (EGFR) was used (Ooi *et al*, 1995), but this interaction has not been demonstrated *in vivo*. Grb10 demonstrates a preference for binding to the IR over other receptor tyrosine kinases (RTKs; Frantz *et al*, 1997; Laviola *et al*, 1997), and has since been shown to play a key role in the negative modulation of insulin signalling *in vivo* (discussed in Chapter Three; Shiura *et al*, 2005; Smith *et al*, 2007). However, the results of *in vitro* studies are conflicting. Over-expression of the human GRB10β isoform in Chinese hamster ovary cells also over-expressing *Insulin receptor* (*Insr*; CHO/IR) inhibited the tyrosine phosphorylation of insulin receptor substrate-1 (IRS-1), a downstream effector of insulin signalling (Liu and Roth, 1995). PI 3-kinase activity was also perturbed. The mode of action of Grb10 in this system appears to be as a physical block to

IR/IRS-1 interaction, rather than suppressing the catalytic activity of the receptor. This was demonstrated in a yeast tri-hybrid experiment, which showed human GRB10ζ inhibited IR/IRS-1 association in a SH2-dependent manner (Wick *et al*, 2003). These *in vitro* studies support the apparent role of Grb10 *in vivo* as a negative regulator of insulin signalling, but other experiments have indicated that Grb10 may have a positive effect on the same signal transduction pathway. Over-expression of Grb10 in differentiated 3T3-L1 adipocyte cells promoted the cellular response to insulin, and correspondingly, dominant-negative Grb10 SH2 peptide mimetics abolished such effects (Deng *et al*, 2003). This is in conflict with the majority of other studies, and may reflect a different role for Grb10 in a context-dependent manner. Grb14 also appears to interact with the IR and, like Grb10, negatively regulates insulin signalling *in vivo* (Cooney *et al*, 2004). Compound *Grb10*/*Grb14* mutant mice exhibit similar phenotypes to single knockout models, suggesting considerable functional redundancy (Smith *et al*, 2007; Holt *et al*, 2009).

Grb7 has been shown to associate with the IR *in vivo*, using co-immunoprecipitation (Kasus-Jacobi *et al*, 2000), but the association appears to be much weaker than that for Grb10 and Grb14, suggesting Grb7 may perform distinct cellular functions (Holt and Siddle, 2005). Consistent with this, *GRB7* is over-expressed in a range of cancers, including breast, gastric and oesophageal cancer cell lines, suggesting it has a positive mitogenic role. *GRB7* is consistently co-amplified in cancers with the tyrosine kinase receptor *HER2*, which is located on the same chromosomal region as *GRB7*, 17q11-q21 (Stein *et al*, 1994; Tanaka *et al*, 1997). Unlike the roles of Grb10 and Grb14, which are widely considered to be inhibitory in growth factor signalling, knock-down of *GRB7* in a breast cancer cell line reduced tyrosine phosphorylation of the receptor and of the mitogenic AKT signalling family, suggesting GRB7 is an activator of growth factor signalling (Bai and Luoh, 2008). Whilst this property was determined in a cancer cell line, GRB7/HER2 interaction also occurs in a normal cellular context, and appears to promote epithelial development in kidney, lung and gut (Leavey *et al*, 1998). Additionally, Grb7 has been shown to stimulate cell growth both *in vitro* and *in vivo* by binding to caveolin-1 (Lee *et al*, 2000). Whether the over-expression of *GRB7* is a common contributory factor to cancer progression requires further investigation, but one study does provide support for this hypothesis (Bai and Luoh, 2008). *GRB7* was over-expressed in a breast cancer cell line stably transfected to express *HER2* (MCF::HER2 cells). Four million of these cells were transplanted subcutaneously into nude mice. Cells transfected with a green fluorescent protein (GFP) control produced small tumours, but those over-expressing *GRB7* produced significantly larger tumours, demonstrating that GRB7 can facilitate HER2-mediated signalling leading to tumour growth, at least in this context.

Human GRB10ζ also interacts with the mitogen-activated protein (MAP) kinase MEK1, as demonstrated by co-immunoprecipitation and *in vitro* binding experiments (Nantel *et al*, 1998). The MAP kinase signalling cascade is key in coupling cellular responses to the binding of growth factors at cell surface receptors. It consists of a series of kinases activated in sequence, thus permitting amplification of the signal. In summary, receptor activation recruits docking proteins, such as Grb2 (unrelated to the Grb7 superfamily) and the guanine nucleotide exchange factor (GEF) Son of sevenless (SOS) which stimulates

activation of Ras by promoting the switching of the Ras-associated GDP molecule for GTP. Ras-GTP dissociates from the complex and activates the first serine/threonine kinase, RAF. In turn, MEK, MAPK and MNK are phosphorylated, which results in the activation of transcription factors such as the cAMP response element binding protein (CREB; Shaywitz and Greenberg, 1999). Both Grb10 and MEK1 have been shown to associate with Raf1 *in vitro*, although, as mentioned previously, Grb10 has not been detected bound to Ras despite possessing a RA domain. The Grb10/MEK1/Raf1 association is phospho-serine/threonine-dependent, but does not require tyrosine phosphorylation (Nantel *et al*, 1998). Raf1 is anti-apoptotic, and indeed the Raf1/Grb10 association is increased in ultraviolet (UV)-irradiated apoptosing cells (Nantel *et al*, 1999). Interestingly, this interaction was also detected in the mitochondria of these cells, suggesting Grb10 may act as a link between activation of receptors at the cell surface and the apoptotic machinery of the mitochondrial outer membrane. These data suggest that GRB10ζ is a promoter of MAP kinase signalling.

Grb10/GRB10 has been implicated in associations with a range of other signalling molecules, both RTKs and non-RTKs. For example, the Eph receptor family member ELK (Eph-related receptor tyrosine kinase), used as bait in a yeast two-hybrid experiment, yielded the Grb10 SH2 domain (Stein *et al*, 1996). In a cellular context, ligand-stimulated activation of ELK caused the recruitment of Grb10 following autophosphorylation of the receptor; indeed, the association was dependent on the phosphorylation of ELK at a critical tyrosine residue. Eph family receptors are implicated in various physiological processes, including cell migration, axon guidance and vascular development (Kullander and Klein, 2002). The Grb10 SH2 domain was also yielded when the Ret tyrosine kinase receptor was used as bait in a yeast two-hybrid assay (Pandey *et al*, 1995), an interaction confirmed *in vitro* and also apparent for Grb7/Ret (Pandey *et al*, 1996). This receptor plays a key role in the development of endocrine organs and the enteric nervous system.

Already mentioned briefly to illustrate the properties of the SH2 domain, the association of Grb10 with c-Abl (Frantz *et al*, 1997) is notable because of its relevance to oncogenesis. Bcr-Abl is an oncoprotein generated by the fusion of part of the Bcr serine/threonine kinase to the tyrosine kinase Abl, encoded by *c-Abl*. This occurs because of the juxtaposition of the breakpoint cluster region on human chromosome 22, at which Bcr is located, to the *c-Abl* gene on chromosome 9 (Chan *et al*, 1987). Bcr-Abl proteins vary in their properties, depending on how much of Bcr is fused to Abl, and typically activate the PI 3-kinase, MAP kinase and STAT signalling cascades. Bcr-Abl isoforms have been implicated in chronic myelogenous leukaemia (CML) and acute lymphoblastic leukaemia (ALL) (reviewed in Advani and Pendergast, 2002).

Grb10 has been implicated in antigen receptor signalling in lymphocytes, by its association with Tec, an interaction again established by yeast two-hybrid experiments (Mano *et al*, 1998). Tec is a non-receptor tyrosine kinase. Although over-expression of *Grb10* does not inhibit the kinase activity of the enzyme, downstream effector activation is inhibited. This was demonstrated by a down-regulation of expression of a luciferase reporter gene driven by the *c-fos* promoter, a classic target of antigen receptor activation.

An interaction between GRB10 and the growth hormone receptor (GHR) has also been demonstrated *in vitro*, mediated by the SH2 domain (Moutoussamy *et al*, 1998). Ligand-induced receptor activation promotes the recruitment and autophosphorylation of Janus kinase 2 (JAK2), which subsequently phosphorylates the GHR cytoplasmic domain. SH2-domain containing proteins, such as Signal transducer and activator of transcription (STAT) family members, are recruited to the receptor and activated. GRB10 physically interacts with JAK2 (Moutossamy *et al*, 1998), and although over-expression of GRB10 had no effect on the phosphorylation of JAK2, GHR or STAT5, it inhibited the transcription of reporter genes containing GH response elements. These data implicate GRB10 in the negative regulation of GH signalling.

In conclusion, Grb10/GRB10 has been shown to potentially associate with a considerable number of cellular signalling molecules, both receptors and non-receptors, and by extrapolation has been implicated in several physiological processes. Whilst some interactions have only been demonstrated by biochemical means (e.g. EGFR), and thus their relevance to physiological conditions questionable, others have been shown *in vitro* (e.g. GHR) and even *in vivo* (e.g. IR). This is also true for the other members of the Grb7 superfamily, and thus these molecules are highly likely candidates for regulating cross-talk between various signalling cascades (Riedel, 2004).

1.2.3 *Grb10* as an imprinted gene

Although Grb10 was cloned in 1995 (Ooi *et al*, 1995), the imprinted nature of the *Grb10* gene was not revealed until 1998 (Miyoshi *et al*, 1998), using a subtractive hybridisation approach to identify novel maternally-expressed genes. Its potential as a candidate for SRS was recognised immediately, and supported two years later by the identification of sequence mutations in the *GRB10* genes of two SRS patients (Yoshihashi *et al*, 2000). The same study confirmed that human *GRB10* was also imprinted, a result previously predicted by the observation of early DNA replication at the locus, a hallmark of imprinted genes (Monk *et al*, 2000). In the same year, Blagitko *et al* (2000) demonstrated that *GRB10* expression in the human foetal brain was specifically from the paternally-inherited copy, whilst peripheral tissues typically demonstrated biallelic expression, with maternal-specific expression in skeletal muscle. The finding of paternally-derived transcripts in the brain was reported as being reciprocal to that found in mouse, but Arnaud *et al* (2003) revealed the conservation of paternal-specific expression in the mouse brain. This study, followed up by Sanz *et al* (2008), characterised tissue- and allele-specific transcripts in considerable detail (Figure 1.2).

The regulation of murine *Grb10* imprinting was elucidated by Arnaud *et al* (2003), Hikichi *et al* (2003) and Sanz *et al* (2008). The promoter region of the gene possesses three CpG islands (Figure 1.2). CpG island 1 (CGI1) is hypomethylated on both alleles in all tissues and stages investigated, including oocytes and sperm, and thus is not a DMR, despite overlapping with the transcription initiation exon for maternally-derived transcripts (exon 1A). Instead, the silencing of the paternal allele in most tissues is achieved by a germline

DMR (CGI2) situated 3' to exon 1A, which is hypermethylated on the maternal chromosome. This is, therefore, an example of hypermethylation being permissive for transcription. Brain-specific transcripts initiate from exons 1B1, 1B2 and 1C, and are under the control of a tissue-specific (somatic) DMR, forming part of CGI3. In peripheral tissues, CGI3 is biallelically hypermethylated, but is hypomethylated on the paternal allele specifically in brain. Although not illustrated in Figure 1.2, differential promoter usage is associated with specific histone tail modifications. Methylation of lysine 27 on histone H3 (H3K27me3) is considered a repressive mark, as it is typically associated with transcriptionally inactive chromatin. This mark was enriched on the unmethylated paternal allele at the germline DMR (CGI2), but this was dissociated in brain (Sanz *et al*, 2008), and is therefore likely to form part of the mechanism for controlling the promoter switch. What is responsible for the initiation of such tissue-specific epigenetic marks remains unsolved.

The first knockout of murine *Grb10* was reported by Charalambous *et al* (2003), in which transcripts were trapped by the integration of a *LacZ* reporter cassette, such that reporter expression was under the control of the endogenous *Grb10* promoter. The allele was termed *Grb10Δ2-4*. This permitted further characterisation of the imprinted nature of the gene, and confirmed that the majority of embryonic and adult expression was derived from the maternally-inherited chromosome. In agreement with Arnaud *et al* (2003), the adult hypothalamus expressed the *LacZ* reporter only when the trapped allele was transmitted through the paternal line (Smith *et al*, 2007). Intriguingly, no reporter expression was detected in the foetal brain, regardless of parental origin, except in the fourth ventricle and choroid plexus, in which *Grb10* was maternally-expressed (Charalambous *et al*, 2003). Immunostaining suggested a more widespread presence of Grb10 protein in the developing brain. To address this shortcoming, Garfield *et al* (submitted) utilised a second transgenic mouse line, containing a *LacZ* reporter cassette integrated more 3' at the *Grb10* locus, termed *Grb10KO*. Inheritance of this trapped allele through the maternal line (*Grb10KO*$^{m/+}$) recapitulated the sites of expression reported by *Grb10Δ2-4*$^{m/+}$. However, extensive expression of *Grb10* in the developing CNS was observed following paternal transmission of the gene trap (*Grb10KO*$^{+/p}$). As discussed previously, the two knockout models also permitted characterisation of the parent-of-origin specific *in vivo* roles for Grb10: maternal expression was fundamental for the regulation of foetal growth and adult metabolism, whilst expression from the paternal allele tempered social behaviour.

1.2.4 Concluding remarks and aims

Despite the wealth of information regarding signalling partners of Grb10, and the characterisation of its roles in foetal growth, postnatal metabolism and adult behaviour, many intriguing questions remain, related both to its *in vivo* function and the control of its imprint. For example, whilst its influence on postnatal metabolism is achieved through the modulation of insulin signalling, it is still not clear through which genetic pathways *Grb10* controls foetal development. Genetic evidence argues strongly against the IGF1 and IGF2 signalling pathways (Charalambous *et al*, 2003; Garfield, 2007). The observation that the paternally-expressed imprinted gene *Dlk1* maps to many of the sites of *Grb10* expression,

and that *Dlk1*-deficient mice exhibit opposite growth effects to *Grb10*-deficient animals, is provocative, and may represent the predominant pathway through which *Grb10* influences growth. An investigation of this potential relationship is currently under way.

Additionally, it is not currently possible to discriminate between the direct influence of *Grb10* on foetal growth, and its indirect influence through effects on the placenta. Is disproportionate placental overgrowth a response to foetal overgrowth, or does an improvement in placental efficiency drive foetal development?

Before the present study was conducted, another pressing issue which required attention was the apparent inability of the *Grb10Δ2-4* allele, when transmitted through the paternal line (*Grb10Δ2-4*$^{+/p}$), to report expression in the developing CNS, in the light of strong reporter expression in this tissue from the paternal *Grb10KO* allele. Indeed, limited characterisation of the *Grb10KO* allele had been performed, and thus it was difficult to speculate on the molecular basis for these differences.

With these points in mind, the current study began with three key aims:

1) to characterise the structure of the *Grb10KO* allele, and perform a molecular demonstration of its efficacy in trapping *Grb10* transcripts;
2) to use this knowledge to address the molecular basis for differences in the reporter expression profiles of the two transgenic models;
3) to expand on existing work demonstrating the influence of *Grb10* on placental development and foetal growth, by characterising the expression profile of *Grb10* in the placenta and the morphological consequences of *Grb10* ablation.

Unexpectedly, the genetic characterisation of the *Grb10KO* allele, and the elucidation of the molecular basis for differences in reporter expression, led to the identification of a previously unidentified site of *Grb10* expression in the adult; namely, the mammary epithelium. We characterised the imprinting status and function of *Grb10* in this tissue, and defined a novel role for maternally-expressed *Grb10* in regulating nutrient transfer from mother to suckling offspring. This extended our previous understanding of the role of *Grb10* as a growth regulator. When viewed in light of the role of *Grb10* in the placenta, which controls nutrient transfer *in utero*, we were able to comment on a more general role for *Grb10* in the control of reproductive strategy.

Chapter Two

Materials and Methods

2.1 Transgenic mouse lines

2.1.1 Animal husbandry

All mouse strains were maintained in accordance with United Kingdom Home Office regulations, on a 13-hour light/11-hour dark cycle, including 30 minutes each of artificial dawn and dusk lighting. Ambient temperature was maintained at 21°C ± 2°C, with a relative humidity of 55 ± 10 %. Animals were permitted unrestricted access to food (CRM formula, Special Diets Services, Essex, UK) and water, and were housed at a density of one to six animals per cage. Cages were individually ventilated.

2.1.2 Transgenic mouse strains

All transgenic strains were maintained on a C57BL/6:CBA mixed background. The *Grb10KO* strain was generated from aggregation chimeras made by Dr Kim Moorwood and Dr Joanne Stewart-Cox, from the XC302 embryonic stem (ES) cell gene trap line (Baygenomics, CA, USA; Garfield *et al*, submitted). The *Grb10Δ2-4* strain was created by Dr William Bennett, using the KST268 ES cell gene trap line (Baygenomics) in an ES cell co-culture method, as previously described (Charalambous *et al*, 2003).

2.1.3 Genotyping of transgenic animals

Genotyping of transgenic stock animals was performed using DNA samples in the polymerase chain reaction (PCR). Ear clips (from adult) or tail clips (from embryo) were boiled for 10 minutes in 600 µl 0.1 M sodium hydroxide (Fisher Scientific, UK), and neutralised with 50 µl 1 M Tris-HCl pH 8.0 (Tris and HCl both from Fisher Scientific). 1 µl (adult ear clip) or 2 µl (embryonic tail clip) of each boiled sample was used as the template in the PCR reaction. DNA from adult ear clips was amplified in a total volume of 20 µl using GoTaq Master Mix (Promega, UK) diluted 1:2, with primers at a final concentration of 0.25 µM each (purchased from Invitrogen, UK; Table 2.1). Embryonic tail DNA was amplified in a total volume of 25 µl using *Kod* Hot-Start DNA Polymerase (Novagen, Germany), according to the manufacturer's instructions. Amplification for all samples was performed on a G-Storm Mark 1 thermal cycler (Gene Technologies Ltd., UK), using the following conditions: initial denaturation for 5 minutes at 95°C, followed by 34 cycles of 60 seconds at 95°C, 60 seconds at 60°C, 60 seconds at 72°C, and a final extension of 72°C for 5 minutes. Following amplification, samples were loaded and run on a 1 % (w/v) agarose (Invitrogen) gel containing 0.5 µg/ml ethidium bromide (Sigma Aldrich, Dorset, UK) in 1x TAE buffer (2 M Tris (Fisher Scientific), 50 mM EDTA (Sigma Aldrich), 5.7 % (v/v) acetic acid (Fisher Scientific)). A 1 kb DNA ladder (Promega) was used for size estimation. DNA was visualised under ultraviolet radiation (AlphaImager 3400).

DNA from e7.5 embryos was obtained by boiling whole embryos in 100 µl 0.1 M sodium hydroxide for 10 minutes. Genotyping was performed by PCR as described for adult ear clips.

Table 2.1 – Sequences of primers used in PCR amplification

Nucleotide sequences are presented for primers used for the purposes of genotyping, mapping of the *LacZ* gene trap cassette, and RT-PCR/qPCR. [1]from Charalambous *et al*, 2003; [2]from Charalambous *et al*, submitted; [3]from Zhu *et al*, 2006. *fwd* – forward; *rev* – reverse.

Application	Template	Primer name	Primer sequence (5' to 3')

2.2 Molecular techniques

All solutions were made according to Sambrook and Russell (2001) with purified and deionised water, prepared with the MilliQ water filtration system (Millipore Corporation, MA, USA), unless otherwise stated.

2.2.1 Genomic DNA isolation from tissue samples

Although DNA for genotyping purposes was isolated from tissue biopsies as described in Section 2.1.3, cleaner DNA preparations were required for other PCR amplification experiments. 500 mg tissue samples were incubated overnight at 55°C in 560 µl digestion buffer (50 mM Tris pH 8.0, 100 mM EDTA, 100 mM NaCl (Fisher Scientific), 1 % sodium dodecyl sulphate (SDS; Fisher Scientific), 350 µg Proteinase K (Sigma Aldrich)). RNA was degraded by the addition of 0.4 µg RNase A (Sigma Aldrich) at 37°C for 1 hour. DNA was precipitated with the addition of NaCl to a final concentration of 1.3 M, followed by an equal volume of chloroform:isoamyl alcohol (24:1; both reagents from Fisher Scientific), and centrifuged at 12,000 x *g* for 10 minutes in a Sorvall Biofuge Pico microcentrifuge. One volume of propan-2-ol (Sigma Aldrich) was added to the aqueous phase and the DNA pelleted by centrifuging as before. The pellet was washed in 70 % ethanol (Fisher Scientific) at 4°C for at least 1 hour and dissolved in an appropriate volume of Tris-EDTA buffer (10 mM Tris pH 8.0, 1 mM EDTA). DNA preparations were stored at -20°C.

2.2.2 RNA isolation from tissue samples

Organs, whole embryos or tissue biopsies were isolated and snap-frozen in liquid Nitrogen (refer to Section 2.4.1 for details on tissue isolation). RNA was purified from frozen samples using TRI reagent (Sigma Aldrich), essentially following the manufacturer's instructions. Briefly, 50-100 mg tissue was homogenised thoroughly in 1 ml ice-cold TRI reagent using a T8.01 homogeniser (GMBH and Co., Germany). After centrifugation at 12,000 x *g* for 10 minutes in a microcentrifuge, the supernatant was transferred to a fresh 1.5 ml microcentrifuge tube (Eppendorf). After adjusting to room temperature for 5 minutes, 0.2 ml chloroform was added and samples were mixed by shaking vigorously for 15 seconds. After standing at room temperature for 15 minutes, samples were centrifuged at 12,000 x *g* for 15 minutes at 4°C. 0.5 ml propan-2-ol was mixed with the aqueous phase and allowed to stand at room temperature for 5-10 minutes. Following centrifugation as before, RNA pellets were washed in 1 ml ice-cold 75 % ethanol and air-dried. RNA was resuspended in 50-200 µl DEPC-treated deionised water (DEPC from Sigma Aldrich) by repeated pipetting of samples warmed to 55°C. Samples for cDNA synthesis were further treated with DNase I, using DNA-*free* (Ambion, TX, USA) as described in the product literature. RNA samples were used immediately or stored at -80°C.

2.2.3 cDNA synthesis

For semi-quantitative reverse transcription PCR (RT-PCR) and amplification of probes for Northern blotting, 1 µg DNase I-treated RNA was heated to 65°C for 5 minutes in a G-Storm Mark 1 thermal cycler in a total volume of 13 µl, with 1 mM dNTP mix (Invitrogen) and 5 µM oligo-dT_{20} (Invitrogen). For quantitative RT-PCR (qPCR), 2 µg DNase I-treated RNA was used in the same reaction. The thermal cycler was paused and samples incubated on ice for 1 minute. The SuperScript III reverse transcriptase system (Invitrogen) was used to synthesise cDNA, following the manufacturer's recommended protocol. A control reaction was also set up, from which the reverse transcriptase enzyme was omitted, permitting accurate interpretation of subsequent PCR amplification.

2.2.4 Semi-quantitative reverse transcription PCR (RT-PCR) on adult brain cDNA

cDNA was synthesised from brain homogenates from wild type, *Grb10Δ2-4*$^{m/+}$ and *Grb10Δ2-4*$^{+/p}$ adult males, as described in Section 2.2.3. 1 µl cDNA from each sample was amplified for 26 cycles using PCR conditions described previously (Section 2.1.3); primers amplified *Grb10* exons 11-16 and β-*actin* (see Table 2.1 for primer sequences). Amplicons were visualised by gel electrophoresis, as described before (Section 2.1.3).

2.2.5 Quantitative real-time PCR (qPCR) analysis

Quantitative real-time PCR with SYBR green was performed with SensiMix (Quantace, UK), according to the manufacturer's instructions. For qPCR on e17.5 placentae, primers were used to amplify *Grb10* exons 3-4, *Grb10* exons 11-16, total *Igf2*, *Igf2P0*, *Slc38a4* and the house-keeping gene *Hprt* (refer to Table 2.1 for primer sequences). The relative standard curve method was employed for quantification (Pfaffl, 2001). Gene expression was normalised to that of *Hprt*, the expression of which did not significantly differ between the datasets (data not shown; Charalambous *et al*, submitted).

The same technique was employed to analyse gene expression in adult pituitary glands, using primers for *Prolactin*, *Growth hormone* and β-*actin* (Table 2.1). Target gene expression was normalised to β-*actin* transcript levels.

For both analyses, the mean of each dataset was compared using the Kruskal-Wallis test, with Dunn's multiple comparison test to compare each group to the relevant control dataset.

qPCR analysis was performed by Dr Marika Charalambous (Department of Physiology, Development and Neuroscience, University of Cambridge).

2.2.6 PCR amplification and cloning of probes for Southern and Northern blotting

Probes for Southern blotting and the DNase I hypersensitivity assay were amplified by PCR from 295 ng genomic DNA, isolated from a wild type adult mouse liver sample as described in Section 2.2.1. Table 2.2 details the primers utilised for the amplification of each probe. Products were amplified using GoTaq Master Mix and PCR conditions described previously (Section 2.1.3).

Probes for Northern blotting were amplified, using the same conditions, from cDNA synthesised from whole wild type e14.5 embryo RNA. Primer sequences are detailed in Table 2.2.

PCR amplicons were purified from 1 % agarose gels using the Wizard SV Gel and PCR Purification Kit (Promega), following the protocol described in the product literature. The pGEM-T Easy vector system (Promega) was used to clone the *Taq*-amplified products, exploiting the single base pair 'A'-tail overhangs generated in the PCR. Ligation reactions contained insert:vector in a 1:1 to 5:1 ratio, 2 x Rapid Ligation Buffer (Promega) and 3 U T4 DNA ligase (Promega), in a 10 µl total volume. Reactions were incubated at 4°C overnight.

Competent *Escherichia coli* DH5α cells were prepared by Dr Masataka Nikaido (University of Bath). A fresh single colony of cells growing on Luria agar (Sigma Aldrich) was picked into 50 ml sterilised SOB medium (2 % (w/v) bactotryptone (BD Biosciences, NJ, USA), 0.5 % (w/v) yeast extract (Oxoid Ltd., Hampshire, UK), 10 mM NaCl, 2.5 mM KCl (Sigma Aldrich), 20 mM Mg^{2+} (Sigma Aldrich)) in a 500 ml conical flask, and shaken at ~250 rpm at 18-25°C. When OD_{600} was between 0.4 and 0.6, cultures were placed on ice for 10 minutes, and cells pelleted by centrifugation at 3000 rpm in a Beckman Coulter Allegra 25R benchtop centrifuge for 10 minutes, at 4°C. Cells were resuspended in 1/3 volume of ice-cold TB medium (10 mM PIPES (Sigma Aldrich), 15 mM $CaCl_2.2H_2O$ (Sigma Aldrich), 250 mM KCl, 55 mM $MnCl_2.4H_2O$ (Sigma Aldrich), pH 6.7) and incubated on ice for 10 minutes. Cells were pelleted as before and resuspended in 4 ml ice-cold TB medium. DMSO (Sigma Aldrich) was added to a final concentration of 7 %, mixed and cells placed on ice for 10 minutes. Cells were snap-frozen in liquid Nitrogen and stored at -80°C. Competency was quantified with known amounts of pBlueScript KS+ vector (Stratagene, CA, USA) and was typically ~10^8 colony forming units (cfu)/µg vector.

Plasmid DNA was purified from the salts of the ligation reaction mix by microdialysis, using 0.025 µm membrane filters (Millipore) floating on deionised water for 30 minutes. Competent cells were incubated with all of the plasmid DNA from the ligation reaction on ice in a pre-chilled 14 ml Falcon tube for 30 minutes. Cells were heat-shocked for 90 seconds at 42°C and chilled on ice for 2 minutes, permitting plasmid uptake. 1 ml pre-warmed Luria Broth (LB) medium (made as directed from LB powder, Sigma Aldrich) was added to the cells, which were allowed to express β-*lactamase*, the enzyme responsible for the degradation of carbenicillin, in the absence of antibiotics, by incubating at 37°C for 1 hour, shaking at 200 rpm (Innova 4230 incubator, New Brunswick Scientific, NJ, USA). 200 µl of cells were plated onto a Luria agar plate, containing 150 µl 100 mg/ml carbenicillin (Bioline, UK), 240 µl 20 mg/ml isopropyl-β-D-thiogalactopyranoside (IPTG; Sigma Aldrich)

Table 2.2 – Southern and Northern hybridisation probes

Primers used for the amplification of probes for Southern and Northern hybridisation, including the DNase I hypersensitivity assay, are presented. [1]from Charalambous *et al*, 2003; [2]from Menheniott *et al*, 2008. *fwd* – forward; *rev* – reverse.

Probe	Amplification template	Primer sequence (5' to 3')

and 300 µl 40 mg/ml 5-bromo-4-chloro-3-indolyl-β-D-galactopyranoside (X-gal; Fermentas, Canada) per 300 ml. Overnight incubation at 37°C was sufficient to visualise colony growth and permit blue/white selection.

White colonies, indicating disruption of the *LacZ* gene on the pGEM-T Easy vector with the PCR amplicon, were picked into 4 ml LB plus 2 µl 100 mg/ml carbenicillin, and propagated overnight at 37°C in a shaking incubator (200 rpm). Cells from 2 ml of each culture were pelleted at 3000 x *g* for 10 minutes, and the plasmid DNA was purified using the Wizard Plus SV miniprep kit (Promega).

Clones were initially screened by appropriate restriction digestion strategies, and then sequenced (MWG Biotech, Germany) using the T7 Promoter primer. A single clone for each probe was propagated in 150 ml LB plus carbenicillin overnight, shaking at 200 rpm, and a large-scale plasmid purification performed using the GenElute HP plasmid maxiprep kit (Sigma Aldrich), according to the manufacturer's guidelines. Final preparations were quantified using a spectrophotometer (Eppendorf BioPhotometer) and stored at 4°C.

Probe fragments were excised from the vector using appropriate restriction digestion. Enzymes and associated digestion buffers were supplied by Promega, and reactions were performed in line with the recommended protocol.

2.2.7 PCR amplification for gene-trap cassette mapping

PCR was performed as described in Section 2.1.3 on 295 ng genomic DNA, isolated from an adult liver biopsy or total e14.5 embryo. Primer sequences are provided in Table 2.1. Amplicons were separated by gel electrophoresis, purified, cloned into pGEM-T Easy and sequenced, as described above. Subsequent genotyping was performed using a subset of the mapping primers (Table 2.1) in PCR.

2.2.8 Southern and Northern blotting

To map the position of the β-*geo* cassette in the *Grb10KO* allele, genomic DNA was purified from liver samples of adult wild type and *Grb10KO*$^{+/p}$ animals, and from a rare *Grb10KO*$^{m/p}$ embryo isolated at e14.5, as described in Section 2.2.1. 12 µg genomic DNA was digested overnight at 37°C with 60 U *Pst*I or *Bam*HI (Promega) in a total volume of 50 µl. Samples were diluted in 6x DNA loading buffer (Promega) and run on a 1 % agarose gel in 1x TAE buffer containing 0.5 µg/ml ethidium bromide, at 25 V for 18 hours.

1 % agarose gels for the separation of RNA for Northern blotting were made in a 6 % formaldehyde (Sigma Aldrich) and 1 x MOPS buffer (20 mM MOPS (Sigma Aldrich), 10 mM sodium acetate (Sigma Aldrich), 1 mM EDTA, pH 7.0), using DEPC-treated distilled water. RNA was purified from homogenised tissue samples as described in Section 2.2.2 and 20-50 µg was diluted in 2x loading buffer (Fermentas). RNA was denatured by heating at 70°C for 10 minutes and loaded onto agarose gels. Electrophoresis was performed in a 1 x MOPS

running buffer for 5-6 hours. All electrophoresis components were cleaned prior to use with 3 % hydrogen peroxide (Sigma Aldrich) and rinsed with DEPC-treated distilled water, to reduce RNase activity.

After electrophoresis, DNA gels were denatured by washing in 1 M NaCl, 0.5 M NaOH for 30 minutes at room temperature, followed by two washes in 1.5 M NaCl, 50 mM Tris, 1 mM EDTA for 15 minutes to neutralise. Nucleic acid (RNA or DNA) was transferred to nitrocellulose membrane (Gene Technologies Ltd.) by capillary blotting for at least 16 hours, using 20x SSC (3 M NaCl, 0.3 M sodium citrate (Sigma Aldrich)) as a buffer. For Northern blotting, transfer equipment was cleaned prior to use as described for electrophoresis. Nucleic acid was cross-linked onto membranes using ultraviolet radiation in a CL-1000 UVP cross-linker at 24000 µJ/cm^2.

Membranes were pre-hybridised in 15 ml Church buffer (50 % (v/v) phosphate buffer (0.95 M Na_2HPO_4 (Fisher Scientific), 0.8 % phosphoric acid (BDH, UK), pH 8.0), 1 mM EDTA, 7 % (w/v) SDS, 1 % (w/v) bovine serum albumin (BSA; Sigma Aldrich)) plus 150 µl sonicated salmon sperm DNA (Sigma Aldrich). Pre-hybridisation was performed in rotating hybridisation bottles overnight at 63.8°C in a Hybaid hybridisation oven. 25 ng of the relevant DNA probe was denatured by boiling for 2 minutes in a total volume of 13 µl. A 5x pre-mixed labelling solution (High Prime, Roche, IN, USA) was added to the sample on ice. 3 µl α^{32}P-dCTP (Perkin Elmer, MA, USA), with an activity of at least 5 µCi/µl, was added to the reaction mix and subsequently incubated at 37°C for 20 minutes.

The reaction mix volume was made up to 100 µl with TE, and labelled probe fragments were purified from unincorporated nucleotides by centrifugation through a Sephadex-G50 column (1200 x *g* for 2 minutes; Sephadex G-50 from Sigma Aldrich). A further 100 µl TE was added to the column and centrifuged again to elute probe fragments. The Klenow enzyme was denatured by the addition of NaOH to a final concentration of 330 mM, incubated for 5 minutes at room temperature, and the mix then neutralised with Tris HCl pH 7.5 to a final concentration of 457 mM. The labelled probe fragments were hybridised with nucleic acid on the relevant membranes overnight at 65°C in the existing Church buffer and salmon sperm DNA solution.

Membranes were washed twice in wash solution 1 (4 % (v/v) phosphate buffer, 5 % (w/v) SDS, 0.5 % (w/v) BSA, 1 mM EDTA) for 15 minutes each, and twice in wash solution 2 (4 % (v/v) phosphate buffer, 1 % (w/v) SDS, 1 mM EDTA) for at least 1 hour each, to remove unbound or loosely associated probe fragments. Membranes were wrapped in clingfilm and exposed to imaging film (GE Healthcare) for up to two weeks at -80°C. Development was performed using an Optimax film processor (GmbH and Co.).

2.2.9 DNase I hypersensitivity assay

Whole brain and liver tissues were dissected from adult wild type male mice and rinsed briefly in 0.1 % phosphate buffered saline (PBS; Oxoid Ltd.). Tissues were individually homogenised in 10 ml ice-cold buffer I (0.3 M sucrose (Sigma Aldrich), 60 mM KCl, 15 mM

NaCl, 5 mM $MgCl_2$ (Sigma Aldrich), 0.1 M EGTA (Sigma Aldrich), 15 mM Tris-HCl pH 7.5, 0.5 mM DTT (Sigma Aldrich), 0.1 mM PMSF (Sigma Aldrich), fresh aprotinin (Sigma Aldrich) to 3.6 ng/ml) using a homogeniser. The resulting homogenates were filtered through four layers of muslin cloth pre-moistened with 2 ml buffer I. Cells were pelleted at 6000 x *g* for 20 minutes in a refrigerated centrifuge (Beckman Coulter Allegra 25R) and re-suspended in 2 ml ice-cold buffer I, pooling the nuclei isolated from each tissue type. Cells were lysed with the addition of an equal volume of ice-cold buffer II (as buffer I, plus 0.4 % (v/v) Igepal CA-630 (Sigma Aldrich)) and incubated on ice for 5 minutes. Lysed cell suspensions were layered onto 8 ml sucrose cushions (1.2 M sucrose, 60 mM KCl, 15 mM NaCl, 5 mM $MgCl_2$, 0.1 M EGTA, 15 mM Tris HCl pH 7.5, 0.5 mM DTT, 0.1 mM PMSF, fresh aprotinin to 3.6 ng/ml) in 14 ml glass centrifuge tubes and centrifuged at 10000 x *g* for 20 minutes at 4°C. Pelleted nuclei were resuspended in 2 ml ice-cold DNase I digestion buffer (as buffer I, without aprotinin or PMSF). 200 µl of each suspension was digested with 0, 120 or 200 U DNase I (Roche) for 20 minutes in a water bath at 25°C. Reactions were terminated with the addition of an equal volume of 20 mM EDTA pH 8.0, 1 % (w/v) SDS. DNase I and DNA-associated proteins were digested at 50°C overnight with proteinase K at a final concentration of 200 µg/ml, previously diluted to 20 mg/ml in TE buffer (10 mM Tris HCl pH 7.5, 1 mM EDTA) and incubated at 37°C for 15 minutes to activate. DNA was extracted twice with phenol:chloroform:isoamyl alcohol (25:24:1); DNA exposed to 0 U DNase I was too viscous to be extracted initially, and was thus sheared first by passing through a 30 gauge syringe needle 3 times. A final extraction with chloroform:isoamyl alcohol was then performed for all samples. DNA was precipitated with the addition of 1/20 volume of 5 M NaCl and one volume of propan-2-ol. After a 5 minute incubation at room temperature, DNA was pelleted by centrifugation at 12000 x *g* for 20 minutes, rinsed in 70 % ethanol, air-dried and resuspended in 50 µl TE buffer.

Purified DNA was quantified and digested at 37°C overnight with an excess of *Bam*HI, according to the manufacturer's guidelines (Promega). Digested DNA was precipitated with an equal volume of propan-2-ol, rinsed in 70 % ethanol, air-dried and dissolved in 50 µl TE buffer. DNA suspensions were quantified as before and 10 µg of each sample mixed with 6x gel loading buffer (Promega) and loaded on a 1 % agarose gel. Samples were electrophoresed overnight at 15 V and transferred to nitrocellulose membrane by capillary blotting, as described for Southern blotting (Section 2.2.8). The blot was challenged with a radiolabelled probe (probe C; Table 2.2) by Southern hybridisation.

2.2.10 Western blotting

Whole e14.5 placentae were homogenised in 1 ml Igepal CA-630 lysis buffer (50 mM Tris HCl pH 8.0, 150 mM NaCl, 1 % (v/v) Igepal CA-630, plus one Roche protease inhibitor cocktail tablet per 10 ml buffer). Samples were incubated on ice for 30 minutes to permit cell lysis and passed through a 21 gauge needle 5 times. Suspensions were centrifuged at 12000 x *g* for 10 minutes at 4°C to pellet cell debris and supernatants further centrifuged at 100000 x *g* for 15 minutes (Beckman TL-100 ultracentrifuge) at 4°C. Total protein

concentration was determined using the BCA protein assay kit (Pierce, IL, USA), and samples stored at -20°C.

20 µg of each sample was mixed with 2x reducing sample buffer (250 mM Tris HCl pH 6.8, 2 % (w/v) SDS, 10 % (v/v) glycerol (Sigma Aldrich), 10 % (v/v) β-mercaptoethanol (Sigma Aldrich), 0.02% (w/v) bromophenol blue (Sigma Aldrich)) and heated to 95°C for 5 minutes. Samples were loaded onto a polyacrylamide gel (resolving gel: 8 % polyacrylamide (National Diagnostics, GA, USA), 0.37 M Tris HCl pH 8.8, 0.1 % SDS, 0.05 % AMPS (Sigma Aldrich), 0.05 % TEMED (ICN Biomedicals Inc., OH, USA); stacking gel: 5 % polyacrylamide, 0.12 M Tris HCl pH 6.8, 0.05 % AMPS, 0.1 % TEMED) alongside pre-stained protein standards (Bio-Rad Laboratories, UK), and run at 100 V for 90 minutes in running buffer (0.1 % SDS, 25 mM Tris, 208 mM glycine (Fluka, Sigma Aldrich)). Protein was transferred onto PVDF membrane (Bio-Rad Laboratories) by wet transfer (25 mM Tris, 192 mM glycine, 20 % (v/v) methanol (Fisher Scientific)). All subsequent incubations were performed on an orbital shaker. The membrane was blocked in 5 % powdered skimmed milk (Tesco, UK), 0.1 % Tween-20 (Sigma Aldrich) in 0.1 % PBS for 2 hours at room temperature. Primary antibodies were diluted in 1 % milk in PBS-T (0.1 % Tween-20, 0.1 % PBS; see Table 2.3 for antibody concentrations used) and applied to the appropriate membranes. Overnight incubation was permitted at 4°C. Membranes were washed three times in 0.1 % PBS-T for 15 minutes per wash, and incubated in peroxidase-conjugated goat anti-rabbit secondary antibody (Vector Laboratories, CA, USA) diluted 1/10000 in 1 % milk in PBS-T for 1 hour at room temperature. Three further washes were performed as before and protein detection was achieved using the ECL-Plus system (GE Healthcare), as directed by the manufacturer. Autoradiography film (GE Healthcare) was developed using an X-ray processor.

Table 2.3 – Primary antibodies utilised for Western blotting and immunohistochemistry

Species indicates the animal in which the antibody was raised. *IHC* – immuno-histochemistry.

Antigen	Species	Application	Concentration	Manufacturer

2.3 *In vitro* techniques

2.3.1 Luciferase assay constructs

pRSV-puroSTAT5B1*6 (Onishi *et al*, 1998) was kindly donated by Dr Fabrice Gouilleux (University of Picardie-Jules Verne, France) with the permission of Dr Toshio Kitamura (University of Tokyo, Japan). pRL-SV40, encoding *Renilla* luciferase, was a gift from Emily Jane-Myatt and Dr David Tosh (University of Bath). Donated plasmids were transformed into competent *E. coli* DH5α cells, as described in Section 2.2.6.

The 799 bp genomic region, incorporating *cis*-regulatory module 1 (CRM1), previously amplified to generate the probe for DNase I hypersensitivity analysis, was excised from pGEM-T Easy using the *Sac*II and *Spe*I restriction enzymes, and sub-cloned into these sites in the pBlueScript KS+ vector. The genomic region was subsequently cloned into the pGL3-Promoter vector (Promega) using *Kpn*I and *Sac*I to generate pGL3-Pro-CRM1, and the integrity of the sequence confirmed by nucleotide sequencing (MWG Biotech, Germany).

Large scale plasmid purifications were performed for all constructs, including pGL3-Promoter alone, as previously described (Section 2.2.6).

2.3.2 Cell maintenance

A frozen aliquot of NIH/3T3 mouse fibroblast cells was kindly donated by Kathy O'Neill and Dr David Tosh (University of Bath). Cells were rapidly thawed and maintained in Dulbecco's modified Eagle's medium (DMEM; Gibco, Invitrogen) plus 10 % (v/v) newborn calf serum (Gibco, Invitrogen), 1 % (v/v) penicillin/streptomycin (Gibco, Invitrogen) and 1 % (v/v) L-glutamine (Gibco, Invitrogen), herein referred to as complete media. Cells were incubated at 37°C in 5 % CO_2 and were maintained in 75 cm^2 flasks (Greiner Bio-One, Belgium). Complete media was changed as required. At around 70 % confluency, cultures were passaged by washing briefly in 0.1 % PBS and detached from the flask with a 5 minute incubation at 37°C with 1 ml 0.05 % trypsin/EDTA (Gibco, Invitrogen) per 25 cm^2. Trypsin/EDTA was neutralised with an equal volume of complete media and transferred to a 15 ml centrifuge tube (Falcon). Cells were pelleted at 180 x *g* for 4 minutes (MSE Mistral 1000 centrifuge) and resuspended in 1 ml complete media, before distributing into fresh flasks. Typically, cultures were split 1/20 every 4-5 days.

2.3.3 Cell transfection

Near-confluent flasks of NIH/3T3 cells were trypsinised as described before, and cells counted by use of a haemocytometer slide. 100000 cells were seeded into each well of four 6-well plates, each well containing 3 ml complete media. The complete media was refreshed the following day. 48 hours after seeding, cells were ~60 % confluent, and

complete media was replaced with DMEM plus 1 % newborn calf serum and 1 % L-glutamine. Cells were incubated at 37°C, 5 % CO_2 in this antibiotic-free media for 4.5 hours.

DNA mixes to be transfected were prepared in separate sterile microcentrifuge tubes, as shown in Table 2.4. Each sample was incubated with 250 µl Optimem medium (Gibco, Invitrogen) for 5 minutes at room temperature. Simultaneously, 10 µl Lipofectamine 2000 (Invitrogen) was incubated with 250 µl Optimem medium at room temperature for 5 minutes, for every replicate. The DNA and Lipofectamine 2000 mixes were pooled and incubated for at least 30 minutes at room temperature. Transfection mixes were added to the appropriate well containing NIH/3T3 cells in antibiotic-free media, mixed gently and incubated for 4.5 hours at 37°C, 5 % CO_2. Media was replaced with complete media, including antibiotics, and cells were left to grow and express recombinant proteins for 48 hours before performing the luciferase assay.

2.3.4 Luciferase assay

The Dual-Luciferase Reporter Assay System (Promega) was used to quantify luciferase activity, and was performed according to the manufacturer's instructions. The passive cell lysis method, rather than active lysis by scraping, was used to liberate cellular proteins. A Microlumat Plus luminometer (EG&G Berthold, Germany) was used to assess the activity of both firefly and *Renilla* luciferase. For each sample, firefly luciferase activity was normalised to that for *Renilla* luciferase, thus controlling for cell viability and transfection efficiency. Data was compared by one-way analysis of variance (ANOVA) with Tukey's post-hoc test, using Prism software.

Table 2.4 – Plasmid DNA transfection mixes

pGL3-Pro – pGL3-Promoter vector (Promega); *pGL3-Pro-CRM1* – pGL3-Promoter vector with *cis*-regulatory module 1 cloned into the multiple cloning site. Constructs are depicted graphically in Figure 5.9.

Mix #	Plasmid	Quantity	Number of replicates

2.4 Histological techniques

2.4.1 Tissue isolation

Tissues were isolated from adult mice following death by cervical dislocation. Embryos, or extra-embryonic material, was obtained following cervical dislocation of the pregnant female, isolation of the uterine horns and subsequent immersion in ice-cold 0.1 % PBS for 5 minutes. Tissue biopsies, or whole organs, were removed, rinsed briefly in 0.1 % PBS and processed as required. Adult mammary glands were spread across APTS-subbed slides to preserve the shape of the gland, protecting the epithelial component as much as possible.

2.4.2 Carmine staining of mammary glands

Wholemount glands were isolated from gravid and lactating females, all 10 weeks of age and previously virgins at mating. For lactating females, litter size was normalised to 7 pups on the day of birth. Glands, adhered to slides as described above, were incubated in Carnoy's fixative (60 % ethanol, 30 % chloroform, 10 % acetic acid) for 3 hours at room temperature, transferred to 70 % ethanol for 15 minutes and hydrated slowly by gradual replacement of the ethanol with tap water, using a gently running tap for ~3 minutes. Carmine alum stain (0.2 % (w/v) carmine dye (BDH), 0.5 % (w/v) aluminium potassium sulphate (Sigma Aldrich)) was prepared by boiling for 20 minutes, allowing to cool and filtering through Whatmann #1 filter paper. Glands were stained in carmine alum for 18 hours at room temperature, and sequentially dehydrated, by incubating for 10 minutes in each of 50 %, 70 %, 90 % and 100 % ethanol. Glands were stored in xylene (Fisher Scientific) and mounted in DePex mounting medium (BDH).

2.4.3 Optical Projection Tomography

Wild type mammary glands isolated at gestational day 12.5 (G12.5), which had previously been stained with carmine alum as described above, were cleared of DePex by incubating at room temperature in xylene for several days. Glands were detached from slides and cleared in four overnight incubations in 100 % methanol, followed by one overnight incubation in benzyl alcohol (Sigma Aldrich). The free-floating glands were embedded in low melting point agarose, which was subsequently trimmed to an octagonal prism, and scanned using a Bioptonics 3100. 400 2-dimensional scans were reconstructed into a 3-dimensional image using Amira software.

2.4.4 Staining for β-galactosidase activity in mammary wholemounts

Glands were isolated and spread across slides as described in Section 2.4.1, and fixed for 2 hours in 2 % (w/v) paraformaldehyde (PFA; Sigma Aldrich), 0.25 % (v/v) glutaraldehyde (Sigma Aldrich), 0.01 % (v/v) Igepal CA-630 in 0.1 % PBS, at room temperature. Glands were washed briefly in 0.1 % PBS and further fixed in 2 mM $MgCl_2$, 0.01 % (w/v) sodium deoxycholate (Sigma Aldrich), 0.02 % (v/v) Igepal CA-630 in 0.1 % PBS for 2 hours at room temperature, rocking gently. Following fixation, glands were incubated in 1 mg/ml X-gal (Sigma Aldrich) in stain base (30 mM $K_4Fe(CN)_6$ (Sigma Aldrich), 30 mM $K_3Fe(CN)_6.3H_2O$ (Sigma Aldrich), 2 mM $MgCl_2$, 0.01 % (w/v) sodium deoxycholate, 0.02 % (v/v) Igepal CA-630 in 0.1 % PBS) for 18 hours at 28°C. X-gal had been previously diluted to 40 mg/ml in N,N-dimethylformamide (DMF; Sigma Aldrich).

After staining, glands were cleared in acetone (Fisher Scientific) for 6.5 hours, dehydrated in an ascending ethanol series as described for carmine alum staining, and stored in xylene. Glands were mounted in DePex for photographing.

2.4.5 Staining for β-galactosidase activity in e8.0 mouse embryos

Eight days after the observation of a cervical plug, pregnant females were sacrificed and uterine horns removed. Embryos were isolated with the aid of a dissecting microscope and washed in 0.1 % PBS. Fixation was performed for 30 minutes at 4°C in 1 % (w/v) formaldehyde (Sigma Aldrich), 0.2 % (v/v) glutaraldehyde, 2 mM $MgCl_2$, 5 mM EGTA, 0.02 % (v/v) Igepal CA-630 in 0.1 % PBS. Embryos were washed at room temperature in three changes of 0.02 % (v/v) Igepal CA-630 in 0.1 % PBS for 30 minutes each. Staining was performed in the dark, using X-gal diluted in stain base, as described in Section 2.4.4. Embryos were post-fixed in 4 % (w/v) PFA in 0.1 % PBS overnight at 4°C.

To permit sectioning, embryos were resin embedded, using Technovit 7100 (Heraeus, Germany). First, they were dehydrated for 30 minutes each in 70 %, 96 % and 100 % ethanol at room temperature. Next, a pre-infiltration step was performed, incubating embryos in a 1:1 ratio of ethanol:infiltration solution A (Heraeus) for 2 hours. Infiltration was performed overnight by incubating embryos in 100 % infiltration solution A. Embryos were embedded in solution B (Heraeus) and polymerisation permitted overnight. Blocks were mounted, ready for sectioning, using Technovit 3040, according to the manufacturer's instructions. Sectioning was performed by Iryna Withington.

Sections were heated to 65°C for 1 hour, then counter-stained in nuclear fast red solution (Vector Laboratories) for 15 minutes. Following a wash with tap water, slides were left to dry at 30°C and mounted in DePex.

2.4.6 Sectioning and staining of the mature mouse placenta

Cryosectioning and assaying for β-galactosidase activity

Placental genotype was determined by PCR amplification of embryonic tail clips, as described in Section 2.1.3. Placentae were fixed for 30 minutes at room temperature in 4 % (w/v) PFA, 0.2 % (v/v) glutaraldehyde in 0.1 % PBS. Tissue was cryo-protected by incubating in 30 % sucrose at 4°C, until the tissue had sunk to the bottom of the tube. After eliminating excess sucrose solution, placentae were embedded in OCT (VWR International, UK) on dry ice and stored at -80°C until sectioning. Sections were cut at a thickness of 8 µm using a Leica CM1850 cryostat, onto polysine slides (Menzel-Gläser, Germany).

X-gal was diluted in stain base, as described previously, and pipetted onto sections in a dark, humidified chamber. Incubation proceeded for 18 hours at 37°C, except where otherwise stated in the text. To permit counter-staining, slides were washed gently in 0.1 % PBS to remove excess X-gal, and cleared in two 2 minute incubations with Histoclear (National Diagnostics). Sections were hydrated in a descending ethanol series, incubating for 2 minutes each in 100 %, 100 %, 95 %, 90 %, 70 %, 50 % ethanol and finally MilliQ water. Sections were stained in filtered nuclear fast red for 90 seconds and dehydrated in 70 % ethanol (15 seconds), 95 % ethanol (15 seconds) and two 100 % ethanol incubations (1 minute each). Sections were prepared for mounting with DePex by two 2 minute incubations in Histoclear.

Assaying for β-galactosidase activity, post-fixing and paraffin sectioning

Placentae were isolated at e14.5, fixed for 30 minutes at 4°C in 4 % (w/v) PFA in 0.1 % PBS, washed briefly in 0.1 % PBS and excess liquid removed on tin foil. Tissues were frozen quickly on dry-ice and sagittally bisected with a razor blade, before being stained in X-gal solution, diluted in stain base as previously, at 28°C. Samples were washed in 0.1 % PBS, fixed overnight in 4 % (w/v) PFA in 0.1 % PBS at 4°C and prepared for sectioning using a Leica tissue processor. Briefly, samples were dehydrated in an ascending ethanol series (2 hours in each of 50 %, 70 %, 90 %, 100 %, 100% ethanol), then cleared twice in Histoclear (2 hours each) and infiltrated with hot wax (three 2 hour incubations). Sections were taken at a thickness of 8 µm (Leica RM2155).

Sections were hydrated, counter-stained with nuclear fast red, dehydrated and mounted, as described above.

Staining for morphological assessment

Whole e14.5 placentae were isolated, fixed overnight in 4 % (w/v) PFA in 0.1 % PBS at 4°C, washed in 0.1 % PBS and stored in 70 % ethanol at 4°C. Samples were dehydrated and sectioned as described above.

To permit staining with haematoxylin and eosin, tissue sections were first cleared of excess wax by two 2 minute washes in Histoclear and hydrated through a descending ethanol series (100 %, 100 %, 95 %, 90 %, 70 %, 50 %), with 1 minute in each solution. Hydration was completed with an incubation in MilliQ water for 1 minute. Nuclear staining was achieved by incubation in filtered Ehrlich's haematoxylin (Raymond Lamb, Fisher Scientific) for 5 minutes. Excess stain was removed under a running tap for ~5 minutes. Sections were placed in 1 % concentrated HCl in 70 % ethanol for 30 seconds, followed by 60 seconds in 1 % NH_3 (Fisher Scientific) in 70 % ethanol. Sections were washed briefly (30 seconds) in 70 % ethanol to remove traces of NH_3, and then stained in filtered eosin (Fisher Scientific) for 5 minutes. Brief washes (~3 seconds) were performed in 70 %, 95 %, 100 % and 100 % ethanol, and sections prepared for mounting with two 2 minute incubations in Histoclear. Slides were mounted with DePex.

2.4.7 Immunohistochemistry

Paraffin-sectioned tissue was cleared in Histoclear as before and hydrated through a descending ethanol series, with a 1 minute incubation in each of 100 %, 95 %, 70 % and 50 % ethanol. Antigen retrieval was achieved by boiling sections in 10 mM citric acid (Sigma Aldrich) three times for 5 minutes each. Endogenous peroxidase activity was quenched by incubating in 0.3 % (v/v) hydrogen peroxide for 30 minutes at room temperature. Sections were rinsed in 0.1 % PBS and blocked for 1 hour in 0.3 % (w/v) BSA, 0.01 % Tween-20 in 0.1 % PBS. Stat5 or Grb7 antibody was diluted in blocking buffer (Table 2.3), applied to slides and left to incubate overnight at 4°C. Negative (no primary antibody) controls were also performed simultaneously.

Sections were washed three times in 0.1 % Tween-20 in 0.1 % PBS for 15 minutes each, removing excess primary antibody. The Vectastain ABC kit (Vector Laboratories) was used for amplification of signal, according to the manufacturer's instructions. Briefly, a biotinylated goat anti-rabbit secondary antibody was reconstituted as instructed in blocking buffer, and applied to sections for 1 hour at room temperature. Sections were washed as before and incubated in Vectastain ABC reagent for 45 minutes, as directed. Five washes of 5 minutes each were performed with 0.1 % PBS, and visualisation of protein localisation was achieved by incubating with DAB substrate (Vector Laboratories) for 10 minutes, prepared according to the manufacturer's guidelines. To remove excess DAB substrate, slides were washed in running water for 5 minutes, and then counter-stained in haematoxylin for 30 seconds. After washing in water, sections were dehydrated in a graded ethanol series of 70 %, 95 % and 100 % ethanol, for 1 minute each, cleared in Histoclear as before and mounted with DePex.

2.4.8 Assessment of apoptosis by TUNEL assay

Fourth (abdominal) mammary glands were isolated from age-matched (all 10 weeks of age and virgins at mating) and litter size-matched females 48 hours after a forced wean at

postnatal day 15. As before, glands were spread over APTS-subbed slides to preserve architecture and shape. Glands were fixed in 10 % neutral-buffered formalin (Sigma Aldrich) overnight at 4°C. Cells undergoing apoptosis were labelled using the ApopTag peroxidase *in situ* apoptosis detection kit (Chemicon International Inc., USA), as described in the associated manual. Working strength peroxidase substrate (Vector Laboratories) was prepared as directed. Counter-staining was achieved with methyl green (Vector Laboratories), then sections were dehydrated in xylene and mounted with DePex, as instructed in the ApopTag peroxidase *in situ* apoptosis detection kit literature.

For a quantitative assessment of TUNEL-positive cells, one representative section from each sample was photographed at 400x magnification at four randomly-selected, non-overlapping sites, using a Nikon Eclipse E800 microscope. TUNEL-positive nuclei were counted as a proportion of the total number of nuclei, and a mean proportion calculated for each sample. Glands from five different females were analysed for each genotype (wild type and *Grb10KO*$^{m/+}$); the mean value for each genotype was compared by Students' T-test, using Prism software.

2.5 Morphological analyses

2.5.1 Assessment of the placenta

Measurement of cell layer thickness

Ten placentae of each genotype were sectioned and stained with haematoxylin and eosin. One representative section close to the midline was randomly-selected from each sample and photographed at 10x magnification, such that the entire section could be visualised in one field. Using Image ProPlus software, the distance from the labyrinth-junctional zone boundary to the foetal edge of the chorionic plate was measured at the centre of each section, as well as the distance from the labyrinth-junctional zone boundary to the junctional zone-decidua boundary. Data was analysed for each measurement using one-way ANOVA with Tukey's post-hoc test, and manipulated using Prism software.

Morphometric analysis

Images of the ten randomly-selected placental sections for each genotype were overlaid with a 8 x 4 grid, dividing the sections into 32 discrete areas. One area was chosen by random number generation. This area, and seven of the surrounding areas, were consistently analysed for each sample. Viewed at 100x magnification, each area was overlaid with a counting grid, and cell type was scored as 'labyrinth', 'spongiotrophoblast', 'glycogen cell' or 'blood vessel', essentially as described (Charalambous *et al*, submitted). The total number of scored cell types per window was pooled for each sample, and used to calculate mean values for each genotype.

Blood vessel area analysis

Images of placental sections were taken at 40x magnification to assess foetal vasculature occupancy. All images had 100 % occupation by labyrinth. First, Image ProPlus was used to manually define the edges of foetal blood vessels through which a cross-section had been taken. This was used to calculate the total area of foetal vasculature, in arbitrary units. Secondly, the number of discrete foetal blood vessels was counted. One representative section from each of ten placentae per genotype, close to the midline, was analysed in this manner. Statistical analyses were performed using Prism software.

2.5.2 Assessment of the mammary gland

Fourth (abdominal) mammary glands isolated at gestational day 12.5 (G12.5) were fixed and stained with carmine alum. Females were 10 weeks of age at mating and previously

virgins. Wholemount glands were consistently photographed at 20x magnification, positioning the edge of the lymph node closest to the leading edge such that it was just visible at the top centre of the image. The number of primary branch points within the window was counted. Five wild type and three *Grb10KO*$^{m/+}$ glands, from separate females, were analysed in this manner.

The distance from the lymph node to the leading edge was also measured, by photographing the same mammary gland wholemounts adjacent to a ruler.

For both measurements, results were analysed with Students' T-test using Prism software.

2.6 *In silico* analyses

2.6.1 Sequence conservation at the *Grb10* locus

The genomic sequences of the orthologous *Grb10* sequences for mouse, human, chimpanzee, cow, *Xenopus tropicalis*, chicken and opossum were retrieved from Ensembl (www.ensembl.org). The relevant Ensembl IDs are provided in the legend to Figure 5.4. ExactPlus (available for public use at http://research.nhgri.nih.gov/exactplus; Antonellis *et al*, 2006) was used to identify short conserved sequences. First, a MultiPipMaker alignment (acgt) file was generated for each of the separate comparisons to be made, and the 'very verbose text (ASCII, compressed)' output submitted to ExactPlus for analysis. The first nucleotide base of the murine *Grb10* sequence was used as the start coordinate to enable a graphical depiction of the alignment on the UCSC Genome Browser (http://genome.ucsc.edu/). The minimum length of exact match to seed was 6 bp. The minimum number of species to seed was equivalent to the number of species for that particular alignment; all species must thus possess at least 6 identical base pairs in sequence for a hit to be reported. The minimum number of species to extend a hit was consistently set at 2; this represented the number of species in which an alignment was required to extend a hit both 5' and 3' to the initial sequence identified. An exons file was submitted to exclude murine exons 1, 2, 3, 4 and 5 from the alignment. Exons 6 to 18 were included as positive controls for sequence conservation. Custom tracks were submitted to the UCSC Genome Browser and viewed in squish format.

2.6.2 Identification of predicted regulatory modules at the *Grb10* locus

The mouse *Grb10* Ensembl gene ID was submitted to PReMod, available for public use at http://genomequebec.mcgill.ca/PReMod/welcome.do. No search restrictions were imposed. Output was viewed as a html file. Details of the software are provided in Blanchette *et al* (2006).

2.6.3 Allen Brain Atlas

The atlas is available for public use at www.brain-map.org. Known sites of *Grb10* expression in the CNS (Garfield *et al*, submitted) were identified in the images of sagittal sections which had been challenged with *in situ* probes to *Stat5a*, *Stat5b*, *Pax1-9* and *Tcf11*. Sites of *Grb10* expression which corresponded with higher levels of *in situ* signal than background noise for each of these transcription factors were recorded.

2.7 Mammary gland function analyses

2.7.1 Mice

For all matings, males were wild type animals. All females used in the cross-fostering study were 7 weeks of age and virgins at mating. On the morning of the observation of a cervical plug, males were removed from females, and prior to giving birth, females were housed individually. On the day of birth, pups were weighed and tattooed on the pads of the paws to permit future identification. This was achieved by injecting a small volume of India ink sub-cutaneously. Litters were normalised to 5-7 pups on the day of birth by arbitrary pup selection, unless an obviously unhealthy pup was apparent. Where appropriate, litters were exchanged between mothers on the day of birth; see Figure 6.3 for the directions of transfer. Provided the genotypes did not compromise the experiment, individual pups were exchanged if it helped to normalise litter size. Pup weight was recorded every subsequent day at approximately the same time until postnatal day 15. During this period, females were permitted unlimited access to food and water. Once culled, pups were genotyped from a tissue biopsy, as described for adult ear clips (Section 2.1.3).

2.7.2 Milk isolation

On postnatal day 15, pups were culled. Mothers were left for ~4 hours to permit milk accumulation and injected intraperitoneally with 0.1 % (w/v) xylazine, 0.5 % (w/v) ketaset in 0.9 % (w/v) NaCl, at 16 µl/g of mouse to induce anaesthesia. Once fully anaesthetised, mice were injected intraperitoneally with 200 µl oxytocin (Sigma Aldrich) at 10 IU/ml, diluted in 0.1 % PBS, to aid milk letdown. After 2-3 minutes, nipples were swabbed with 70 % ethanol to make them erect, and gentle vacuum pressure was applied in combination with massaging of the gland. The vacuum was provided by a pipette aid electric pump, connected to a 1.5 ml collecting tube, which in turn was connected to a shortened yellow pipette tip sitting comfortably around the nipple (see Figure 6.7*a* and *b*). Up to 150 µl milk could be collected per mouse. Females were culled by cervical dislocation under terminal anaesthesia, and pituitary glands isolated and snap-frozen.

2.7.3 Milk analysis

A small volume (~20 µl) of each milk sample was centrifuged in a plugged borosilicate glass capillary tube (Harvard Apparatus Ltd., Kent, UK) for 20 minutes at 3000 rpm in a Sorvall Biofuge Pico microcentrifuge, to separate fat from protein. The relative proportion of fat in the sample was measured using a ruler. Data was analysed using Prism software and statistical analysis performed by one-way ANOVA with Tukey's post-hoc test. Capillary tubes were sliced to remove the fat. Protein was retrieved from the capillary tube and diluted 1/5 in buffer (50 mM Tris HCl pH 8.0, 150 mM NaCl, 1 % (v/v) Igepal CA-630).

Samples were boiled for 10 minutes with an equal volume of 2x reducing sample buffer (recipe in Section 2.2.10) and loaded onto a 15 % Criterion Tris-HCl gel (Bio-Rad Laboratories) alongside pre-stained molecular weight standards, as described for Western blotting.

After suitable protein separation, the gel was fixed in 50 % ethanol, 10 % acetic acid for 1 hour at room temperature, rocking gently, and then transferred to 50 % methanol, 10 % acetic acid overnight, again rocking gently. The following day, the gel was stained with Coomassie blue (0.1 % (w/v) Coomassie blue (Raymond Lamb), 20 % (v/v) methanol, 10 % (v/v) acetic acid) at room temperature for 3 hours with gentle agitation. Destaining was performed using 50 % methanol, 10 % acetic acid. Solution was changed frequently until most background staining had been eliminated. Gels were stored in 5 % acetic acid and photographed with an AlphaImager 3400.

Chapter Three

Genetic characterisation of the Grb10KO *allele and its influence during early mouse development*

3.1 Introduction

Many of the early analyses of murine Grb10/human GRB10 employed yeast two-hybrid assays and *in vitro* manipulations to elucidate potential binding partners. Indeed, Grb10 was first identified in a bacterial expression library screen, using the tyrosine-phosphorylated carboxy-terminus of the epidermal growth factor receptor (EGFR; Ooi *et al*, 1995). Later screens identified further potential binding partners of Grb10, including other tyrosine kinase receptors, such as the insulin and insulin-like growth factor I receptors (He *et al*, 1998), and Bcr-Abl (Bai *et al*, 1998). More recently, two intracellular binding partners, termed Grb10 interacting GYF proteins 1 (GIGYF1) and GIGYF2, have been identified using yeast two-hybrid screening with the N-terminus of Grb10 (Giovannone *et al*, 2003). Grb10, as an adaptor protein, appears to link the GIGYFs with the IGF1 receptor, thereby modulating IGF1 signalling. Other intracellular signalling partners have been identified by biochemical means, including the growth hormone receptor (GHR), insulin receptor (IR), MEK1, ELK and Tec, as discussed in Chapter One (Stein *et al*, 1996; Frantz *et al*, 1997; Mano *et al*, 1998; Moutoussamy *et al*, 1998; Nantel *et al*, 1998).

Such biochemical studies have been key in shaping the direction of research on the cellular functions of Grb10, but they have an important limitation. The artificial conditions in which the experiments are performed can force associations which might otherwise occur only weakly in a cell, or indeed, not at all if two proteins exhibit different tissue distributions. Therefore, some of the identified 'binding partners' might not be physiologically relevant. *In vitro* analyses can often confirm or argue against a molecular interaction; for example, such experiments have failed to identify Grb10 as a true binding partner of the EGFR, despite being a strong candidate from biochemical analyses.

One shortcoming of both biochemical and *in vitro* analyses is that they may provide limited information about the physiological relevance of an interaction. As discussed in Chapter One, several *in vitro* studies have described Grb10 as a negative regulator of insulin signalling (Liu and Roth, 1995; Wick *et al*, 2003). However, these experiments fail to answer several important questions about the functions of Grb10 in a physiological context: How significant is Grb10 in regulating insulin signalling? Does Grb10 act in all insulin target tissues? Is *Grb10* over-expression a risk factor for diabetes?

Transgenic animal models can complement biochemical and *in vitro* analyses, and can often help to address some of these shortcomings, providing important information about the physiological relevance of molecular interactions. Shiura *et al* (2005) describe a mouse model in which ectopic *Grb10* is expressed under the control of the chicken β-*actin* promoter, increasing transcripts of this gene by 1.2 to 1.4-fold in tissues examined, relative to wild type controls. Growth retardation manifested 4 weeks after birth, with a 10-15 % reduction in weight compared with wild type controls at 4 months. Adult mice also exhibited insulin resistance, with blood glucose levels remaining significantly higher than wild type controls 60 minutes after insulin administration. The result correlated with an impaired ability to clear glucose following glucose injection. This study supported the

findings of *in vitro* experiments, suggesting that Grb10 negatively regulates insulin signalling, but only the transgenic model enabled the function of Grb10 to be described in a physiological context, demonstrating the important homeostatic role for Grb10 in maintaining circulating blood glucose levels.

The function of Grb10 as a modulator of insulin signalling was also confirmed from *in vivo* knock-out experiments. Smith *et al* (2007) utilised a transgenic mouse line in which Grb10 protein had been ablated by the incorporation of a gene-trap cassette in the endogenous *Grb10* locus (*Grb10Δ2-4*). Converse to results reported for *Grb10* over-expression mice, animals inheriting the *Grb10Δ2-4* allele through the maternal line (*Grb10Δ2-4*$^{m/+}$), effectively ablating Grb10 from peripheral tissues, displayed improved whole-body glucose tolerance and insulin sensitivity. Dual X-ray absorptiometry performed on whole 6-month old *Grb10Δ2-4*$^{m/+}$ animals revealed an increase in muscle mass with a concomitant reduced adiposity, also confirmed by the wet weights of individual muscles and fat depots. Whilst an increase in the mass of muscle, a key glucose deposition tissue, might partially account for the improved ability to clear circulating glucose, *Grb10Δ2-4*$^{m/+}$ mice exhibited higher levels of IR in both skeletal muscle and fat than wild type counterparts. RNAi-mediated suppression of *Grb10* activity suggests that, whilst the levels of IR message are not influenced by *Grb10*, insulin-stimulated ubiquitination of the IR may be the mechanistic basis for this *in vivo* observation, with Grb10 acting to promote receptor internalisation and presumably proteasomal-targeting (Ramos *et al*, 2006). The absence of Grb10 in *Grb10Δ2-4*$^{m/+}$ animals also correlated with an increased proportion of phosphorylated insulin receptor substrate-1 (IRS-1). Taken together, these results confirm the role of Grb10 in peripheral tissues as a negative regulator of insulin signalling, but also highlight the importance of transgenic models in extrapolating *in vitro* observations to the whole-organism level.

In addition to ablating full-length transcripts, the gene-trap cassette integrated at the *Grb10* locus to generate the *Grb10Δ2-4* allele includes a *LacZ* reporter gene, expression of which is driven by the endogenous promoter (Charalambous *et al*, 2003). This genetic tool offers the opportunity to track sites of *Grb10* expression during development and in adulthood. Whilst this can also be achieved using *in situ* hybridisation and immunohistochemistry, these latter techniques offer limited scope for the study of uniparental expression, being indiscriminate in their recognition of protein or mRNA derived from each parental allele. Transmission of an integrated reporter gene, however, can be parent-specific. Transmitting *Grb10Δ2-4* through the maternal line reported widespread embryonic expression at e14.5, including skeletal and cardiac muscle, liver and bronchioles, as well as pancreatic buds and developing tubules in the kidney (Charalambous *et al*, 2003). Expression of *LacZ* from a paternally-inherited copy of *Grb10Δ2-4* reported a more restricted profile, including some cells of the heart, gut, umbilicus, lungs and tongue. A contribution from both alleles was apparent in cartilage tissue, although expression from the maternally-inherited allele appeared greater.

Interestingly, immunohistochemistry identified Grb10 protein in the developing central nervous system (CNS), a site not reported following inheritance of *Grb10Δ2-4* through

either parental line (Charalambous *et al*, 2003). A second transgenic allele, created in the same gene-trapping experiment, also ablated full-length *Grb10* transcripts and reported *Grb10* expression. This allele, herein referred to as *Grb10KO*, confirmed the embryonic expression profile identified previously, but also reported expression in the developing CNS following paternal inheritance (Garfield *et al*, submitted). Strikingly, this identifies *Grb10* as the only gene with such a reciprocal imprinting pattern, in which peripheral expression is predominantly from the maternally-inherited allele, while the paternally-derived copy is the near-exclusive source of transcripts in the CNS. Other genes display imprinted expression in a tissue-specific manner, but not a complete switch from one imprinted allele to the other. Murine *Blcap_v1a*, for example, is expressed broadly but only imprinted in the brain (Schulz *et al*, 2008). Conversely, *Igf2* is expressed and imprinted in most tissues, but in the choroid plexus epithelium is expressed from both parental alleles (DeChiara *et al*, 1991; Charalambous *et al*, 2004).

The inability of *Grb10Δ2-4* to report expression in the CNS is addressed in Chapter Five.

Sites of *Grb10* expression during adulthood are relatively restricted, being predominant in skeletal muscle, adipose tissue and endocrine cells of the pancreas, thus correlating with the role for Grb10 in mediating insulin signalling. Expression is also detected in the Leydig cells of the testis, the oviduct and uterine horns of the female reproductive system, and some cell populations of the CNS (Smith *et al*, 2007; Garfield *et al*, submitted). The reciprocal imprinting pattern, however, persists into adulthood, with transcripts in the CNS continuing to arise almost exclusively from the paternally-inherited allele, with the exception of the epithelium of the choroid plexus, the ventricular ependymal layers and the meninges (Garfield *et al*, submitted).

Whilst the gene-trap cassette in the *Grb10Δ2-4* allele has been mapped (Charalambous *et al*, 2003), the exact position of the same cassette in *Grb10KO* remained to be elucidated. 5' RACE data suggested the *LacZ* reporter gene splices onto the end of exon 7 in transcripts originating from the *Grb10* promoter, thereby implying the reporter cassette must lie 3' of this exon. Knowing the site of cassette integration is critical to understanding the relationship between gene and phenotype. An integration site between exons 1A and 1C, for example, from which peripheral- and brain-specific transcripts initiate, respectively, might fail to ablate functional Grb10 in the CNS.

This Chapter describes the mapping experiments performed to identify the integration site of the β-*geo* cassette into the *Grb10* locus, thereby creating the *Grb10KO* allele. The efficacy of the gene-trap in ablating full-length *Grb10* transcripts is demonstrated. With detailed knowledge of the allelic structure, a key phenotypic difference between mice inheriting *Grb10KO* and *Grb10Δ2-4* is addressed.

3.2 Results

3.2.1 Mapping of the gene-trap cassette integration site in the *Grb10KO* allele

Both the *Grb10Δ2-4* and *Grb10KO* alleles were generated in a commercial gene-trapping experiment, in which a β-*geo* cassette was randomly integrated into the genome of embryonic stem (ES) cells (Stryke *et al*, 2003). This cassette consists of four key features: a 5' splice acceptor (SA) sequence, onto which transcripts initiating upstream splice; a *LacZ* reporter gene, enabling characterisation of the expression profile of the trapped gene; a *neo* resistance gene for ES cell selection; and a 3' poly-adenylation (poly-(A) or pA) sequence to prematurely terminate host gene transcripts. Transgenic mice harbouring the *Grb10KO* or *Grb10Δ2-4* allele were generated as described in Section 2.1.2. Southern blotting and polymerase chain reaction (PCR)-based mapping experiments for *Grb10Δ2-4* demonstrated that the β-*geo* cassette had replaced ~38 kb of the *Grb10* locus, including exons 2-4 (Charalambous *et al*, 2003).

5' RACE experiments performed from *Grb10KO* ES cells, utilising a primer complimentary to the 5' end of the *LacZ* reporter gene, indicated that β-*geo* splices onto the end of exon 7 of transcripts arising at the *Grb10* locus (Bay Genomics, University of California). This suggested the cassette had integrated between exons 7 and 8, and provided a focus for initial mapping experiments.

The first mapping strategy employed in the present study involved the use of nine primer pairs, each with an amplicon size of between 470 bp and 680 bp, which together provided complete coverage of intron 7. At the site of cassette integration, one or more of these primer pairs would fail to amplify from DNA homozygous for the *Grb10KO* allele. Embryos at 14.5 days post-coitum (e14.5), based on the observation of a cervical plug, were isolated from *Grb10KO*$^{m/+}$ x *Grb10KO*$^{m/+}$ crosses. Bisected embryos were stained for *LacZ* expression and *Grb10KO*$^{m/p}$ conceptuses identified by the presence of staining in both the central nervous system and mesodermally-derived tissues (indicating paternal and maternal inheritance of the *Grb10KO* allele, respectively). DNA isolated from tissue biopsies from these and wild type embryos was subjected to PCR using the nine primer pairs spanning intron 7. Amplicons, however, were observed from all nine primer pairs using both wild type and *Grb10KO*$^{m/p}$ DNA as template (data not shown). Additionally, semi-quantitative PCR failed to detect a difference between wild type and *Grb10KO*$^{m/+}$ DNA (data not shown), together suggesting the cassette integration site may not lie in intron 7.

To allow for the possibility that the integration site may be further downstream, Southern blotting was performed on wild type, *Grb10KO*$^{+/p}$ and *Grb10KO*$^{m/p}$ DNA, using digest strategies which would enable screening of the genomic region from 984 bp upstream of exon 7 to the 3' end of exon 9 (Figure 3.1*a*). First, *Bam*HI-digested genomic DNA was challenged with a radiolabelled probe (probe A) spanning the exon 7/intron 7 boundary. A 4.5 kb digestion fragment was identified in DNA from all three genotypes, indicating that

the β-*geo* cassette had not integrated upstream of the intron 7 *Bam*HI recognition site (Figure 3.1*b*).

A second digest strategy, utilising *Pst*I, identified a restriction fragment length polymorphism (Figure 3.1*c*). Probing of wild type DNA generated the 6.7 kb *Pst*I digestion fragment expected from the endogenous sequence (Figure 3.1*a*). An additional digestion fragment was apparent from the probing of *Grb10KO*$^{+/p}$ genomic DNA, estimated to be ~10 kb. This fragment was also present in DNA isolated from a *Grb10KO*$^{m/p}$ embryo, whilst the 6.7 kb fragment was absent, suggesting these represent the *Grb10KO* and wild type alleles, respectively.

The 5'-most *Pst*I site in the β-*geo* cassette is positioned 4.7 kb into the β-*geo* sequence, putting the start of the cassette ~5.3 kb downstream of the endogenous *Pst*I site in intron 6 (Figure 3.1*a*). This result implied that the integration site is close to or within exon 8. Using a similar approach to that described previously, overlapping primer pairs were designed to span the 3' end of intron 7 to the 5' end of intron 9, and PCR amplification performed on wild type and *Grb10KO*$^{m/p}$ DNA isolates (Figure 3.2*a*). Whilst primer Sets A and C successfully amplified DNA of both genotypes, primer Set B failed to amplify from *Grb10KO*$^{m/p}$ DNA (Figure 3.2*b*). The absence of an amplicon from DNA homozygous for the *Grb10KO* allele, suggested this 392 bp region might contain the site of cassette integration.

In order to map the integration site to the base pair resolution, PCR amplification was performed on *Grb10KO*$^{m/p}$ DNA using the forward primer of primer Set B in combination with two reverse primers complimentary to sites within the β-*geo* cassette (β-R1 and β-R2, Figure 3.2*a*). Both of these primer combinations produced amplification products, neither of which were observed using wild type DNA as a template (not shown). Both products were cloned into the pGEM-T Easy vector, as described in Section 2.2.7, and sequenced. The sequencing results from both clones corroborated, indicating that the 5' end of the integration site is within exon 8, 11 bp from the 3' end (Figure 3.2*c*).

The integration of the β-*geo* cassette to generate the *Grb10Δ2-4* allele caused the deletion of ~38 kb of the endogenous *Grb10* locus (Charalambous *et al*, 2003). To confirm whether *Grb10KO* was generated by a simple insertion event, or if it too was subject to a sequence deletion, the current study next mapped the 3' end of the β-*geo* cassette by PCR. A forward primer located close to the 3' end of the cassette (β-F1, Figure 3.2*a*), with the reverse primer from primer Set B, produced an amplicon from *Grb10KO*$^{m/p}$ embryo DNA which was cloned and sequenced, as before. This confirmed that the insertion of the β-*geo* cassette had deleted 12 bp of the *Grb10* locus, including 11 bp from exon 8 and 1 bp from intron 8 (Figures 3.2*a* and 3.2*c*).

Additionally, 825 bp at the 5' end of the β-*geo* cassette sequence were deleted during the integration. However, 707 bp 5' to the splice acceptor sequence were retained, and 5' RACE experiments confirmed correct splicing of the β-*geo* cassette onto *Grb10* exon 7 (Bay Genomics, University of California).

a

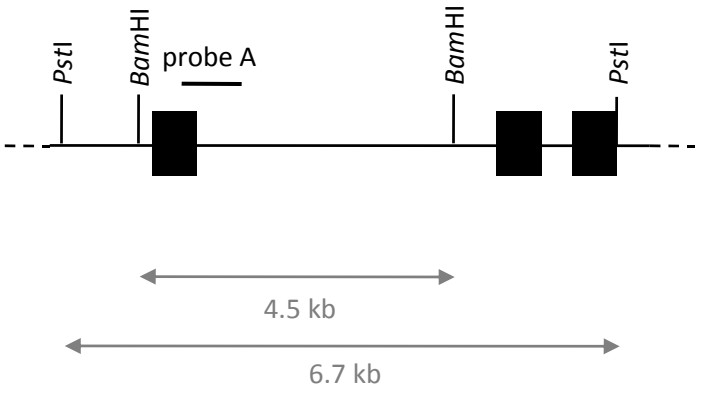
PstI
BamHI
probe A
BamHI
PstI
4.5 kb
6.7 kb

b

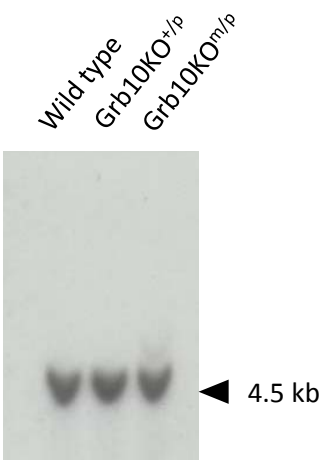
BamHI
digest
Wild type
Grb10KO+/p
Grb10KOm/p
4.5 kb

c

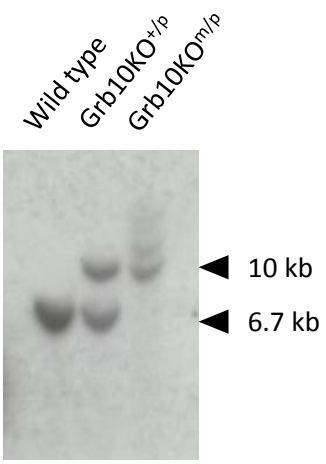
PstI
digest
Wild type
Grb10KO+/p
Grb10KOm/p
10 kb
6.7 kb

a

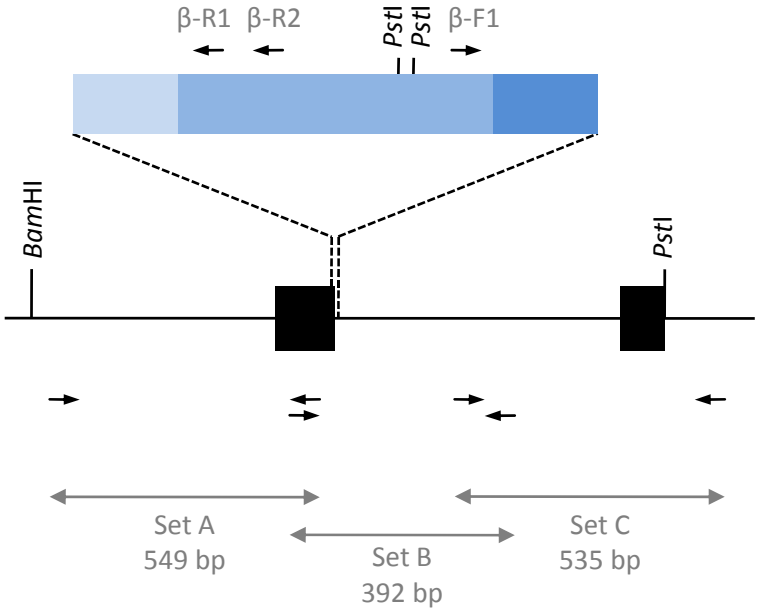

b

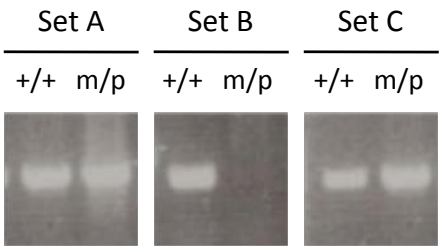

c

Exon 8

ACACCTCACATGTGATGGTTCTCCCTACAGAGAGGTGCCTGGAGGACCATGA

GATCGTGGTCCAAGTGGAGAGTACCATGCCAAGTGAGAGCAAATTCTTATTC

AGAAAGAATTATGCGAAGTACGAGTTCTTTA|AGAATCCAGTGG|TAAGTCT

CCTGAAATCTTGGAGTTA

3.2.2 The *Grb10KO* allele effectively ablates full-length *Grb10* transcripts

Mice inheriting the *Grb10KO* allele through the maternal line demonstrate similar embryonic growth and adult metabolic phenotypes to those previously described for *Grb10Δ2-4*$^{m/+}$ animals (Charalambous *et al*, 2003; Smith *et al*, 2007; Garfield, 2007; Garfield *et al*, submitted), suggesting effective ablation of functional Grb10 protein. However, a demonstration of the absence of full-length *Grb10* transcripts was required to confirm the efficacy of the β-*geo* cassette insertion.

Total RNA isolated from wild type e14.5 embryos, as well as embryos inheriting the *Grb10KO* allele through each of the parental lines, was size-fractionated on a denaturing gel and probed for full-length *Grb10* transcripts, using a cDNA probe spanning exons 11-16 (probe B; Figure 3.3*a*; Charalambous *et al*, 2003). *Grb10* transcripts of 5.5 kb were detected in wild type RNA and with a similar intensity in RNA isolated from *Grb10KO*$^{+/p}$ embryos (Figure 3.3*b*). The expression of *Grb10* transcripts in a *Grb10KO*$^{m/+}$ embryo was considerably reduced, confirming both the effective ablation of full-length *Grb10* transcripts and the imprinted nature of the gene. A low level of signal representing 5.5 kb transcripts was apparent in this RNA sample, presumably reflecting *Grb10* expression from the paternally-inherited allele in the central nervous system and other discrete sites of both mesodermal and endodermal origin (see Section 3.1). The same samples were challenged with a probe hybridising to *Gapdh* transcripts, confirming equal loading.

A lower molecular weight species of ~2.5 kb was apparent in both wild type and *Grb10KO*$^{+/p}$ RNA samples, which was also detected on a Northern blot probing placental RNA at e14.5 (data not shown). This could represent non-specific probe hybridisation, but this is unlikely due to the absence of this product in *Grb10KO*$^{m/+}$ RNA. This implies that a shorter transcript of *Grb10*, yet to be described, may exist, which forms a small proportion of the total pool, at least in whole embryo and placental isolates. Key, however, is that this transcript is ablated from the *Grb10KO* allele. Potential functional redundancy with full-length *Grb10* will not, therefore, compromise the phenotypic characterisation of mice inheriting this allele.

3.2.3 *Grb10* is expressed from the paternally-derived allele in adult brain

Whilst mice inheriting the *Grb10Δ2-4* allele did not report *Grb10* expression in the CNS, immunohistochemistry experiments suggested active transcription and translation of this gene in the brain (Charalambous *et al*, 2003). Corroborating this, analysis of the *LacZ* reporter expression profile from adult mice harbouring the *Grb10KO* allele, demonstrated *Grb10* expression in a subset of neurons, including some cells of the thalamus, hypothalamus, midbrain and hindbrain, as well as the ventral spinal cord (for a complete list, see Garfield *et al*, submitted). Specifically, expression of the *LacZ* reporter was observed only following inheritance of the *Grb10KO* allele through the paternal line.

To confirm the imprinted status of *Grb10* in this tissue, RNA isolated from the brains of adult mice inheriting the gene-trap allele through each of the parental lines, as well as a

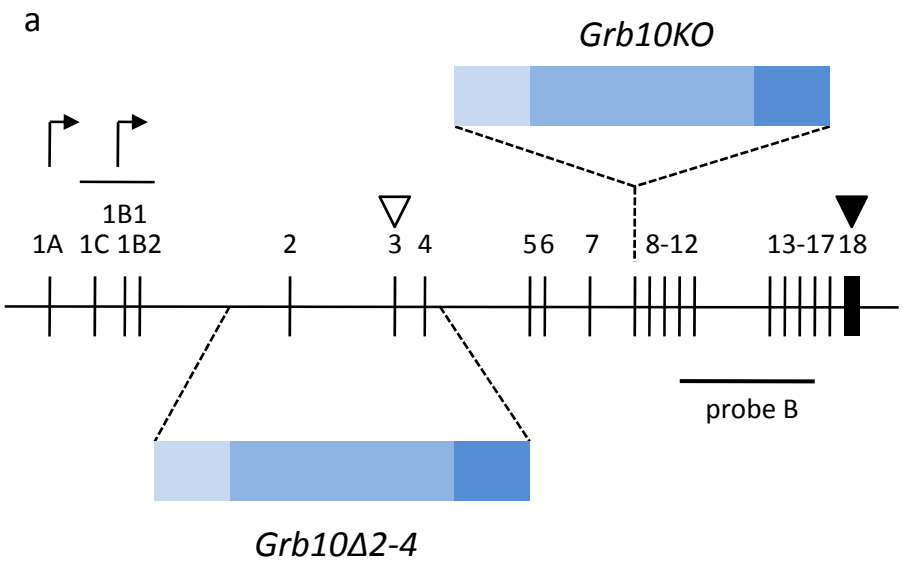
a
Grb10KO
1B1
1A 1C 1B2
2
3 4
5 6 7
8-12
13-17
18
probe B
Grb10Δ2-4

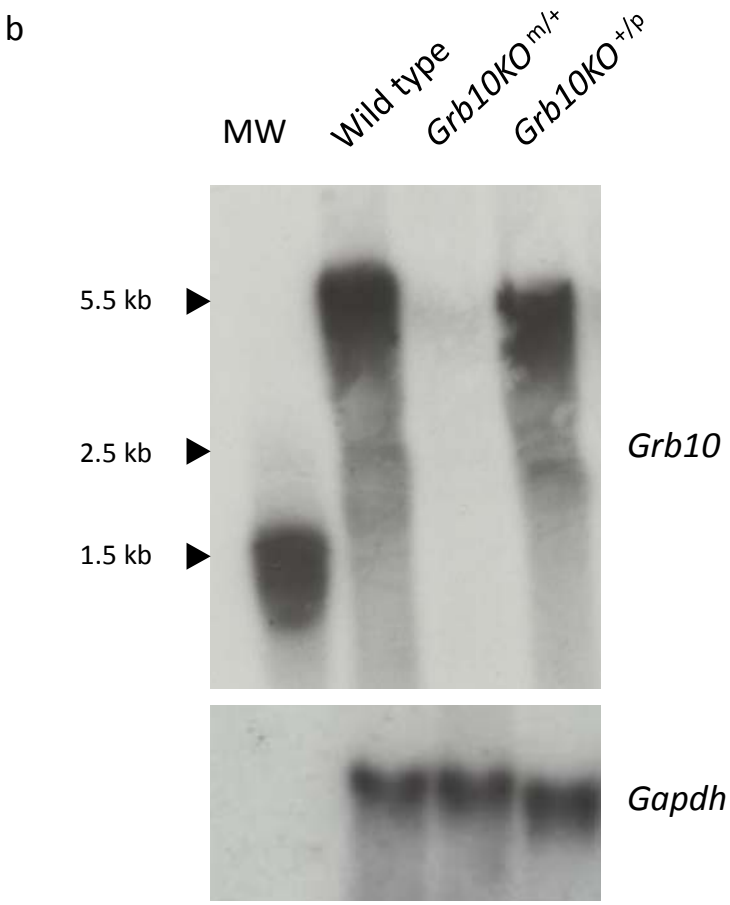
b
MW
Wild type
Grb10KO m/+
Grb10KO +/p
5.5 kb
2.5 kb
1.5 kb
Grb10
Gapdh

a

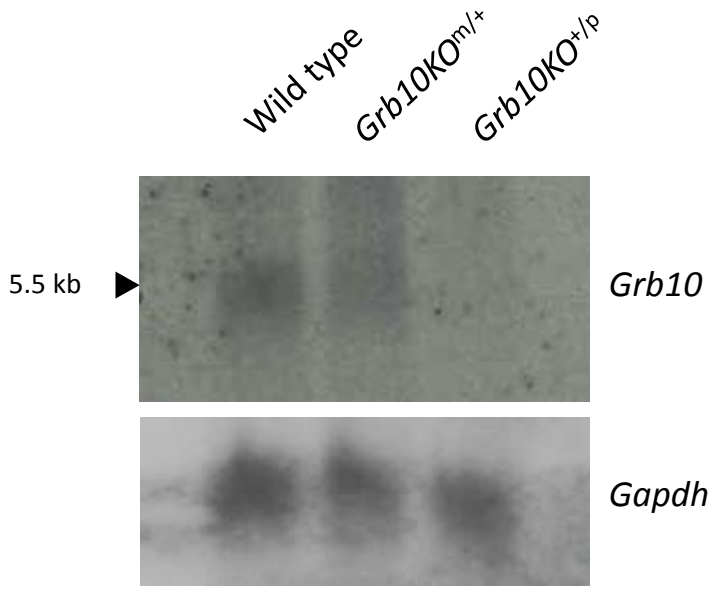
Wild type
Grb10KO m/+
Grb10KO +/p
5.5 kb
Grb10
Gapdh

b

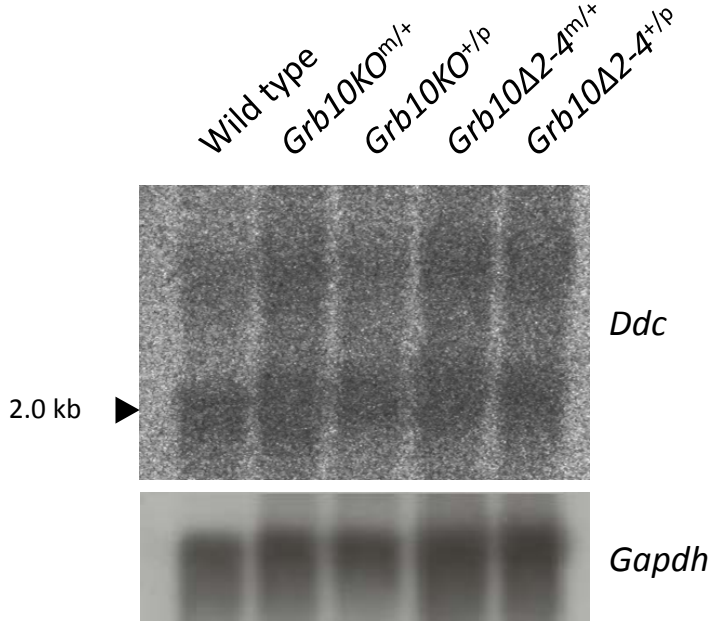
Wild type
Grb10KO m/+
Grb10KO +/p
Grb10Δ2-4 m/+
Grb10Δ2-4 +/p
2.0 kb
Ddc
Gapdh

wild type control, was probed for *Grb10* (Figure 3.4*a*). Probe B (Figure 3.3*a*) detected 5.5 kb transcripts in RNA from wild type and *Grb10KO*$^{m/+}$ adult brain samples, but not from a *Grb10KO*$^{+/p}$ brain, confirming the reciprocal imprint between peripheral tissues and the CNS.

Previous experiments have demonstrated that *Grb10* and its neighbouring gene *Dopa decarboxylase* (*Ddc*) form an imprinted cluster, sharing regulatory domains (Menheniott *et al*, 2008; Shiura *et al*, 2009). To confirm that the insertion of a β-*geo* cassette at the *Grb10* locus, and indeed the ablation of *Grb10* transcripts, does not influence the expression of *Ddc* in the adult brain, Northern blotting was performed on adult brain RNA samples using a probe specific to *Ddc*. No changes in the level of expression of the characterised 2.0 kb *Ddc* transcript, or of a higher molecular weight species, were observed following the inheritance of *Grb10KO* or *Grb10Δ2-4* through either parental line (Figure 3.4*b*).

3.2.4 *Grb10KO*$^{m/p}$ mice do not conform to the expected Mendelian ratio at e14.5

The mapping strategies employed to locate the integration site of the β-*geo* cassette in the *Grb10KO* allele, utilised DNA purified from *Grb10KO*$^{m/p}$ embryos (Section 3.2.1). Embryos isolated from *Grb10KO*$^{m/+}$ x *Grb10KO*$^{m/+}$ crosses were genotyped initially on the basis of *LacZ* reporter expression. Those reporting expression from both the maternally- and paternally-inherited alleles appeared to occur infrequently at e14.5. This was initially attributed to the limitation of genotyping embryos in this manner, in which reporter expression in the brain can be obscured by that in the surrounding mesodermal tissue.

Identification of the β-*geo* cassette integration site permitted derivation of a genotyping strategy which could discriminate between the wild type and *Grb10KO* alleles, thus enabling definitive identification of heterozygous and homozygous embryos. The genotyping strategy utilised primer Set B (Figure 3.2*a* and *b*) to indicate the presence of a wild type allele. The forward primer of Set B with a reverse primer in the β-*geo* cassette (β-R1; Figure 3.2*a*) were used to amplify from the *Grb10KO* allele. Table 3.1 presents the numbers of offspring of each genotype isolated at e14.5 from *Grb10KO*$^{m/+}$ x *Grb10KO*$^{m/+}$ crosses. Chi-squared analysis confirmed that the ratio of genotypes deviated significantly from that expected under Mendelian laws of inheritance ($p = 0.017$). Chi-squared analysis (not shown) performed on the same data set, but excluding *Grb10KO*$^{m/p}$ embryos, confirmed that the ratio of wild type and heterozygous animals conformed to that expected ($\chi^2 = 0.8$; $p = 0.670$), implying a lethality effect in *Grb10KO*$^{m/p}$ conceptuses.

3.2.5 The *Grb10KO* allele is predicted to give rise to a truncated Grb10 polypeptide

Intriguingly, mice inheriting two copies of the *Grb10Δ2-4* allele do conform to the expected Mendelian ratio (Table 3.2; $p = 0.709$, Chi-squared analysis), and have been studied, as adults, in metabolic experiments (Smith *et al*, 2007). The complete ablation of functional Grb10 protein is, therefore, an insufficient explanation for the scarcity of *Grb10KO*$^{m/p}$

Table 3.1 – Number of offspring of each genotype produced from *Grb10KO*$^{m/+}$ x *Grb10KO*$^{m/+}$ crosses at e14.5

Isolated embryos were initially screened for *LacZ* reporter expression to identify those with the *Grb10KO*$^{+/p}$ genotype. Tissue biopsies were genotyped by PCR as described in the text to differentiate *Grb10KO*$^{m/p}$ from *Grb10KO*$^{m/+}$ embryos ($\chi^2 = 10.19$; $p = 0.017$).

Genotype	Observed number of embryos	Expected number of embryos

Table 3.2 – Number of offspring of each genotype produced from *Grb10Δ2-4*$^{m/+}$ x *Grb10Δ2-4*$^{m/+}$ crosses surviving to adulthood

Adult mice from *Grb10Δ2-4*$^{m/+}$ x *Grb10Δ2-4*$^{m/+}$ crosses were genotyped from ear biopsies by PCR as described in Smith *et al*, 2007 ($\chi^2 = 0.6875$; $p = 0.709$). Refer to Table 2.1 for relevant primer sequences.

Genotype	Observed number of mice	Expected number of mice

a

Exon 7

GAUGUCAAAGUCUUUAGUGAAGAUGGGACCAGCAAAGUGGUGGAGAU

--D--V--K--V--F--S--E--D--G--T--S--K--V--V--E--

UCUAACCGACAUGACAGCCAGGGACCUGUGCCAGCUGCUGGUUUACA

I--L--T--D--M--T--A--R--D--L--C--Q--L--L--V--Y-

AAAGUCACUGUGUGGAUGACAACAGCUGGACUCUGGUGGAACACCAC

-K--S--H--C--V--D--D--N--S--W--T--L--V--E--H--H

CCACAACUGGGAUUAGGUCCCAGGUCCCGAAAACCAAAGAAGAAGAA

--P--Q--L--G--L--G--P--R--S--R--K--P--K--K--K--

CGCAGAUCGCAUCGAUAACUUCGUAUAG

N--A--D--R--I--D--L--F--V--STOP

b

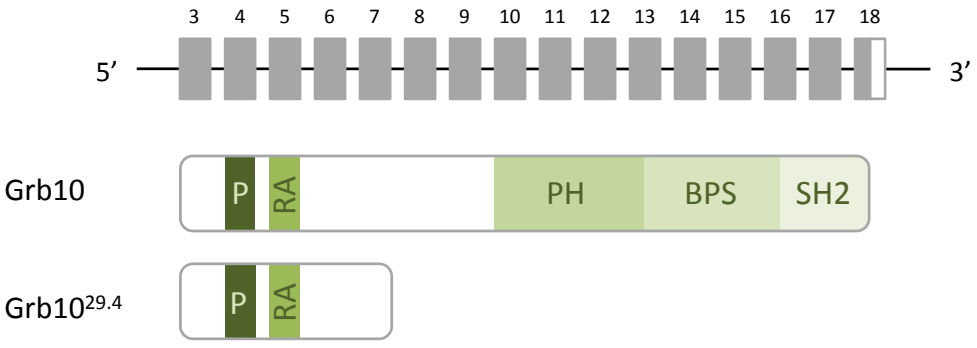

embryos at e14.5. Mapping of the two gene-trap alleles, however, revealed a key difference. Integration of the β-*geo* cassette in *Grb10KO* is downstream of the endogenous translational start site in exon 3, whereas this has been abolished in *Grb10Δ2-4* (Figure 3.3*a*). Therefore, whilst the *LacZ* reporter is under the control of the endogenous *Grb10* promoter in both transgenic alleles, only the *Grb10KO* allele would be expected to produce a *Grb10-LacZ* fusion protein. The presence of an in-frame stop codon created by gene-trap integration might terminate translation early for a subset of transcripts arising from the *Grb10KO* locus, potentially producing a truncated Grb10 protein species. Clearly, such premature termination could not occur for all transcripts, given the ability of *LacZ* to report sites of *Grb10* expression. This 'skipping' of a stop codon is referred to as translational read through, and has been documented at several loci in mammals, as well as bacteria and yeast (Williams *et al*, 2004; Tate *et al*, 1995).

The size of such a truncated protein species was predicted from the known sequence of the *Grb10KO* allele, based on the position of the first in-frame stop codon downstream of exon 3 (Figure 3.5*a*). This analysis predicted a polypeptide of 267 amino acids, consisting of 248 residues to the 3' end of exon 7 in the endogenous *Grb10* sequence, and an additional 19 residues from the β-*geo* cassette. The molecular weight of such a species was predicted to be ~29.4 kDa, assuming a mean molecular weight of 110 per amino acid molecule, and is herein referred to as $Grb10^{29.4}$. The only functional motifs predicted within this translated sequence would be the proline-rich and Ras-associating domains (Figure 3.5*b*).

Western blotting of whole wild type, *Grb10Δ2-4*$^{m/+}$ and *Grb10KO*$^{m/+}$ neonate lysates was performed, using a N-terminal antibody raised against Grb10, aiming to detect this truncated protein species. Such a protein should be absent from wild type and *Grb10Δ2-4*$^{m/+}$ samples. Western blotting failed to detect this predicted protein (data not shown).

3.2.6 $Grb10^{29.4}$ may be biallelically expressed in the developing heart

As embryos inheriting just one copy of *Grb10KO* from either parental line were viable, it followed that this truncated molecule must only confer lethality when present as two copies. The imprinted nature of *Grb10* restricts the number of sites at which biallelic expression would permit sufficient levels of $Grb10^{29.4}$ for such an effect. The scarcity of foetuses homozygous for *Grb10KO* at e14.5 implied a site of biallelic expression prior to this developmental stage. Sanz *et al* (2008) describe expression of *Grb10* from the paternally-derived allele at the anterior visceral endoderm (AVE), an early patterning centre partly responsible for establishing anterior-posterior polarity (Thomas and Beddington, 1996). It is unclear from this published work whether AVE expression is exclusively from this allele, or if there is also a contribution from the maternally-inherited copy.

To address this issue, *LacZ* reporter expression was examined in e8.0 embryos inheriting the *Grb10KO* allele from one parent. Examination of whole embryos revealed apparently widespread expression in foetal tissue from the maternally-derived allele, whereas the paternal contribution was localised to a population of cells close to the early headfold

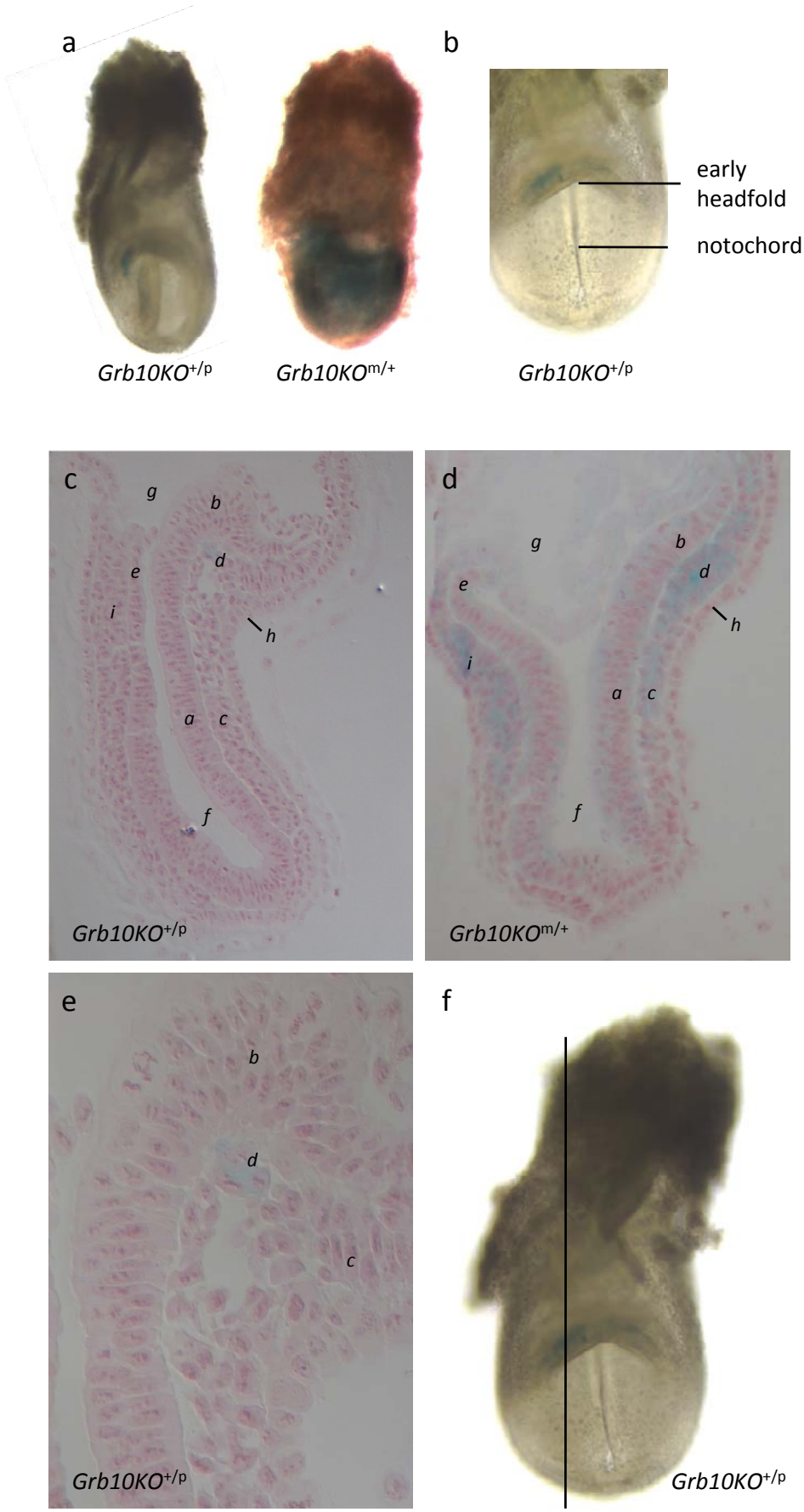
a
b
early
headfold
notochord
Grb10KO+/p
Grb10KOm/+
Grb10KO+/p
c
g
b
d
e
i
h
a
c
f
Grb10KO+/p
d
g
b
d
e
h
i
a
c
f
Grb10KOm/+
e
b
d
c
Grb10KO+/p
f
Grb10KO+/p

region (Figure 3.6*a* and *b*). These stained embryos were resin-embedded, sagittally-sectioned and counter-stained with nuclear fast red to permit a more detailed analysis of reporter expression. Sectioning of both embryos revealed a morphology consistent with Theiler Stage late 11/early 12. The *Grb10KO*$^{+/p}$ embryo showed a more marked headfold than the *Grb10KO*$^{m/+}$ embryo (Figure 3.6*c* and *d*), suggesting the *Grb10KO*$^{+/p}$ conceptus was further developed by a few hours. *LacZ* expression from the paternally-derived allele was indeed restricted to a few cells (position of the sections shown is illustrated in Figure 3.6*f*). However, the position of these cells was inconsistent with the location of the anterior visceral endoderm, being situated in the mesodermal layer adjacent and posterior to the presumptive neural ectoderm (Figure 3.6*e*). These cells represented endocardial or myocardial cells of the heart tube, the primordia of the embryonic heart. Expression appeared strongest in the right heart tube (Figure 3.6*b*), suggesting a possible involvement of Grb10 in establishing or maintaining left-right asymmetry in this tissue.

Reporter expression was readily detected in the mesodermal layer of the sectioned *Grb10KO*$^{m/+}$ embryo (Figure 3.6*d*). Expression was strongest in the anterior mesoderm, becoming weaker towards the centre of the embryo, but could also be readily detected in the posterior mesoderm. Anterior mesodermal cells were presumed to include those of the developing heart tube, and the strong β-galactosidase activity detected in all cells in the region suggested *Grb10* may be biallelically-expressed in this structure. No reporter expression was apparent in the AVE, although weak activity could be detected in a subset of ectodermal cells.

3.2.7 *Grb10KO*$^{m/p}$ embryos are viable at e7.5

To help elucidate the mechanism responsible for embryonic lethality in *Grb10KO*$^{m/p}$ conceptuses, the viability of embryos at e7.5 was examined. Embryos were collected from *Grb10KO*$^{m/+}$ x *Grb10KO*$^{m/+}$ crosses and genotyped by PCR as described in Section 2.1.3. Table 3.3 presents the number of embryos of each genotype generated in these crosses. Chi-squared analysis confirmed no significant deviation from the expected ratios, implying that all genotypes were viable at this developmental stage ($p = 0.243$).

Table 3.3 – Number of offspring of each genotype produced from *Grb10KO*$^{m/+}$ x *Grb10KO*$^{m/+}$ crosses at e7.5

Embryos from *Grb10KO*$^{m/+}$ x *Grb10KO*$^{m/+}$ crosses were isolated at e7.5 and genotyped by PCR, as described in the text ($\chi^2 = 2.83$; $p = 0.243$).

Genotype	Observed number of embryos	Expected number of embryos

3.3 Discussion

Despite numerous biochemical and *in vitro* studies of Grb10 identifying potential binding partners and implicating the protein in various intracellular signalling cascades, the relevance of these interactions to physiological processes require further investigation. Indeed, many such assays have demonstrated the involvement of Grb10 in insulin signalling, an example for which there is support for a corresponding *in vivo* role, yet at face value even these studies fail to agree on whether Grb10 is a positive or negative modulator. Chinese hamster ovary cells over-expressing human *Insr* (CHO/IR) exhibited reduced tyrosine phosphorylation of two downstream effector molecules, insulin receptor substrate-1 (IRS-1) and GTPase-activating-protein-associated protein, following insulin stimulation, when *Grb10* was stably transfected and expressed (Liu *et al*, 1995). The reduced activity of these effector molecules implied a role for Grb10 in attenuation of insulin signalling, and was corroborated by the increased tyrosine phosphorylation of IRS-1 in muscle of *Grb10Δ2-4*$^{m/+}$ mice (Smith *et al*, 2007). Further *in vitro* analyses provided a mechanistic basis for this role, demonstrating reduced insulin-stimulated IR ubiquitination and internalisation following RNAi-mediated suppression of endogenous Grb10 (Ramos *et al*, 2006). Conversely, Wang *et al* (1999) implicated Grb10 as a positive mitogenic mediator of insulin signalling. NIH/3T3 fibroblasts, over-expressing the human IR, were micro-injected with the Grb10-SH2 domain as a dominant negative competitor of endogenous Grb10-mediated signalling. Following a period of starvation, insulin treatment of these cells failed to stimulate DNA synthesis at a rate comparable with micro-injected controls. This effect of Grb10-SH2 was explained as an interference with normal mitogenic signalling, mediated by the full-length Grb10 protein.

Such shortcomings of *in vitro* experimentation can be often be addressed using *in vivo* models. Transgenic models are often the most valuable, in which a specific gene or regulatory element can be manipulated, phenotypic consequences observed and the subsequent normal function elucidated. This is the case for mice inheriting the *Grb10Δ2-4* allele, used to demonstrate both the developmental and metabolic effects of *Grb10* expressed from the maternally-derived allele in peripheral tissues (Charalambous *et al*, 2003; Smith *et al*, 2007). However, the integrated *LacZ* reporter in this transgenic model did not fully recapitulate endogenous *Grb10* expression, failing to match immunohistochemical detection of Grb10 protein in the brain. Integration of the *LacZ* reporter elsewhere at the locus, generating the *Grb10KO* allele, did confirm expression in the CNS, but only following inheritance through the paternal line (Garfield *et al*, submitted). In contrast to its role in peripheral tissues, Grb10 was shown to modulate social dominance in the brain.

To confirm that the *LacZ* gene in *Grb10KO* was indeed reporting *Grb10* expression, and that ablation of transcripts at this locus was responsible for the observed social dominance phenotype, it was first necessary to map the integration site of the β-*geo* cassette. Southern blotting and PCR-based strategies identified a deletion of 12 bp of the endogenous sequence at the exon 8/intron 8 boundary, which were replaced by the β-*geo*

cassette. Such a short deleted sequence is in contrast with the ~38 kb removed in the generation of the *Grb10Δ2-4* allele (Charalambous *et al*, 2003), but is more consistent with the integration of the β-*geo* cassette at other loci (for example, Beigneux *et al*, 2006). Interestingly, two other studies have described the insertion site in *Grb10KO*, with both reporting integration in intron 7 (Wang *et al*, 2007; Sanz *et al*, 2008), inconsistent with that identified in the present study. However, few published details of the mapping experiments are provided in the latter publication, whilst those described in Wang *et al* (2007) rely solely upon 5' RACE sequencing, demonstrating splicing of the *LacZ* reporter onto exon 7. No mapping at the level of genomic sequence is reported. Indeed, the absence of exon 8 in transcripts initiating at the *Grb10* promoter from the *Grb10KO* allele is initially surprising, but can be most likely accounted for by the strength of the β-*geo* splice acceptor sequence, which might out-compete that of exon 8 for recognition by spliceosomes. The 3' splice acceptor sequences do differ for exon 8 and β-*geo*. Whilst the consensus sequence is 10 consecutive pyrimidine residues, followed by any base (N), then a cytosine (C) and invariably adenine-guanine (AG), the acceptor sequence for exon 8 consists of only 8 initial pyrimidines. β-*geo*, on the other hand, possesses an initial run of 8 pyrimidines, but this run is interrupted by two guanines. The close physical proximity of the two acceptor sequences, and the possibility that this sequence difference increases the probability of spliceosome recognition for β-*geo*, might account for the absence of exon 8 in transcripts from the *Grb10KO* allele. Although 825 bp at the 5' extreme of the β-*geo* cassette were deleted during integration, the splice acceptor sequence was fully retained, and thus the deletion does not apparently affect its ability to splice, a result supported by both 5' RACE and visualisation of reporter gene activity.

The failure of RNA polymerase to generate full-length transcripts from the *Grb10KO* allele, thus demonstrating the efficacy of the gene-trap, was confirmed by Northern blotting. Consistent with previous reports, the majority of embryonic expression during mid-gestation arose from the maternally-inherited allele, although a contribution from the paternally-derived copy was also detected, presumably representing transcripts in the CNS and other specific peripheral tissue sites. The detection of a ~2.5 kb transcript from both embryonic and placental RNA isolates cannot be explained by the current literature, implying an as-yet uncharacterised transcript variant of *Grb10*. This might be produced from an alternative transcription initiation site, or arise through splicing out of several exons, although at least some of exons 11 to 16 must remain to be detected by the probe. Alternatively, a weak poly-(A) signal within an exon might cause premature termination in a subset of transcripts. Whilst elucidation of the structure and function of the ~2.5 kb transcript would be of interest, it is important to note that its contribution to the *Grb10* transcript pool is relatively small. Additionally, the effective ablation of this transcript in *Grb10KO*$^{m/+}$ embryos discounts the possibility of redundancy with full-length Grb10 influencing functional characterisation of the protein.

The reversal of the *Grb10* imprint in both the developing and adult mouse CNS has thus far been demonstrated only by use of the *LacZ* reporter gene. To confirm this result at the genetic level, Northern blotting was performed on adult brain tissue, with full-length *Grb10* transcripts being readily detected in wild type and *Grb10KO*$^{m/+}$ brain, but undetected in

Grb10KO$^{+/p}$ brain, a pattern opposite to that demonstrated in whole embryo. These results support the recent demonstration of biased expression from the paternally-derived allele in human foetal brain and spinal cord (Monk *et al*, 2009). Interestingly, expression in other human foetal tissues is apparently biallelic, an observation inconsistent with that observed in mouse. This might be attributable to the differences in mating habits of mouse and human. A female of the former species will carry litters of multiple paternities throughout her lifetime, and thus there is an evolutionary argument for antagonism between the two parental genomes (see Section 1.1.2 for further details of the parental conflict hypothesis). Multiple paternities are less frequent in humans, with a single male generally siring the offspring of one female, and thus the basis for conflict is reduced. Alternatively, the limitations of assessing allele-specific expression using RT-PCR, which is highly susceptible to contamination and may amplify a low level of leakage from the 'silent' allele, might mask the retention of *Grb10* imprinting in humans.

Disrupting the expression of *Grb10*, using either *Grb10KO* or *Grb10Δ2-4*, did not affect expression of the neighbouring gene *Ddc*, at least in adult brain. This was predicted as the germline differentially methylated region (DMR) at the *Grb10* locus, shown also to regulate *Ddc* imprinting (Shiura *et al*, 2009), is not removed in either allele, and indeed the imprinting status of *Grb10* itself is not disrupted. Additionally, only a specific transcript of *Ddc*, referred to as *Ddc_exon1a*, is imprinted, and expression is localised to trabecular cardiomyocytes in the developing heart (Menheniott *et al*, 2008). Indeed, no parent-of-origin specific expression was detected in neonatal brain. Although both the *Ddc* and *Ddc_exon1a* transcripts are ~2 kb, the probe used in Northern blotting also detected a higher molecular weight transcript in all RNA samples. A similar species was previously detected in Northern blotting for *Ddc* (Menheniott *et al*, 2008) although its nature was not described. The transcript probably represents a variant of *Ddc*, because its expression profile during development mirrors that of the full-length message (Menheniott *et al*, 2008), and could be a result of poly-(A) run-on.

The demonstration that both the *Grb10KO* and *Grb10Δ2-4* alleles ablate functional Grb10 protein suggested that mice inheriting either of these alleles through the same parental line would display identical phenotypes. One difference, the inability of *Grb10Δ2-4* to report expression in the CNS, has already been observed, and is the subject of Chapter Five. However, the observation that embryos homozygous for the *Grb10KO* allele deviated significantly from the predicted Mendelian ratio at e14.5, supported through both *LacZ* staining experiments and PCR genotyping, was unexpected given that *Grb10Δ2-4*$^{m/p}$ animals are viable (Smith *et al*, 2007). This observation was also reported by another group utilising mice carrying the *Grb10KO* allele, but no mechanistic explanation was provided (Cao *et al*, 2008). Integration of the β-*geo* cassette in *Grb10KO* is 3' to the translation initiation site, which is deleted in *Grb10Δ2-4*, therefore potentially enabling a small protein species to be generated. Identification of the first in-frame stop codon in the β-*geo* cassette sequence predicted a ~29.4 kDa protein, referred to as Grb10$^{29.4}$. This protein could not be detected in lysates of *Grb10KO*$^{m/+}$ neonates using Western blotting. This might reflect a high turnover of the protein species, or its accumulation in a tissue- and/or stage-specific manner. Alternatively, the result might be a consequence of the limitations of the antibodies

employed. The majority of antibodies commercially-available for Grb10 and described in the literature are raised against the C-terminus of the protein, and were thus inappropriate for detection of Grb10$^{29.4}$. Two N-terminal antibodies were sourced but these failed even to differentiate between wild type and *Grb10KO*$^{m/+}$ samples for full-length Grb10, suggesting non-specific epitope recognition. An alternative approach might be to perform immunoprecipitation using an antibody raised against proline-rich domains, for example, followed by Western blotting for the Grb10 N-terminus, thereby reducing the number of protein species blotted and possibly eliminating some of the non-specific detection. It might also be valuable to examine protein lysates from various tissues and developmental stages.

If the only functional domains of Grb10$^{29.4}$ are a proline-rich region and a Ras-associating domain, this might sequester intracellular signalling molecules, preventing their interaction with upstream regulators or downstream targets which would otherwise be brought into close proximity by binding to other domains of Grb10. GIGYF1 and GIGYF2 were identified in a yeast two-hybrid assay using the N-terminus of Grb10 as bait, including the proline-rich region but not other conserved structural motifs (Giovannone *et al*, 2003). In fibroblasts over-expressing *Igf1r*, stimulation with IGF1 increases Grb10-GIGYF1/2 interaction above the basal state, and this complex transiently binds to the IGF1R, suggesting GIGYF1 and GIGYF2 modulate IGF1 signalling via Grb10 (Giovannone *et al*, 2003). The interaction between Grb10 and the IGF1R has been demonstrated in many studies (reviewed in Morrione, 2003) and occurs through the SH2 and BPS domains of Grb10 (He *et al*, 1998; Stein *et al*, 2001). Conceivably, Grb10$^{29.4}$, which lacks the SH2 and BPS domains, might sequester GIGYF molecules and prevent their regulation of IGF1 signalling, potentially disrupting development.

If this system is to explain the lethality of *Grb10KO*$^{m/p}$ conceptuses, it must be correlated to dosage. Embryos inheriting the transgenic allele from either parent are viable and born with the expected frequency, suggesting monoallelic expression of Grb10$^{29.4}$ is compatible with life. Given the imprinted nature of *Grb10*, a 'double dosage' can only occur at one of the few sites of biallelic expression. We considered the anterior visceral endoderm as a candidate site, for which expression from the paternally-inherited allele has previously been described (Sanz *et al*, 2008), but a contribution from the opposite allele not discounted. *LacZ* staining of a *Grb10KO*$^{+/p}$ embryo at e8.0, however, was inconsistent with expression at this anterior signalling centre, instead localising to the myocardial or endocardial cells of the heart tube. Analysis of *LacZ*-stained whole embryos essentially recapitulated that described in Sanz *et al* (2008), suggesting a misinterpretation of the site as AVE, rather than aberrant reporter expression. Indeed, it was only possible to identify the mesodermal origin of these cells following sectioning of stained embryos. Heart tube expression was further supported by comparison with mouse embryos harbouring a *LacZ* gene driven by the *Xenopus* MLC2 promoter, a gene encoding a regulatory myosin light chain of the cardiac muscle contraction apparatus (Latinkić *et al*, 2004). At e7.5, the expression profile was very similar to that observed for *Grb10* at e8.0, although *Grb10* appeared to be more localised to the right heart tube, implying a possible role in the establishment or maintenance of left-right asymmetry in this structure. This observation is

consistent with reporter expression from the paternally-derived allele being restricted to a subset of cardiomyocytes in the developing right ventricle at e14.5, but not the left (Garfield, 2007).

Reporter expression in a *Grb10KO*$^{m/+}$ embryo was more widespread in the mesodermal layer than that observed for the *Grb10KO*$^{+/p}$ embryo. Importantly, this included strong reporter expression in the anterior mesoderm, presumed to include the myocardial and endocardial cells of the heart tube. This is consistent with the observation that expression from the maternally-inherited allele is widespread in the heart at e14.5, being strongest in the myocardial cells of the atria and ventricles (Garfield, 2007). Given this, it is likely that the right heart tube may represent a site of biallelic expression of *Grb10* in wild type conceptuses, and of *Grb10*$^{29.4}$ in *Grb10KO*$^{m/p}$ conceptuses. This might account for the lethality associated with homozygosity for the *Grb10KO* allele.

The majority of signals stimulating development of the heart tube are members of the Wnt, FGF and BMP families, with which Grb10 has not previously been implicated. However, the expression profile of vascular endothelial growth factor (VEGF) includes myocardial and some endocardial cells of the heart tube, first apparent at e8.5 (Miquerol *et al*, 1999), although it is interesting to note that *Grb10* expression is detected earlier than this. An interaction between Grb10 and VEGF receptor 2 (VEGF-R2) has been demonstrated *in vitro*, with Grb10 positively promoting downstream signalling cascades (Giorgetti-Peraldi *et al*, 2001). At e14.5, VEGF expression is detected strongly in the ventricles and weakly in the atria, being mostly restricted to myocardial cells, similar to *Grb10*. VEGF signalling therefore represents a candidate pathway disrupted by the dominant negative protein isoform in *Grb10KO*$^{m/p}$ foetuses. The direct interaction between VEGF receptors and Grb10 requires an intact SH2 domain (Giorgetti-Peraldi *et al*, 2001), which Grb10$^{29.4}$ lacks. However, VEGF influences a number of cellular processes through VEGF-R2, including gene transcription in a pathway reliant on Ras (Meadows *et al*, 2001). *Vegfr2*$^{-/-}$ embryos die by e8.5-9.5, exhibiting defects in the development of endothelial and haematopoietic precursors, suggestive of an important role in vascular development (Shalaby *et al*, 1995). However, this receptor is also expressed in the heart tube at e7.5 (Yamaguchi *et al*, 1993). Heart-specific ablation of *Vegfr2* has not been reported, but this might confer lethality at a later stage. If a sufficient dose of Grb10$^{29.4}$ sequesters Ras, preventing VEGF signalling in the heart, this might represent the mechanism by which *Grb10KO* homozygosity confers lethality.

The only proteins identified to-date to interact with the proline-rich domain are GIGYF1 and GIGYF2. These proteins are modulators of IGF1 signalling and have not been associated with events downstream of the VEGF receptors. An anti-apoptotic role for IGF1 has been documented in cultured rat cardiomyocytes (Wang *et al*, 1998), and has also been shown to stimulate adult myocardial stem cell regeneration (reviewed in Opgaard and Wang, 2005). Whether IGF1 signalling is important for stem cell differentiation or to prevent apoptosis in the developing heart remains unclear, but might represent another candidate pathway for disruption by Grb10$^{29.4}$.

Whilst these pathways might be perturbed by expression of Grb10$^{29.4}$ from both parental chromosomes, this does not necessarily implicate Grb10 in these pathways during normal heart development. Nonetheless, the biallelic expression of *Grb10* in the right heart tube is intriguing, and is certainly suggestive of a role in mediating one or more signalling cascades in this tissue. Grb10 is not crucial for heart development because *Grb10Δ2-4*$^{m/p}$ embryos survive to adulthood at the expected Mendelian ratio.

It would be valuable to examine heart development in *Grb10KO*$^{m/p}$ embryos. An initial analysis might involve the use of a marker (e.g. *Nkx2.5* (Komuro and Izumo, 1993)) in *in situ* hybridisation to assess morphology. Perhaps compartmentalisation fails to occur. This would be consistent with the apparent asymmetric expression of *Grb10*, which might be required to establish, during looping of the heart tube, or maintain the structural differences between the left and right heart. Additionally, further analysis of the developmental time point of lethality would help to underpin the mechanism responsible, although viability at e7.5 is consistent with an incorrectly developed heart being the cause. Mice mutant for *Nkx2.5*, a master transcription factor required for correct heart formation, die at e9.0-10.0, due to the failure of looping morphogenesis which creates the left-right asymmetry of the organ (Lyons *et al*, 1995). The apparent localisation of *Grb10* to the right heart tube might also imply incorrect looping in *Grb10KO*$^{m/p}$ conceptuses. Thus, e10.0 might be the next developmental time point at which to examine the viability of mutant embryos.

The genetic characterisation of the *Grb10KO* allele has enabled a clear demonstration of its ability to accurately report parent-of-origin-specific expression, and has confirmed the opposite imprint between the central nervous system and peripheral tissues. Detailed knowledge of the allelic structure has also aided in the explanation of a key phenotypic difference between mice inheriting the *Grb10KO* and *Grb10Δ2-4* alleles. Other phenotypic differences are discussed in subsequent Chapters and are explained in the light of this knowledge.

Chapter Four

Expression and function of Grb10 *in the mature mouse placenta*

4.1 Introduction

The placenta is a transient organ arising from extra-embryonic cell lineages, which is essential to support development of the foetus in eutherian mammals. Placental cell lineages arise very early in mouse development, with trophectoderm and extra-embryonic ectoderm cells differentiating even before implantation. The function of the placenta is to mediate interactions between the developing foetus and the mother in two ways. Firstly, the placenta must permit the transfer of nutrients from mother to foetus, and the simultaneous transfer of waste products from foetus to mother. To this end, it has evolved as a highly efficient exchange barrier. The foetal circulation is intimately associated with the placenta; a network of endothelium-bound capillaries branches out from the chorionic plate into the labyrinth and are connected to the foetus by the umbilicus. Maternal blood flows through spaces not bound by an endothelium, but directly contacts cytotrophoblast cells of embryonic origin. In this way, foetal and maternal blood never make contact, but are separated by just three cell layers (excluding the foetal endothelium). Nutrients can be extracted from the maternal blood into the foetal circulation through four mechanisms: solvent drag describes the process through which solutes are transported across membranes by the flow of water; endo- and exocytosis involve the internalisation and subsequent release of membrane-bound proteins; diffusion of hydrophilic molecules can occur across cell membranes; and transporter molecules can actively pump substrates across (Sibley and Boyd, 1988). Paracellular diffusion and active transport are probably the most significant mechanisms for nutrient transfer across the placenta (Sibley *et al*, 1997).

The second key function of the placenta is as an endocrine organ. A range of hormones, including members of the prolactin and growth hormone families, are released from the placenta into both the foetal and maternal blood circulations. Crucially, these hormones help stimulate the preparations necessary in the mother for the processes of birth and lactation. This system of communication between tissues of embryonic origin and the mother is discussed in more detail later.

The structure of the human placenta is somewhat different to that of the murine placenta, although the function is identical (reviewed in Cross *et al*, 2003). In both cases, the uterine epithelium (endometrium) is invaded such that maternal blood can flow into the placenta. This invasion is achieved by trophoblast giant cells in mouse, and extravillous cytotrophoblast cells in human. The maternal blood makes direct contact with trophoblast cells. The three trophoblast layers of the mouse placenta (one layer of mononucleated, cuboidal cytotrophoblast cells, plus two layers of syncytiotrophoblast) contrast with the single syncytial layer and underlying trophoblast stem cell layer of humans. This means that there are four membranes lying between the maternal and foetal blood in humans, with a six membrane exchange barrier in mouse.

The ability of a placenta to transfer nutrients from the maternal to the foetal circulation is dependent upon five key factors, reviewed here briefly. First, the size of the placenta is directly correlated to the surface area available for nutrient exchange and thus its

efficiency. Larger embryos and neonates are associated with increased placental wet weights in a range of species, including mouse (Fowden, 2006). However, the size of the placenta can, in turn, be dictated by the demands of the foetus, as well as environmental factors. Nutritional restriction in pregnant sheep during mid-gestation, when the placenta shows the most rapid growth, reduces placental expansion, but towards the end of gestation, the placenta compensates by becoming larger than those of sheep with sufficient access to nutrients (Oliver *et al*, 2005). Such a compensation is presumably demanded by the foetus at a critical point to prevent abortion.

The morphology of the placenta can also dramatically influence nutrient transfer capacity. Indeed, the mouse placenta achieves its maximum wet weight at e16.5, but the labyrinth continues to expand up to e18.5, with a concomitant reduction in the proportion of the placenta occupied by the junctional zone (Coan *et al*, 2004). This correlates with increased foetal growth until term. Additionally, the barrier thickness between the maternal blood and foetal blood circulation is reduced between mid- and late-gestation, effectively increasing the theoretical diffusion capacity of the mouse placenta by 15- to 20-fold (Coan *et al*, 2004).

As the transfer of some molecules is dependent on active transport, the availability of transporter molecules, as well as their affinity and localisation, also influences placental efficiency. The system A transporter family, one member of which is encoded by the imprinted gene *Slc38a4* (Smith *et al*, 2003), transfers small amino acids, whilst glucose is transferred by the GLUT1 and GLUT3 glucose transporters. The activities and expression levels of each of these transporters can be influenced by both hormonal and environmental stimuli.

Although often overlooked, the placenta itself requires nutrients and oxygen to perform its functions. Like the foetus, it must rely on nutrients extracted from maternal blood. Remarkably, ruminant placental tissues utilise 50-70 % of the glucose and oxygen taken up by the uterus (Fowden, 1997). This is required for the metabolic activities of the placenta, which include secondary active transport and amino acid deamination to supply the foetus with essential amino acids. The metabolic efficiency of the placenta therefore affects its nutrient transfer efficiency.

Finally, hormones of placental origin are key in regulating placental efficiency. Progesterone and placental lactogen, for example, promote maternal glucose delivery to the foetus. Proliferin is produced in the mid-gestation human placenta and secreted into the maternal and foetal circulations (Jackson *et al*, 1994). This hormone has angiogenic properties, and thus promotes blood flow, improving the conditions for nutrient exchange. Whilst proliferin is a circulating hormone and can potentially have a wide range of targets, at least part of its effects are realised locally. Evidence for a paracrine signalling effect includes the expression of proliferin receptors on labyrinth endothelial cells (Jackson *et al*, 1994). In such a manner, these hormones affect the rate of nutrient transfer and thus regulate placental efficiency.

As well as this direct mediation of placental efficiency, hormones produced by the placenta have a broader role in the communication between foetus and mother. For example, prolactin is secreted from the rat decidua and supplements pituitary prolactin levels, maintaining progesterone secretion by the corpus luteum. In turn, progesterone promotes maternal weight gain and fat deposition (Grueso *et al*, 2001; Freemark, 2006). Decidual prolactin also performs a paracrine function, suppressing the expression of genes detrimental to pregnancy within the decidua (Bao *et al*, 2007). Placental lactogens, secreted from the syncytiotrophoblast of the human placenta (McWilliams and Boime, 1980), target a range of maternal organs, preparing them for birth and lactation. One obvious target is the mammary gland, in which ductal branching is stimulated to permit milk synthesis and let-down after birth (Thordarson *et al*, 1986). However, placental lactogens also stimulate regions of the brain; this includes the generation of new olfactory interneurons, most likely to promote recognition of offspring by smell, critical for rearing (Shingo *et al*, 2003). Placental lactogens also promote maternal care behaviours (Bridges *et al*, 1996). The placenta is thus important in priming the mother for rearing.

Genes subject to genomic imprinting appear to play central roles in controlling the supply of, and demand for, maternal nutrients. Paternally-expressed *Igf2* is a classic paradigm, whose role has been elegantly demonstrated by both *in vivo* knockout and over-expression studies. *Igf2* is expressed in all extra-embryonic cell types of the mature mouse placenta, a significant proportion of which is derived from a placental-specific promoter element, *P0*. These *Igf2P0* transcripts are particularly abundant in the placental labyrinth (Constância *et al*, 2002). Their significance to the total pool of *Igf2* is clearly apparent given that *Igf2P0*-specific knockout mice exhibit a placental growth restriction very similar to that of total *Igf2* null animals (DeChiara *et al*, 1991; Constância *et al*, 2002; Reik *et al*, 2003). The growth restriction is dramatic, with a 30-40 % reduction in placental wet weight. Conversely, *Igf2* over-expression engenders placentomegaly. This is most dramatically achieved in transgenic mouse models exhibiting loss of imprinting of *Igf2* together with ablation of *Igf2r*, which degrades excess IGF2; in such cases, placentae can range from 140 % to 230 % of the wild type mass (Eggenschwiler *et al*, 1997).

Whilst the loss of *Igf2P0* from the placenta is associated with both placental and foetal growth restriction, there is not a linear correlation between the two. Placental growth restriction is observed from e11.5 onwards, with foetal growth retardation not manifesting until the end of gestation (96 % and 78 % of wild type foetuses at e15.5 and e18.5, respectively; Constância *et al*, 2002). These data implied that *Igf2P0* null placentae are more efficient during mid-gestation. To address the exchange properties, radiolabelled tracer compounds were injected into the jugular vein of a pregnant female mouse, and foetuses harvested 1-5 minutes later. Following homogenisation of the embryos, the activity of the radiolabelled tracer was detected using a scintillation counter, thus providing a method for quantitatively assessing placental transfer capacity. Gravid females at e15.5, at which stage the *Igf2P0* null placenta is smaller but the embryo is similar to wild type, and at e18.5, when both are significantly smaller than wild type, were injected with ^{51}Cr-EDTA and ^{14}C-MeAIB. ^{51}Cr-EDTA is a hydrophilic molecule, and can be used as a measure of passive diffusion through the placenta. ^{14}C-MeAIB is an amino acid analogue, which cannot

be metabolised, and is specifically transported by the system A transporter in the placenta. Within embryos at e15.5, the accumulation of ^{51}Cr-EDTA, measured as units per gram of placenta, was 80 % that of wild type controls. This was reduced to 60 % of wild type controls at e18.5, suggesting that passive permeability is severely reduced in *Igf2P0* null placentae, presumably a consequence of reduced placental size. However, the accumulation of ^{14}C-MeAIB in mutant embryos was 155 % that of wild type controls at e15.5, when considered per gram of placenta. In effect, this resulted in mutant embryos receiving the same actual amount of the amino acid analogue as wild types, consistent with them being a similar size. This was reduced to 116 % of wild type levels per gram of placenta at e18.5, equating to 74 % of the actual amount received by wild type foetuses. This correlated with the foetal growth restriction recorded at this stage. Thus, whilst passive permeability is reduced in *Igf2P0* null placentae, the increased efficiency of secondary active transport compensates at the earlier stage of gestation, maintaining foetal mass. At the later stage, this compensation is insufficient to meet foetal demands, resulting in growth retardation. This compensation appears to be achieved by promotion of both amino acid and glucose transport (Constância *et al*, 2005).

These data imply two key points: 1) that the foetus can demand more nutrients following placental growth restriction; and 2) that the placenta is able to respond to this demand. Imprinted genes have also been implicated in this process. Indeed, IGF2 itself is probably part of this mechanism. *In vitro* experiments have demonstrated that exogenous IGF2 can promote amino acid transport in labyrinthine trophoblast cells in culture (Karl, 1995). This suggests that the placenta can differentiate between IGF2 produced within the organ and that produced by the foetus, possibly through the positioning of receptors on the syncytiotrophoblast membrane. One prediction of this hypothesis is that mice lacking functional *Igf2* in the embryo as well as the placenta would fail to promote system A transporter upregulation, as observed in *Igf2P0* null placentae (Reik *et al*, 2003). In support of this, total *Igf2* null mice are growth retarded from e11.5 onwards, and indeed, do not show increased levels of system A transporter expression (Constância *et al*, 2002; Constância *et al*, 2005). As such, *Igf2* mediates both the foetal demand for, and placental supply of, maternal nutrients.

This conclusion can be extended to many other imprinted genes. Indeed, the imprinted cluster on mouse distal chromosome 7, which includes *Igf2*, incorporates a number of genes involved in this system. Genes of this cluster expressed from the maternally-inherited chromosome negatively control placental supply. Deletion of maternally-expressed *Ipl* produces a large placenta, but a 'normal' embryo; an increase in supply but not demand (Frank *et al*, 2002). The same is true for *p57KIP2* mutants, again an imprinted gene expressed from the maternally-derived chromosome (Takahashi *et al*, 2000). This imprinting cluster therefore contains a 'strong demand' promoter (*Igf2* expressed in the foetus), a 'strong supply' promoter (*Igf2*, predominantly *Igf2P0*, expressed in the placenta), and at least two 'supply suppressors' (Reik *et al*, 2003). This effect can be extended to genes on other imprinted clusters. The imprinted system A transporter *Slc38a4* is expressed from the paternally-derived chromosome. As well as being upregulated in response to foetal demand in *Igf2P0* deficient placentae (Constância *et al*, 2005), genetic

ablation of *Slc38a4* generates growth retarded embryos (G. Kelsey, personal communication), identifying the gene as a supply promoter. That the positive effects on supply and demand are mediated by paternally-expressed transcripts (*Igf2*, *Igf2P0* and *Slc38a4*), which are antagonised by the negative influences of maternally-expressed genes (*Ipl*, *p57KIP2*), is strong evidence for the parental conflict hypothesis.

The placental growth effects following the transmission of a dysfunctional *Grb10* allele through the maternal line also conform to the parental conflict hypothesis. *Grb10Δ2-4*$^{m/+}$ placentae are overgrown from e14.5, whilst foetuses exhibit overgrowth from e12.5 (Charalambous *et al*, 2003). This also correlates with an increased placental efficiency (Charalambous *et al*, submitted). At e17.5, the foetal:placental wet weight ratio is ~10 % more for *Grb10Δ2-4*$^{m/+}$ conceptuses than for wild type or *Grb10Δ2-4*$^{+/p}$ embryos, suggesting that the normal function for *Grb10* expressed from the maternally-inherited allele in the placenta is to limit efficiency. Although the mechanistic basis of this remains to be elucidated, the labyrinthine volume of *Grb10Δ2-4*$^{m/+}$ placentae is disproportionately increased. Thus, a larger surface area for nutrient exchange is probably at least partly responsible.

This Chapter identifies an additional possible mechanism for the improved efficiency observed in placentae lacking a maternally-inherited functional *Grb10* allele. This mechanism is correlated with the expression profile for the gene in this organ, which is established in detail in the present study. This work builds on our existing knowledge, identifying *Grb10* as a probable player in mediating foetal demand and placental supply.

4.2 Results

4.2.1 *Grb10* is expressed from both parental alleles in the placental labyrinth

To examine the expression profile of *Grb10* in the late gestation placenta, *Grb10KO*$^{m/+}$ and *Grb10KO*$^{+/p}$ placentae were isolated 14 days after the observation of a cervical plug (e14.5), cryosectioned and assayed for β-galactosidase activity. No enzyme activity, assessed by the presence of a blue precipitate, was detected when wild type placentae were treated in an identical manner (data not shown), confirming the reliability of the assay in reporting *LacZ*, and by inference *Grb10*, expression. Incubation with X-gal substrate for 18 hours revealed strong reporter expression in the labyrinth and chorionic plate of *Grb10KO*$^{m/+}$ placentae, as well as in a subset of cells in the embryonic yolk sac (Figure 4.1*a* and *c*). No reporter expression was detected in the junctional zone or maternal decidua. *Grb10KO*$^{+/p}$ placental sections reported expression exclusively in the labyrinth, although β-galactosidase activity was weaker than that detected in *Grb10KO*$^{m/+}$ placental sections, despite being stained simultaneously (Figure 4.1*b* and *d*). No contributions from the paternally-inherited chromosome were detected in the chorionic plate or yolk sac.

Higher magnification views of e14.5 *Grb10KO*$^{m/+}$ placental sections assayed for β-galactosidase activity suggested that expression might be limited to a subset of labyrinthine cells, as some trophoblast nuclei did not appear to associate with positively-stained cytoplasm (Figure 4.1*e*). Similarly, reporter expression from the *Grb10KO*$^{+/p}$ allele appeared to be excluded from some cells of the labyrinth (Figure 4.1*f*). However, these sections did not permit more detailed analyses of cell type-specific expression.

4.2.2 Allele- and cell-specific expression of *Grb10* in extra-embryonic tissues

To enable a detailed examination of reporter expression in specific cell types, placentae were isolated as before, stained and fixed using a different technique (Section 2.4.6), which permitted better preservation of tissue morphology.

Consistent with the expression profile observed from cryosectioned placentae, reporter expression was absent from the maternal tissue and junctional zone of both *Grb10KO*$^{m/+}$ and *Grb10KO*$^{+/p}$ placentae (data not shown). Expression was detected in cells of the labyrinth and chorionic plate following maternal transmission of the gene-trap allele, but was absent from the chorionic plate after paternal transmission (Figure 4.2*a* and *b*).

In *Grb10KO*$^{m/+}$ placental sections, positive *LacZ* expression was detected in the cytoplasm of foetal endothelial cells and syncytiotrophoblast cells (Figure 4.2*c*). The cytoplasm of cytotrophoblast cells, identifiable by their larger nuclei, did not report expression.

The foetal endothelial cells of *Grb10KO*$^{+/p}$ placentae were also positive for *LacZ* expression, suggesting a contribution from both alleles to the transcriptome in this cell type (Figure

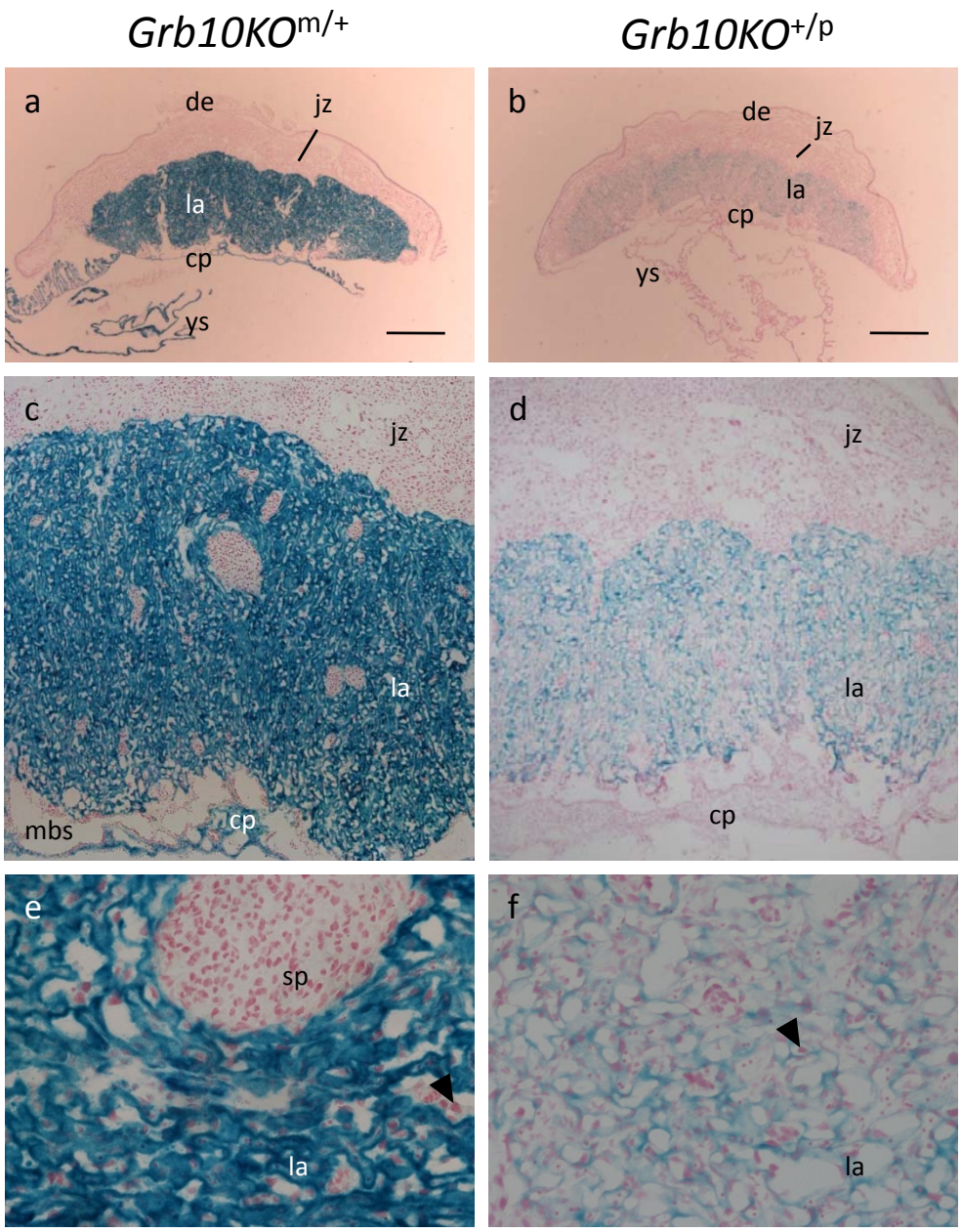
Grb10KO m/+
Grb10KO +/p
a
de
jz
la
cp
ys
b
de
jz
la
cp
ys
c
jz
la
mbs
cp
d
jz
la
cp
e
sp
la
f
la

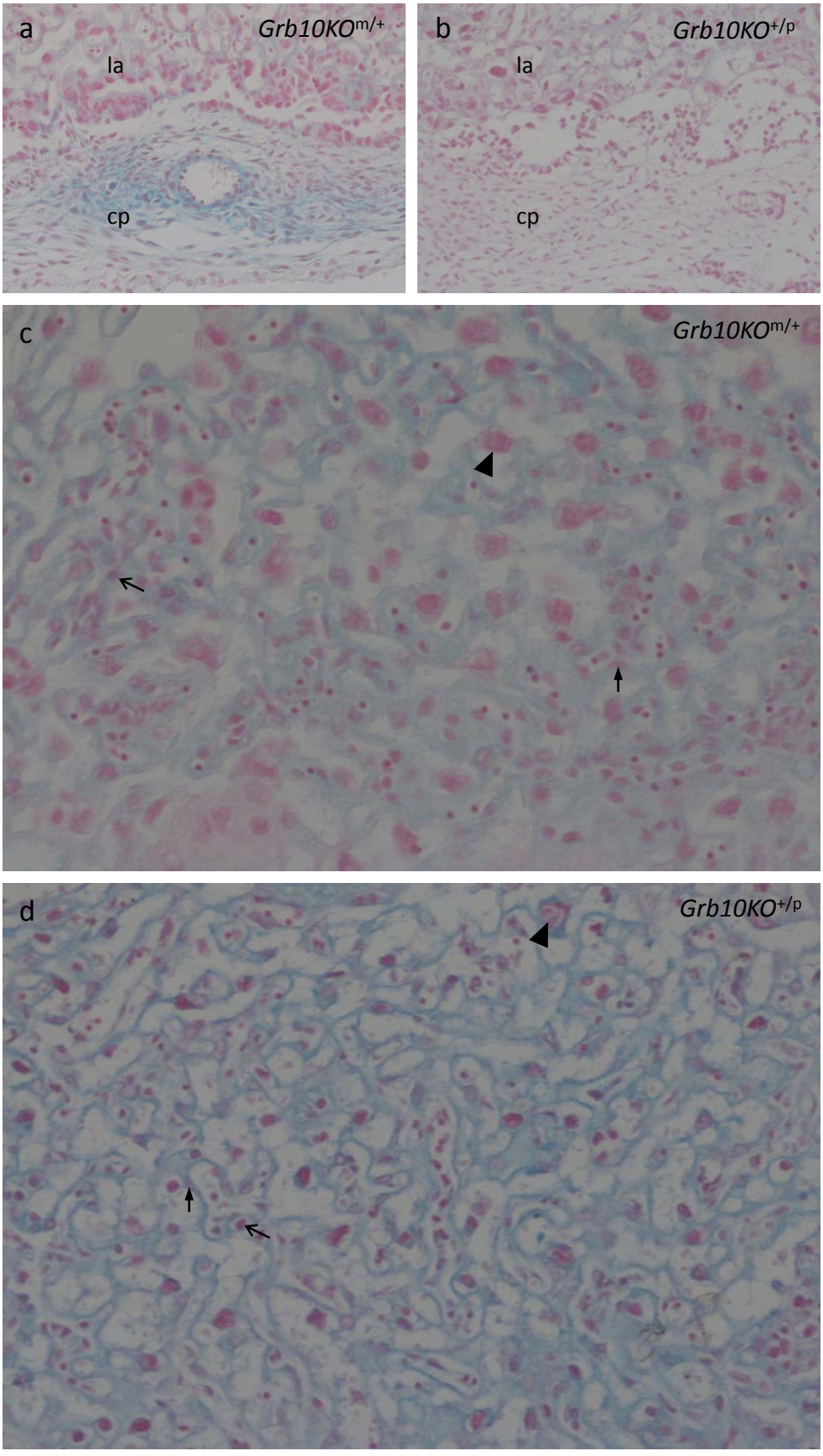
a
Grb10KO m/+
la
cp
b
Grb10KO +/p
la
cp
c
Grb10KO m/+
d
Grb10KO +/p

4.2*d*). Intriguingly, trophoblast expression appeared to be reciprocal to that from the maternally-inherited chromosome. Positive staining was detected in the cytoplasm associated with the large nuclei of cytotrophoblast cells, whilst *LacZ* could not be detected around at least some of the syncytiotrophoblast nuclei, suggesting one or both syncytial layers may not express *Grb10* from the paternally-inherited chromosome.

4.2.3 Allelic bias of *Grb10* expression in the placental labyrinth

Comparative staining performed on cryosections of *Grb10KO*$^{m/+}$ and *Grb10KO*$^{+/p}$ placentae suggested the contribution from the paternally-inherited chromosome in this organ was smaller than that from the maternally-derived copy. To assess the relative contribution in a quantitative manner, quantitative real-time PCR (qPCR) analysis was performed on total placental RNA using primers amplifying full-length *Grb10* transcripts in the context of one deleted allele.

We chose to perform this analysis on e17.5 placentae, to correlate with the improved placental efficiency associated with ablation of *Grb10* on the maternally-inherited chromosome (Charalambous *et al*, submitted). Analyses of reporter expression performed in the present study confirmed the persistence of a contribution from both parental alleles at this stage, with an expression pattern consistent with that observed at e14.5 (data not shown). To integrate with unpublished data from other studies, placentae inheriting the *Grb10Δ2-4* allele through each of the parental lines, as well as wild type controls, were analysed.

Amplification was performed using two primer pairs. The first pair was complimentary to sequences within exons 3 and 4, situated within the deleted endogenous sequence of the allele, and thus represented expression exclusively from the wild type copy (see Figure 3.3*a* for details of the genomic structure of the *Grb10Δ2-4* allele). The second pair amplified exons 11 to 16, downstream of the deletion. Any differences in amplification between the two primer pairs might suggest splicing of transcripts from the *Grb10Δ2-4* allele onto downstream exons, and thus ineffective trapping. Expression from each placenta was normalised to that of *Hprt*, a housekeeping gene, the expression of which did not differ between the genotypes (data not shown).

Similar results were obtained using both primer pairs (Figure 4.3*a* and *b*). When normalised to total *Grb10* expression levels in wild type placentae, maternal transmission of the *Grb10Δ2-4* allele resulted in a 70 % reduction in transcripts, confirming that the maternally-inherited chromosome is the source of the majority of *Grb10* transcripts in this organ. Amplification from *Grb10Δ2-4*$^{+/p}$ placentae produced a complimentary 30-40 % reduction in transcripts. This provided quantitative support for the differing levels of β-galactosidase activity detected in *Grb10KO*$^{m/+}$ and *Grb10KO*$^{+/p}$ placental sections (Figure 4.1). Additionally, the additive levels of expression from each of the parental alleles in the context of a deleted copy are similar to that from wild type placentae, suggesting the wild type allele is unable to compensate for *Grb10* deletion by upregulating its transcription.

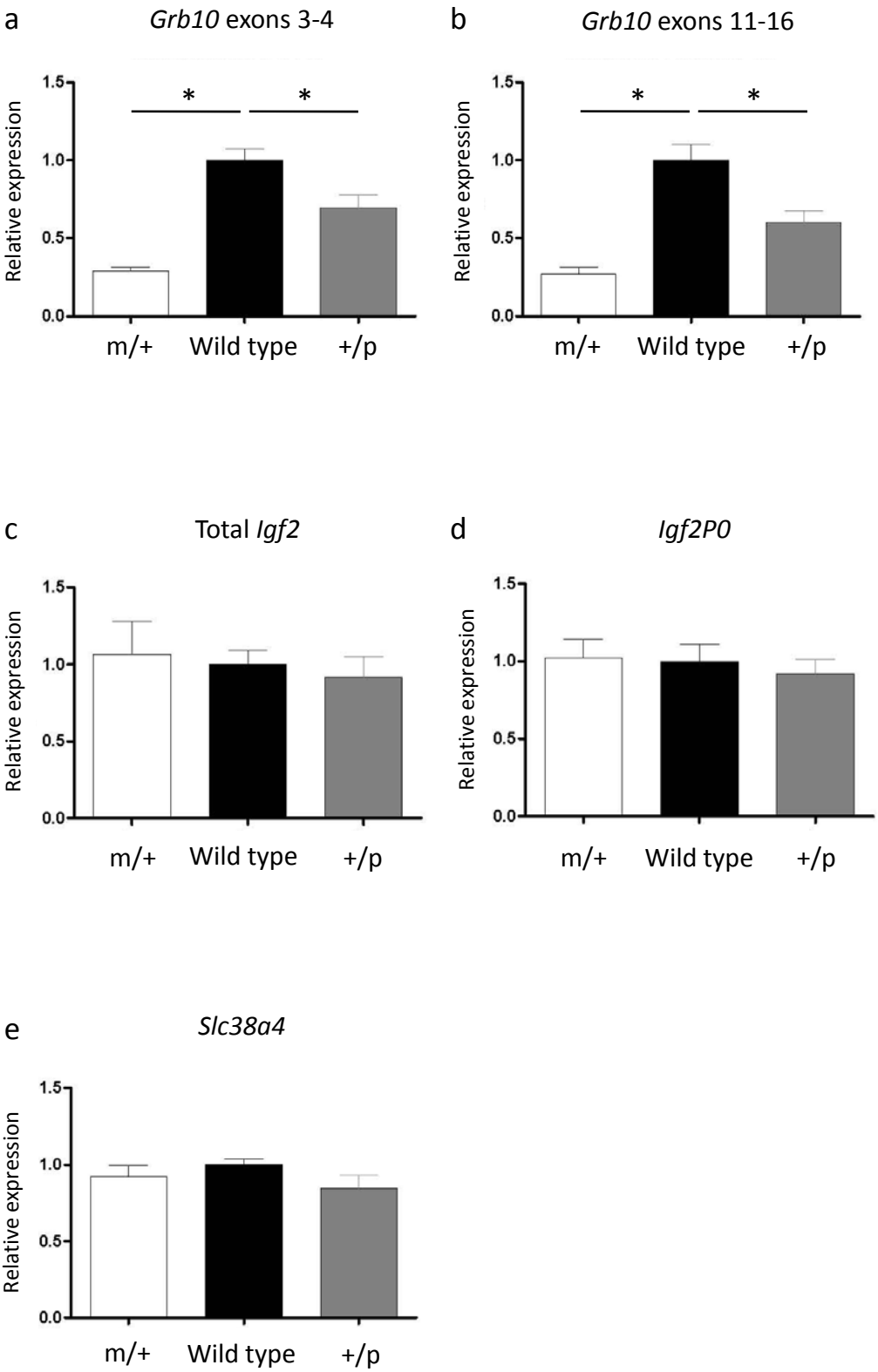
a
Grb10 exons 3-4
Relative expression
1.5
1.0
0.5
0.0
*
*
m/+
Wild type
+/p
b
Grb10 exons 11-16
Relative expression
1.5
1.0
0.5
0.0
*
*
m/+
Wild type
+/p
c
Total *Igf2*
Relative expression
1.5
1.0
0.5
0.0
m/+
Wild type
+/p
d
Igf2P0
Relative expression
1.5
1.0
0.5
0.0
m/+
Wild type
+/p
e
Slc38a4
Relative expression
1.5
1.0
0.5
0.0
m/+
Wild type
+/p

4.2.4 The expression of imprinted genes associated with improved placental efficiency is unaffected by the loss of *Grb10*

A previous study identified an enhanced placental efficiency phenotype following maternal transmission of *Grb10Δ2-4* (Charalambous *et al*, submitted). This was first detected at e17.5, at which stage the ratio of foetal:placental wet weight was 10 % greater than that of wild type or *Grb10Δ2-4*$^{+/p}$ controls. To begin to dissect the mechanism for this enhanced efficiency, qPCR was performed on e17.5 placentae of all three genotypes, using primers complimentary to imprinted genes previously associated with influencing placental efficiency.

In wild type mice, elevated levels of the placental-specific *Igf2P0* transcript are associated with improved placental efficiency (Coan *et al*, 2008). An opposite phenotype is observed upon deletion of the *Igf2P0* transcript (Constancia *et al*, 2002). No differences were observed in the levels of *Igf2P0*, nor of total *Igf2*, between wild type, *Grb10Δ2-4*$^{m/+}$ and *Grb10Δ2-4*$^{+/p}$ placentae (Figure 4.3*c* and *d*). Similarly, expression of the imprinted system A transporter *Slc38a4*, which partially compensates for a reduced efficiency in *Igf2P0* null placentae, was not affected by Grb10 ablation (Figure 4.3*e*).

These results suggested that *Grb10* does not mediate placental efficiency through the molecular pathway involving *Igf2P0* and *Slc38a4*.

4.2.5 *Grb10KO*$^{m/+}$ placentae and embryos exhibit overgrowth

To permit further investigation of the mechanism responsible for the enhanced placental efficiency phenotype, placentae inheriting the *Grb10KO* allele through each of the parental lines were isolated at e14.5. Although a statistically significant improvement in efficiency is not detected until e17.5 (Charalambous *et al*, submitted), previous studies have confirmed that both embryo and placenta are overgrown at e14.5 when inheriting a dysfunctional *Grb10* allele through the maternal line. This is true for both *Grb10Δ2-4*$^{m/+}$ (Charalambous *et al*, 2003) and *Grb10KO*$^{m/+}$ (Garfield *et al*, submitted) conceptuses. Consistent with these reports, *Grb10KO*$^{m/+}$ embryos isolated in the present study were 18 % larger than wild type controls at e14.5 (Figure 4.4*a*), a statistically significant increase. According to these data, *Grb10KO*$^{+/p}$ embryos were also significantly larger than wild type controls at this stage, a result inconsistent with previous analyses (Garfield *et al*, submitted). There was greater variance within this data set, which also had a smaller population size than that of the other data sets, providing the most likely reason for this discrepancy.

Consistent with previous reports, *Grb10KO*$^{m/+}$ placentae were larger than wild type and *Grb10KO*$^{+/p}$ controls at this stage (Figure 4.4*b*). However, this did not correlate with an improved placental efficiency, as assessed by the ratio of foetal:placental wet weight (Figure 4.4*c*). *Grb10KO*$^{+/p}$ placentae also failed to show a difference in efficiency. These results are supported by previous studies using *Grb10Δ2-4* animals, in which an enhanced efficiency was not observed until later in gestation (Charalambous *et al*, submitted).

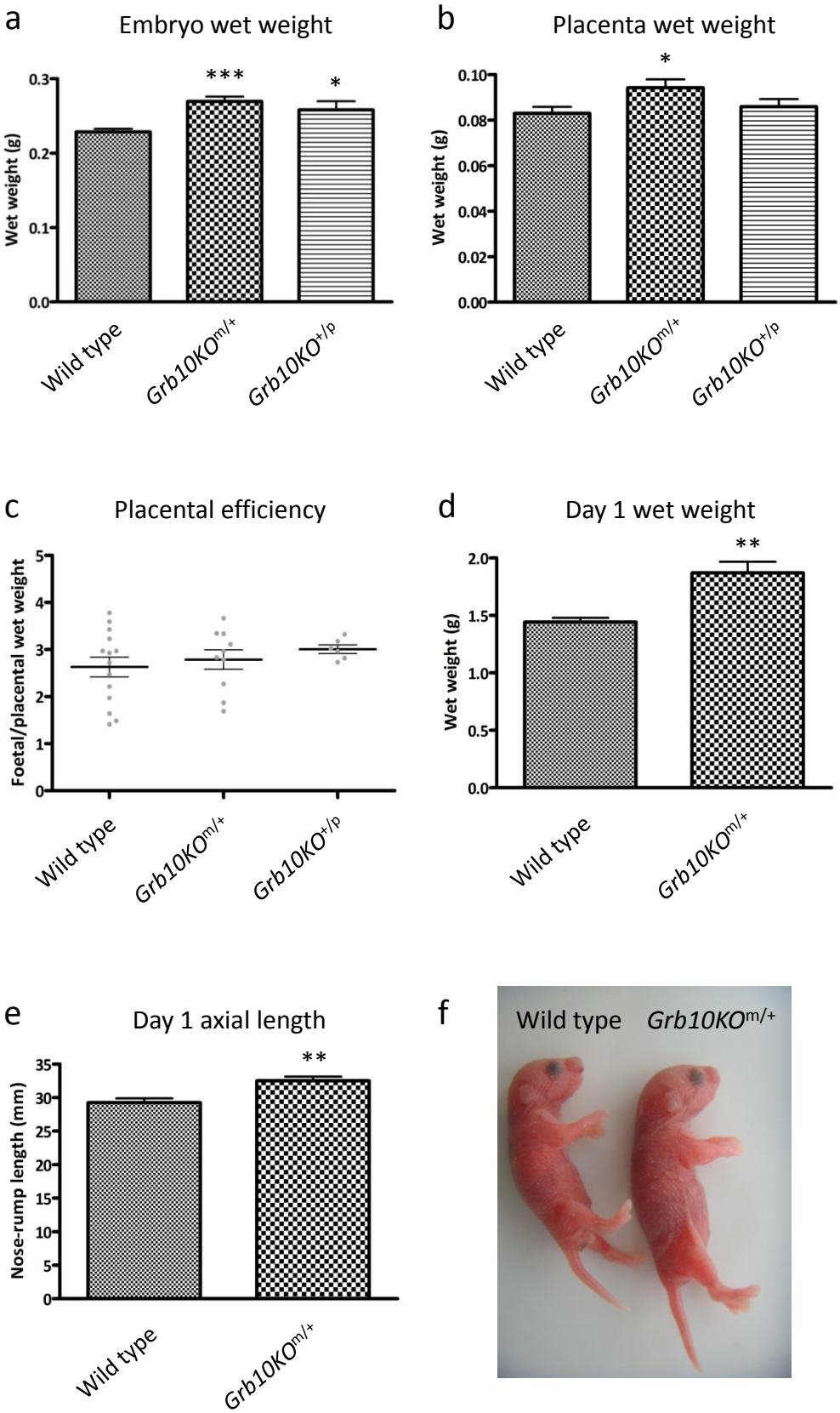
a
Embryo wet weight
Wet weight (g)
0.3
0.2
0.1
0.0
***
*
Wild type
Grb10KO m/+
Grb10KO +/p
b
Placenta wet weight
Wet weight (g)
0.10
0.08
0.06
0.04
0.02
0.00
*
Wild type
Grb10KO m/+
Grb10KO +/p
c
Placental efficiency
Foetal/placental wet weight
5
4
3
2
1
0
Wild type
Grb10KO m/+
Grb10KO +/p
d
Day 1 wet weight
Wet weight (g)
2.0
1.5
1.0
0.5
0.0
**
Wild type
Grb10KO m/+
e
Day 1 axial length
Nose-rump length (mm)
35
30
25
20
15
10
5
0
**
Wild type
Grb10KO m/+
f
Wild type
Grb10KO m/+

4.2.6 Overgrowth persists in *Grb10KO*$^{m/+}$ day 1 neonates

The overgrowth of *Grb10KO*$^{m/+}$ pups *in utero*, first detected at e12.5, persists into the neonatal period. On the day of birth, *Grb10KO*$^{m/+}$ neonates were significantly heavier than wild type littermates (Figure 4.4*d*), a result consistent with previous reports. In the current study, *Grb10KO*$^{+/p}$ neonates were not examined as they have previously been shown not to exhibit a growth phenotype (Garfield *et al*, submitted). At least part of the overgrowth was attributed to an increased axial length on the day of birth (Figure 4.4*e*), suggesting a possible involvement of *Grb10* in long bone growth or formation. Both the increased size and length of *Grb10KO*$^{m/+}$ pups relative to wild type littermates was clearly apparent from a visual comparison (Figure 4.4*f*).

4.2.7 The labyrinth is disproportionately overgrown in *Grb10KO*$^{m/+}$ placentae

Next, we examined the basis of the overgrowth observed at e14.5 in *Grb10KO*$^{m/+}$ placentae. Imaging software was utilised to measure the depth of the labyrinth and junctional zone close to the centre of the placenta, as described in Section 2.5.1. Specifically, the distance from the labyrinth-junctional zone boundary to the foetal edge of the chorionic plate was measured, as well as the distance from the labyrinth-junctional zone boundary to the junctional zone-decidua boundary ('labyrinth and chorionic plate' and 'junctional zone', respectively; Figure 4.5*a*). One randomly-selected section from each of ten placentae was analysed for each genotype, but the analysis was performed without knowledge of genotype-section correlation. Representative wild type and *Grb10KO*$^{m/+}$ sections are shown in Figure 4.5*c*. The differences in labyrinth depth are clearly illustrated. Although the junctional zone of this *Grb10KO*$^{m/+}$ section is thinner, this was not a statistically significant result when comparing ten samples of each genotype.

Both wild type and *Grb10KO*$^{+/p}$ placentae exhibited similar properties, with the labyrinth and chorionic plate contributing 56 % of the wild type and 58 % of the *Grb10KO*$^{+/p}$ total placental depth. There was also no significant difference in the actual placental depth between these two genotypes. When *Grb10* was ablated on the maternally-derived chromosome, however, the labyrinth and chorionic plate were disproportionately enlarged. Together, these contributed to 64 % of the total placental depth, whilst the actual depth of the junctional zone did not differ significantly from that of wild type and *Grb10KO*$^{+/p}$ placentae. This resulted in an increase in the total placental depth of *Grb10KO*$^{m/+}$ placentae.

Morphometric assessments, in which labyrinthine cells in a fixed number of windows were counted, confirmed the increased size of the labyrinth in placentae inheriting the *Grb10KO* allele through the maternal line (Figure 4.5*b*). An identical analysis was performed for *Grb10KO*$^{+/p}$ placentae, which also exhibited a small but highly significant increase in labyrinthine volume relative to wild type.

a

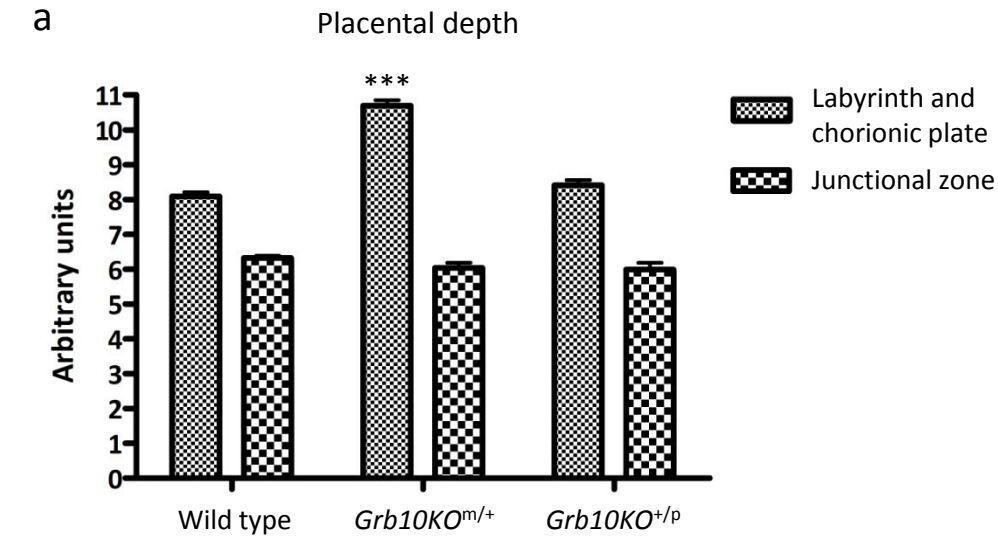
Placental depth
***
Arbitrary units
11
10
9
8
7
6
5
4
3
2
1
0
Wild type
Grb10KOm/+
Grb10KO+/p
Labyrinth and chorionic plate
Junctional zone

b

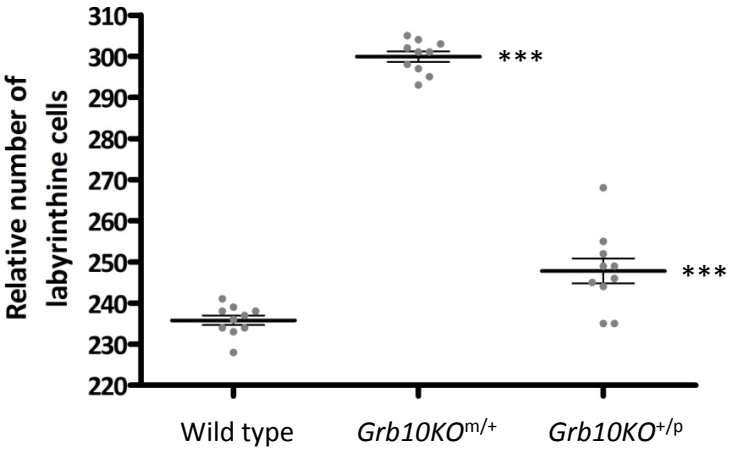
Morphometric assessment of labyrinth
Relative number of labyrinthine cells
310
300
290
280
270
260
250
240
230
220
***
***
Wild type
Grb10KOm/+
Grb10KO+/p

c

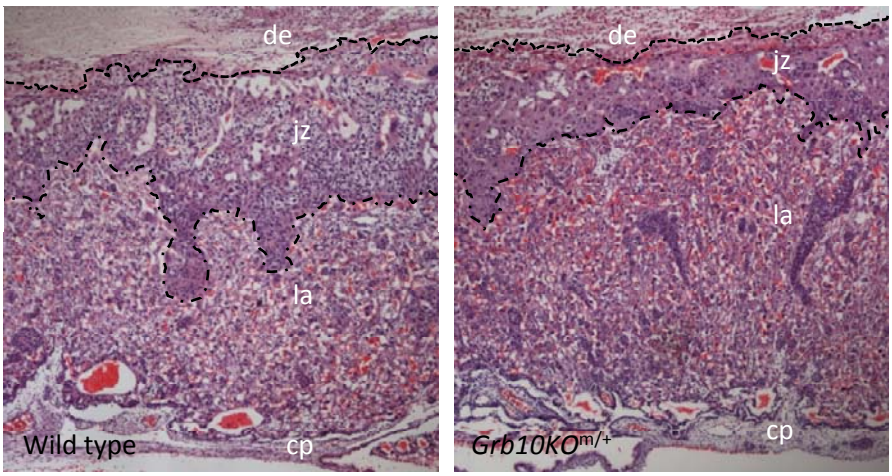
de
jz
la
cp
Wild type
de
jz
la
cp
Grb10KOm/+

4.2.8 *Grb10KO*$^{m/+}$ placentae exhibit an increased foetal vasculature

Given that *Grb10* is expressed from the maternally-derived allele on the foetal side of the labyrinthine trophoblast, as well as in foetal endothelial cells, we hypothesised that the improved placental efficiency, associated with ablation of maternally-inherited *Grb10*, might be mediated by an increased surface area of foetal vasculature. Again, representative sections from ten placentae were analysed for each genotype, without knowledge of genotype-section correlation. First, the total surface area of foetal blood vessels was measured in a fixed window, as described in Section 2.5.1. This was significantly increased in *Grb10KO*$^{m/+}$ placentae relative to wild type and *Grb10KO*$^{+/p}$ samples (Figure 4.6*a*).

These data were supported by counts of discrete cross-sections through foetal capillaries. Only inheritance of a dysfunctional *Grb10* allele through the maternal line resulted in a significantly higher number of foetal blood capillaries, suggestive of more extensive foetal vascularisation (Figure 4.6*b*).

Whilst the *Grb10KO*$^{m/+}$ placental sections had 34 % more discrete cross-sections through foetal capillaries than wild type controls, the total foetal vasculature surface area was increased by 43 %, suggesting that foetal blood vessels are both larger and more numerous in *Grb10KO*$^{m/+}$ placentae. This might increase the surface area for nutrient exchange, providing a possible mechanism for improved placental efficiency.

4.2.9 No evidence for compensation by *Grb7* following ablation of the maternally-derived *Grb10* allele

Whilst the molecular pathways within which Grb10 operates in the placenta are unknown, both Grb10 and its homolog Grb7 have been implicated in common signalling pathways, including that of the insulin receptor (Smith *et al*, 2007; Shiura *et al*, 2005; Kasus-Jacobi *et al*, 2000). This raises the possibility of partial functional redundancy, such that one protein may compensate for the loss of the other. This can inhibit the dissection of *in vivo* function following a gene knockout.

To assess the possibility that Grb7 might partially compensate for the absence of Grb10 in *Grb10KO*$^{m/+}$ placentae, the expression profile of *Grb7* in this organ was first determined. Unlike *Grb10*, which is restricted to the chorionic plate and a subset of labyrinthine cells, Grb7 protein was detected in all extra-embryonic layers of the mature wild type mouse placenta, using immunohistochemistry (Figure 4.7*a(i)*). This included very strong expression in the chorionic plate and labyrinth (Figure 4.7*a(ii)*). Indeed, all cell types of the labyrinth appeared to express *Grb7*, although this was strongest in the foetal endothelium and the cytotrophoblast layer immediately adjacent to the maternal blood spaces (Figure 4.7*a(iii)*). No protein was detected in the maternal decidua (data not shown), nor in a control sample in which primary antibody was omitted (Figure 4.7*a(iv)*).

a

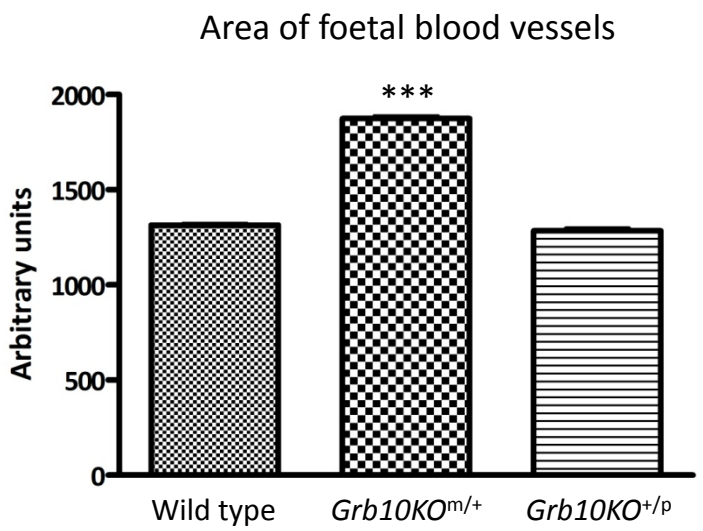
Area of foetal blood vessels
***
2000
1500
1000
500
0
Arbitrary units
Wild type
Grb10KOm/+
Grb10KO+/p

b

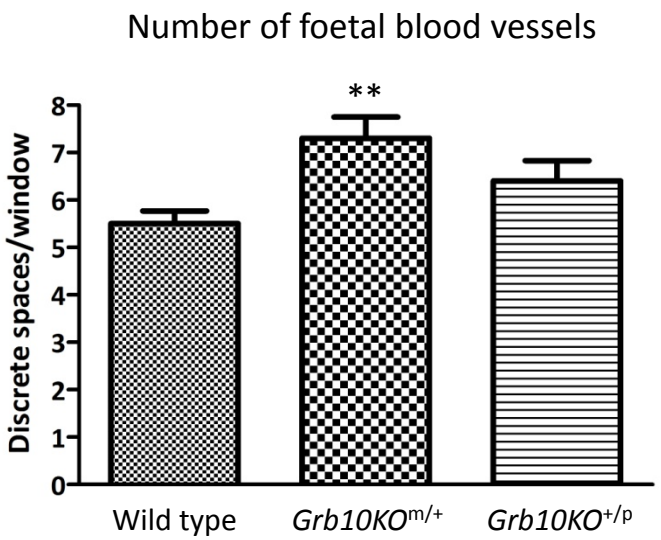
Number of foetal blood vessels
**
8
7
6
5
4
3
2
1
0
Discrete spaces/window
Wild type
Grb10KOm/+
Grb10KO+/p

a

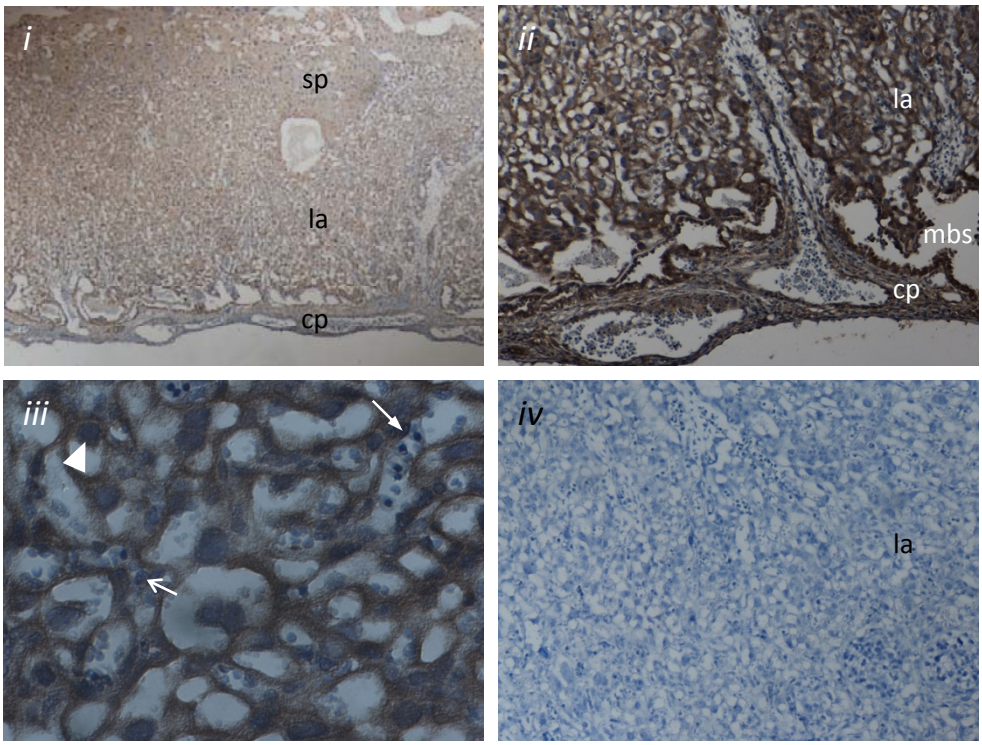
i
sp
la
cp
ii
la
mbs
cp
iii
iv
la

b

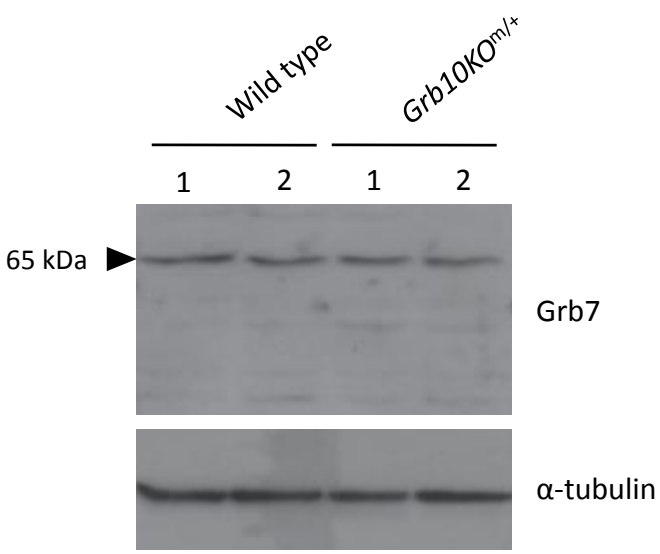
Wild type
Grb10KO m/+
1
2
1
2
65 kDa
Grb7
α-tubulin

Western blotting utilising an anti-Grb7 antibody revealed no differences in the levels of the 65 kDa Grb7 protein in *Grb10KO*$^{m/+}$ placental homogenates, relative to wild type (Figure 4.7*b*). Signal representing α-tubulin was also consistent in each sample, confirming equal loading of protein. Thus, although *Grb7* and *Grb10* are strongly expressed in foetal endothelial cells, and display co-expression in other cell types of the mature mouse placenta, Grb7 protein levels are unaffected by the considerable reduction in *Grb10* transcripts in *Grb10KO*$^{m/+}$ placentae.

4.3 Discussion

The function of *Grb10* in the mature mouse placenta has already been described by our group (Charalambous *et al*, submitted). In effect, *Grb10* limits placental efficiency, thereby controlling embryonic growth. The present study aimed to extend this work in two ways: firstly, to obtain a more detailed understanding of allele-specific contributions in each cell type of the placenta; and secondly, to begin to address the mechanistic basis for an improved placental efficiency phenotype, following ablation of *Grb10* on the maternally-inherited chromosome.

Previous analyses of *Grb10* expression in the placenta utilised the *Grb10Δ2-4* allele, from which expression of the *LacZ* reporter is relatively weak, most probably due to the deletion of an enhancer element which is active in this organ (see Chapter Five for more details). Parent-specific transmission of the *Grb10KO* allele circumvented this issue, and revealed a significant contribution from the paternally-inherited copy in the placental labyrinth, although this appeared weaker than expression from the maternally-derived chromosome. No reporter expression had previously been detected from *Grb10Δ2-4*$^{+/p}$ placentae. To confirm that this was not a result of ineffective trapping of *Grb10* transcripts by the β-*geo* cassette, quantitative real-time PCR (qPCR) was performed using primers amplifying full-length *Grb10* transcripts, on wild type, *Grb10Δ2-4*$^{m/+}$ and *Grb10Δ2-4*$^{+/p}$ total placental RNA. Consistent with *LacZ* staining of *Grb10KO* placental sections, the maternally-inherited *Grb10* allele was found to contribute ~70 % of transcripts, and accordingly, 30-40 % of transcripts arose from the paternally-derived copy. This result was achieved using primers situated within the deleted endogenous sequence of the *Grb10Δ2-4* allele, as well as primers downstream of the β-*geo* cassette, confirming effective trapping of *Grb10* transcripts arising from the transgenic allele.

In conclusion, the parent-of-origin specific *LacZ* reporter expression profile from the *Grb10KO* allele matches that obtained through qPCR from the *Grb10Δ2-4* allele, suggesting that both transgenic mouse lines are suitable models for studying *Grb10* expression and function in the placenta.

The poor morphology of cryosectioned and *LacZ* stained placentae did not permit a cell-specific examination of *Grb10* expression. An alternative preparation technique improved the preservation of tissue morphology, whilst still enabling visualisation of *LacZ* reporter expression. In these sections, consistent with the analysis of cryosectioned placentae, *Grb10* was expressed from the maternally-inherited chromosome in the labyrinth, chorionic plate and a subset of cells in the yolk sac. The paternal chromosome did not contribute any *Grb10* transcripts to the chorionic plate or yolk sac, but was detected in some cells of the labyrinth.

Within the labyrinth, both alleles were expressed in the foetal endothelium, lining the foetal capillaries. In the trophoblast layers, expression appeared to be reciprocal. *Grb10* from the maternally-inherited chromosome was excluded from the mononucleated

cytotrophoblast cells, but appeared to be expressed in both syncytiotrophoblast cell layers. Paternal expression, on the other hand, appeared to be more closely associated with large nuclei, implying expression in the cytotrophoblast layer. Most of the cytoplasm surrounding the smaller nuclei of the syncytial layers was devoid of staining, suggesting *Grb10* is not expressed from the paternally-inherited chromosome in one or both syncytial layers. Indeed, reporter expression in *Grb10KO*$^{+/p}$ placental sections appeared more restricted to the boundaries of foetal vessels and maternal blood spaces, consistent with this observation, whilst *Grb10KO*$^{m/+}$ placentae showed more diffuse *LacZ* reporter expression, which was relatively weak around the edges of maternal blood spaces.

The structure of the human placenta is different to that of the mouse. *Grb10* expression in the human villous trophoblast is exclusively from the maternally-derived allele (Monk *et al*, 2009), and it is this layer which is associated with the regulation of nutrient transfer, suggesting the conservation of the *Grb10* imprint is coupled to this function. However, the human placenta as a whole demonstrates an approximate 1:1 ratio of maternal:paternal expression (Monk *et al*, 2009), contrasting with the ~2.3:1 ratio revealed in the present study for mouse. It is not clear whether this 1:1 ratio reflects biallelic *Grb10* expression or cell-specific imprinting. Clearly, this cannot be addressed in human tissue using a *LacZ* gene-trap, and would require single cell RT-PCR analysis.

Having deduced the expression profile in greater detail, we next confirmed that mice inheriting the *Grb10KO* allele through the maternal line demonstrated a similar growth phenotype to *Grb10Δ2-4*$^{m/+}$ animals. Both *Grb10KO*$^{m/+}$ placentae and embryos were significantly larger than wild type controls at e14.5, and this persisted on the day of birth. Interestingly, we attributed part of this increased wet weight at the neonatal stage to an extended axial length, suggesting *Grb10* may be involved in the formation or growth of long bones. Since *Grb10Δ2-4*$^{m/+}$ adult mice also have more muscle and less fat (Smith *et al*, 2007), *Grb10* might possibly be involved in the fate decision of mesenchymal stem cells, which give rise to myocytes, adipocytes and osteocytes, among others (reviewed in Liu *et al*, 2009).

We next used the *Grb10KO* model to investigate the mechanistic basis for an improved placental efficiency phenotype following ablation of the gene on the maternally-derived chromosome. The increased placental wet weight at e14.5 correlated with a disproportionate overgrowth of the labyrinth, an effect also recorded for *Grb10Δ2-4*$^{m/+}$ placentae at a later stage (Charalambous *et al*, submitted). This was initially demonstrated by measuring the thickness of the labyrinth and junctional zone in cross-sections close to the midline of placental samples. The highly significant increase in labyrinth and chorionic plate depth in *Grb10KO*$^{m/+}$ placentae was not matched by a concomitant reduction in junctional zone depth. In a previous study, the wet weight of the junctional zone in *Grb10Δ2-4*$^{m/+}$ placentae remained comparable to wild type controls (Charalambous *et al*, submitted). A larger labyrinth might, therefore, be expected to spread the junctional zone more thinly across its surface, but the effect may be too subtle to detect using this approach.

The increase in labyrinthine volume was further supported by morphometric analysis, which confirmed that labyrinthine cells were over-represented in *Grb10KO*$^{m/+}$ placentae. A small, but highly significant, increase in labyrinthine volume was detected in *Grb10KO*$^{+/p}$ placentae using this technique. Such an effect has not previously been observed (Charalambous *et al*, submitted). Given that the associated embryos of this dataset were also significantly larger than wild type controls, again a result not reported in previous studies, the effect is perhaps not surprising. It is possible that some of the *Grb10KO*$^{+/p}$ embryos and placentae were isolated at a stage closer to e15.0 or even e15.5, which compromises the comparison. As pregnancy is detected in females by the examination of cervical plugs only once per day, there is a large window within which mating may have been performed. In support of this, there is a much greater variance in this dataset than the wild type and *Grb10KO*$^{m/+}$ datasets, and indeed, the variance is significantly different ($p = 0.0056$; Bartlett's test for equal variances). As the embryos were isolated from two separate litters, one litter may have been at e14.5, with the other a few hours older, explaining this difference. Embryos should be accurately staged at isolation, using key features which define specific developmental time points.

Whilst a disproportionately enlarged labyrinth has been reported in *Grb10Δ2-4*$^{m/+}$ mice at e17.5, a whole placental overgrowth effect is apparent from e14.5 onwards. The current study confirmed that the earlier stages of the effect are also a consequence of labyrinthine overgrowth, although morphometric analysis on cells of the junctional zone was not performed. With this knowledge, plus the data demonstrating that *Grb10* is expressed from the maternally-derived allele in the cell layers closest to the foetal capillaries, we hypothesised that the improved placental efficiency phenotype might arise from an increased area of foetal vasculature. The total surface area of foetal capillaries in cross-sections through *Grb10KO*$^{m/+}$ placentae was significantly higher than in wild type or *Grb10KO*$^{+/p}$ controls. Interestingly, this was reflected by an increased number of discrete foetal vasculature spaces, implying that the greater surface area is, at least in part, a consequence of increased capillary branching. The mean cross-sectional surface area of capillaries in each placental section was not established, but would be valuable in deducing the relative significance of more capillaries versus larger capillaries.

This represents the first indication of a mechanistic basis for improved placental efficiency in *Grb10* mutant mice. The ablation of functional *Grb10* from the maternally-derived chromosome would reduce *Grb10* transcripts in the foetal endothelium, and remove most or all transcripts from the two multinucleated syncytiotrophoblast layers. This is associated with an increase in mass of the placental labyrinth, which is, at least in part, caused by enhanced foetal vascularisation, presumably a result of endothelial cell proliferation. This results in a larger surface area for nutrient exchange, either by active transport or passive diffusion. Inversely, this implies that the normal role of *Grb10* is to restrict endothelial cell proliferation, and so limit the nutrient transfer capacity, or efficiency, of the placenta. The predominance of *Grb10* expression in the endothelium suggests a response to factors in the foetal circulation. This is supported by immunohistochemistry experiments which show Grb10 protein localising to the capillary side of endothelial cells (Charalambous *et al*, submitted).

This role for Grb10 in the placenta fits our existing knowledge of *Grb10* on three levels. Firstly, *Grb10* is typically a negative regulator of growth factor signalling, and thus could act to dampen hormonal demands from the foetal circulation, restricting the extraction of nutrients from the maternal blood. Secondly, the protein is an inhibitor of cell proliferation. *Grb10KO*$^{m/+}$ primary mouse embryonic fibroblasts grow more rapidly than their wild type counterparts (Garfield, 2007). Thus, in its normal role, Grb10 might restrict endothelial cell proliferation, and by extrapolation vascularisation, again limiting nutrient transfer by restricting the surface area available for nutrient exchange. Finally, our model is consistent with the parental conflict hypothesis, which predicts that maternally-expressed genes in the placenta will function to limit nutrient exchange, thereby maximising the lifetime reproductive success of the mother. Further evidence of this role comes from the retention of the *Grb10* imprint in the human villous trophoblast layer, an essential cell layer involved in nutrient transfer (Monk *et al*, 2009).

Whilst *Grb10* is predominantly expressed from the maternally-inherited chromosome in the mouse placenta, a significant minority is derived from the other copy. That no growth phenotypes have been associated with ablation of the paternally-inherited *Grb10* allele might be a reflection of its relatively low contribution to the *Grb10* transcript pool, or might be a consequence of cell-specific expression. We found that expression in at least one of the syncytiotrophoblast layers, if not both, is exclusively from the maternally-inherited allele, which also accounts for the majority of endothelial expression (Charalambous *et al*, submitted). The syncytiotrophoblast in particular is associated with a nutrient transfer function. The role of paternally-expressed *Grb10* remains to be elucidated, but this study suggests it may play a minor role in influencing growth.

If the ratio of cell-type contributions to the labyrinth remained the same, but the labyrinthine volume was simply increased in *Grb10KO*$^{m/+}$ placentae, it is possible that this increased volume would be adequate to explain the improved efficiency. However, we were unable to associate all of the foetal overgrowth to the increase in labyrinthine volume in *Grb10KO*$^{m/+}$ embryos (Charalambous and Cowley, unpublished data), suggesting this is an insufficient explanation to account for the phenotype. This adds weight to the hypothesis that an increased foetal vasculature is the mechanistic basis. This preliminary study needs to be extended by performing stereological assessments of *Grb10KO*$^{m/+}$ placentae, as defined previously (Coan *et al*, 2004). Subtle differences in placental morphology can be detected in this way, and, by inference, can say much about nutrient transfer capacities. This could potentially be followed up with radiolabelled tracer transfer assays, such as those performed on *Igf2P0* null mice (Constância *et al*, 2002), to directly measure transfer capacity.

Additionally, we noted that levels of *Igf2P0*, total *Igf2* and *Slc38a4* did not differ between wild type, *Grb10Δ2-4*$^{m/+}$ and *Grb10Δ2-4*$^{+/p}$ placentae at e17.5. *Igf2P0* mutant placentae exhibit growth restriction from e12.5, but associated embryos remain the same size as wild type littermates until e16.5, from which point they are growth retarded (Constância *et al*, 2002). As such, mutant placentae are more efficient at these earlier stages. This somewhat paradoxical finding is explained by an increase in active transport, which acts to

compensate for the reduced surface area limiting passive nutrient diffusion. *Slc38a4* is a key mediator of this compensation, a gene which is also imprinted (Smith *et al*, 2003). That the expression of these genes was not altered by ablation of *Grb10* suggests the mechanism is independent of *Igf2*. This is supported by genetic experiments which demonstrated that ablation of *Grb10* from the maternally-inherited chromosome promoted embryonic and placental overgrowth, even in the absence of *Igf2* (Charalambous *et al*, 2003). The growth pathway through which *Grb10* mediates its effects is yet to be identified, although preliminary data suggests *Grb10* might be epistatic, and antagonistic, to the paternally-expressed gene *Dlk1* in some tissues (Madon, Cowley, Garfield and Ward, unpublished data). The *in vivo* function of *Dlk1* is to promote embryonic growth (da Rocha *et al*, 2009). However, this may not be the predominant growth pathway involving *Grb10* in the placenta. Firstly, *Dlk1* expression is limited to the foetal endothelium (Yevtodiyenko and Schmidt, 2006), whilst *Grb10* is also present in the trophoblast. Secondly, genetic experiments have demonstrated that *Grb10Δ2-4*$^{m/+}$*/Dlk1KO*$^{+/p}$ double mutant mice display a compound placental growth phenotype with additive effects of both mutations, whereas embryonic growth of double mutants is similar to *Grb10Δ2-4*$^{m/+}$ single mutants (Madon, Cowley, Garfield and Ward, unpublished data). Therefore, the pathway(s) within which *Grb10* acts in the placenta remain to be elucidated.

The larger labyrinth resulting from maternal transmission of a dysfunctional *Grb10* allele might be expected to engender increased levels of *Igf2* expression. However, the predominant *Igf2* transcript in the labyrinth is *Igf2P0*; the ablation of this transcript results in a placental growth deficit close to that for total *Igf2* null mice, demonstrating the importance of *Igf2P0* in this organ (DeChiara *et al*, 1991; Constância *et al*, 2002). The expression of this transcript is restricted to trophoblast cells, and is absent from the endothelium. Therefore, if the increased labyrinthine volume in *Grb10Δ2-4*$^{m/+}$ and *Grb10KO*$^{m/+}$ placentae is a consequence of increased foetal vasculature and hyperproliferation of endothelial cells, *Igf2* levels would most likely remain unaffected.

We found no evidence of compensation for *Grb10* depletion by the homolog *Grb7*. This adaptor protein displayed a more widespread expression profile in the placenta, including cells of the junctional zone. Within the labyrinth, Grb7 protein was most strongly expressed in the foetal endothelium, where *Grb10* is expressed from both alleles, and the cytotrophoblast layer, in which *Grb10* is monoallelically-expressed from the paternally-inherited chromosome. Whilst this profile potentially enables partial functional redundancy, we detected no changes in the levels of native Grb7 protein following ablation of 70 % of *Grb10* transcripts. This could be extended to examine the levels of phosphorylated Grb7, as an indication of activated protein (Chu *et al*, 2009). The assessment of placental size in *Grb10KO*$^{m/+}$*/Grb7KO*$^{-/-}$ double mutants might also be more helpful in revealing the extent of compensation. Whilst Grb10 and Grb7 have both been implicated in mediating insulin signalling, there is also evidence of redundancy between Grb10 and Grb14 (Holt *et al*, 2009). Again, the expression profile of *Grb14* in the placenta is unknown, and would be the first step towards identifying any redundancy. Like *Grb10*, the pathways within which *Grb7* and *Grb14* act in the placenta remain unclear.

Finally, the *Grb10KO*$^{m/+}$ (or *Grb10Δ2-4*$^{m/+}$) placenta is the first example, to our knowledge, of an overgrown placenta which is more efficient. The ablation of other maternally-expressed genes can cause placental hyperplasia, without an associated improvement in efficiency. The *Ipl* mutant placenta, for example, exhibits hyperplasia but associated embryos are the same size as wild type littermates (Frank *et al*, 2002). This phenotype was interpreted as an increase in supply but not demand, suggesting *Ipl* is a supply suppressor. As a maternally-expressed gene, *Ipl* conforms to the parental conflict hypothesis. Whilst ablation of *Grb10* from the maternally-inherited chromosome similarly confers placentomegaly, it also engenders embryonic overgrowth. Interpreted in the same manner, this identifies *Grb10* as both a supply suppressor and a demand suppressor. At first glance, the expression of a demand suppressor in the embryo might not appear to be in the embryo's best interests. However, this is based on the assumption that the greater the nutrients extracted from the mother, the more advantageous for the embryo. This is certainly not the case. Studies of human births indicate that the optimal birth weight (i.e. that associated with least risk of mortality) is just above the mean birth weight for a population (Sansing and Chinnici, 1976). The risk of mortality increases beyond this threshold. Indeed, overgrowth following ablation of *Grb10* from the maternally-derived allele results in a 12 % neonatal lethality (Charalambous *et al*, 2003). As such, there exists a threshold of nutrient demand beyond which the embryo would be disadvantaged. In normal situations, this threshold is presumably not usually reached because the maternally-expressed genes in the placenta act first to limit nutrient transfer, in the interests of the mother. In unusual situations, where nutrients are in excess (such as due to a very efficient placenta), demand suppressors are activated at a higher threshold to dampen demand, and prevent dangerous embryonic overgrowth.

Being able to dissect the relative contributions of placental *Grb10* and embryonic *Grb10* to the control of growth would, therefore, be of considerable value. Ablation of *Grb10* specifically in one or the other would enable this. Depletion of *Grb10* exclusively in the embryo could be achieved by a tissue-specific rescue, in which *Grb10* expression is driven from a placental-specific promoter on a *Grb10KO*$^{m/+}$ background, although recapitulating endogenous levels of expression would be challenging. Alternatively, the technique of tetraploid rescue could be employed (Nagy and Rossant, 1993). This permits the development of a 'wild type' placenta associated with an embryo carrying a targeted mutation. Thus, the individual contributions of placenta and embryo to the embryonic phenotype can be determined.

Additional evidence for *Grb10* as a demand suppressor comes from the investigation of postnatal nutrient demand. Cross-fostering experiments involving wild type and *Grb10KO*$^{m/+}$ mothers and pups essentially enable a dissociation of mother and pup genotype. This allows the influence of the pup genotype on nutrient demand to be considered in isolation. These experiments are detailed in Chapter Six, and will be discussed in the context of *Grb10* in the placenta in Chapter Seven.

Chapter Five

Tissue-specific regulation of Grb10 *expression by Signal transducer and activator of transcription (Stat) 5*

5.1 Introduction

Sir Francis Crick enunciated what is now commonly referred to as the 'central dogma of molecular biology' in 1958 (Crick, 1958). He postulated that information flowed from deoxyribonucleic acid (DNA) to protein, through a messenger ribonucleic acid (mRNA) intermediate. Key to this model was that the information flow was unidirectional, such that the sequence information of a protein, or more specifically the chain of amino acids forming a polypeptide, could not be used to synthesise DNA. This hypothesis has since been extended to include the system of reverse transcription, in which sequence information can be passed 'backward' from mRNA to produce complimentary DNA (cDNA) under certain conditions.

Although Crick's model accounted for the majority of the experimental evidence of the day, and was accurate in its interpretation, it tells us nothing about the mechanisms through which this information flow is achieved. However, the publication of the central dogma model was highly influential in shaping the direction of subsequent research in molecular biology, and as a result, has unearthed a highly complex and delicately tuned system responsible for regulating this transfer of information. Here, we address briefly how the system is initiated: what regulates, both spatially and temporally, the initiation of transcription?

The polymerisation of RNA molecules to generate mRNA is catalysed by the enzyme RNA polymerase, of which there are three classes in eukaryotes. Polypeptide-encoding mRNA is synthesised by RNA polymerase II. When a gene is to be transcribed, this enzyme binds to the promoter sequence, normally situated 5' to the transcription start point, and recruits co-factors to produce the basal transcription apparatus (reviewed in Thomas and Chiang, 2006). A minimal set of co-factors are an absolute requirement for transcription initiation. The TATA-binding protein (TBP), for example, recognises a consensus sequence ~25 bp upstream of most promoters, referred to as the TATA box because of its high content of AT pairs. The substitution of a single base pair within the TATA box strongly reduces the efficiency of transcription from the associated promoter, and therefore represents one crude mechanism by which the number of transcripts arising can be controlled. TBP recruits various, typically ~11, TBP-associated factors (TAFs). Some TAFs are tissue-specific, representing the first mechanism through which differences in the transcriptome may be achieved between differentiated cell types. The basal transcription apparatus consists of many more proteins, including TFIIH, an enzyme with helicase, ATPase and kinase activities. Its helicase activity separates the double stranded DNA template to permit transcription by RNA polymerase II, a function requiring ATP hydrolysis using its ATPase activity.

More refined levels of gene expression are achieved in each differentiated cell type according to their requirements. For example, whilst proteins involved in the cytoskeleton are expressed at comparable levels in most cell types ('housekeeping' genes), a differentiated β cell of the pancreas requires high levels of insulin transcript relative to all other cell types. Enhancer elements in the DNA sequence are partially responsible for this

additional control of transcription. Enhancers are consensus sequences which recruit transcription factors. A transcription factor, when bound to a target sequence, may alter the structure of the DNA molecule, making it more accessible to the basal transcription unit, or may provide an entry site for RNA polymerase II which associates with the DNA and migrates along the molecule until it encounters TBP bound to a TATA box. Enhancer sequences may be situated immediately adjacent to a promoter, or can be several kilobases away, either up or downstream. Transcription factors bound to distal enhancers may physically interact with proteins of the transcription apparatus which are bound to the promoter, through chromatin looping. Indeed, specific sequences between different chromosomes are found to physically associate more frequently than would be expected by chance, suggesting enhancers may influence gene transcription in an inter-chromosomal manner (Ling *et al*, 2006).

Silencers can function to reduce the rate of transcription to below that of the basal level. This may be necessary where expression of a gene might be detrimental to a cell. In a manner similar to that for enhancers, proteins are recruited to silencers, which can physically block the passage of RNA polymerase II along the DNA molecule.

A further mechanism for the control of transcription initiation may be achieved by DNA sequences which do not bind proteins *per se*, but instead are 'permissive' for the process. This is exemplified by CpG islands, regions of sequence rich in CpG dinucleotides, which overlap 72 % of human gene promoters (Saxonov *et al*, 2006). Indeed, CpG islands are typically associated with a permissive chromatin structure; in other words, a conformation which permits access by transcription factors and ultimately RNA polymerase II. Evidence for the importance of CpG islands in this role includes the relatively high frequency with which sequences similar to promoters, TATA boxes and enhancers occur in the genome. Perhaps CpG islands help to differentiate 'real' from 'bogus' transcription factor binding sites.

This also suggests that, as well as DNA sequence information, chromatin structure is an important contributor to the regulation of gene transcription. This influence is commonly observed in *Drosophila melanogaster*; genes which are juxtaposed to heterochromatic regions are often silenced, and this effect is heritable. This is referred to as position-effect variegation (PEV). Whilst the traditional view is that such an effect is achieved by compacting the gene in question, green fluorescent protein (GFP) tagging experiments have demonstrated that silent chromatin is highly dynamic over a short time period, with an overall reduction in its accessibility to transcription factors (Festenstein *et al*, 2003; Cheutin *et al*, 2003). This implies that factors affecting nucleosome stability are key in regulating chromatin structure, and by extrapolation, the initiation of gene transcription.

It is well-established that transcription factors typically bind at sites devoid of nucleosomes, a property exploited in DNase I hypersensitivity assays. Such nucleosome eviction can be achieved through several means. First, nucleosomes exhibit a preference for certain nucleotide sequences, such that left alone, they would not be evenly spaced along the DNA molecule (Drew and Travers, 1985; Stockdale *et al*, 2006). Put another way, this means a DNA sequence can discourage the association of a nucleosome. Second, chromatin

assembly proteins can shift nucleosome positioning. The ISW2 protein in budding yeast appears to manipulate nucleosomes into energetically unfavourable positions, at which they can actively interfere with transcription (Whitehouse and Tsukiyama, 2006). The histone composition of nucleosomes can also influence positioning. Nucleosomes are composed of an octamer of histones, consisting of two copies each of H2A, H2B, H3 and H4. However, there are subtypes, or variants, of each histone molecule, which typically associate with heterochromatic or euchromatic regions. The H2 histone variant, H2A.Z, for example, localises to active chromatin at the *c-myc* locus, and might 'mark' a nucleosome for eviction (Farris *et al*, 2005). Finally, histone tail modifications are extensive in the genome and highly dynamic. The most important are those of the $(H_3\text{-}H_4)_2$ tetramer. Acetylated H3 tails prevent interactions with other nucleosome components, resulting in destabilisation (reviewed in Henikoff, 2007). Conversely, methylation of a histone 3 molecule on lysine 9 (H3K9) recruits heterochromatin protein 1 (HP1), which interacts with the methylated K9 residue of another histone 3 molecule, either within a nucleosome or that of an adjacent complex, stabilising the structure (Jacobs and Khorasanizadeh, 2002; Motamedi *et al*, 2008). Tail modifications therefore strengthen or weaken anchoring of a nucleosome to the chromatin and thus influence its susceptibility to eviction.

Together, these mechanisms enable gene transcription to be controlled in a well-refined manner, such that each gene is transcribed at a different rate according to how many transcripts are required. Imprinted genes require an additional level of regulatory complexity: they must be expressed monoallelically in a parent-of-origin specific manner. This is achieved by using a similar arsenal of mechanisms to those described for biallelically-expressed genes, but in the context of one active and one silent allele. For imprinted genes, therefore, the key questions are: 1) how are the parental alleles differentiated; and 2) how is this information used to engender monoallelic expression?

CpG islands, as discussed previously, are common to many gene loci, both imprinted and non-imprinted. Although a CpG island alone is, therefore, insufficient to distinguish between the two, the majority of CpG islands in the genome are hypomethylated. Imprinted genes have exploited this property; associated CpG islands are differentially-methylated on the two parental alleles, marking them out from biallelically-expressed genes. Such differentially methylated regions (DMRs) may be shared between two or more imprinted genes located in a cluster, such as in the *H19*/*Igf2* reciprocally-imprinted gene pair. Indeed, this locus exemplifies many of the mechanisms utilised by imprinted genes to achieve monoallelic expression, and the considerable extent to which these have been dissected makes *H19*/*Igf2* a good example with which to illustrate imprinted gene regulation.

H19 is situated ~80 kb downstream of *Igf2* on mouse chromosome 7, and this clustering is conserved on human chromosome 11. *H19* is expressed from the maternally-inherited copy in most tissues, whereas *Igf2* transcripts arise predominantly from the paternally-derived allele. The locus contains four DMRs, although one is tissue-specific and not required for establishing this reciprocal imprint in the majority of somatic tissues. A germline differentially methylated insulator element (termed the *H19* differentially methylated domain (DMD)) is positioned 2-4 kb upstream of the *H19* locus, and is methylated on the

paternally-inherited chromosome. A germline DMR is one whose differential methylation is established during germ cell development and persists in all developmental stages and somatic tissues, as discussed in Chapter One. DMR1 and DMR2 are positioned adjacent to the *Igf2* promoter, and both are paternally hypermethylated. DMR0 is a placental-specific, maternally hypermethylated DMR, giving rise to the *Igf2P0* transcript, whose function is discussed in Chapter Four.

The *H19* DMD contains several binding sites for the zinc finger protein CCCTC-binding factor (CTCF; Bell and Felsenfeld, 2000). On the unmethylated maternally-inherited allele, CTCF associates with these binding sites, and recruits other proteins to form a complex. This is likely to include the cohesion proteins RAD21 and SMC1, which have been shown to associate with CTCF at the *H19*/*Igf2* locus in a parental-allele specific manner, but a function has not been confirmed (Stedman *et al*, 2008). This complex prevents access of downstream enhancer elements to the promoter region of *Igf2*, thereby functioning as a boundary element (Bell and Fesenfeld, 2000). Specifically, this is achieved by a physical interaction between proteins bound at the DMD and those at DMR1, adjacent to the *Igf2* promoter (Murrell *et al*, 2004). Such distal interactions occur through chromatin looping, as demonstrated by chromosome conformation capture. As a consequence, *Igf2* is silenced on the maternally-derived chromosome and *H19* expressed.

On the paternal allele, the *H19* DMD is hypermethylated, abrogating CTCF binding and functioning of the boundary. In the absence of CTCF, the DMD physically interacts with the methylated DMR2, also positioned close to the *Igf2* promoter. This interaction, again demonstrated by chromosome conformation capture (Murrell *et al*, 2004), suggests the importance of proteins other than those of the CTCF complex in this system. As a result of the DMD-DMR2 interaction, the *Igf2* promoter is brought into close proximity to the downstream enhancer elements, and the gene transcribed. In this way, DMR2 can be considered an activator element, whilst DMR1 is a silencer. This is supported by deletion studies, in which ablation of maternal DMR1 confers biallelic *Igf2* expression, whereas DMR2 disruption does not influence imprinting, but reduces transcriptional activation (Constancia *et al*, 2000; Murrell *et al*, 2001).

The silencing of *H19* on the paternally-inherited chromosome is achieved by a mechanism independent of the reciprocal *H19*/*Igf2* imprint, although remarkably, involves a 1.2 kb genomic element situated within the germline DMD. Deletion of this element resulted in the relaxation of *H19* silencing following paternal transmission, but did not interfere with *Igf2* expression or imprinting (Drewell *et al*, 2000). Similarly, the patterns of DNA methylation at the locus were unaffected.

A further level of regulation at this locus was suggested by a modification of the chromosome conformation capture technique which permitted identification of previously unknown remote interacting sequences (Ling *et al*, 2006). This screen pulled out an intergenic sequence on mouse chromosome 11, between the *Wsb1* and *Nf1* genes, which physically interacted with the DMD, implying an inter-chromosomal interaction. This was confirmed using fluorescent *in situ* hybridisation, in which co-localisation between the two regions was identified in 30-40 % of nuclei examined. Further, this interaction was allele

specific, involving exclusively maternally-inherited chromosome 7, and paternally-inherited chromosome 11. No such localisation was detected following CTCF depletion, demonstrating the importance of this protein in mediating the physical interaction. CTCF depletion reduced *Wsb1* and *Nf1* transcription from paternal chromosome 11 by ~50 %, while expression from the other copy was unaffected. As would be expected, loss of imprinting of *Igf2* also resulted from ablation of CTCF. These results are intriguing, as they suggest long-range chromatin interactions need not be confined to the same chromosome, but that regulatory sequences on different chromosomes can contribute to the finely tuned system of gene transcription. Assessing the effect of deleting the *Wsb1-Nf1* intergenic region on *H19*/*Igf2* expression and imprinting status, in the presence of functional CTCF, would be of great interest. *Nf1* and *Wsb1* are also clustered on human chromosome 17, suggesting this inter-chromosomal interaction may be conserved between species.

The imprinting mechanisms described for *H19*/*Igf2* act in concert with the 'usual suspects' to regulate spatial and temporal expression. This includes an array of endodermal and mesodermal enhancer elements, as well as those specific to terminally-differentiated cell types (reviewed in Arney, 2003). Although not characterised for *Igf2* and *H19*, histone variants and tail modifications are likely to associate with the promoter regions in a parent-of-origin specific manner. These are likely to be both permissive and repressive, consistent with the imprinted expression patterns of the two genes. Indeed, in some situations, histone tail modifications alone have been shown to regulate imprinting, entirely independent of DNA methylation. This is exemplified by *MEDEA*, an endosperm-specific imprinted gene in *Arabidopsis*. Unlike the examples described previously, *MEDEA* transcription is kept active on the maternally-inherited chromosome by demethylation (Gehring *et al*, 2006). This process is catalysed by DEMETER, a glycosylase/lyase which excises methyl-cytosine residues and subsequently repairs the DNA, with the effect of actively demethylating nucleotides. The paternally-derived allele is silenced in a mechanism reliant solely upon histone tail modification. The allele is enriched in the repressive methylation of H3 lysine 27 (H3K27me), controlled by Polycomb group proteins expressed from the maternal chromosome, including the product of the *MEDEA* gene itself. It is believed that histone modification is an evolutionarily more ancient imprinting mechanism, and that DNA methylation, which is more stable, evolved later as a maintenance mark (Reik and Lewis, 2005).

This Chapter describes the identification and characterisation of a tissue-specific enhancer element at the *Grb10* locus, which acts independently of the imprinting status of the gene to regulate transcription. This discovery explains a key phenotypic difference between mice inheriting the *Grb10KO* and *Grb10Δ2-4* alleles. Finally, we identify a novel tissue in which *Grb10* is imprinted in the adult mouse, which has implications for understanding the physiological significance, and thus the evolution, of genomic imprinting.

5.2 Results

5.2.1 *Grb10Δ2-4* fails to report *Grb10* expression in the developing central nervous system

Immunohistochemistry experiments on sagittally-bisected mouse embryos at 14.5 days post-coitum (e14.5) revealed the presence of Grb10 protein in the developing brain (Charalambous *et al*, 2003). The *LacZ* reporter expressed from the *Grb10Δ2-4* allele, however, did not report expression in this tissue in bisected embryos. Conversely, the *Grb10KO* allele fully recapitulated endogenous *Grb10* expression, including mirroring antibody staining in the developing CNS (Garfield, 2007). Specifically, expression in this tissue was almost exclusively from the paternally-inherited allele, despite the majority of transcripts in embryonic tissues arising from the other copy (Figure 5.1*a* and *b*). This reciprocal imprinting pattern persisted into adulthood (Figure 3.4*a*).

A direct comparison between foetuses inheriting the two reporter alleles through the maternal line revealed an essentially identical expression profile, with an abundance of β-galactosidase in most tissues of both mesodermal and endodermal origin, including heart, cartilage of the ribs, tongue and lungs, as described previously (Figure 5.1*a* and *c*; Section 3.1; Charalambous *et al*, 2003). The contribution from the maternally-inherited allele was also apparent in the choroid plexus in both transgenic lines.

The apparent absence of reporter expression in the CNS following paternal transmission of *Grb10Δ2-4* is striking when compared with a matched conceptus inheriting the *Grb10KO* allele (Figure 5.1*b* and *d*). Indeed, the *Grb10Δ2-4*$^{+/p}$ foetus presented in Figure 5.1*d* was incubated in X-gal substrate for longer than the *Grb10KO*$^{+/p}$ counterpart, explaining the apparent increase in levels of reporter expression in peripheral tissues, including tongue, cartilage of the ribs and ventricles of the developing heart. Despite this extended staining period, no reporter expression was detected in any cells of the midbrain, hindbrain or ventral spinal cord, at the resolution of a bisected embryo.

5.2.2 Two models could account for *Grb10KO* and *Grb10Δ2-4* reporter differences

The observation of differences in reporter expression profiles following paternal inheritance of *Grb10KO* and *Grb10Δ2-4* was initially unexpected, given that both alleles were generated from the integration of a β-*geo* cassette into the same locus. The genomic structures of the two alleles were analysed and models devised to account for the observed differences. Figure 5.2*a* presents the structure of the wild type *Grb10* allele, and displays the alternative initiation exons utilised for brain-specific transcripts, as discussed in Chapter One (Arnaud *et al*, 2003; Hikichi *et al*, 2003; Sanz *et al*, 2008).

Our first model described splicing around the β-*geo* cassette in transcripts arising from the *Grb10Δ2-4* allele (Figure 5.2*b*). Detailed mapping of the *Grb10KO* allele (Section 3.2.1)

Maternal transmission (m/+)

Paternal transmission (+/p)

Grb10KO

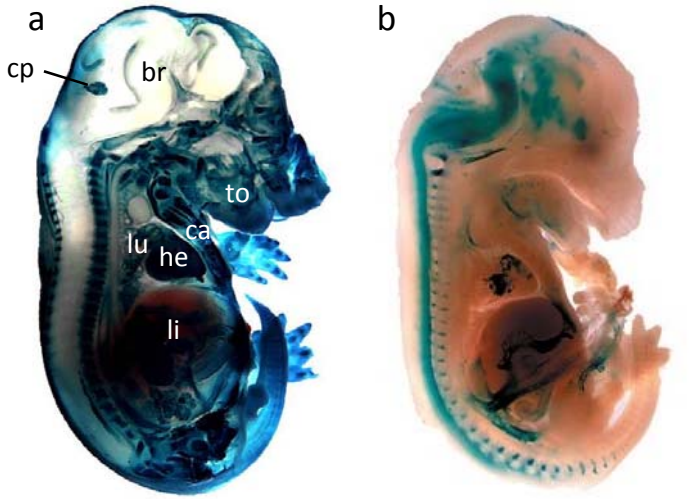

Grb10Δ2-4

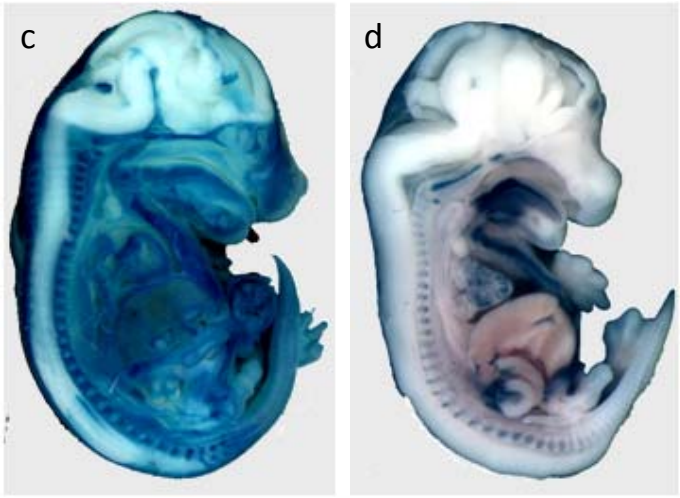

a Wild type

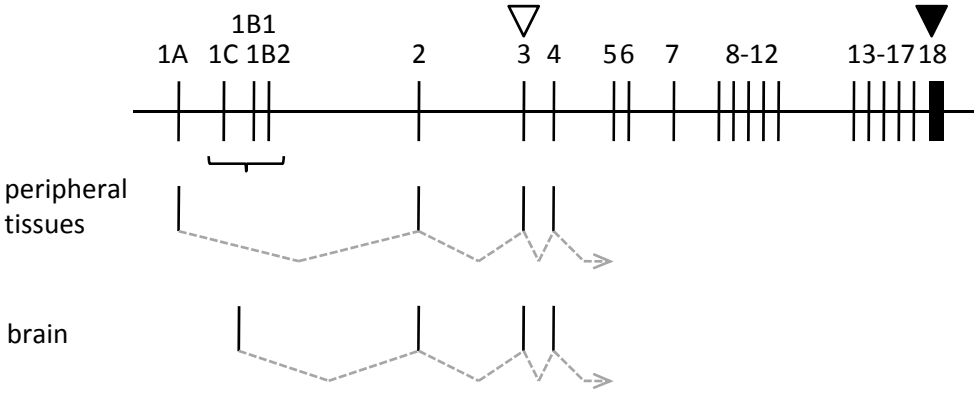

b *Grb10Δ2-4* – splicing around β-*geo* cassette in the CNS

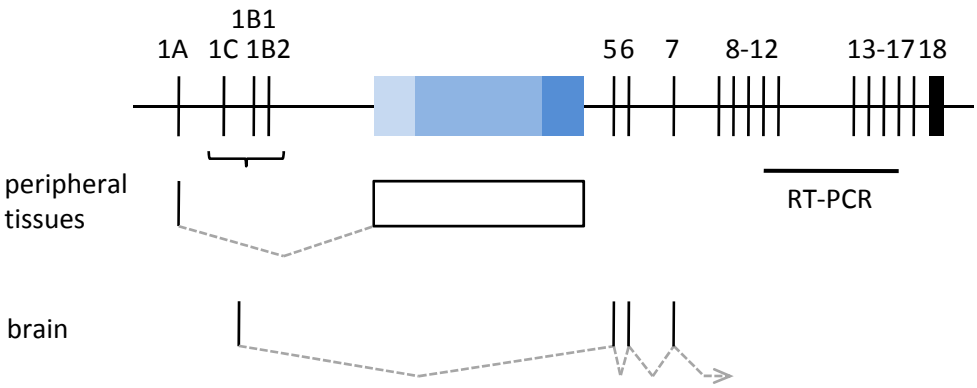

c *Grb10Δ2-4* – deletion of a CNS-specific enhancer

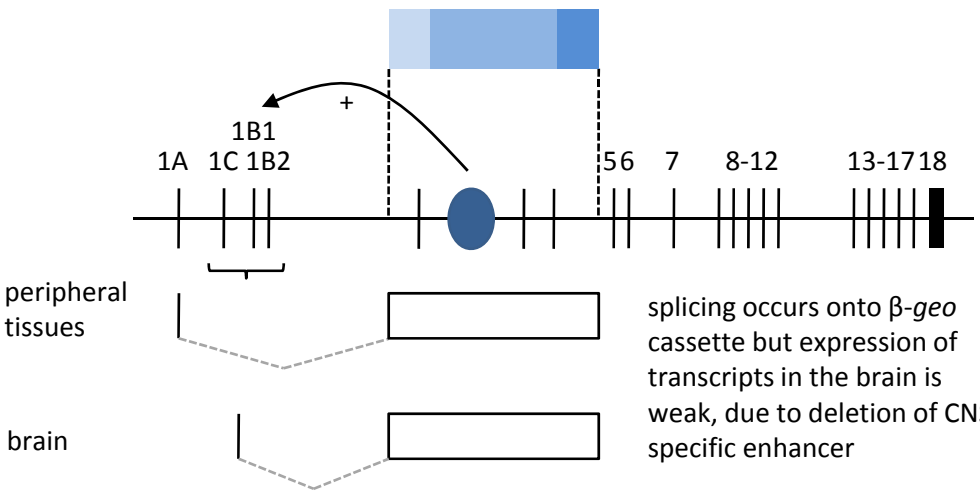

splicing occurs onto β-*geo* cassette but expression of transcripts in the brain is weak, due to deletion of CNS-specific enhancer

revealed a deletion of 825 bp at the 5' end of the β-*geo* cassette, although this did not include the splice acceptor sequence. Such a deletion, perhaps including the splice acceptor, might also have occurred during the integration to create the *Grb10Δ2-4* allele. As a consequence, transcripts arising from the *Grb10* promoter region would fail to splice onto the *LacZ* reporter, either terminating prematurely or splicing onto a downstream exon. The latter option appeared unlikely due to the inability to detect transcripts in *Grb10Δ2-4*$^{m/+}$ embryo RNA using a probe complimentary to exon 18, 3' to the β-*geo* cassette (Charalambous *et al*, 2003). Moreover, neither option could account for the accurate reporting of *Grb10* transcripts in tissues outside of the central nervous system; a deletion of the splice acceptor sequence at the genomic level would persist in all tissues. A modification of this model proposed that splicing around the β-*geo* cassette might be an event specific to the CNS, such that the splice acceptor sequence is retained and utilised only in peripheral tissues (Figure 5.2*b*).

An alternative model proposed the deletion of an enhancer element following integration of the β-*geo* cassette to generate the *Grb10Δ2-4* allele (Figure 5.2*c*). The activity of such an element may be restricted to the CNS, such that the levels of transcripts in peripheral tissues are not affected by its deletion. About 38 kb of genomic sequence was lost in the creation of *Grb10Δ2-4* (Charalambous *et al*, 2003), within which an enhancer element may reside.

5.2.3 No evidence for splicing around the β-*geo* cassette in the *Grb10Δ2-4*$^{+/p}$ brain

To address the possibility that the β-*geo* cassette failed to trap brain-specific transcripts initiating at the *Grb10Δ2-4* allele, semi-quantitative RT-PCR was performed on wild type, *Grb10Δ2-4*$^{m/+}$ and *Grb10Δ2-4*$^{+/p}$ total brain RNA. Primers were designed to anneal to the *Grb10* cDNA sequence downstream of the β-*geo* cassette, specifically amplifying a 505 bp region spanning exons 11 to 16 (Figure 5.2*b, horizontal bar*).

Amplification using primers specific to the housekeeping gene β-*actin* demonstrated comparable concentrations of cDNA for all samples analysed, and no amplification products could be detected in samples from which reverse transcriptase was omitted (–RT), confirming the absence of genomic DNA (Figure 5.3). *Grb10* primers amplified to a similar extent from wild type and *Grb10Δ2-4*$^{m/+}$ cDNA, consistent with our findings that most transcripts in the brain are not expressed from the maternally-inherited chromosome (Figure 3.3; Figure 5.1*a* and *c*). Amplification from *Grb10Δ2-4*$^{+/p}$ cDNA was considerably reduced, demonstrating the effective trapping of the majority of *Grb10* transcripts in the brain following paternal inheritance of the *Grb10Δ2-4* allele. If transcripts were splicing around the β-*geo* cassette in the brain, amplification from *Grb10Δ2-4*$^{+/p}$ cDNA would be expected to be comparable to that from wild type cDNA. The low level of *Grb10* transcripts detected in *Grb10Δ2-4*$^{+/p}$ brain supports the observation of transcription from the maternally-derived allele in non-neural sites (choroid plexus, ependymal layers and meninges), utilising the *LacZ* reporter in *Grb10KO* mice (Figure 5.1*a*; Garfield, 2007). In conclusion, the result argues against the splicing model as an explanation for the absence of *LacZ* transcripts in the brains of *Grb10Δ2-4*$^{+/p}$ mice.

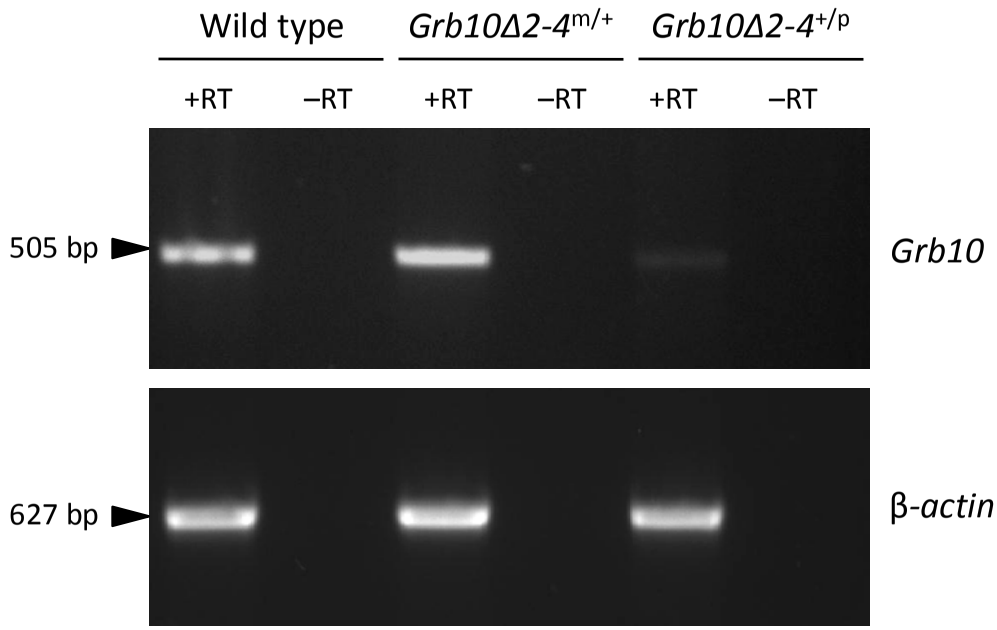
Wild type
Grb10Δ2-4m/+
Grb10Δ2-4+/p
+RT
–RT
+RT
–RT
+RT
–RT
505 bp
Grb10
627 bp
β-actin

5.2.4 Conserved intronic sequences represent potential enhancer elements

We addressed the possibility that the deleted endogenous sequence from the *Grb10Δ2-4* allele might harbour a CNS-specific enhancer element. Initially, sequence alignments between different mammalian species were performed. The programme ExactPlus (Antonellis *et al*, 2006) was utilised to identify short (≥ 6 bp) conserved sequences at the *Grb10* locus, which might represent transcription factor binding sites. To prevent interference from exonic sequences, which would be expected to retain a high degree of conservation, exons 1 to 5 were eliminated from the alignment. Exons 6 to 18 were included as positive controls for the detection of conserved sequence. Similarly, the 5' and 3' extremities of introns can display a high degree of conservation, due to the presence of splice recognition sequences. Thus, 15 bp at both ends of introns 1, 2, 3 and 4 were also excluded from the analysis. Further details of the parameters employed are described in Section 2.6.1.

An initial alignment between the mouse and human *Grb10* sequences revealed extensive conservation. Figure 5.4 provides a graphical depiction of the alignment, created by importing the ExactPlus output into the UCSC Genome Browser as a custom track. Genomic regions in which two or more short conserved sequences are clustered (that is, positioned within a few base pairs of each other) are represented by vertical dark red bars. The height of a bar is a reflection of the total number of conserved base pairs within that cluster. Clusters of short conserved sequences included a considerable proportion of most introns, as well as exons 6 to 18, confirming the suitability of the parameters in detecting homology. The addition of the chimpanzee *Grb10* sequence made a negligible difference to the comparison, but the close evolutionary relatedness of human and chimpanzee might account for this. Inclusion of the *Grb10* sequence from a fourth mammal, namely cow, revealed a much smaller number of short conserved sequence clusters, which were a subset of those identified from the mouse-human-chimpanzee alignment. Most of the conserved intronic clusters were positioned in introns 1-4, several of which were within the limits of the deleted endogenous region (Figure 5.4, *lower bar*) and therefore candidates for further investigation.

Using the same parameters, the murine *Grb10* sequence was aligned with the frog ortholog. Clusters of conserved intronic sequences between these two species formed a subset of those identified from the alignment of the four eutherian mammals. Similarly, comparison of the mouse and chicken *Grb10* sequences identified conserved sites already determined from previous alignments. Finally, the mouse *Grb10* sequence was compared with the ortholog from opossum. The conservation profile for this alignment incorporated a larger number of clusters identified from the mouse-human-chimpanzee-cow alignment than for the mouse-frog or mouse-chicken comparisons, consistent with a closer evolutionary relatedness between mouse and opossum than frog or chicken.

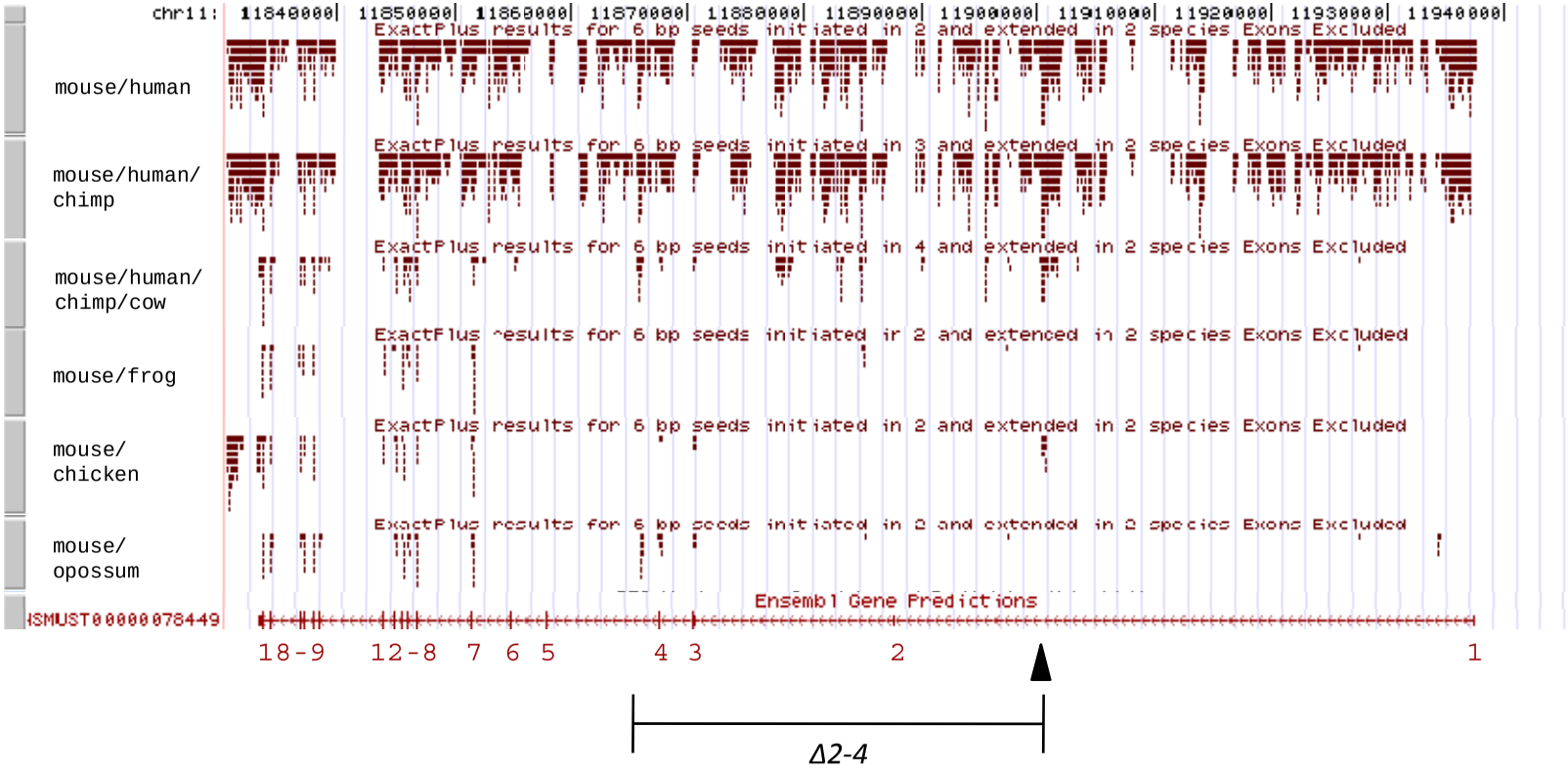
chr11: 11840000 11850000 11860000 11870000 11880000 11890000 11900000 11910000 11920000 11930000 11940000
mouse/human
ExactPlus results for 6 bp seeds initiated in 2 and extended in 2 species Exons Excluded
mouse/human/ chimp
ExactPlus results for 6 bp seeds initiated in 3 and extended in 2 species Exons Excluded
mouse/human/ chimp/cow
ExactPlus results for 6 bp seeds initiated in 4 and extended in 2 species Exons Excluded
mouse/frog
ExactPlus results for 6 bp seeds initiated in 2 and extended in 2 species Exons Excluded
mouse/ chicken
ExactPlus results for 6 bp seeds initiated in 2 and extended in 2 species Exons Excluded
mouse/ opossum
ExactPlus results for 6 bp seeds initiated in 2 and extended in 2 species Exons Excluded
Ensembl Gene Predictions
ENSMUST00000078449
18-9 12-8 7 6 5 4 3 2 1
Δ2-4

5.2.5 Identification of a conserved sequence with consensus transcription factor binding sites

Whilst a sequence alignment between homologous genes separated through speciation can highlight possibilities for further analyses, the result does not permit conclusions to be drawn about the biological significance, if any, of conserved regions. In order to specifically search for regulatory elements, the entire *Grb10* locus was screened against a database of known consensus transcription factor binding sites, using the programme PReMod (Blanchette *et al*, 2006). This screen identified a single *cis*-regulatory module (CRM) candidate at the locus, which did not map to any previously described regulatory elements. The structure of this CRM, herein referred to as *cis*-regulatory module 1 (CRM1), is shown in Figure 5.5. The 70 bp sequence consists of several potential transcription factor binding sites, which have been ranked in relative order of similarity to their consensus recognition sequence; thus, numeric scores (Figure 5.5, *right*), calculated using an algorithm in the PReMod software, reflect the likelihood that a transcription factor binds at the site.

The highest scoring 'hit' consisted of two sequences, in tandem repeat, which show similarity to the consensus recognition sequence for Signal transducer and activator of transcription (Stat)5b. Other potential binding sites within the cluster included two sequences similar to a generic Pax protein consensus site. The tandem repeat sequences potentially recognised by Stat5b are also similar to those bound by the closely-related protein Stat5a, although a lower numeric score reflects a greater dissimilarity with the Stat5a consensus. Sequences related to those recognised by the bZIP transcription factor Tcf11 and the POU-domain transcription factor Tst-1 were also identified, but achieved the lowest likelihood scores. Worthy of note is that several of these potential recognition sites overlap.

The 70 bp CRM1 region incorporated or overlapped with three of the short conserved sequences identified using ExactPlus, which formed a cluster (Figure 5.4, *black arrowhead* and Figure 5.6), suggesting much of this regulatory module has been retained in the genome through multiple speciation events. Indeed, a large proportion of the module was highly conserved between five of the orthologs examined; this included the *Grb10* sequences of the four eutherian mammals, as well as chicken. Despite some variation within CRM1, the putative recognition sequences for Stat5b, identified as the most likely active candidates by PReMod because of their similarity to the consensus, were perfectly conserved between the five species (Figure 5.6).

The position of CRM1 within the deleted endogenous sequence of the *Grb10Δ2-4* allele suggested it was a suitable candidate for the CNS-specific enhancer element proposed in the model in Figure 5.2*c*.

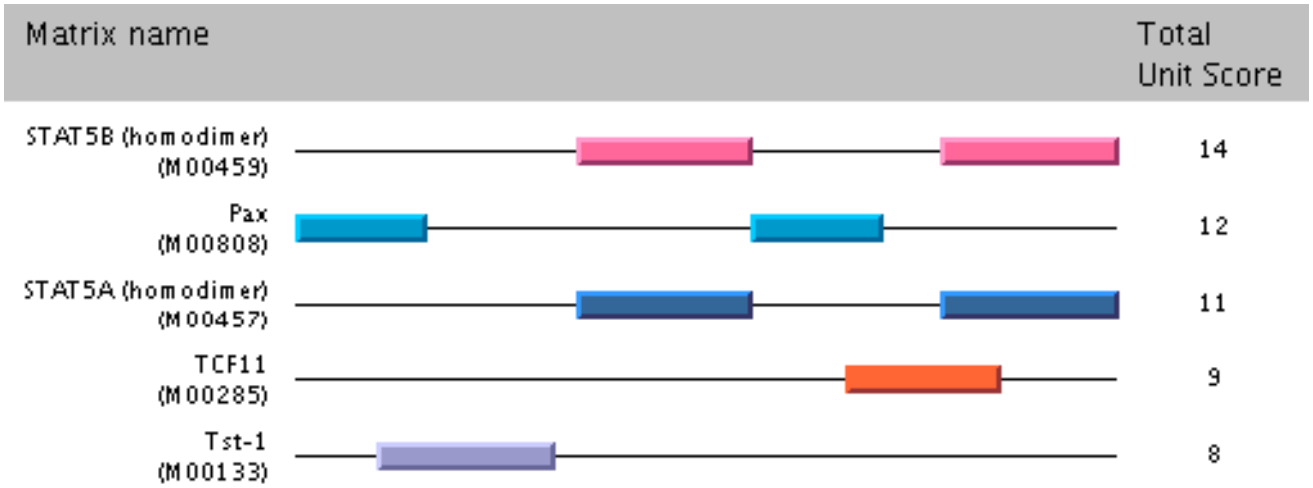
Matrix name
Total Unit Score
STAT5B (homodimer) (M00459)
14
Pax (M00808)
12
STAT5A (homodimer) (M00457)
11
TCF11 (M00285)
9
Tst-1 (M00133)
8

PReMod
ExactPlus
>gi|mod010470 chr11:11895215-11895285 (UCSC March 2005)
CTGGAACCCACTGTAAATCATCTTGTTTTCTGAGAAATTCTGGAACTGTCATCTAATTTTCCAGGAACAC
11900412-11900447 Length: 36
Mouse CAGATTGCTCAAGACTGGAACCCACTGTAAATCATC
Human ACGACTGCTCAAGACTGGAACCCATTGTAAATCATC
Chimp ACGATTGCTCAAGACTGGAACCCATTGTAAATCATC
Cow CATATTACTCAAGACT-GAATGCACTGTAAATCATC
Chick CAGATTGCAAAAGAACGGAA-ACACAGTAAATCATC
11900451-11900479 Length: 29
Mouse TTTTCTGAGAAATTCTGGAACTGTCATCT
Human TATTCTGAGAAATTCTGGAACTGTCATCT
Chimp TATTCTGAGAAATTCTGGAACTGTCATCT
Cow TGTTCTGAGAAATTCTGGAACTGTCAGCT
Chick TTTTCTGAGAAATTCTGGGACTATGTTCT
11900481-11900495 Length: 15
Mouse ATTTTCCAGGAACAC
Human ATTTTCCAGGAACAA
Chimp ATTTTCCAGGAACAA
Cow ATTTTCCAGGAACAC
Chick AATTTCCAGGAACAG

5.2.6 *Cis*-regulatory module 1 is hypersensitive to DNase I in brain chromatin

The tissue-specific activity of promoter and enhancer sequences is often achieved through differences in chromatin conformation; a transcription factor may only be capable of binding to a recognition sequence if such a site is physically accessible. The ability of chromatin to adopt 'open' and 'closed' states is thus responsible for many of the differences in gene expression observed between differentiated tissues.

To examine the accessibility of CRM1 to transcription factors, and thus assess its potential as a transcription factor binding site *in vivo*, chromatin isolated from adult wild type brain and liver samples was exposed to varying concentrations of DNase I. This enzyme possesses endonuclease activity, but is restricted in its digestion of genomic DNA by the presence of nucleosomes. Following a 20 minute incubation with DNase I, DNA was purified, cleaved with *Bam*HI, and subsequently prepared for Southern analysis using a probe complimentary to CRM1 and the surrounding genomic sequence (probe C; Figure 5.7*a*).

A 6 kb *Bam*HI digestion fragment was apparent in all samples exposed to DNase I, regardless of tissue origin (Figure 5.7*b*). A species of smaller molecular weight was observed in the brain chromatin sample challenged with the highest amount of DNase I (200 Units (U)). This fragment maps to the 3.8 kb DNase I digestion fragment expected if CRM1 was in an 'open' conformation (Figure 5.7*a*). Probe C did not detect this digestion fragment in brain samples exposed to 0 or 120 U of DNase I. Moreover, this fragment was not detected in samples of liver chromatin exposed to the same conditions, consistent with the hypothesis that CRM1 is a CNS-specific enhancer, and is inaccessible to transcription factors in the liver. Although probe C was complimentary to genomic sequence both 5' and 3' to CRM1, it did not detect a fragment consistent with the expected 2.2 kb DNase I digestion product.

5.2.7 Grb10 and Stat5b are co-expressed in the mature mouse brain

Potential binding sites for several transcription factors were identified within CRM1 (Figure 5.5). To validate which of these, if any, were likely candidates for regulating transcription of *Grb10* in the CNS, an examination of their expression profiles in the brain was performed. Grb10 protein is not ubiquitous in this organ, being restricted to specific cell populations of the midbrain and hindbrain (Garfield *et al*, submitted). We utilised the comprehensive database of *in situ* hybridisation images collated in the Allen Brain Atlas, available for public use at www.brain-map.org, and systematically screened all known sites of *Grb10* expression in the brain for *in situ* signal representing each of the candidate transcription factors.

a

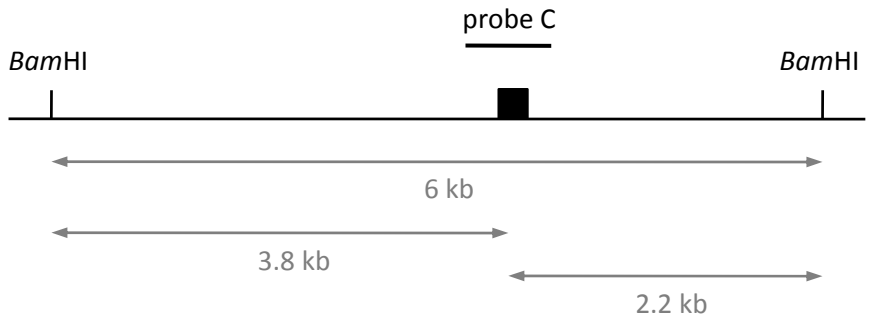
probe C
BamHI
BamHI
6 kb
3.8 kb
2.2 kb

b

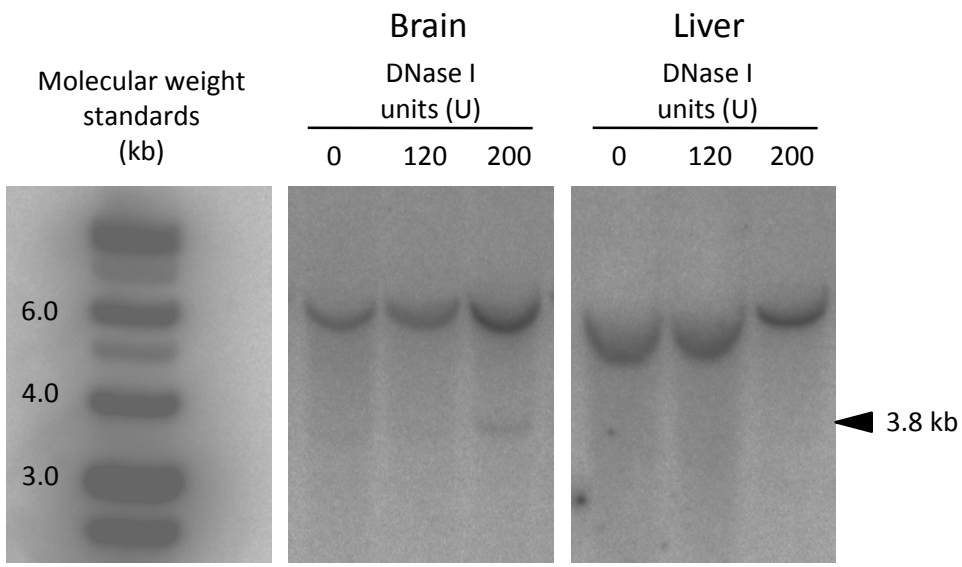
Brain
Liver
Molecular weight standards (kb)
DNase I units (U)
0
120
200
DNase I units (U)
0
120
200
6.0
4.0
3.0
3.8 kb

Stat5b

Within CRM1, the transcription factor binding sequence with closest similarity to its consensus was that for Stat5b. Use of the expression summary graphs available from the Allen Brain Atlas revealed a similar profile of expression to *Grb10*, with strong signal for both apparent in the hypothalamus. Sites at which *Grb10* expression was essentially undetectable, including the cortex and hippocampus, demonstrated the lowest levels of *Stat5b*, with the single exception of the cerebellum, in which *Stat5b* signal was relatively strong.

To examine sites of expression at a more detailed resolution, *in situ* hybridisation images for *Stat5b* and *Grb10*, from coronal sections, were manually screened. Like *Grb10*, *Stat5b* was not ubiquitous within the regions identified from the expression summary graphs, but was restricted to specific cell populations. Indeed, *Stat5b* could be detected in the majority of sites at which *Grb10* expression has previously been described, including, for example, the locus coeruleus and the Edinger-Westphal and arcuate nuclei. A striking overlap was revealed from a direct comparison of *Stat5b in situ* images with those of the *LacZ* reporter in *Grb10KO*$^{+/p}$ brain sections, representing *Grb10*. Three representative sites are presented in Figure 5.8. The medial habenular nucleus, located in the epithalamus, contained high levels of β-galactosidase relative to surrounding neuronal cells, and this was mirrored by a more intense *in situ* signal for *Stat5b* at this site (Figure 5.8*a* and *b*). Similarly, cells of the dorsal raphe nucleus demonstrated high levels of *LacZ* expression, and *in situ* signal for *Stat5b* was higher than the general background levels (Figure 5.8*c* and *d*). Perhaps the most convincing demonstration of co-expression was at the substantia nigra, wherein *Grb10* is restricted to the pars compacta and almost entirely absent from the pars reticulata (Figure 5.8*e*). Consistent with this, *Stat5b* was clearly detected in the substantia nigra pars compacta, but no signal above the level of background noise could be detected in the pars reticulata (Figure 5.8*f*).

A section-by-section analysis was performed for all other candidate transcription factors shown in Figure 5.5, but none displayed such a tight co-expression with Grb10 as *Stat5b*. Outlined below is an overview of expression of the remaining candidates, using the expression summary graphs available from the Allen Brain Atlas (images not shown).

Pax

The Pax recognition sequence identified within CRM1 was a generic consensus sequence, potentially capable of being bound by any member of the Pax transcription factor family. Screening was therefore performed for all nine described *Pax* genes. Consistent with previously published reports (Blake *et al*, 2008 and references therein), *Pax6* was found to have the widest expression profile in the adult brain, with *in situ* hybridisation signal strongest in cells of the cerebellum, hypothalamus, thalamus and olfactory bulb. The profile for *Pax1* was similar to that for *Pax4*, with apparently highest expression in the olfactory bulb, cerebral cortex and hippocampal region for both. *In situ* hybridisation for

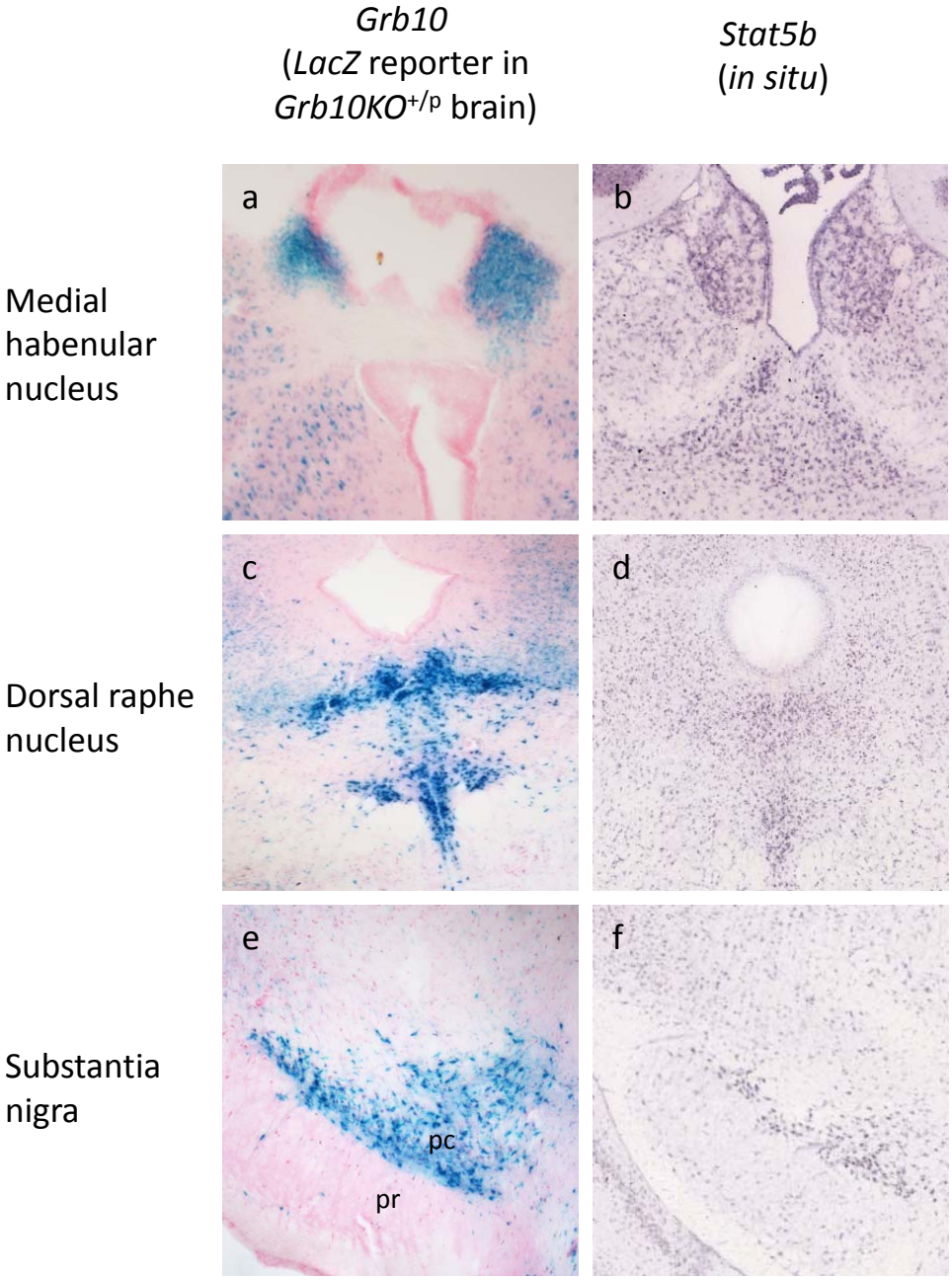
Grb10
(*LacZ* reporter in
Grb10KO$^{+/p}$ brain)
Stat5b
(*in situ*)
Medial habenular nucleus
Dorsal raphe nucleus
Substantia nigra
a
b
c
d
e
f
pc
pr

the remaining *Pax* genes revealed relatively low levels of expression, a result matched by the manual examination of sagittal sections.

Stat5a

Despite significant structural similarity with Stat5b, the expression of *Stat5a* was strongest in the medulla and cortex, sites at which both its homolog and *Grb10* are expressed weakly. Additionally, *Stat5a* expression was almost undetectable in the hypothalamus, a key site of *Grb10* transcription. Thus, although Figure 5.5 identifies both Stat5a and Stat5b as being potentially able to recognise the same 9 bp sequence, the expression profile of Stat5a essentially eliminates it as a candidate.

Tcf11

The expression summary graph for this transcription factor implied an ubiquitous profile, with high levels of *in situ* signal detected in all regions of the brain. However, the protein is encoded by the gene *Nfe2l1*, previously described as being transcriptionally active in erythrocytes (Caterina *et al*, 1994), but not identified in neurons. This explained the widespread distribution of the transcription factor in the brain and, further, excluded it as a candidate for regulating *Grb10* expression.

Tst-1

In situ hybridisation images of this POU-domain transcription factor were unavailable from the Allen Brain Atlas, but its expression profile in the rat brain has been characterised in some detail (He *et al*, 1989). Transcripts were most abundant in the cortex and parabigeminal nucleus of the mature rat brain, representing a subset of the cells in which *Tst-1* was detected during embryonic development. This restricted adult expression profile rendered Tst-1 an unlikely candidate for regulating the transcription of *Grb10* in the brain.

5.2.8 CRM1 has enhancer capacity in the presence of constitutively active Stat5b

Comparison of the expression profiles of each of the transcription factors shown in Figure 5.5 identified Stat5b as the strongest candidate for regulating *Grb10* transcription in the CNS. To confirm that CRM1 is indeed an enhancer element, and that its activity can be controlled by the binding of Stat5b, an *in vitro* luciferase assay was performed using NIH/3T3 mouse fibroblasts.

A 799 bp region, containing the 70 bp CRM1, was amplified by PCR from wild type DNA (Section 2.3.1). The resulting fragment was cloned upstream of the minimal SV40 promoter sequence in the pGL3-Promoter vector (Figure 5.9*a*), creating a construct herein referred to

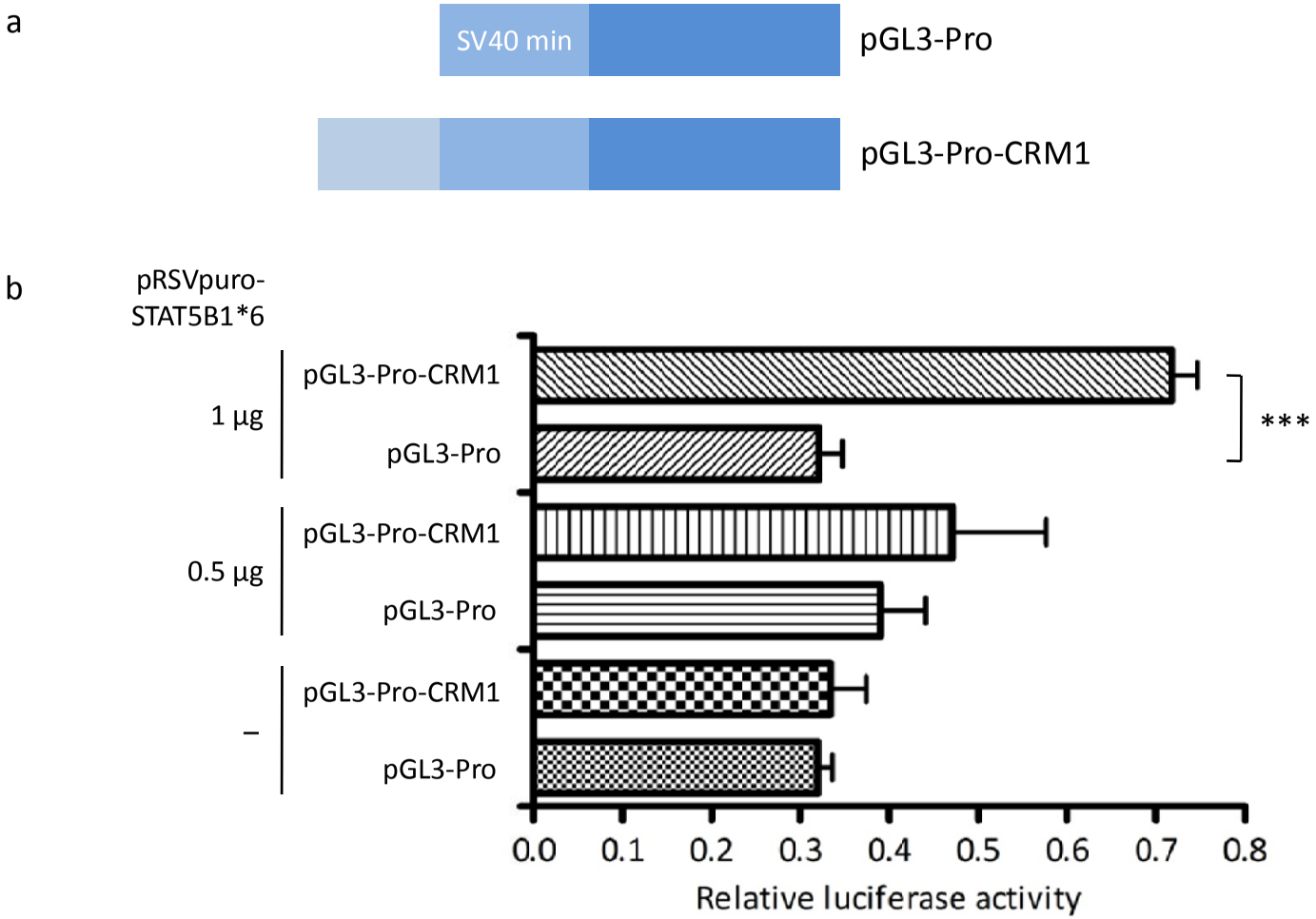
a
SV40 min
pGL3-Pro
pGL3-Pro-CRM1
b
pRSVpuro-
STAT5B1*6
1 µg
0.5 µg
–
pGL3-Pro-CRM1
pGL3-Pro
pGL3-Pro-CRM1
pGL3-Pro
pGL3-Pro-CRM1
pGL3-Pro
***
0.0
0.1
0.2
0.3
0.4
0.5
0.6
0.7
0.8
Relative luciferase activity

as pGL3-Pro-CRM1. This vector also contained the gene encoding firefly luciferase, positioned immediately downstream of the minimal promoter and thus under the influence of CRM1.

First, empty vector (pGL3-Pro; Figure 5.9*a*) or pGL3-Pro-CRM1 were co-transfected with pRL-SV40, a construct expressing *Renilla* luciferase, into NIH/3T3 fibroblasts. The activity of firefly luciferase was detected 48 hours later and normalised to levels of *Renilla* luciferase, thereby controlling for any variability in transfection efficiency and cell viability. The presence of CRM1 upstream of firefly luciferase did not, on its own, significantly influence transcription of this reporter, with no difference observed from transfecting empty vector (Figure 5.9*b*).

Next, the influence of a constitutively active Stat5b mutant (pRSVpuro-STAT5B1*6; Onishi *et al*, 1998) on luciferase expression was examined. As before, cells were transfected with pGL3-Pro or pGL3-Pro-CRM1 alongside pRL-SV40, but 0.5 µg or 1 µg of pRSVpuro-STAT5B1*6 was also introduced. Neither amount of constitutively active Stat5b influenced luciferase activity when co-transfected with empty vector (Figure 5.9*b*). 0.5 µg constitutively active Stat5b appeared to increase luciferase activity in the presence of CRM1, although this did not reach statistical significance. Co-transfecting 1 µg of the constitutively active Stat5b construct with pGL3-Pro-CRM1 increased luciferase activity to 2.2 times the level of that achieved with empty vector, a statistically significant change. These results suggested that the combination of active Stat5b with the presence of CRM1 enhanced reporter gene expression, and that this response appeared to be dose-dependent.

This established that CRM1, *in vitro*, was an element with enhancer properties which could be stimulated by the presence of active Stat5b.

5.2.9 CRM1 may also be active in the placenta

Chapter Four characterised both the transcriptional activity and phenotypic influence of *Grb10* on the late-gestation placenta, using the *Grb10KO* allele as a tool. Previous, unpublished, experiments had suggested that the *Grb10Δ2-4* allele was a poor reporter of *Grb10* expression in this organ, but a direct comparison with the *Grb10KO* allele had not been performed. We wished to examine relative reporter expression from the two alleles in the placenta, with a view to determining whether this might be another site at which CRM1 could be active.

As described in Section 4.2.1, both the parental alleles contribute to the *Grb10* transcript pool in the placental labyrinth and chorionic plate, with biased expression from the maternally-inherited chromosome (images reproduced in Figure 5.10*a* and *b*). Placentae developing from the extraembryonic tissues of *Grb10KO*$^{m/+}$, *Grb10KO*$^{+/p}$, *Grb10Δ2-4*$^{m/+}$ and *Grb10Δ2-4*$^{+/p}$ embryos were isolated at e14.5, cryosectioned and stained simultaneously for *LacZ* expression for 18 hours. Figure 5.10*d* confirms both the profile and allelic-bias of *Grb10* expression in the late-gestation placenta, as described in Chapter Four, using

Grb10KO as a reporter. Reporter expression in *Grb10Δ2-4*$^{m/+}$ placentae was considerably reduced, with only a few trophoblast cells staining positive for *LacZ*, despite the use of identical conditions and substrate solution. *Grb10Δ2-4*$^{+/p}$ placentae were entirely devoid of positive staining.

Whilst *Grb10Δ2-4*$^{+/p}$ brains stained *in situ* in a sagittally-bisected embryo appeared not to express any *LacZ* reporter, staining of sectioned adult brains revealed a weak activity which mapped to the sites of expression described for *Grb10KO* (Garfield, 2007; Garfield *et al*, submitted). To determine whether this was also the case for the placenta, *Grb10Δ2-4*$^{m/+}$ and *Grb10Δ2-4*$^{+/p}$ sections were incubated in X-gal substrate for 60 hours. This extended incubation time revealed correctly localised positive reporter expression, but only for the placenta carrying the maternally-inherited *Grb10Δ2-4* allele (Figure 5.10*c*). No signal could be detected from *Grb10Δ2-4*$^{+/p}$ placentae (not shown), reflecting the significantly smaller contribution of this allele to the *Grb10* transcript pool (Figure 4.3).

5.2.10 Stat5 is expressed in extra-embryonic tissues of the late-gestation placenta

Whilst the expression of *Stat5b* in the adult brain appeared to mirror that for *Grb10* closely, no published reports describe the sites of *Stat5* expression in the mouse placenta, although one study has identified the presence of Stat5b transcripts in a human placental cDNA library (Sawka-Verhelle *et al*, 1997). Wild type embryos were sacrificed at e14.5 and their corresponding placentae embedded in wax and sectioned. Immunohistochemistry, using a pan-Stat5 primary antibody, detected protein in all extra-embryonic layers of the placenta, including labyrinth, chorionic plate and spongiotrophoblast (Figure 5.11*a*). No staining was detected in the absence of primary antibody (Figure 5.11*d*). A detailed view of the labyrinth identified Stat5 in the cytoplasm of all cell types, excluding foetal and maternal red blood cells (Figure 5.11*b*). Nuclear localisation, indicating Stat5 actively promoting gene transcription in response to hormonal stimulus, was varied. Whilst all foetal endothelial cells examined demonstrated nuclear as well as cytosolic localisation of Stat5, only a subset of cytotrophoblast and syncytiotrophoblast nuclei were positive for the protein.

Stat5 was detected in both the cytoplasm and nuclei of the majority of spongiotrophoblast cells, whereas the nuclei of trophoblast giant cells and glycogen cells rarely stained positive (Figure 5.11*c*). No signal was detected in the decidua, forming the maternal contribution to this organ.

The widespread expression of Stat5 in the late-gestation placenta is consistent with this protein regulating *Grb10* transcription, although its presence in cells which are not positive for *Grb10* implicate other gene targets.

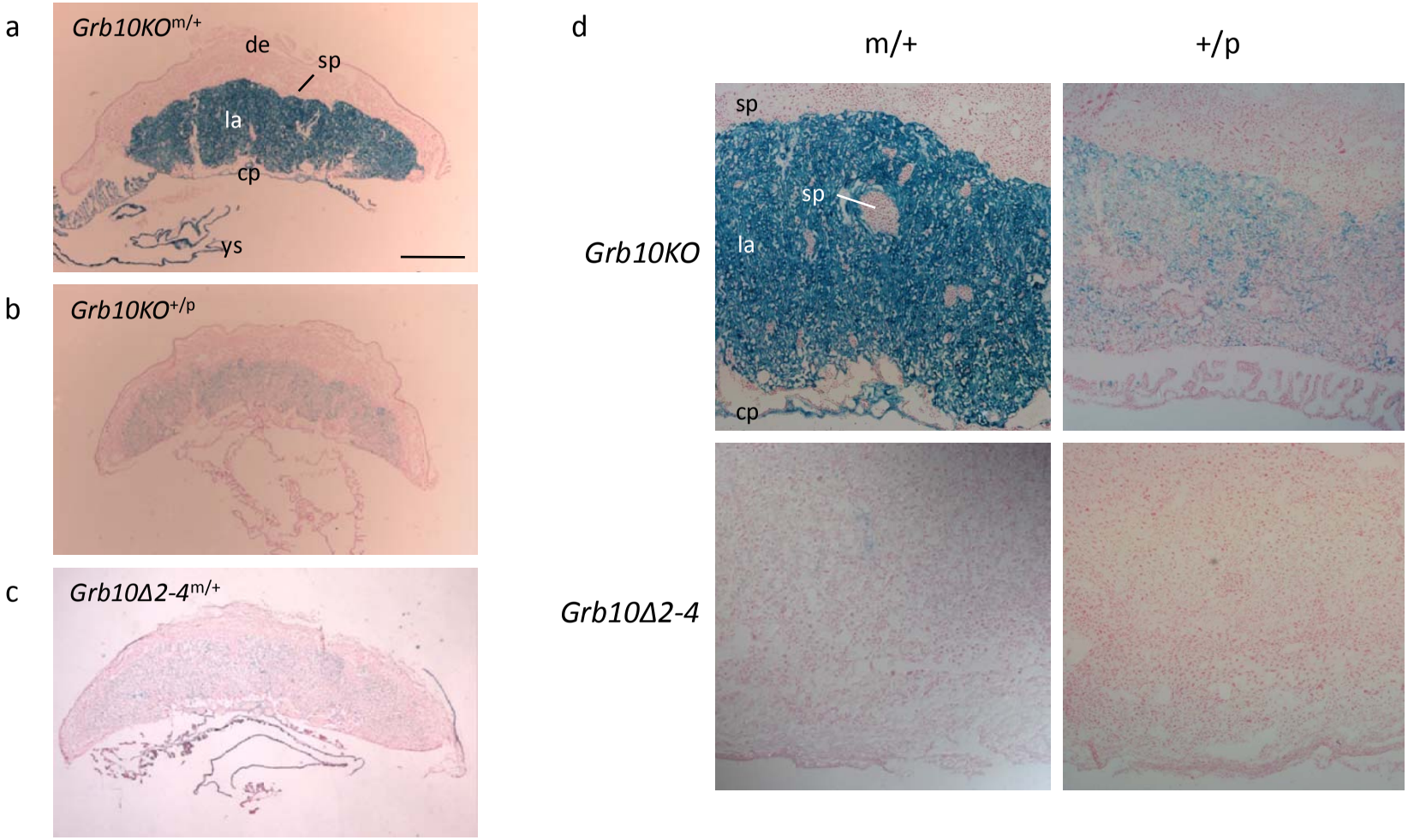
a
Grb10KO m/+
de
sp
la
cp
ys
b
Grb10KO +/p
c
Grb10Δ2-4 m/+
d
m/+
+/p
Grb10KO
sp
sp
la
cp
Grb10Δ2-4

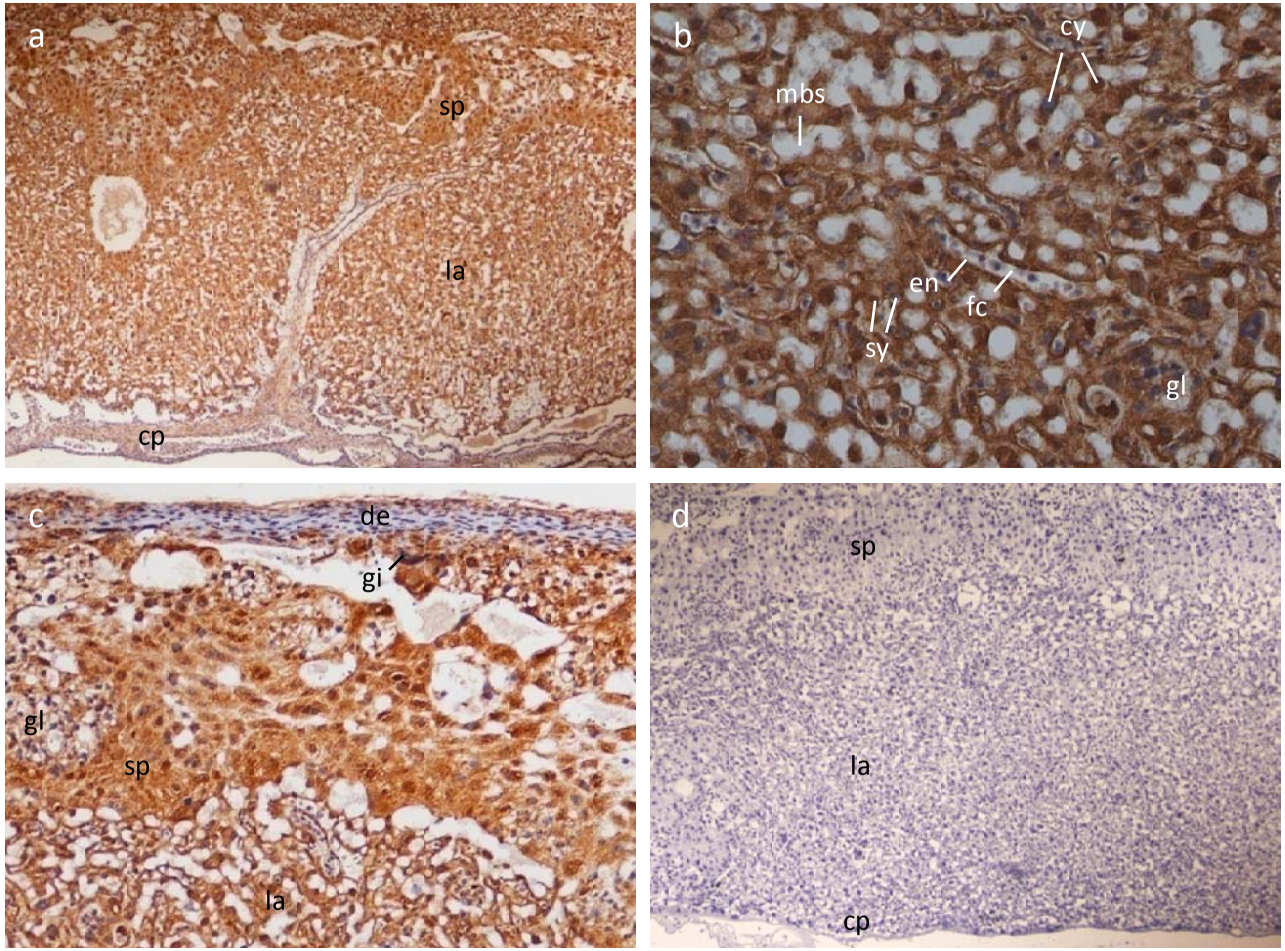
a
sp
la
cp
b
cy
mbs
en
fc
sy
gl
c
de
gi
gl
sp
la
d
sp
la
cp

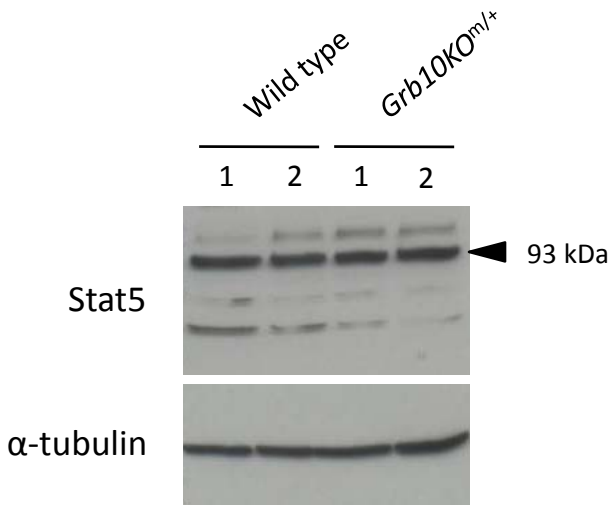
Wild type
Grb10KO m/+
1
2
1
2
93 kDa
Stat5
α-tubulin

5.2.11 *Grb10* depletion does not influence Stat5 protein levels in the placenta

If *Grb10* is a transcriptional target of Stat5, its expression may be required to maintain Stat5 levels in a positive feedback loop. Western blotting of protein isolates from two wild type and two *Grb10KO*$^{m/+}$ e14.5 placentae was performed using a pan-Stat5 antibody (Figure 5.12). No differences in levels of the 93 kDa native protein, nor in the levels of α-tubulin, employed as a loading control, were observed between any of the samples. This suggested *Grb10* does not influence Stat5 protein levels in the placenta.

5.2.12 Stat5 regulates *Grb10* transcription in the mammary gland in a pregnancy-dependent manner

A previous study identified *Grb10* as a likely transcriptional target of Stat5a in mammary epithelial cells (Clarkson *et al*, 2006). In that study, a conditionally active Stat5a protein construct was transduced into an immortal mammary epithelial cell line, and a microarray experiment performed to compare the transcriptomes of induced and uninduced cells. Upon induction of Stat5a, *Grb10* expression was increased 3.6-fold, making it the gene with the fifth most-altered expression level in the microarray. This supported our current model of a transcriptional level interaction, and suggested that Stat5 binding at CRM1 might be required for *Grb10* expression in the mammary epithelium. A related study, utilising microarrays, characterised the expression profile of *Grb10* through gestation, lactation and involution (Clarkson *et al*, 2003). *Grb10* appeared to be activated in a pregnancy-dependent manner.

These data provided two testable hypotheses: 1) that mice inheriting the *Grb10KO* allele should report an expression profile in this tissue similar to that characterised by microarray analysis; and 2) that *LacZ* expression from the *Grb10Δ2-4* allele should be weaker, due to the deletion of CRM1.

First, mammary glands were excised from wild type, *Grb10KO*$^{m/+}$ and *Grb10KO*$^{+/p}$ virgin females, fixed and stained for *LacZ* expression. No reporter expression was observed, implying an absence of *Grb10* in post-pubertal but pre-gestation females (data not shown).

Next, the expression of *Grb10* in the adult mammary gland was characterised at three stages, corresponding to early gestation (gestational day 7.5; G7.5), mid-gestation (G12.5) and postpartum (postnatal day 6; P6). Fourth (abdominal) mammary glands were isolated from the right side of wild type, *Grb10KO*$^{m/+}$ and *Grb10KO*$^{+/p}$ females, all age-matched to 10 weeks at conception. These were fixed and stained for *LacZ* expression for 18 hours. The mammary gland undergoes dramatic branching morphogenesis during gestation, so glands from the left side were excised from wild type females at the same stages, and stained with carmine alum to correlate expression with structure.

At G7.5, no reporter expression was apparent in glands of any genotype (Figure 5.13), consistent with that seen for virgin animals. At this stage, the extent of branching was limited, with the majority of tissue composed of adipocytes (Figure 5.13, *left panel*). By G12.5, cell proliferation had produced a denser network of branches, and individual

clusters of epithelial cells were clearly apparent. Reporter expression at this stage was observed in a subset of epithelial cells in the *Grb10KO*$^{m/+}$ gland, spreading out from the lymph node. Cells located closer to the nipple stained negative for *LacZ* at this stage. Glands excised from wild type and *Grb10KO*$^{+/p}$ females did not report expression, confirming the validity of the stain and the retained imprint of *Grb10*, respectively. The imprinted nature was further confirmed at P6, with all epithelial cells appearing to report positive *LacZ* expression when the transgenic allele was inherited maternally, but no expression from *Grb10KO*$^{+/p}$ glands. Similarly, wild type glands remained devoid of staining. At this stage, dense clusters of milk-secreting epithelial cells were observed from carmine alum staining.

To test the hypothesis that deletion of CRM1 will result in reduced reporter expression in *Grb10Δ2-4*$^{m/+}$ mammary epithelial cells relative to *Grb10KO*$^{m/+}$, staining was repeated at all stages on glands excised from *Grb10Δ2-4*$^{m/+}$ females, again 10 weeks old at conception. After 18 hours of incubation, no reporter expression was observed at any stage, including P6 when expression from *Grb10KO* is greatest. This was consistent with the proposed model, and, alongside data from previous studies, confirmed mammary epithelial tissue as an additional site at which Stat5 regulates *Grb10* transcription.

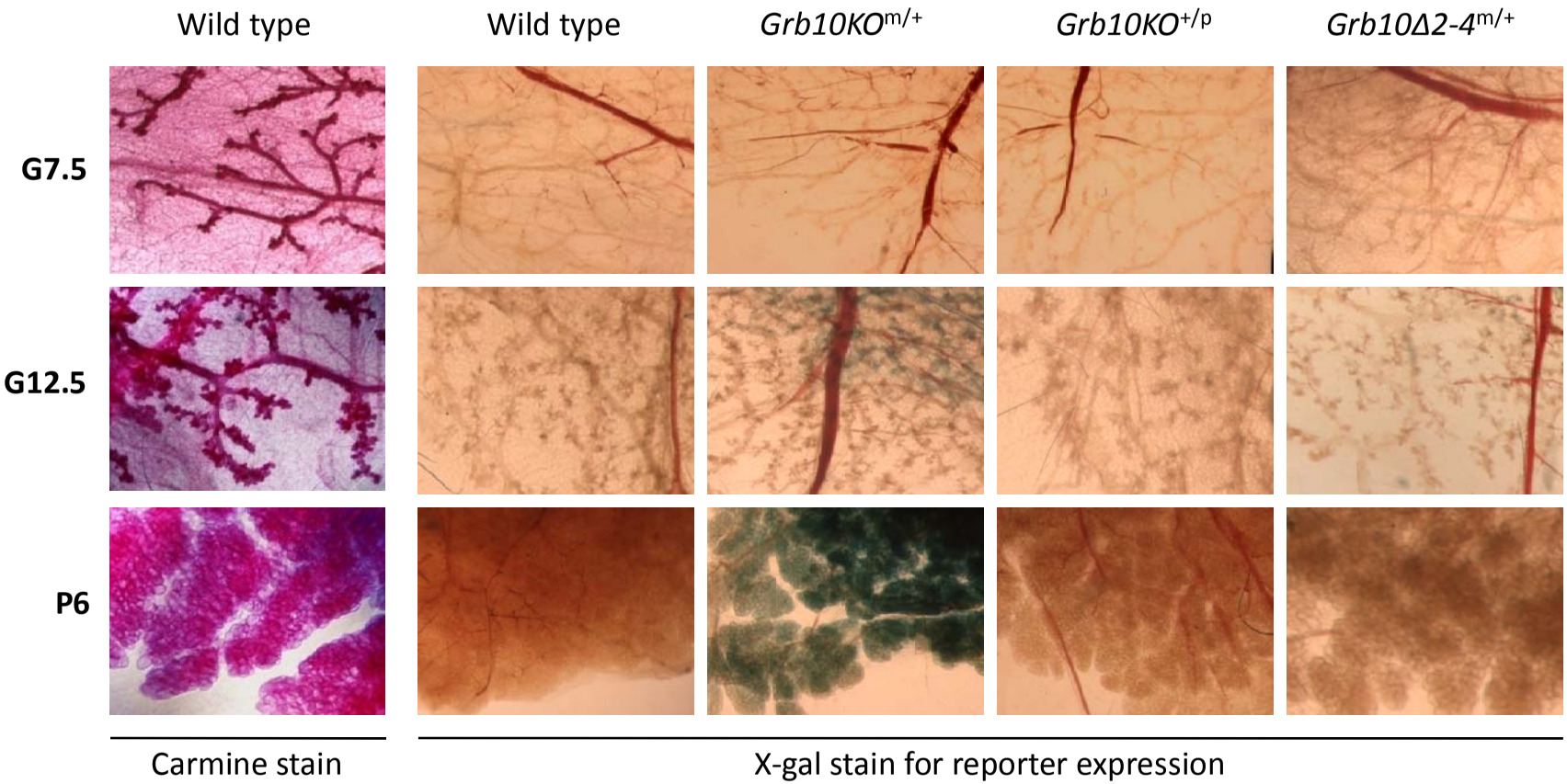
Wild type
Wild type
Grb10KOm/+
Grb10KO+/p
Grb10Δ2-4m/+
G7.5
G12.5
P6
Carmine stain
X-gal stain for reporter expression

5.3 Discussion

Using a range of tools, we have identified a highly conserved intronic sequence at the *Grb10* locus, which may bind Stat5 in a tissue-specific manner and can promote *Grb10* transcription.

Previous work from our laboratory determined the presence of Grb10 protein in the developing mouse brain using immunohistochemical analysis, but this was not recapitulated by assaying for β-galactosidase activity in mice possessing a copy of the *Grb10Δ2-4* allele (Charalambous *et al*, 2003). Studies utilising *Grb10KO* mice found that *LacZ* reporter expression from this allele matched all sites at which Grb10 protein was detected, but showed a requirement for both parental alleles to be expressed. In particular, reporter expression in the CNS was only detected when the *Grb10KO* allele was inherited through the paternal line (Garfield, 2007; Garfield *et al*, submitted). Figure 5.1 presents *LacZ* stained, sagittally-bisected embryos to permit a direct comparison between these genotypes. Inconsistent fixation techniques are responsible for the differences in quality observed, but the key results are plainly illustrated.

Firstly, maternal transmission of both transgenic alleles produced identical reporter expression profiles, with an abundance of β-galactosidase in most tissues of mesodermal and endodermal origin, as described previously. Although not presented here, expression from both alleles, when maternally-inherited, was detected in the epidermis (Garfield, 2007). The most striking observation is the absence of reporter staining in the majority of the CNS. One clear exception is the epithelium of the choroid plexus, although staining of coronally-sectioned brains also revealed a contribution from the maternal allele in ventricular ependymal layers and the meninges (Garfield *et al*, submitted). All three sites consist of non-neural cells, and indeed, the choroid plexus epithelium is synonymous with unusual patterns of imprinted gene expression. Of particular interest is the absence of imprinting at the *H19*/*Igf2* locus in this tissue (DeChiara *et al*, 1991). As a consequence, *H19* is biallelically-silenced, whilst *Igf2* is biallelically-expressed. This escape from imprinting appears to be achieved through biallelic hypermethylation of some CpG dinucleotides within the germline differentially methylated domain (DMD), the differential methylation of which is responsible for establishing imprinting at the locus. This hypermethylation results in the exclusion of CTCF from these sites on both alleles and a subsequent de-regulation of the imprint (Menheniott *et al*, submitted). Interestingly, *Igf2* retained its imprint within closely-associated stromal cells of the choroid plexus (Charalambous *et al*, 2004), cells in which *Grb10* is expressed from the paternally-derived allele (Garfield, 2007). Thus, unlike the *H19*/*Igf2* locus, *Grb10* does not escape imprinting but is reciprocally-imprinted between the epithelium and the stroma. This pattern is limited to embryonic development, as in adulthood, the maternally-inherited *Grb10* allele does not contribute any transcripts to the CNS. Further dissection of the developmental and mechanistic basis, as well as the function, of this reciprocal imprint between two intimately related tissues is required.

Secondly, a comparison of *Grb10KO*$^{m/+}$ and *Grb10KO*$^{+/p}$ foetuses confirmed that the paternally-inherited allele is the predominant contributor of transcripts in the CNS, thereby establishing a reciprocal imprint between the CNS and peripheral tissues (Garfield *et al*, submitted). Unlike the reciprocal imprint between the epithelium and stromal cells of the choroid plexus, the CNS/peripheral tissue imprinting pattern persists in adulthood, as demonstrated by Northern blotting in the present study (Figure 3.4*a*) and *LacZ* staining of adult tissues (Smith *et al*, 2007; Garfield *et al*, submitted). Intriguingly, this correlates with differences in the function of maternally- and paternally-expressed *Grb10*, with the former regulating insulin metabolism and the latter modulating social dominance. The evolutionary basis for such a system is still unclear, but given that *Grb10* is the only identified gene to exhibit allele-specific imprinting in both directions, a system conserved in humans (Arnaud *et al*, 2003; Monk *et al*, 2009), further investigation is necessitated. This should include further dissection of the signalling pathways which *Grb10* mediates in the brain and peripheral tissues.

The final key observation is from the comparison of *Grb10Δ2-4*$^{+/p}$ and *Grb10KO*$^{+/p}$ embryos; specifically, the failure of *Grb10Δ2-4* to report expression in the CNS. Assaying for β-galactosidase activity apparently revealed no such reduction in the peripheral sites of paternal expression, including the ventricles of the heart, tongue and others. This suggested that, in the developing embryo, the mechanism responsible for the difference was specific to the CNS. To address this, the structures of the two alleles were compared. This was possible as a result of the mapping experiments for *Grb10KO* described in Chapter Three, and the published details for *Grb10Δ2-4* (Charalambous *et al*, 2003). Based on this comparison of the *Grb10KO* and *Grb10Δ2-4* alleles, two models were proposed to account for the differences in CNS reporter expression, whilst retaining similar peripheral tissue expression profiles.

One model described differences in splicing between transcripts arising from *Grb10Δ2-4* in the CNS and elsewhere. Brain-specific transcripts initiate at alternative leader exons, and epigenetic systems are responsible for regulating this promoter switch (Arnaud *et al*, 2003; Sanz *et al*, 2008). These, in turn, confer higher order chromatin conformation rearrangements, potentially interfering with the ability of transcripts to splice onto the β-*geo* cassette. The promoter switch at the *Grb10* locus is achieved in part by differential methylation at a brain-specific DMR; in other tissues, this site is biallelically hypermethylated (see Section 1.2.3). One of the brain-specific leader exons, 1C, initiates within this DMR and thus its accessibility to the transcription machinery may be directly regulated by methylation at this site. However, exons 1B1 and 1B2 are located within the germline DMR, which retains its maternal hypermethylation in the brain as in all tissues. Thus, a different epigenetic system, histone tail modifications, is also responsible for regulating the promoter switch. In particular, the repressive histone modification H3K27me3 was found to associate with the unmethylated paternal allele within the germline DMR, but this was dissociated in the brain (Sanz *et al*, 2008). These two regulatory systems, differential DNA methylation and histone tail modification, ensure that differential promoter usage is tightly coupled to reciprocal imprinting.

The higher order chromatin conformation changes induced by such epigenetic systems result in the exclusion or inclusion of transcription factors, or indeed distal enhancers through chromatin looping (Murrell *et al*, 2004), from promoter sites. These higher order structures might adversely affect the accessibility of small nuclear ribonucleoprotein particles, which catalyse splicing, to the β-*geo* splice acceptor in the brains of *Grb10Δ2-4*$^{+/p}$ mice. This may force splicing around the cassette, onto a downstream exon, and could account for the successful splicing of transcripts onto the β-*geo* cassette in other tissues. However, the considerable reduction in full-length *Grb10* transcripts detected in the brains of *Grb10Δ2-4*$^{+/p}$ animals, relative to wild type and maternal transmission controls, argues against this model.

Further evidence arguing against the influence of chromatin conformation causing splicing around the β-*geo* cassette, is derived from the observation that *Grb10Δ2-4* fails to report expression in the mammary epithelium, a site at which expression is exclusively from the maternally-inherited chromosome. Although no study has characterised the exon structure of *Grb10* transcripts in the mammary epithelium, and thus it is not possible to rule out that the initiation exons 1B1, 1B2 or 1C are utilised, this seems an unlikely scenario given that the mechanisms for initiating transcription at these exons are tightly coupled to silencing of the maternal and activation of the paternal alleles. This suggests that *Grb10* transcripts in the mammary tissue initiate at exon 1A, and chromatin conformation is therefore different to that in the brain. This makes the sharing of a splicing event by brain and mammary epithelium, as a consequence of such epigenetic modifications, seem unlikely.

An alternative explanation proposed the existence of an enhancer element at the *Grb10* locus, situated within the deleted region of *Grb10Δ2-4*. If this enhancer was active only in the CNS of the developing embryo, it might account for the failure of *Grb10Δ2-4*$^{+/p}$ embryos to report CNS expression. To this end, an alignment between the *Grb10* orthologs of various species was performed, using software called ExactPlus (Antonellis *et al*, 2006), which enabled the identification of short conserved sequences which might represent enhancer elements. Both the mouse-human and mouse-human-chimpanzee alignments revealed extensive intronic conservation, suggesting relatively limited sequence evolution since the divergence of the rodent and primate lineages 61.7 million years ago (MYA; Benton and Donoghue, 2007). Indeed, very few differences were observed between these two alignments, reflecting the ~99 % genomic sequence similarity between human and chimpanzee (Kehrer-Sawatzki and Cooper, 2007; and references therein). The addition of the bovine *Grb10* sequence resulted in a 'filtering' effect of conserved sites, such that clusters of short conserved sequences formed a subset of those identified from the aforementioned comparisons. *Grb10* is imprinted in human and mouse, and the high degree of genome similarity between human and chimpanzee would predict the retention of imprinting in this species, although this is yet to be confirmed. Imprinting is also active in the cow, and although *Grb10* expression has been detected in parthenogenetic peri-implantation bovine embryos, the status of the paternally-inherited allele remains unknown (Tveden-Nyborg *et al*, 2008). Assuming retention of imprinting at this locus in these four eutherian mammals, conservation of DMRs might be expected. However, the only short conserved sequence between the four species at the 5' end of the locus mapped

to a run of GT repeats, situated between the germline and somatic DMRs. A function for these repeats has not previously been described, although other repeat sequences specific to the 5' end of mouse *Grb10* have been shown to bind CTCF, and are thus implicated in regulating imprinting at the locus (Hikichi *et al*, 2003). The current study failed to detect conserved CTCF binding sites between mouse and human, consistent with the observation that these are specific to murine *Grb10*. The apparent lack of conservation of DMRs might reflect the importance of epigenetic, rather than sequence-based, regulation of imprinting, such that there is evolutionary pressure to retain a high GC content, but not to conserve the intermediate sequence.

Alignments of *Grb10* orthologs between more distantly related species, using *Xenopus tropicalis* and chicken as representatives of the amphibian and bird classes, and opossum as a representative of marsupials, revealed a fewer number of conserved intronic sites. Interestingly, those identified in the mouse-frog comparison were a subset of those found in the eutherian mammal alignment. That these sites have retained conservation through ~330 million years (Benton and Donoghue, 2007) potentially implies a functional significance, and might perhaps represent other regulatory elements worthy of future investigation.

Many imprinted genes retain their monoallelic expression status in marsupials; studies of the tammar wallaby, *Macropus eugenii*, have shown that *IGF2*, *IGF2R*, *Insulin*, *PEG1*/*MEST* and *PEG10* are all imprinted in both foetus and placenta (Suzuki *et al*, 2007; Renfree *et al*, 2008). Whilst wallaby is the archetypal marsupial for examining imprinted genes, the status of *Grb10* has not yet been revealed, although characterisation is in progress (M. Renfree and J. Stringer, personal communication). The most overwhelming limitation is that the wallaby genome sequence is still to be completed. This also prohibits inclusion of wallaby in the ExactPlus alignment, and thus the opossum sequence presented a suitable alternative (although in this species too, the imprinting status of *Grb10* has not been defined). The mouse-opossum alignment represented an 'intermediate' between the mouse-frog and mouse-human-chimpanzee-cow comparisons, reflecting the opossum's closer relatedness to eutherian mammals.

A single intronic sequence was conserved between the eutherian mammals examined and chicken. That there is no other intron sequence similarity in the entire *Grb10* locus suggests a functional significance for this site. In support of this, the sequence mapped to the only *cis*-regulatory module identified in the mouse *Grb10* sequence using PReMod. Indeed, a direct comparison between the PReMod and ExactPlus outputs for this region, referred to as *cis*-regulatory module 1 (CRM1), revealed a 73 % base pair conservation of CRM1 across all five of these species. Of further interest is that CRM1 was positioned within the portion of the *Grb10* locus deleted during the creation of the *Grb10Δ2-4* allele, and was therefore a strong candidate for the predicted missing enhancer.

CRM1 included several putative transcription factor binding sites; the PReMod software identifies clusters of sequences with similarity to consensus sites registered in the TransFac 7.2 database, and subsequently filters them with an alignment between mouse and rat (Blanchette *et al*, 2006). The overlapping nature of these sequences is intriguing, and

supports previous analyses that transcription factor recognition sequences tightly cluster; in evolutionary terms, this might permit greater opportunity for the emergence of co-regulation by multiple factors and thus more refined control of expression, or in situations of more than one copy of the same transcription factor binding sequence, might simply assist transcription factors in finding their target sites (Zhang *et al*, 2006).

It is pertinent to note that the analyses performed using ExactPlus and PReMod are not entirely independent, although they address different questions. PReMod filters noise after identifying candidate clusters by aligning them between the mouse and rat orthologous sequences. This additional level of screening is the basis for the ExactPlus analysis, and thus it is not surprising that CRM1 was also identified using this programme. However, the two approaches are complimentary, and in fact, PReMod overcomes a considerable limitation of the ExactPlus analysis. Exons 1 to 5 were excluded from the ExactPlus alignment such that the strong conservation expected within exons would not cloud the search for potential enhancer elements. Enhancer elements can reside within exons (Reed, 1996), and this exclusion is thus a limitation. PReMod, on the other hand, does not discriminate between exonic and intronic sequence.

Following the identification of CRM1 from bioinformatic analyses, the present study progressed to characterise its properties and to identify Stat5 as a highly likely candidate for binding. Initially, CRM1 was examined *in vivo*. A DNase I hypersensitivity assay confirmed that the site was hypersensitive to endonuclease digestion, and thus devoid of nucleosomes, in the brain. This was not the case for the liver, consistent with the prediction that CRM1 is a CNS-specific enhancer. Whilst this demonstration of tissue-specific activity is clear, adult liver was not the most suitable control tissue, as *Grb10* transcription is switched off in the neonatal liver and not reactivated in adulthood (Smith *et al*, 2007). A more suitable comparison might be drawn between brain and kidney, for example, in which *Grb10* continues to be expressed in adulthood but would be predicted to be independent of CRM1 (due to no loss of reporter activity in the kidneys of *Grb10Δ2-4*$^{m/+}$ mice).

Manual screening of an extensive database of *in situ* hybridisation images in the adult mouse brain was subsequently performed, cataloguing the expression profiles of each of the transcription factor candidates identified by PReMod. A prerequisite for activating *Grb10* transcription is co-expression. Only Stat5b displayed considerable overlap with *Grb10*, and this was the transcription factor whose putative binding sites were most closely related to the consensus. Stat5b expression was apparent in almost all sites of the brain at which *Grb10* has been characterised (Garfield *et al*, submitted), although the high level of Stat5b expression in the cerebellum is inconsistent. The expression profiles of the other candidates corresponded with previously published analyses (Blake *et al*, 2008; He *et al*, 1989).

The roles of Stat5b as a signal transducer are well-characterised. Following the binding of a cytokine to a cell surface receptor, Stat5b is phosphorylated by Janus kinases (JAKs), dimerises and translocates to the nucleus, wherein it binds to recognition sequences of target genes and promotes their transcription. Studies have demonstrated a role for Stat5 in mediating signalling downstream of prolactin (Wakao *et al*, 1994), growth hormone,

interleukins and erythropoietin (Gouilleux *et al*, 1995), but the relative contributions of Stat5a and Stat5b to each of these pathways depends on the tissue in question. Generally, Stat5b plays a more prominent role in hepatocytes and regulatory T cells. It also plays a critical role in the hypothalamus. Stat5b-deficient mice showed an impaired ability to respond to circulating prolactin, but also displayed grossly elevated levels of prolactin secretion (Grattan *et al*, 2001). This somewhat paradoxical finding was explained by the role of Stat5b in regulating prolactin secretion, forming part of a negative feedback loop between the pituitary and hypothalamus.

Conversely, Stat5a has a more significant role in the response of mammary epithelial cells to prolactin and, by extrapolation, is fundamental for mammary alveolar development and milk secretion (Liu *et al*, 1997). Although Stat5b deficiency does not produce the same phenotype, compound mouse mutants (*Stat5a*$^{-/-}$/*Stat5b*$^{-/-}$) have an even more dramatic phenotype, suggesting some functional redundancy in this system, and the ability for Stat5a to compensate for Stat5b (Udy *et al*, 1997; Teglund *et al*, 1998).

Although the expression profile in the adult brain renders Stat5a an unlikely candidate for activating *Grb10* in this tissue, we cannot rule out the possibility that this protein binds at CRM1 in the mammary epithelium, or indeed, in the placental labyrinth. Elucidation of the function of *Grb10* in the mammary epithelium, described in Chapter Six, did not help to determine whether *Grb10* is activated by Stat5a or Stat5b. This remains an issue to be resolved. Perhaps Stat5 proteins bind indiscriminately to CRM1 in this tissue, or CRM1 might show a higher affinity for one protein over the other.

We next confirmed the enhancer capacity of CRM1, and its ability to respond to Stat5b, *in vitro* using a luciferase assay. The presence of CRM1 cloned upstream of a minimal promoter driving luciferase had no influence, on its own, on luciferase expression as assessed by assaying for enzyme activity. Whilst NIH/3T3 cells express endogenous Stat5 protein (Chen *et al*, 1997), phosphorylated dimers may have been at a level insufficient to drive luciferase expression above that detectable from the empty vector control. Co-transfection with a constitutively active Stat5b mutant, pRSVpuro-STAT5B1*6 (Onishi *et al*, 1998), increased luciferase activity levels in cells containing pGL3-Pro-CRM1, but not pGL3-Pro. This effect appeared to follow a dose-dependent trend, although co-transfection of 2 µg of the constitutively active mutant did not produce as strong an effect as that observed with 1 µg (data not shown). This is probably a consequence of toxic levels of mutant protein, which had a detrimental effect on normal cellular processes.

Whilst the effect of constitutively active Stat5b is dramatic and clearly demonstrates the capacity of CRM1 to bind Stat5b, this result may not necessarily extrapolate to *in vivo* systems. CRM1 might, for example, bind a Pax family transcription factor *in vivo*, identified as a candidate from the PReMod screen. The retention of a Stat5b binding site due to the clustering effect discussed previously might enable an interaction between Stat5b and CRM1 to be 'forced' in an *in vitro* manipulation. However, when considered in light of additional evidence, including the perfect conservation of the Stat5 binding site in chicken and four eutherian mammals, and the co-expression of *Stat5b* and *Grb10* in the adult brain, Stat5 emerges as a strong candidate for regulating *Grb10* expression *in vivo*. The luciferase

assay could be extended to examine the effects of over-expressing the other candidate transcription factors. Additional benefit might be derived from mutating the conserved Stat5 binding sites within the pGL3-Pro-CRM1 construct, predicting loss of the enhanced luciferase activity when 1 µg pRSVpuro-STAT5B1*6 is also transfected.

A demonstration of the tissue-specific nature of this interaction might be achieved by performing similar luciferase assays in different cell lines. A prediction might be that the interaction is effective in a neuronal cell line, such as the N2a neuroblastoma cell line, or a placental labyrinth cell line, such as the HRP.1 cell line (Soares *et al*, 1987), but not a cell line with characteristics of differentiated epidermal cells, for example. However, the nature of this experiment, in which non-physiological levels of activated Stat5b protein are expressed, might not be subtle enough to differentiate such a tissue-specific interaction. Instead, chromatin immunoprecipitation (ChIP), using an antibody to Stat5, could be employed on tissue isolates. This would provide a more refined method for demonstrating tissue-specific interaction, and, moreover, would represent binding *in vivo*. A further advantage would be achieved by the use of precipitating antibodies recognising specific Stat5 isoforms. Antibodies capable of this specificity, and with suitability to ChIP, have been described previously (Moucadel and Constantinescu, 2005). By utilising these antibodies in ChIP on brain, placenta and mammary gland chromatin, we could confirm which of the proteins is responsible for *Grb10* regulation in each of these tissues.

In the absence of such chromatin immunoprecipitation data, the result of effectively deleting the CRM1 *in vivo*, using *Grb10Δ2-4*, provides a clear demonstration of a tissue-specific activity. Arguably, the deletion of ~38 kb of endogenous sequence to generate this allele might also have removed other candidate enhancer elements, and as such may be considered unrefined. Perhaps conclusions cannot be drawn from this result alone, but when considered alongside the data from this and other studies (discussed shortly) the evidence is much more convincing.

In addition to the developing CNS, the inability of the *Grb10Δ2-4* allele to report expression in the placental labyrinth, suggests CRM1 might also be utilised in this tissue. The weak reporter expression in *Grb10Δ2-4*$^{m/+}$ placentae detected after prolonged incubation in X-gal substrate is reminiscent of that in the brain, and fits the model that transcription still occurs from the locus, but is weak in the absence of CRM1. The role of Stat5 is not defined in this organ, although a previous study has confirmed the presence of *Stat5b* transcript in whole mouse placenta (Sawka-Verhelle *et al*, 1997). We examined the placental expression pattern of *Stat5* using immunohistochemistry, although our approach did not permit discrimination between Stat5a and Stat5b. Protein was detected in all cell types derived from extra-embryonic precursors in the mature mouse placenta. The maternal contribution to the placenta, the decidua, did not contain Stat5 protein. The nuclear localisation of the protein, suggestive of a role in promoting transcription of target genes, was variable. All foetal endothelial cells examined showed nuclear and cytosolic localisation of Stat5, consistent with the strong expression of *Grb10* in these cells (Figure 4.2). Syncytiotrophoblast and cytotrophoblast cells displayed a mixed result, with only some cells reporting nuclear as well as cytosolic localisation. The reasons why only a subset of these cells have detectable levels of Stat5 in the nucleus are unclear. In the case of the

multi-nucleated syncytiotrophoblast cells, transcription of Stat5 target genes from just a few nuclei might be sufficient to maintain adequate levels of protein in the cytoplasm. Alternatively, the antigen retrieval process may not have been sufficient to permeabilise all nuclei and thus permit antibody access. The experiment should be repeated and the method of antigen retrieval optimised to resolve this issue. Nevertheless, Stat5 is expressed in all cells positive for Grb10, suggesting it could regulate *Grb10* transcription in the labyrinth. No changes in the levels of Stat5 protein could be detected in *Grb10KO*$^{m/+}$ placentae, suggesting *Grb10* does not regulate *Stat5* expression in a feedback loop. This might be expected given the range of transcriptional targets of Stat5. The persistence of *Grb10* expression from the paternally-inherited chromosome in *Grb10KO*$^{m/+}$ placentae might also prevent detection of the effect; adult brain might be a more suitable tissue to examine in this manner. It may be valuable to extend this analysis to examine phosphorylation levels of Stat5 following *Grb10* ablation, which would be indicative of the levels of active Stat5 protein, rather than total cellular levels.

An entirely independent study is suggestive of a Stat5-*Grb10* transcriptional level interaction. As discussed previously, Stat5a is a key mediator of mammary epithelial cell proliferation and preparation for lactation. Clarkson *et al* (2006) describe an experiment in which an inducible Stat5a construct was transduced into KIM-2 cells, an immortal mammary epithelial cell line. A microarray experiment comparing the transcriptomes of induced and uninduced cells revealed a dramatic increase in *Grb10* transcript levels upon Stat5a induction. A further study, employing microarray analysis of whole mammary gland expression during gestation, lactation and involution, demonstrated that *Grb10* was expressed in a pregnancy-dependent manner in this tissue (Clarkson *et al*, 2003). We used the observations from these two studies to create two testable hypotheses: first, that reporter expression from *Grb10KO* should reflect the previously defined expression profile for *Grb10* in this tissue; and second, that mice inheriting the *Grb10Δ2-4* allele would fail to report mammary epithelial expression because Stat5 binding to CRM1 is required to promote transcription.

In both cases, the hypotheses were shown to be correct. No *Grb10* expression could be detected in virgin females or at day 7.5 of gestation, using *Grb10KO*, consistent with the observation of low levels of transcript in the mammary glands of virgin females and at day 5 of gestation reported by Clarkson *et al* (2003). A subset of epithelial cells closest to the lymph node were positive for β-galactosidase in *Grb10KO*$^{m/+}$ females at day 12.5 of gestation. The microarray published in Clarkson *et al* (2003) did not report much difference between days 5, 10 and 15 of gestation, slightly inconsistent with this finding. However, *LacZ* expression was restricted to a small population of cells, and further analysis of the raw microarray data, available for public access at www.path.cam.ac.uk/~madgroup/gene_expression.shtml, revealed that *Grb10* expression at all these time points was below the threshold value at which expression is considered to be 'true' (R. Clarkson, personal communication). If a value falls below this threshold, it is not possible to differentiate between the absence of expression and low levels of transcript. The restricted expression of *Grb10* at day 12.5 of gestation presumably reflects a gradual change in the

transcriptome of epithelial cells which is coupled to proliferation and branching morphogenesis, with 'older' cells altering their transcriptional profiles first.

At postnatal day 6, the mammary glands from lactating *Grb10KO*$^{m/+}$ females stained strongly for *LacZ* expression, consistent with the reported up-regulation of *Grb10* transcripts throughout lactation (Clarkson *et al*, 2003). Mammary epithelial tissue comprises two differentiated cell types, luminal and myoepithelial cells, and whether or not this profile of *Grb10* transcription is apparent in both sub-populations remains unclear. Indeed, the KIM-2 immortalised mammary epithelial cell line is a heterogeneous population of the two, as well as some stromal cells, although luminal epithelial cells constitute 95 % of the total (Gordon *et al*, 2000). Cryosectioned *Grb10KO*$^{m/+}$ mammary glands should be assayed for β-galactosidase activity to resolve this issue.

As predicted, mammary glands isolated from *Grb10Δ2-4*$^{m/+}$ females did not report expression at any of the stages analysed. This was reminiscent of the *Grb10KO*/*Grb10Δ2-4* differences observed in brain and placenta, and again implied the necessity of CRM1 to permit transcription from the locus.

The final key observation from this experiment was the retention of the *Grb10* imprint in the mammary epithelium. This is of particular interest because the majority of the development of this tissue occurs in adulthood (during gestation), and indeed, *Grb10* transcription is not activated until this stage. The traditional view of imprinted genes, centred around the parental conflict hypothesis, proposes that imprinting is only important during development (or more specifically, from fertilisation to weaning). This does not make imprinted genes redundant in adulthood, but simply implies their imprinting status is no longer relevant. That *Grb10* is silenced on the paternally-inherited chromosome in the mammary tissue may arise from the fact that imprinting is already established in other peripheral tissues. In other words, the differential methylation and histone modification patterns which distinguish the maternal and paternal chromosomes are already laid down in mammary epithelial cells, so during gestation, the cells, requiring Grb10 protein, simply activate the allele with permissive epigenetic marks.

A counter-argument is that the *Grb10* imprint is quite amenable to manipulation during development. Expression in the developing heart at e8.0 appears to be biallelic (Chapter Three). The paternal contribution is still detectable at e14.5 in the right ventricle, but expression from the maternally-inherited chromosome is ubiquitous in the heart at this stage, suggesting a combination of both biallelic and monoallelic expression in one organ (Garfield, 2007). If the imprinting status of *Grb10* is not important in the adult mammary gland, why not prepare the developing mammary mesenchyme for future biallelic expression?

The discovery of the influence of genomic imprinting on maternal care behaviours was originally attributed to the parental conflict hypothesis. A classic example is that of *Peg3*, in which mutation impaired maternal behaviour, often resulting in neonatal lethality (Li *et al*, 1999). However, the conflict hypothesis is an inadequate explanation for this observation. The *Peg3* mutation, inherited through the paternal line, would influence the maternal behaviours of the daughters, not the current mate. As such, the benefits of any paternally-

expressed *Peg3* would be realised by the subsequent generation, but grandparental effects are inconsistent with the hypothesis: an allele transmitted from father to daughter is as likely to be transmitted to the daughter's offspring (the 'grandchildren') as an allele transmitted from her mother (Hurst *et al*, 2000). In this respect, imprinting in the mammary gland, if it were to affect the development of suckling offspring, engenders similar arguments to that proposed for the brain. In summary, the parental conflict hypothesis is inadequate to explain our observation.

An alternative hypothesis, which can partially account for the influence of imprinting on maternal behaviours, and thus, by extrapolation, might also apply to the influence on mammary gland function, is the maternal-offspring coadaptation theory (Wolf and Hager, 2006). There is much evidence that selection has favoured the fixation of complementary maternal and offspring traits, which positively affect offspring development. This is not restricted to *in utero*. A correlation between offspring begging behaviour and maternal response was recorded in great tits, for example (Kölliker *et al*, 2000). This model describes how genomic imprinting is favoured when a gene influences coadaptive traits in mother and offspring. This might fit the expression of *Grb10* from the maternally-inherited chromosome in the mammary gland. This will be discussed further in the light of data demonstrating the function of *Grb10* in this tissue, the subject of Chapter Six.

Finally, it is important to note that the Stat5-induced transcription of *Grb10* is independent of the *Grb10* imprinting status. The observation that CRM1 is active in the developing CNS caused us to question if Stat5 might form part of the mechanism responsible for achieving expression from the paternally-derived allele, whilst expression was predominantly from the maternally-inherited copy in most other tissues. However, the discovery of its influence in the mammary epithelium and placental labyrinth, where *Grb10* is expressed from the maternally-derived alleles and from both alleles, respectively, argued against this role. Instead, Stat5 simply interacts with whichever allele is active. This independence is supported by the conservation of the Stat5 binding site in the chicken *Grb10* locus, which is not subject to imprinting.

A working model to explain the regulation of transcription from the *Grb10KO* and *Grb10Δ2-4* alleles in the brain is presented in Figure 5.14, and explains the reduced levels of β-galactosidase activity observed in some tissues following inheritance of *Grb10Δ2-4*. The figure shows the influence of Stat5 determined in the present study in the context of differential methylation and promoter usage, established previously (Arnaud *et al*, 2003; Sanz *et al*, 2008). Putative CTCF binding sites reside within the brain-specific DMR (CGI3), and CTCF is reported to bind in a methylation-sensitive manner (Hikichi *et al*, 2003). However, the influence of CTCF on transcription is not addressed in this model, as binding has not been demonstrated in the brain. Whilst the model describes the situation in the CNS, in which transcription is from the paternally-inherited allele, it is equally applicable to expression from the other allele, or both alleles, in the mammary gland and placenta, although the initiation exons may differ.

The evidence that Stat5 regulates *Grb10* transcription in a tissue-specific manner is strong, and includes a range of data from *in silico*, *in vivo* and *in vitro* experiments, as well as data

from an independent study. The physiological significance of this interaction is the subject of the next Chapter.

a *Grb10KO*

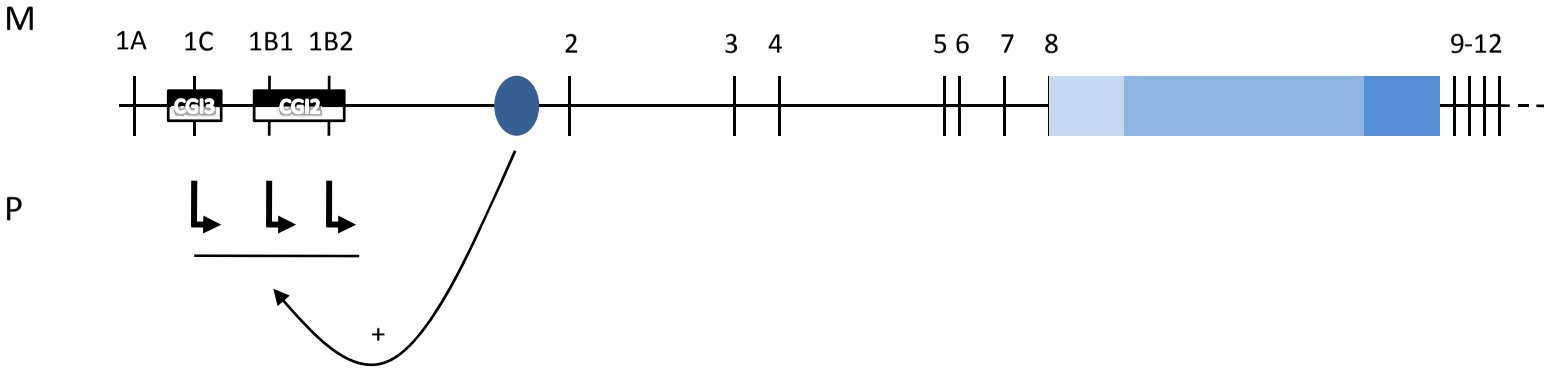

b *Grb10Δ2-4*

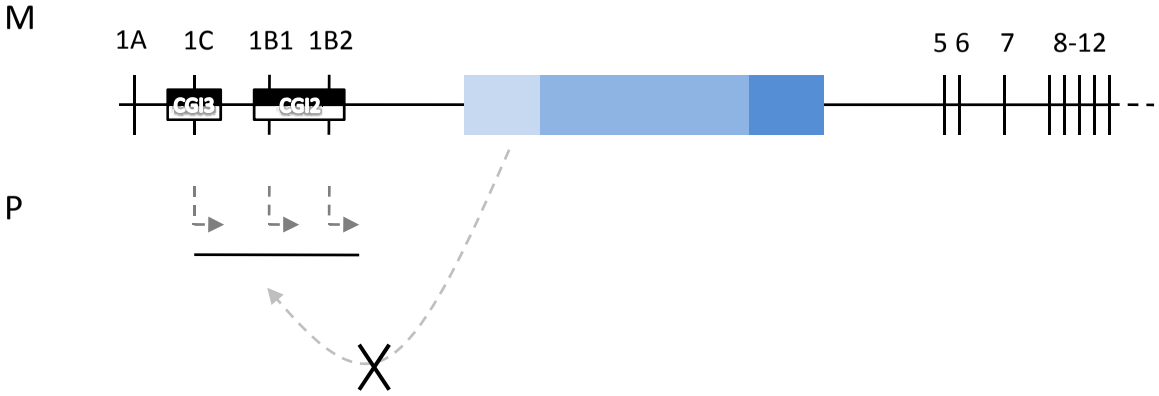

Chapter Six

Investigating the function of Grb10 *in the adult mouse mammary gland*

6.1 Introduction

The mammary gland is an unusual organ because much of its development occurs during adulthood, in response to pregnancy. Like the placenta, it is specific to mammals, including eutherians and marsupials, but not monotremes. Its primary function is the provision of nutrients to suckling offspring, although in addition to milk proteins, immune factors are also secreted, providing offspring with assistance in overcoming infections. At birth, the sterile human foetal intestine is rapidly colonised by bacteria, many of which secrete endotoxins which may be detrimental to neonatal health. The neonatal adaptive immune system is relatively immature to cope with such challenges. Factors secreted in breast milk have been shown to stimulate neonatal release of inflammatory cytokines and chemokines, thus priming the immature immune system (Vidal *et al*, 2001). Indeed, breast-fed infants display a lower incidence of gastro-intestinal diseases than those bottle-fed from birth (Howie *et al*, 1990). Additionally, suckling promotes mother-offspring bonding, which may have other developmental benefits, such as promoting learning, particularly in higher mammals (Peaker, 2002). However, such benefits may not be directly attributed to suckling, but simply a consequence of the extended nurture period typical of higher mammals.

Mammary gland development is characterised by three main stages: embryonic, pubertal and adult. This is true for both mice and humans, and whilst many of the molecular processes are very similar, there are some key differences, such as the number of glands developing. Two milk lines develop in the mouse embryo at e10.5, running bi-laterally along the anterior-posterior axis, from the forelimb to hindlimb. These are ectodermal in origin and are essentially multi-layered ridges, along which ectodermal cells migrate, congregate and grow into the underlying mesenchyme, forming the mammary placodes. Five such placodes, which are bulb-shaped buds, occur along each of the milk lines, and appear in a reproducible pattern: bud pair 3 (thoracic), pair 4 (abdominal), then pairs 1 and 5 together (cervical and inguinal, respectively), and finally pair 2 (upper thoracic) (Veltmaat *et al*, 2003), although this order is disputed (Eblaghie *et al*, 2004). Their positions are determined by local factors, and as such, the development of each pair is independently regulated. Mice deficient for *Fgf10*, or its receptor *Fgfr2b*, lose all bud pairs except pair 4 (Mailleux *et al*, 2002). *Tbx3* deficient mice often lose all bud pairs, although pair 2 is occasionally retained (Eblaghie *et al*, 2004). Further evidence for the importance of paracrine signalling includes the competency of mammary epithelium to develop into a salivary gland-like structure, if recombined with salivary gland mesenchyme and transplanted (Sakakura *et al*, 1976). However, despite producing a structure reminiscent of a salivary gland, the recombined and transplanted mammary epithelium still retained its ability to respond to pituitary prolactin, suggesting signals from the mesenchyme influenced the branching pattern but not the differentiation of the epithelium. In contrast, embryonic skin epithelium isolated at e12.5 will form milk-producing mammary glands if combined with mammary mesenchyme and transplanted (Cunha *et al*, 1995). The instructive nature of the mammary mesenchyme is perhaps best illustrated by the

differentiation of chick and duck epidermis, which normally form feathers, to become branched mammary tissue when recombined with rabbit mammary mesenchyme (Propper and Gomot, 1973). Embryonic mammary gland development also appears to be independent of the hormonal stimuli required for pubertal and adult development, as the ablation of the receptors for oestrogen, progesterone, growth hormone (GH) or prolactin (PRL) appear to have no effect (Sternlicht *et al*, 2006).

Distinct epithelial buds are apparent at e13.5. Until this point, bud development has proceeded identically in male and female mice, but androgen receptors are activated in male buds, causing them to degenerate (Kratochwil and Schwartz, 1976). As a consequence, adult male mice do not possess mammary glands, unlike the situation in humans. At around e15.5, the epithelial buds of female mouse embryos secrete parathyroid hormone-related protein (PTHrP), which sensitises surrounding mesenchymal cells to the autocrine factor bone morphogenetic protein (BMP)4. This promotes epithelial outgrowth into the mammary fat pad precursor, and suppresses hair follicle formation (Hens *et al*, 2007). Such mammary sprouts, as they are termed, produce small tree-like structures which spread through the fat pad precursor, bearing between 10 and 15 small branches. This process is stochastic, such that two pair 4 glands isolated from different individuals will show different patterns of branching (Sternlicht *et al*, 2006). At e18.5, gland development is arrested until puberty, although allometric growth persists.

In humans, a single pair of mammary placodes form, which become apparent within the first trimester of pregnancy. The structure is also somewhat different, with several rudimentary trees converging at the nipple, rather than the single tree observed in mice. Foetal exposure to maternal hormones causes increased branching relative to that which might be expected, such that at birth, human breasts are competent to secrete milk. Once outside of the womb, such stimulus is removed, triggering a phase of gland involution. This is followed by an allometric growth phase similar to that observed for mice.

During puberty, circulating oestrogen levels rise, promoting the development of terminal end buds (TEBs) at the duct tips. These proliferate and invade further into the mammary fat pad. Proliferation is coupled to bifurcation, such that TEBs generate new ductal branches. In mice, ablation of the gene encoding oestrogen receptor α (ERα) causes failure of TEB development and a consequential failure of invasion into the mammary fat pad (Mallepell *et al*, 2006). During pubertal development, lumen are formed by apoptosis of epithelial cells (Humphreys *et al*, 1996). Further side branches form with each ovarian stimulation, such that the mammary glands of older virgin females are more developed than those of younger females.

Growth hormone is also required for correct pubertal mammary gland development, as demonstrated in mice deficient for the growth hormone receptor (GHR; Gallego *et al*, 2001). Exogenous *Igf1* can rescue hypophysectomised mice (which lack a pituitary gland), suggesting that expression of this gene is downstream of GH signalling (Kleinberg *et al*, 2000). Evidence for the importance of local, rather than systemic IGF1, comes from the observation of normal mammary gland branching in mice with a liver-specific deletion of *Igf1*, which reduces circulating levels by ~75 % (Richards *et al*, 2004). Glands deficient for

the *Igf1* receptor (*Igf1r*) transplanted into wild type fat pads exhibit impaired development (Bonnette and Hadsell, 2001), suggesting that *Igf1r* is required in epithelial cells, whereas GHR is specifically required in the stroma (Gallego *et al*, 2001). Together, this implies that GH secreted from the pituitary gland drives *Igf1* expression in the stroma, which signals to adjacent epithelial cells, further highlighting the intimate relationship between epithelium and stroma (Sternlicht *et al*, 2006).

During pregnancy, further morphological changes occur in the mammary gland to prepare for lactation. These are ultimately stimulated by the developing placenta, which secretes hormones such as placental lactogens into the maternal blood circulation, as discussed in Chapter Four. Imprinted genes have been implicated in this system; mouse placentae deficient for the paternally-expressed gene *Peg3* fail to stimulate increased maternal feeding and weight gain, even when the pregnant females are themselves wild type (Curley *et al*, 2004). Prolactin secreted from the rat decidua promotes progesterone secretion by the corpus luteum. This hormone promotes maternal weight gain (Grueso *et al*, 2001), suggesting *Peg3* might be implicated in this system. Another key role of progesterone is to induce extensive side-branching of the rudimentary epithelial tree in the mammary gland. This is mediated through canonical Wnt signalling (Hiremath *et al*, 2007). In combination with PRL, progesterone promotes the differentiation of epithelial cells to alveoli, the structures responsible for synthesising and secreting milk proteins. Both progesterone and prolactin receptors (PRLR) are required for successful pregnancy-induced branching morphogenesis (Ormandy *et al*, 1997; Brisken *et al*, 1998). It would be interesting to examine the mammary glands of wild type females carrying *Peg3* mutant offspring, to see if this process is also perturbed.

The PRLR on mammary epithelial cells is activated by both PRL and placental lactogens. Upon ligand binding, the receptor activates the Jak2-Stat5 signalling cascade, driving the differentiation of alveoli and the expression of milk protein genes. Both β-casein (Happ and Groner, 1993; Wakao *et al*, 1994) and whey acidic protein (WAP; Li and Rosen, 1995) are direct transcriptional targets of Stat5. *Stat5a*$^{-/-}$ mice exhibit curtailed lobuloalveolar outgrowth during pregnancy, and a failure to lactate (Liu *et al*, 1997). *Stat5b*$^{-/-}$ mice display a less dramatic mammary gland development phenotype, and although the relevant milk proteins genes are expressed, milk volume is reduced (Udy *et al*, 1997). Compound mutants show a more dramatic phenotype than either of the single mutants, suggesting some functional redundancy (Teglund *et al*, 1998). Recently, the ETS family transcription factor Elf5 has been revealed as a critical downstream effector of PRL signalling (Harris *et al*, 2006; Choi *et al*, 2009). Although the homozygous *Elf5*$^{-/-}$ mice exhibit embryonic lethality, the phenotype of *Elf5*$^{+/-}$ mice is very similar to that of *Prlr*$^{+/-}$ animals, which display haploinsufficiency and cannot successfully raise litters (Ormandy *et al*, 1997). Transgenic expression of *Elf5* in *Prlr*$^{-/-}$ mice rescued mammary gland development and even milk protein expression (Harris *et al*, 2006). Intriguingly, this was due to the promotion of *Stat5a* expression, which is a downstream target of Elf5. It is not clear whether *Elf5* expression itself is activated by Stat5a, or if PRL signalling may also be mediated by a Stat5a-independent mechanism.

Stat5 signalling is controlled by a negative feedback loop involving Suppressor of cytokine signalling (Socs) proteins, the expression of which are induced by Stat5a (Harris *et al*, 2006). Socs proteins, predominantly Socs1 and Socs3, bind to the PRLR and Jak2 via a central SH2 domain, and inhibit kinase activity (Hennighausen and Robinson, 2008). Caveolin-1, a membrane-bound protein, also interacts with Jak2 and acts as an inhibitor of PRL signalling; *Caveolin-1* deficiency causes elevated Stat5a levels in the mammary glands and premature lactation during pregnancy (Park *et al*, 2002).

Whilst hormone release from the placenta prepares the mammary gland for lactation, such that milk is being synthesised and secreted by the time of parturition, pituitary PRL becomes the key determinant of milk output after birth. This, in turn, is controlled by a milieu of factors, both environmental and reproductive. Stress, for example, will suppress PRL secretion, as will light, causing PRL release to occur with a circadian rhythm (reviewed in Freeman *et al*, 2000). Both mating and suckling promote release. All such inputs are transduced by the hypothalamus, which secretes a range of both prolactin-releasing factors (PRFs) and prolactin-inhibiting factors (PIFs). These act directly on the PRL secreting lactotroph cells, situated in the anterior pituitary gland. Lactotrophs typically have high spontaneous secretory activity, and thus the regulation exerted by the hypothalamus is predominantly inhibitory (Freeman *et al*, 2000). Dopamine is a tonic inhibitor of PRL secretion, and is synthesised and released by a subset of dopaminergic neurons referred to as tuberoinfundibular (TIDA) neurons, located in the arcuate nucleus. Dopamine enters the hypophyseal long portal vessels and is transported to the anterior pituitary. Lactotrophs in the pituitary express the D_2 subclass of dopamine receptors (Caron *et al*, 1978), and suppress PRL secretion in response to ligand-induced receptor activation. Dopamine receptor-blocking agents, such as haloperidol, can rescue PRL release in dopamine-treated pituitary glands *ex vivo* (MacLeod and Lehmeyer, 1974). Suckling suppresses dopamine release from the TIDA neurons, removing the inhibition on lactotrophs and thus promoting PRL synthesis (Callahan *et al*, 1996).

At weaning, the mammary gland undergoes dramatic remodelling, in which epithelial cells apoptose and the gland regresses to a near-pre-pregnant state. Involution, as this remodelling is termed, is a two-step process. The first phase, lasting approximately 48 hours, is characterised by a down-regulation in the transcription of Stat5-dependent survival factors. This is mediated by local signals. The accumulation of milk in the ducts of the glands feeds back to suppress further milk production. The key signalling molecule in this system is serotonin (5-hydroxytryptamine; 5-HT). Levels of tryptophan hydroxylase (TPH1), the rate-limiting enzyme for 5-HT synthesis, increase during lactation (Matsuda *et al*, 2004). This was shown to directly correlate with levels of 5-HT, which is present in both epithelial cells and milk (Stull *et al*, 2007). The negative influence of 5-HT on the production of milk proteins was demonstrated in primary explant cultures, in which exogenous 5-HT suppressed the expression of genes such as β-*casein* in a dose-dependent manner, even in the presence of PRL (Matsuda *et al*, 2004). Although initial experiments suggested that *Tph1* expression was PRL-dependent, further investigation revealed that expression is driven by milk stasis (Pai and Horseman, 2008).

Phase I is characterised not only by this suppression of Stat5-mediated signalling, but the associated switch to Stat3-mediated gene expression. Stat3 is activated by the cytokine leukaemia inhibitory factor (LIF; Kritikou *et al*, 2003), and translocates to the nucleus to promote the expression of death- or remodelling-related genes (Clarkson *et al*, 2006). Other indirect gene targets include those which are antagonistic to growth-promoting pathways. For example, Stat3 activates *C/ebp*δ expression, encoding a transcription factor which in turn induces the expression of *Igfbp5*, encoding the insulin-like growth factor binding protein 5 (Hutt *et al*, 2000). This molecule binds to and suppresses the activity of *Igf1*, antagonising the growth-promoting effects of this pathway (Ning *et al*, 2007). Other Stat3 targets reinforce the involution pathway: transforming growth factor (TGF) β3, for example, is induced within a few hours of a forced-wean, and promotes phosphorylation, and subsequent activation, of Stat3 (Nguyen and Pollard, 2000). The involution switch is rapid; LIF transcription increases 30-fold within 12 hours of a forced-wean (Kritikou *et al*, 2003). *Lif* is itself expressed from the mammary gland, and thus is an autocrine or paracrine regulator, but the mechanism for the induction of *Lif* expression is not clear. During embryonic development, *Lif* is probably controlled by oestrogen or progesterone (Kritikou *et al*, 2003) but these are unlikely activators of mammary gland expression. It is conceivable that the accumulation of 5-HT is responsible for inducing *Lif*, but a causal link has not yet been found.

Epithelial cell apoptosis in the mammary gland is in part triggered by the upregulation of negative regulatory subunits of PI(3) kinase, which are direct transcriptional targets of Stat3. This diminishes levels of phosphorylated AKT, a serine/threonine kinase, which during lactation provides an over-riding survival signal (Schwertfeger *et al*, 2001; Watson, 2006).

Whilst phase I is characterised by the highest number of terminal deoxynucleotidyl transferase dUTP nick-end labelling (TUNEL)-positive cells, indicative of apoptosis, the process remains reversible. The reintroduction of a suckling stimulus will rescue milk protein production, by promoting pituitary PRL release and clearing 5-HT which has accumulated in static milk. Phase II of involution, initiated about 48 hours after a forced-wean, is, however, irreversible. This phase is marked by extensive tissue remodelling. The lobuloalveolar structures collapse and epithelial cell positions are reoccupied by adipocytes. Matrix metalloproteases (MMPs) are key to this process. Expressed by the stroma, they breakdown the extracellular matrix (ECM), which reinforces epithelial cell apoptosis (Pullan *et al*, 1996). The huge volume of cell debris produced in such a short period of time as a consequence of apoptosis is dealt with by both professional and non-professional phagocytes, including mammary epithelial cells themselves (Monks *et al*, 2005). Such cells migrate to the involuting mammary gland in response to inflammatory mediators, such as *Growth-related oncogene 1*, a neutrophil-attracting chemokine, secreted early in phase I (Stein *et al*, 2004).

The observation that *Grb10* is expressed in a pregnancy-dependent manner in the adult mammary gland, probably under the control of PRL-Stat5, caused us to investigate its associated function. The retention of the *Grb10* imprint in this tissue was also intriguing, as,

to our knowledge, this was a precedent. Despite no apparent gross morphological defects in *Grb10KO*$^{m/+}$ mammary glands, our investigations revealed that the gene promotes mammary gland function, consistent with the idea that PRL/Stat5-dependent genes are 'survival factors' in this tissue. Moreover, *Grb10* expressed from the maternally-inherited chromosome mediated a supply/demand system between lactating mother and suckling pup. This finding may have implications for understanding the evolution of genomic imprinting.

6.2 Results

6.2.1 *Grb10* ablation does not engender gross morphological changes in the adult mammary gland

To address the function of *Grb10* in the adult mammary gland, we first examined the gross morphology of fourth (abdominal) glands isolated from wild type, *Grb10KO*$^{m/+}$ and *Grb10KO*$^{+/p}$ females, during gestation and lactation. Glands were stained with carmine alum for visualisation of ductal branching (Figure 6.1). The glands of virgin females were not examined as *Grb10* is expressed in a pregnancy-dependent manner in this organ (Figure 5.13).

At gestational day 7.5 (G7.5), the mammary glands of all genotypes consisted of a rudimentary ductal tree (Figure 6.1), which occupied a small proportion of the total mammary fat pad (not shown). Terminal end buds (TEBs), with their characteristic bifurcating structure, were observed at the ends of the ducts. These had penetrated further into the fat pad by G12.5 and generated new primary ducts by bifurcation. Secondary ductal branches were also visible sprouting laterally from the primary ducts. Mammary glands isolated from lactating females (postnatal day 6; P6) consisted of dense clusters of alveolar structures, the staining of which obscured the visualisation of ducts. At this stage, glands occupied a large proportion of the associated mammary fat pad (not shown). No morphological differences were observed at this resolution between glands of any genotype at the stages examined.

Morphological characterisation was extended by quantifying the number of branch points within a fixed window at G12.5, as described in Section 2.5.2. Only wild type and *Grb10KO*$^{m/+}$ glands were analysed in this manner, as *Grb10* is expressed from the maternally-inherited chromosome in this organ, and thus a morphological difference was not expected between *Grb10KO*$^{+/p}$ and wild type glands. No significant difference in the number of branch points was observed between the wild type and *Grb10KO*$^{m/+}$ glands examined (Figure 6.2*a*). Similarly, the distance between the lymph node and the leading edge was not significantly different between glands of the two genotypes (Figure 6.2*b*).

6.2.2 Pilot study: assessment of mammary gland morphology by Optical Projection Tomography (OPT)

Whilst wholemount and histological analyses of mammary glands are invaluable in examining tissue morphology, they are typically limited to an assessment in two dimensions (2D). It can, therefore, be difficult to extrapolate this information to comment on the three-dimensional (3D) structure of a mammary gland. This could be useful in addressing the total volume of ductal branches, for example, rather than inferring this from measurements of length or number of branch points.

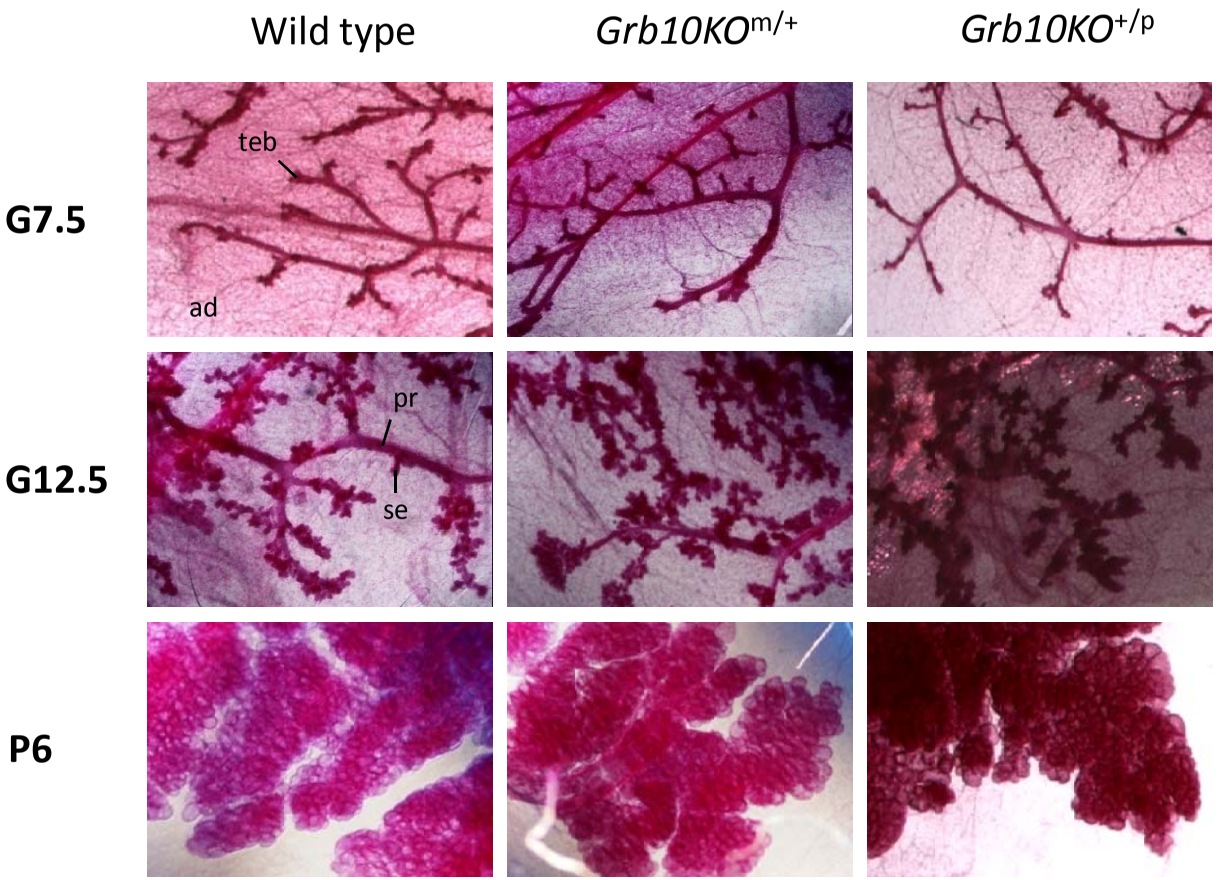
Wild type
Grb10KO m/+
Grb10KO +/p
G7.5
G12.5
P6
teb
ad
pr
se

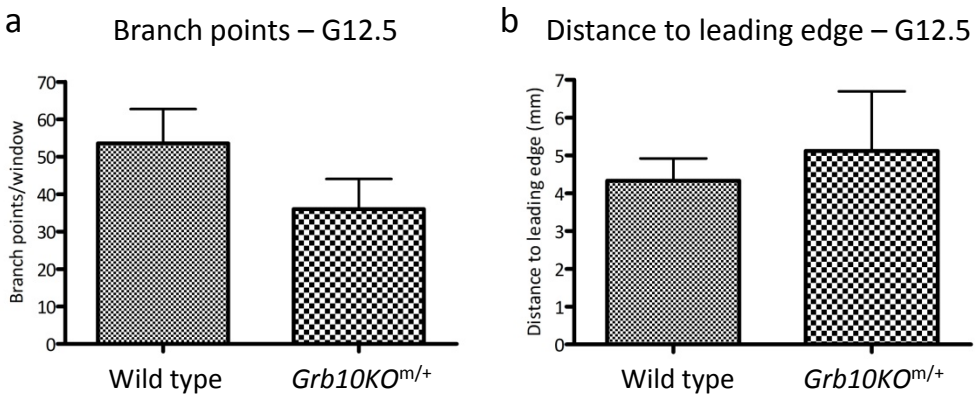
a
Branch points – G12.5
Branch points/window
70
60
50
40
30
20
10
0
Wild type
Grb10KOm/+
b
Distance to leading edge – G12.5
Distance to leading edge (mm)
7
6
5
4
3
2
1
0
Wild type
Grb10KOm/+

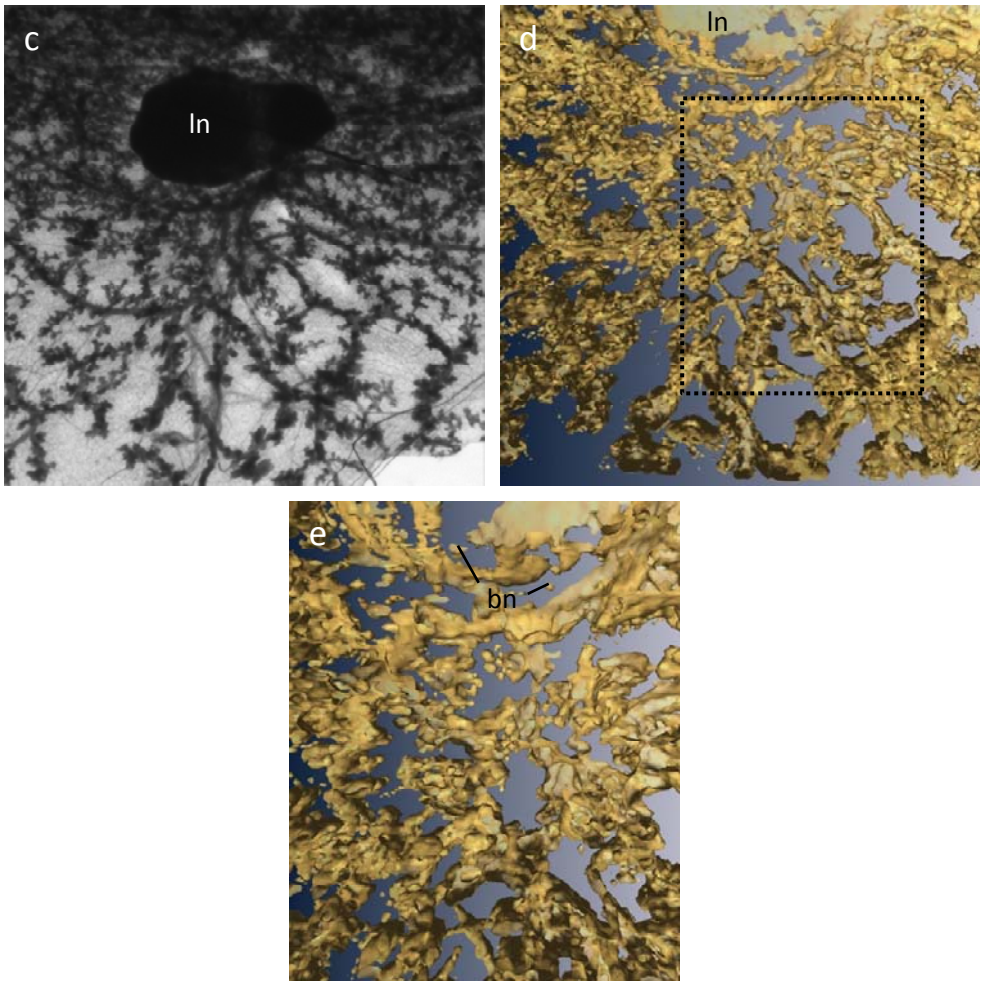
c
ln
d
ln
e
bn

To address this shortcoming, wild type mammary glands isolated at G12.5 were prepared for Optical Projection Tomography scanning. We wished to determine if this technique offered a suitable method for 3D mammary gland assessment. 400 2D scans of each gland were performed; a representative scan is shown in Figure 6.2*c*. Primary and secondary branches, as well as TEBs, are visible in this scan. Computer software stacked these 2D scans to produce a 3D reconstruction of the organ, which could be manipulated on screen to permit viewing from any angle. It was difficult to distinguish between branches and TEBs in these reconstructions, or indeed to identify the extent of individual primary ducts (Figure 6.2*d*). The denser network of branches closer to the lymph node observed from the 2D scan was apparent from the reconstruction. Viewing the reconstruction at a higher magnification emphasised the difficulty in distinguishing specific structures, and revealed a considerable level of noise, in which background staining had been misinterpreted as part of the gland structure (Figure 6.2*e*).

6.2.3 *Grb10* mediates a supply/demand system between suckling pup and lactating mother

Work described in Chapter Five identified a likely candidate site for the binding of the transcription factor Stat5 at the *Grb10* locus. Binding of Stat5 appeared to be necessary for the expression of *Grb10* in the adult mammary gland (Figure 5.13), supporting a previous study identifying *Grb10* as a highly likely transcriptional target of Stat5 in mammary epithelial cell cultures, a probable response to prolactin binding to cell surface receptors (Clarkson *et al*, 2006). This is further supported by the observation that *Grb10* is expressed in a pregnancy-dependent manner in the mammary gland. Further characterisation of *Grb10KO*$^{m/+}$ mammary glands therefore focussed on the identification of a phenotype which might be associated with a perturbation of prolactin action. As pup growth during the neonatal period is correlated with mammary gland function, we tracked the growth of individual pups in litters suckled by wild type and *Grb10KO*$^{m/+}$ females.

Cross-fostering experiments enable the independent phenotypic examination of mother and pup genotypes

Wild type females were mated with wild type males to produce pure wild type litters (Figure 6.3*a(i)*). *Grb10KO*$^{m/+}$ females were also mated with wild type males, producing mixed litters of both wild type and *Grb10KO*$^{m/+}$ offspring (Figure 6.3*a(ii)*). All females were 7 weeks of age at mating, and were previously virgins. Litters were normalised to between 5 and 7 pups on the day of birth. Pups were tattooed on the pads of their paws according to a devised scheme, such that the growth of individual pups could be tracked from the day of birth, and pups posthumously genotyped (Figure 6.5*a*).

Whilst it was possible from these crosses to compare the growth of wild type pups born to a wild type mother with wild type pups born to a *Grb10KO*$^{m/+}$ mother, those born to a *Grb10KO*$^{m/+}$ mother also had *Grb10KO*$^{m/+}$ siblings. These transgenic animals are larger than

a Genetic crosses

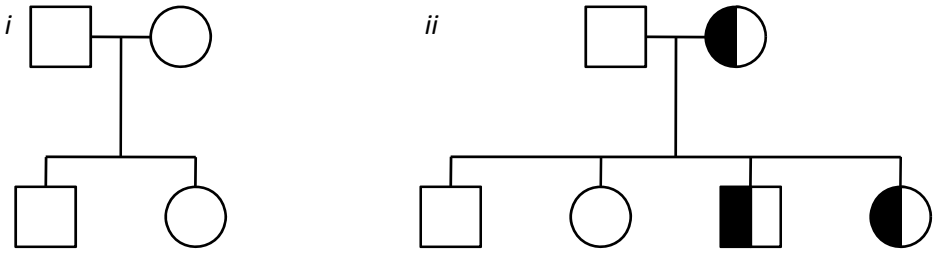

b Mother-pup relationships

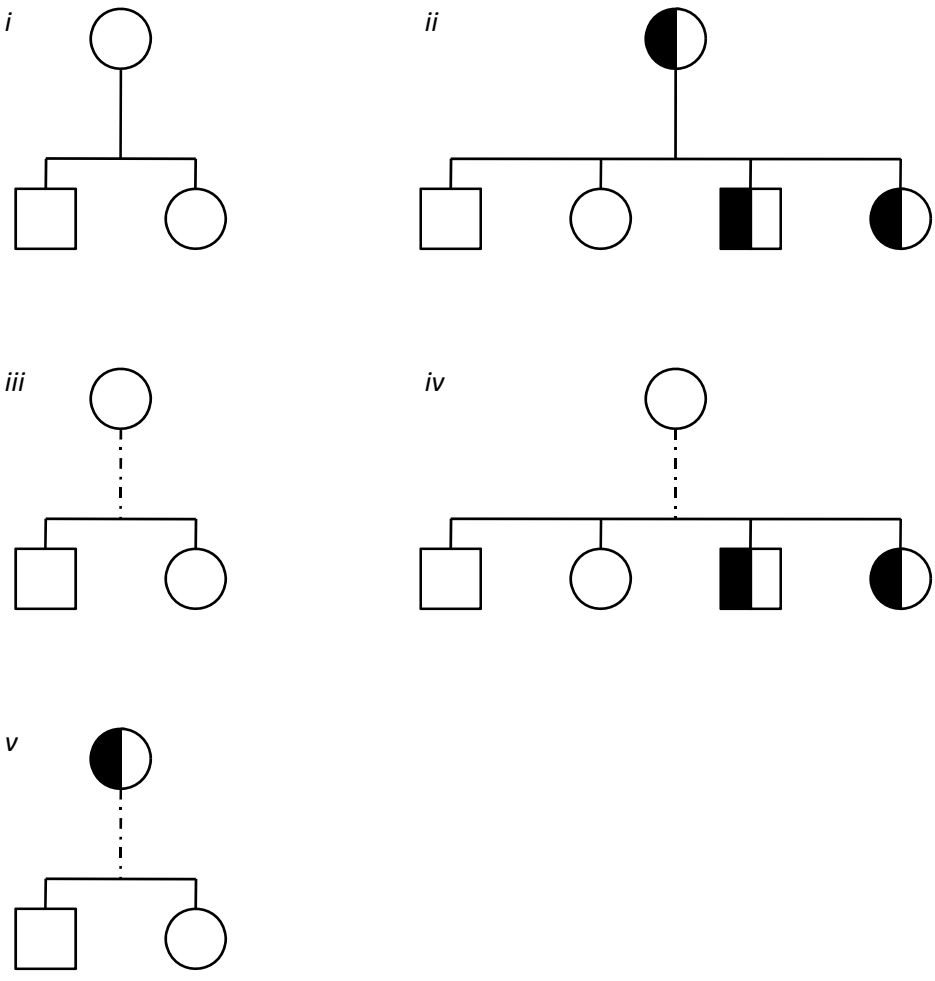

their wild type sibs on the day of birth (Figure 4.4*d* and *f*), and thus might have indirectly influenced the growth of wild type animals in the same litter, by outcompeting them for access to a nipple, for example. To differentiate between the influence of maternal and offspring genotype on pup growth, we devised a cross-fostering strategy, outlined below. As before, all females were 7 weeks of age at mating, and were previously virgins.

Some *Grb10KO*$^{m/+}$ females, having given birth to both wild type and *Grb10KO*$^{m/+}$ pups (a 'mixed litter'), were permitted to raise their own biological offspring (Figure 6.3*b(ii)*). Other *Grb10KO*$^{m/+}$ females had their biological offspring removed on the day of birth and replaced with pure wild type litters (Figure 6.3*b(v)*). The reciprocal was also performed, such that some wild type females raised mixed litters (Figure 6.3*b(iv)*). To control for the process of cross-fostering, ensuring that this in itself did not influence pup growth, some wild type females were permitted to raise their own biological offspring, whilst other wild type females were given pure wild type litters from a separate mating (Figure 6.3*b(i)* and *(iii)*).

No differences in the neonatal growth of male and female pups

To determine if it was necessary to separate datasets according to pup gender, the weights of male and female pups raised by their biological mothers were compared on the day of birth (postnatal day 1), and at postnatal days 8 and 15. Male and female pups born to wild type mothers displayed a similar range of weight values at all time points examined, with no statistically significant differences in mean weight, as assessed by Students' T-test (Figure 6.4). This was also the case for male and female wild type pups born to *Grb10KO*$^{m/+}$ mothers, and male and female *Grb10KO*$^{m/+}$ pups.

The lack of apparent difference in weight between male and female pups, both wild type and transgenic, permitted the consolidation of data from separate genders, creating larger sample sizes and more robust statistical comparisons.

The process of cross-fostering does not influence pup growth

To eliminate the process of cross-fostering as a parameter influencing postnatal pup growth, the weights of wild type pups born to and raised by their biological wild type mothers were compared with the weights of wild type pups cross-fostered to non-biological wild type mothers (Figure 6.3*b(i)* and *(iii)*). No difference between the two datasets was observed on the day of birth, the day after cross-fostering (day 2) or after 15 days of suckling (Figure 6.5*b*), as assessed by Students' T-test. The growth trajectories of the two datasets in the interim period were also very similar (data not shown). Finally, the two datasets were compared at postnatal days 1, 8 and 15 alongside other datasets using one-way analysis of variance (ANOVA). No significant differences were observed at any of the time points (Table 6.1). Together, these results confirmed that the process of cross-fostering itself did not affect postnatal pup growth.

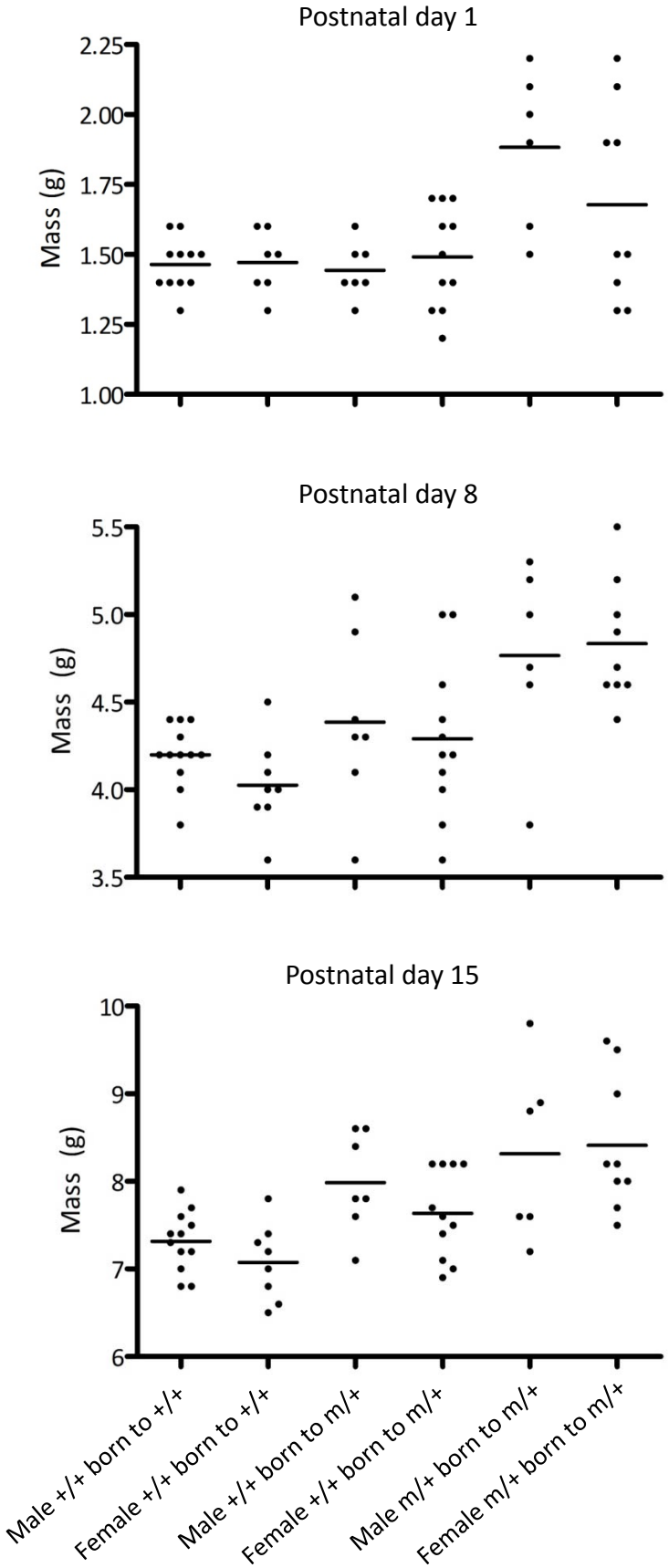
Postnatal day 1
Mass (g)
2.25
2.00
1.75
1.50
1.25
1.00
Postnatal day 8
Mass (g)
5.5
5.0
4.5
4.0
3.5
Postnatal day 15
Mass (g)
10
9
8
7
6
Male +/+ born to +/+
Female +/+ born to +/+
Male +/+ born to m/+
Female +/+ born to m/+
Male m/+ born to m/+
Female m/+ born to m/+

a

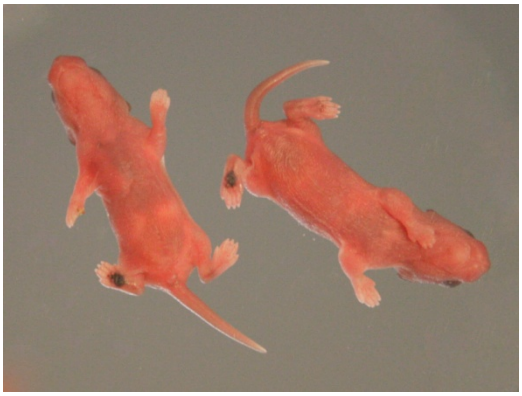

b

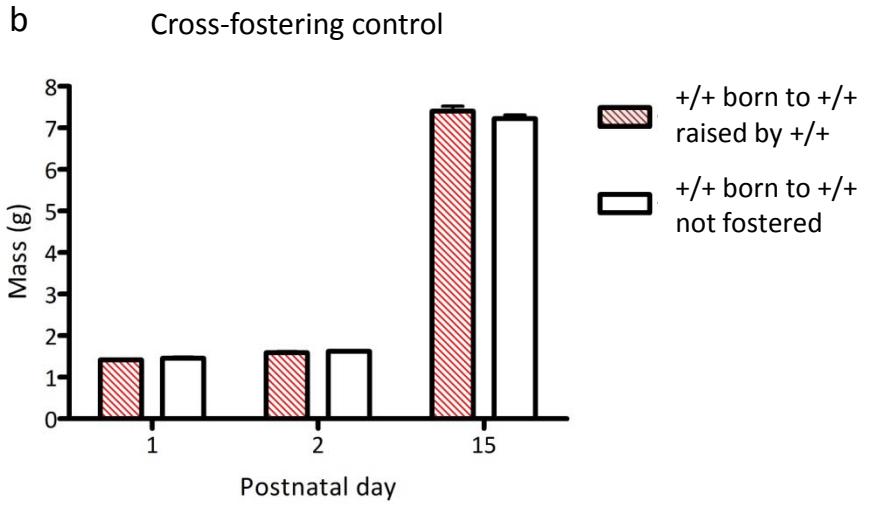
Cross-fostering control
Mass (g)
0
1
2
3
4
5
6
7
8
1
2
15
Postnatal day
+/+ born to +/+ raised by +/+
+/+ born to +/+ not fostered

c

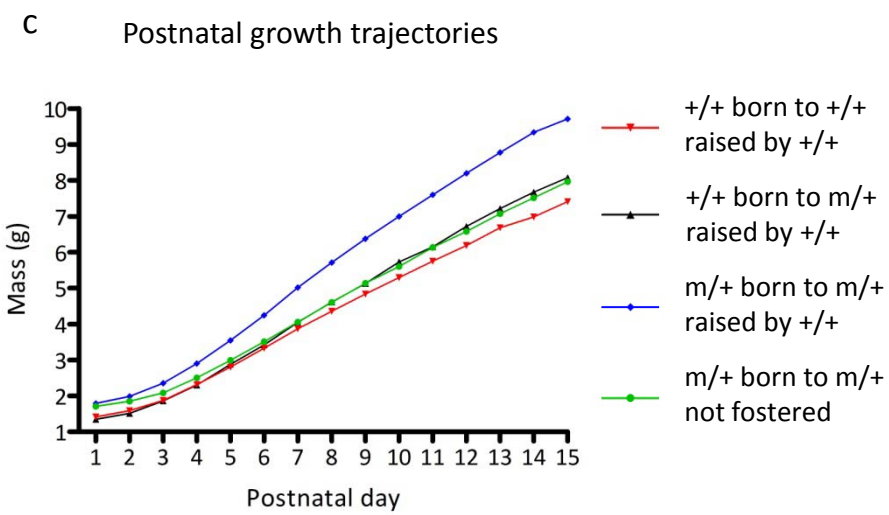
Postnatal growth trajectories
Mass (g)
1
2
3
4
5
6
7
8
9
10
1 2 3 4 5 6 7 8 9 10 11 12 13 14 15
Postnatal day
+/+ born to +/+ raised by +/+
+/+ born to m/+ raised by +/+
m/+ born to m/+ raised by +/+
m/+ born to m/+ not fostered

a Postnatal day 1

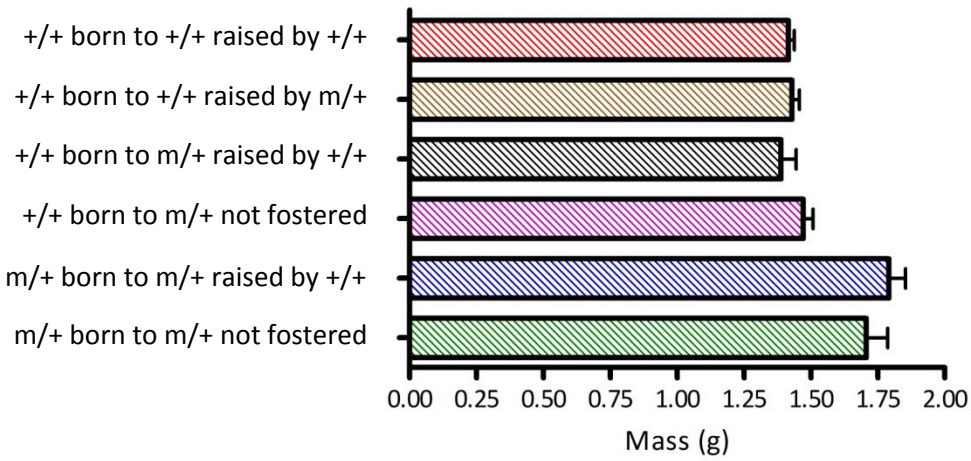

b Postnatal day 8

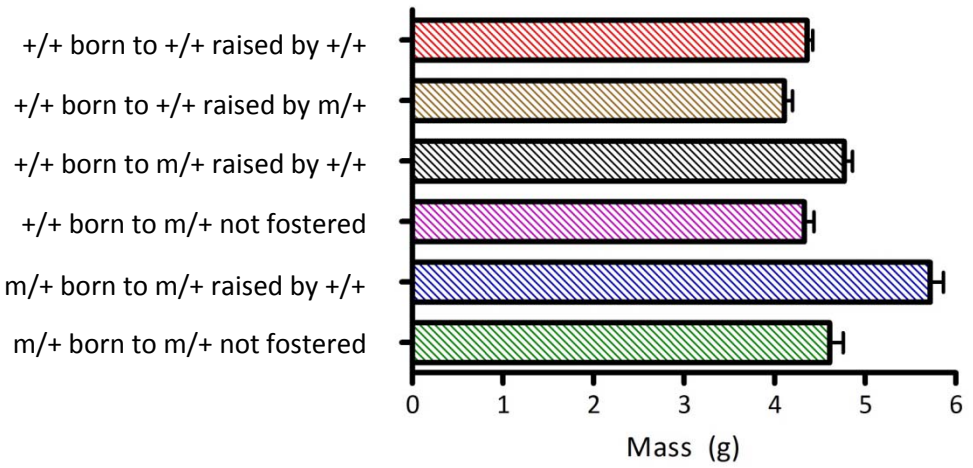

c Postnatal day 15

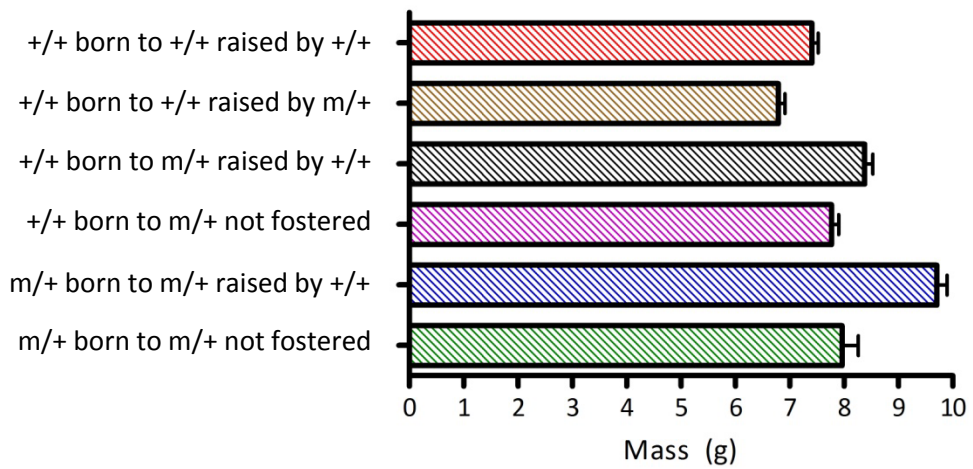

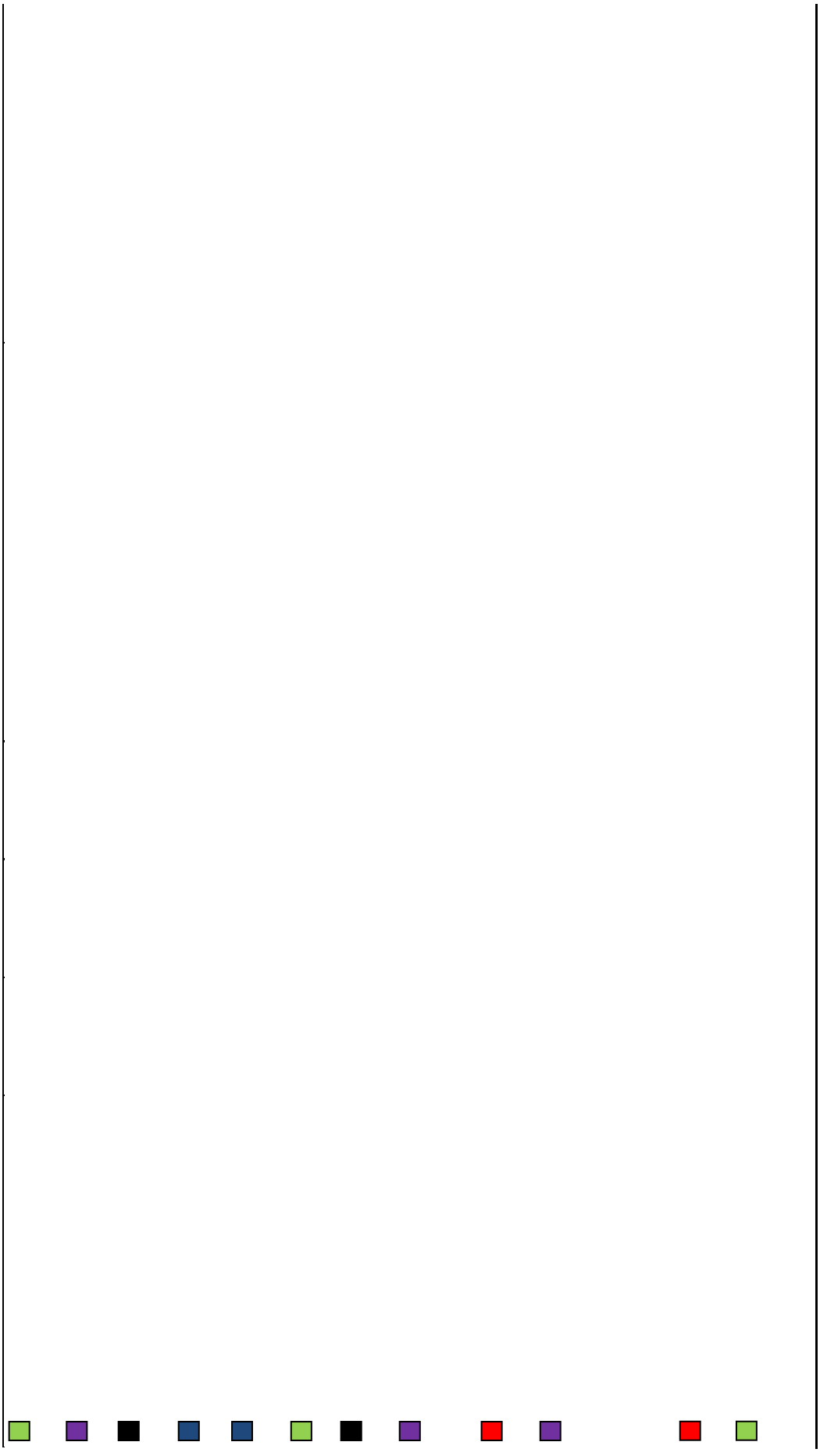

Grb10KO$^{m/+}$ *pups display an increased demand for nutrients*

To examine growth differences in a quantitative manner, the weights of pups in each dataset were compared at postnatal days 1, 8 and 15 by one-way ANOVA. The results of these comparisons are presented in Table 6.1 and can be correlated with bar graphs in Figure 6.6. The growth trajectories of selected datasets are shown in Figure 6.5*c*. To aid the reader, each dataset has been assigned a colour code, which corresponds to the coloured boxes in Table 6.1, and the coloured lines and bars of Figures 6.5*c* and 6.6.

The weights of wild type pups in a pure litter (*red*) were indistinguishable from those of wild type pups in a mixed litter (*black*) on the day of birth. When both groups were suckled by wild type foster mothers, there was a trend towards an increased weight among wild type pups in a mixed litter at day 8. The difference became statistically significant at day 15.

This effect was also observed when the suckling mother was transgenic. Again, wild type pups in a mixed litter (*purple*) grew at a faster rate than those in a pure wild type litter (*brown*). The effect was again not revealed until day 15, although there was a trend in this direction at day 8.

These observations suggested that the presence of *Grb10KO*$^{m/+}$ pups in a litter benefitted wild type sibs, implying that the larger *Grb10KO*$^{m/+}$ pups displayed an increased demand for maternal nutrients.

Grb10KO$^{m/+}$ *mothers display an impaired ability to supply nutrients*

To deduce more about the influence of the suckling mother's genotype, wild type pups in a pure wild type litter were raised by wild type (*red*) and *Grb10KO*$^{m/+}$ (*brown*) mothers. Whilst these were indistinguishable on the day of birth, by day 8 there was a trend towards increased weight in the group raised by wild type mothers, which was significant on day 15 by one-way ANOVA. This implied that *Grb10KO*$^{m/+}$ mothers supplied less nutrients to suckling pups than wild type control mothers.

Grb10KO$^{m/+}$ *mothers display an impaired response to high nutrient demand*

Grb10KO$^{m/+}$ pups were larger than their wild type sibs on the day of birth, but when suckled by a *Grb10KO*$^{m/+}$ mother (*green*), normalised to wild type sibling weight by day 8 (*purple*). By one-way ANOVA, these *Grb10KO*$^{m/+}$ pups were also indistinguishable from wild type pups in a pure litter raised by wild type mothers at days 8 and 15 (*red*). This normalisation was not observed when mixed litters were raised by wild type mothers (*black* and *blue*). Indeed, *Grb10KO*$^{m/+}$ pups raised by wild type mothers (*blue*) were considerably larger at day 15 than *Grb10KO*$^{m/+}$ pups raised by their biological mothers (*green*). This suggested that whilst wild type mothers responded well to an increase in demand, *Grb10KO*$^{m/+}$ mothers responded relatively poorly. However, their response was not abolished entirely

as wild type pups in a mixed litter raised by a *Grb10KO*$^{m/+}$ mother (*purple*) still grew at a faster rate than wild type pups in a pure litter raised by a *Grb10KO*$^{m/+}$ mother (*brown*).

The benefits to a wild type pup of having Grb10KO$^{m/+}$ *siblings are offset by suckling from a* Grb10KO$^{m/+}$ *mother*

Wild type pups in a mixed litter raised by a *Grb10KO*$^{m/+}$ mother (*purple*) had a very similar growth profile to wild type pups in a pure wild type litter raised by a wild type mother (*red*). This suggested that the benefit to a wild type pup of having transgenic siblings, which demand more nutrients, is offset by suckling from a transgenic mother, who is a relatively poor supplier of nutrients.

6.2.4 Milk quality is not the molecular basis for the observed differences in maternal provisioning

To address the mechanistic basis for reduced nutrient supply from *Grb10KO*$^{m/+}$ females, and increased response to high demand in wild type females, milk was isolated from some of the mothers raising cross-fostered litters (Figure 6.7*a* and *b*).

First, the proportion of fat in the milk was assessed. For all datasets examined, the mean fat content was between 23 and 26 %, with no significant differences observed between any of the genotypes (assessed by one-way ANOVA; Figure 6.7*c*).

Following the removal of fat, milk protein content was analysed by sodium dodecyl sulphate (SDS) polyacrylamide gel electrophoresis (PAGE; Figure 6.7*d*). Key milk proteins, including albumin, whey acidic protein (WAP) and α- and β-caseins, were detected in all samples, as well as other protein species observed in previous analyses but not identified (Kumar *et al*, 1994; Hurley, 2009, Milk composition and synthesis resource library, http://classes.ansci.illinois.edu/ansc438/Milkcompsynth/milkcompsynthresources.html).
Equal volumes of milk protein were loaded for each sample, to permit a direct comparison of protein content. Although there was some variation in relative total protein levels between individuals, this did not correlate with genotype.

Together, this data suggested that milk quality was probably not the basis for reduced provisioning of *Grb10KO*$^{m/+}$ females, or for increased provisioning of wild type females when suckling mixed litters, although subtle differences in milk quality cannot be excluded as part of the mechanism.

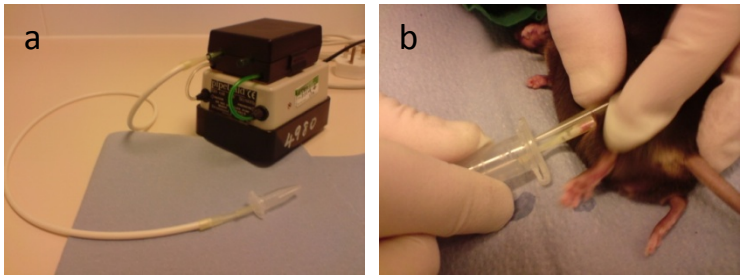
a
b

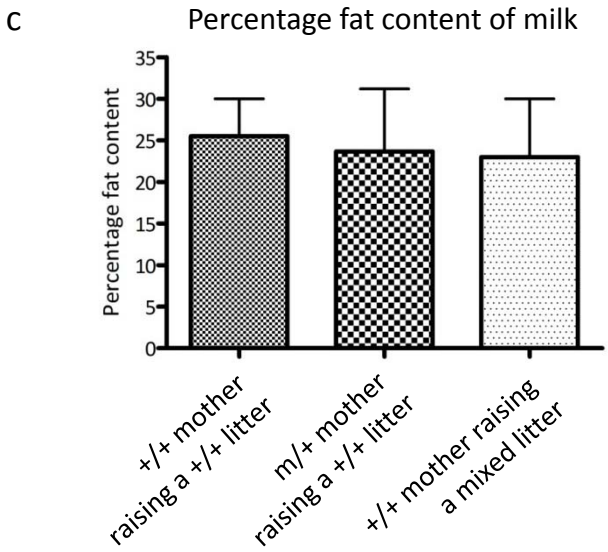
c
Percentage fat content of milk
Percentage fat content
35
30
25
20
15
10
5
0
+/+ mother raising a +/+ litter
m/+ mother raising a +/+ litter
+/+ mother raising a mixed litter

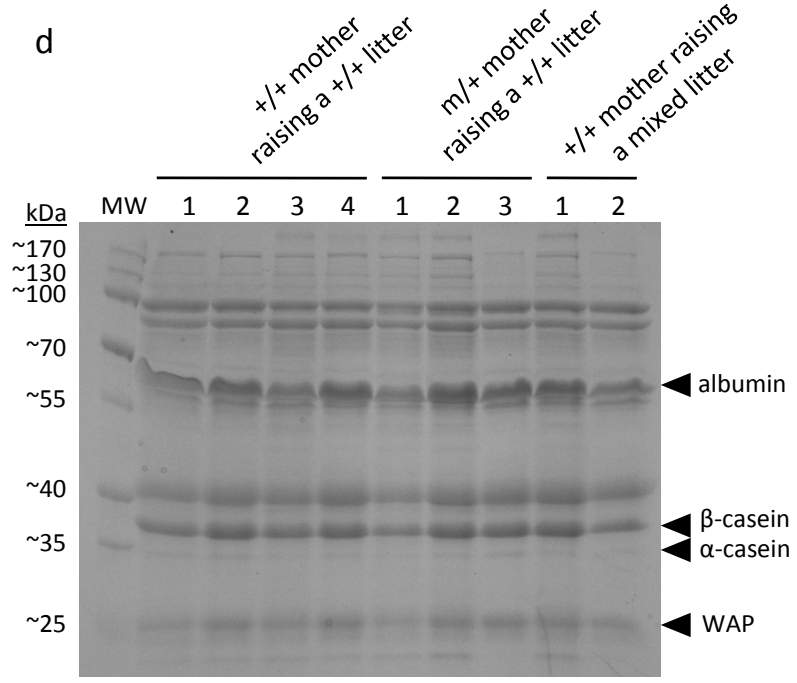
d
+/+ mother raising a +/+ litter
m/+ mother raising a +/+ litter
+/+ mother raising a mixed litter
kDa
MW
1
2
3
4
1
2
3
1
2
~170
~130
~100
~70
~55
~40
~35
~25
albumin
β-casein
α-casein
WAP

6.2.5 *Grb10KO*$^{m/+}$ lactating females display elevated pituitary *Prolactin* expression

Although differences in milk quality did not appear to be the basis for the reduced provisioning of *Grb10KO*$^{m/+}$ mothers, we examined whether expression of *Prolactin* in the pituitary glands might be perturbed. Poor nutrient suppliers might be expected to display reduced levels of *Prolactin* expression.

At the end of the experimental period (i.e. on postnatal day 15), mothers were dissected and total RNA extracted from pituitary glands for examination by quantitative real-time PCR (qPCR). The levels of *Prolactin* and *Growth hormone* transcripts were assessed. Figure 6.8 shows expression levels of these two genes normalised to the levels of *Actin*, a house-keeping gene.

Grb10KO$^{m/+}$ females exhibited elevated pituitary *Prolactin* expression relative to wild type control females, when both groups were suckling pure wild type litters (Figure 6.8*a*). This was statistically significant when assessed by the Kruskal-Wallis test. This was contrary to our original hypothesis, and demonstrated that reduced pituitary *Prolactin* expression was not the basis for poor provisioning among *Grb10KO*$^{m/+}$ mothers.

Additionally, *Prolactin* expression in wild type mothers was unaffected by the genotype of fostered pups, with no significant differences observed between wild type mothers raising wild type pups and those raising mixed litters. The expression of *Growth hormone* did not differ significantly between any of the groups examined (Figure 6.8*b*).

6.2.6 *Grb10KO*$^{m/+}$ mammary glands exhibit a trend towards more rapid involution

In the mammary epithelium, genes activated in response to prolactin, through Stat5, are predicted to play positive roles in the function of the mammary gland, either by promoting gland differentiation or branching, or by promoting milk protein synthesis or release (Clarkson *et al*, 2006). In this manner, Stat5 and its downstream 'survival factors' protect against Stat3-mediated apoptosis; over-expression of *Stat5a in vivo* delays involution (Iavnilovitch *et al*, 2002). As *Grb10* appeared to promote mammary gland function, and might thus be classified as a 'survival factor', we addressed whether *Grb10KO*$^{m/+}$ glands exhibited more rapid involution.

To address this possibility, glands were isolated from age-matched and litter size-matched females 48 hours after a forced-wean. This time point corresponded with the transition from the reversible phase I to irreversible phase II of involution. Glands were sectioned and fragmented nuclei, indicative of apoptosing cells, identified by terminal deoxynucleotidyl transferase dUTP nick-end labelling (TUNEL). Figure 6.9*b* shows an illustrative wild type gland section subjected to TUNEL and subsequently counter-stained with methyl green. Epithelial cells were easily identifiable by their relatively small size when compared with stromal cells. A sub-population of epithelial cells were TUNEL-positive. Randomly-selected sections from five wild type and five *Grb10KO*$^{m/+}$ glands were assessed for TUNEL-positive nuclei in a quantitative manner. Representative images for this quantification are shown in

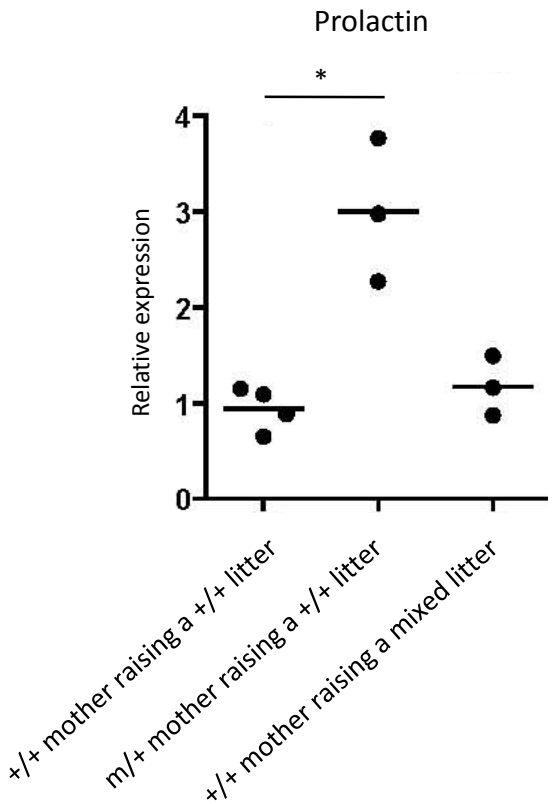
Prolactin
*
Relative expression
4
3
2
1
0
+/+ mother raising a +/+ litter
m/+ mother raising a +/+ litter
+/+ mother raising a mixed litter

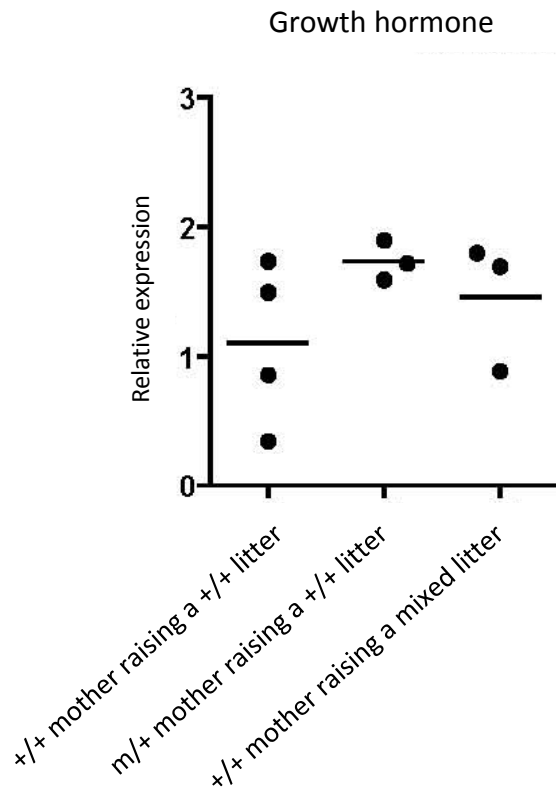
Growth hormone
Relative expression
3
2
1
0
+/+ mother raising a +/+ litter
m/+ mother raising a +/+ litter
+/+ mother raising a mixed litter

a

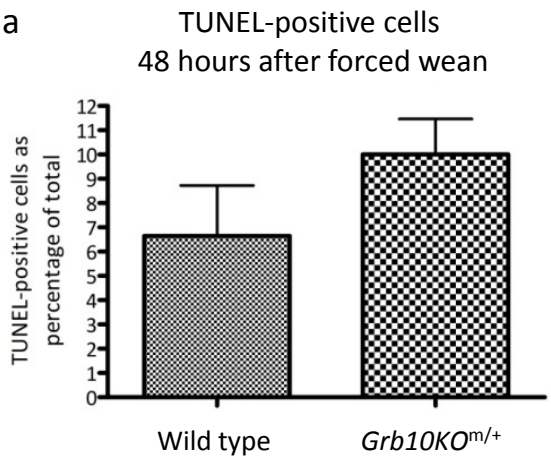
TUNEL-positive cells
48 hours after forced wean
TUNEL-positive cells as percentage of total
0
1
2
3
4
5
6
7
8
9
10
11
12
Wild type
Grb10KOm/+

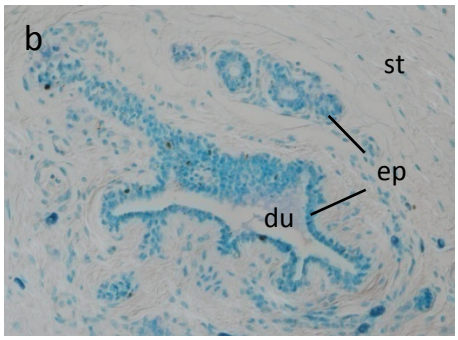
b
st
ep
du

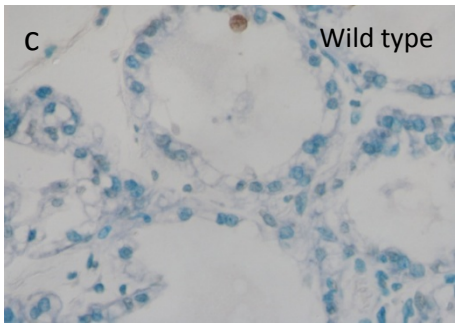
c
Wild type

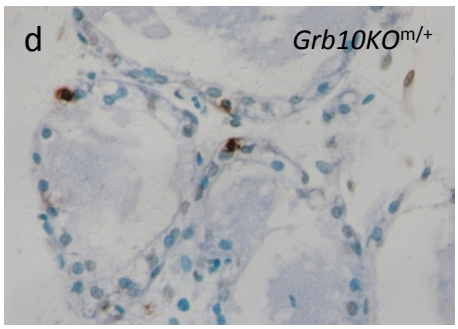
d
Grb10KOm/+

Figure 6.9*c* and *d*. The assessment was performed 'blind' without knowledge of the corresponding genotypes. No significant difference was observed between wild type and *Grb10KO*$^{m/+}$ glands, when TUNEL-positive cells were considered as a proportion of the total number of cells counted (Figure 6.9*a*). However, *Grb10KO*$^{m/+}$ glands did exhibit a trend towards a larger proportion of TUNEL-positive nuclei, consistent with the hypothesis of *Grb10* as a Stat5-dependent mammary gland survival factor.

6.3 Discussion

Work described in Chapter Five revealed a probable Stat5 binding site at the *Grb10* locus. This supported the results of another study identifying *Grb10* as a likely target of this transcription factor, downstream of prolactin receptor activation (Clarkson *et al*, 2006). The presence of the Stat5 binding site appeared to be necessary for the *in vivo* expression of a *LacZ* transgene knocked-in to the *Grb10* locus, in mammary epithelial cells (Figure 5.13). The current study also revealed that the expression of *Grb10* in this tissue is pregnancy-dependent, providing support for the hypothesis that *Grb10* expression is activated in response to prolactin through Stat5. Typically, genes activated via this pathway are proposed to promote mammary gland function, and are therefore termed 'survival factors'. Aside from this general hypothesis, nothing was previously known of the role of *Grb10* in the mammary gland. We thus characterised the effect of *Grb10* ablation on gland structure and function, with a view to finding evidence of perturbation of prolactin action. Whilst no obvious changes to mammary gland development or growth were observed, the present study revealed that *Grb10KO*$^{m/+}$ females were less capable of supplying nutrients to suckling offspring, consistent with a role for *Grb10* as a promoter of prolactin action in the mammary gland. However, the study also revealed an unexpected result: that *Grb10* mediates a system of supply and demand between lactating mother and suckling pup.

Comparable mammary glands from wild type, *Grb10KO*$^{m/+}$ and *Grb10KO*$^{+/p}$ females were isolated at early- and mid-gestation, and during lactation. These were fixed and stained with carmine alum. The epithelial cell proliferation and invasion of the mammary fat pad observed for wild type glands were consistent with previous descriptions (Hennighausen, Biology of the Mammary Gland, http://mammary.nih.gov/index.html). Glands isolated from *Grb10KO*$^{m/+}$ and *Grb10KO*$^{+/p}$ females did not obviously differ in their morphology to wild type controls. No difference was expected in *Grb10KO*$^{+/p}$ glands as *Grb10* transcription is exclusively from the maternally-inherited chromosome in this tissue (Figure 5.13), and thus *Grb10KO*$^{+/p}$ glands still retain functional Grb10 protein. If *Grb10* is a prolactin/Stat5-dependent survival factor, ablation of *Grb10* in this tissue might be expected to perturb branching morphogenesis, but this was not observed. Although the Stat5 proteins have many transcriptional targets (Basham *et al*, 2008), and thus the absence of *Grb10* alone is unlikely to result in such a dramatic phenotype as the compound *Stat5a/b* ablation, a more subtle effect may have been predicted.

The absence of a gross morphological defect was supported by quantitative measurements. *Grb10* ablation did not significantly alter the number of branch points within a fixed area, implying that epithelial cell proliferation was not affected. Similarly, the distance from the lymph node to the leading edge did not change, although such a measurement may be expected to remain quite constant between individuals, unless their body size proportions are dramatically altered. Whilst *Grb10KO*$^{m/+}$ animals are larger than their littermates in late gestation and early neonatal stages, this overgrowth normalises to that of wild type

controls within a few days (provided the pups are nurtured by their biological mothers; discussed later).

Further quantitative assessments might have included a measurement of the overall size of the mammary fat pad, and percentage occupation by epithelial cells and ducts. Such an analysis was not performed because a phenotype of *Grb10KO*$^{m/+}$ animals in adulthood is a reduced fat mass (Smith *et al*, 2007). Thus, it would be difficult to differentiate between an effect specific to the mammary gland and a more global phenotype.

Subtle differences in gland architecture, such as the total ductal volume, for example, are difficult to determine from the analysis of wholemount glands in two-dimensions. A three-dimensional assessment may provide more accurate data, and may be sufficient to detect a subtle phenotype. To this end, a pilot study was initiated to examine isolated and carmine alum-stained mammary glands using Optical Projection Tomography (OPT). This technique permits the stacking of multiple 2D scans of a tissue sample to generate a 3D reconstruction. Considerable success with this technique has already been documented for *in situ* hybridisation on developing chicken embryos (Fisher *et al*, 2008). Wild type glands at G12.5 were utilised in the present analysis. Despite scanning at the highest resolution currently available with the present equipment, the output was not an accurate representation of gland morphology. One key issue was the discrimination between 'real' structures and background staining; the threshold of acceptance could be altered over a wide-ranging scale, but it was impossible to eliminate all background without compromising real gland structures. This might be improved by de-staining the glands before preparing for OPT analysis, or by staining for a shorter time. At present, the current OPT output is inappropriate for quantitative assessment, but this might be possible with methodological improvements.

It is pertinent to note that the quantitative analyses performed in the present study used glands isolated at G12.5. This corresponds with a low-level of *Grb10* expression in the mammary epithelium, and thus might be too early to detect any subtle phenotypic change. However, branch measurements become challenging in glands more developed than G12.5, as the network of ducts and alveoli make it difficult to identify and track individual branches. Thus, being able to compare glands removed at later gestational, and even in lactational, stages by OPT would be a considerable advantage. As already highlighted, there is scope for this technique to be optimised for such an application.

Although no gross morphological defects could be attributed to *Grb10* ablation in the mammary gland, we wished to assay the function of the gland, using postnatal pup growth as an endpoint measure. In this manner, any subtle changes in gene transcription or duct ultrastructure which might ultimately affect milk secretion or synthesis would hopefully be revealed. Previous studies have examined pup growth as a direct correlate of mammary gland function (Wlodek *et al*, 2003; Manhès *et al*, 2006). In the current study, wild type and *Grb10KO*$^{m/+}$ females were mated with wild type males to produce pure wild type and mixed litters, respectively. All females were seven weeks of age at mating, and were previously virgins. It was necessary to control for age and pregnancy number because both of these factors influence mammary gland function; although glands undergo involution after the

weaning of pups, they typically retain more branches than that observed in virgin animals. To track pups over the first 15 days of growth, a method to identify individuals was necessary. This was particularly important in mixed litters, such that after culling, pups could be genotyped and correlated with their respective weights. *Grb10KO*$^{m/+}$ animals are overgrown at birth (Charalambous *et al*, 2003), and thus their growth had to be recorded separately to their wild type sibs. Various methods were employed to enable the identification of individual pups, including the marking of skin with permanent waterproof ink. This was rapidly washed off by the mother and did not permit long-term identification. To circumvent this issue, tattooing was used, in which a small volume of India ink was injected under the skin and thus could not be removed by washing. As the mice were of a mixed C57BL/6:CBA origin, they developed agouti or black pigmentation within a few days, which obscured tattoo marks, regardless of ink colour. However, the pads of the paws remain pink throughout postnatal life, offering the most suitable location for tattoo marks to be easily seen. Further, this created the opportunity to develop a scheme in which differential paw tattoo combinations could be correlated with a number system. This provided an easy and consistent means for identifying individual pups, and caused limited distress to the animals involved. Indeed, the tattoo marks on control animals not utilised in the present study were still clearly visible six months or more after application.

Although tattoo marks enabled the discrimination between wild type and transgenic littermates, thus permitting wild type pups born to a *Grb10KO*$^{m/+}$ mother to be compared with wild type pups born to a wild type mother, the comparison could potentially be confounded by the presence of transgenic pups in litters suckling from a transgenic mother. This was a particular concern because *Grb10KO*$^{m/+}$ pups are overgrown at birth, offering a potential advantage in competing with wild type littermates for access to a nipple. To uncouple the influence of maternal genotype and sibling genotype on wild type pup growth, a cross-fostering study was designed. This included a control for the process of cross-fostering, in which pure wild type litters suckled by their biological wild type mothers were compared with pure wild type litters raised by foster wild type mothers. On the day of birth, both groups were indistinguishable, confirming that neither exhibited a growth advantage. 24 hours after fostering, at which point any negative effects of cross-fostering, such as desertion, would be expected to manifest, there remained no difference in weight between the datasets. This persisted until the end of the experimental period, confirming that the process of cross-fostering in itself did not influence pup growth. All pups in all datasets were tattooed, to ensure that tattooing could also be eliminated as a parameter influencing weight gain.

Before analysing the growth data from the cross-fostering study, we first examined the growth of wild type and *Grb10KO*$^{m/+}$ pups raised by their biological mothers, separated by gender. Three time points were examined which spanned the experimental period. At all time points, pups of both genders displayed a considerable range of weight values, and there were no significant differences between the mean values for male and female pups in matched litters. This correlates with previous observations that body weight sexual dimorphism does not manifest until after weaning, when sex-specific differences in the pulsatile release of growth hormone develop (Lichanska and Waters, 2008). The lack of any

statistically significant difference in weight between the genders enabled the pooling of data for subsequent analyses, and thus larger population sizes with more robust statistical comparisons.

Analysis of postnatal pup growth in the cross-fostering experiment revealed several points of interest. Firstly, wild type pups in a mixed litter were indistinguishable from wild type pups in a pure litter on the day of birth. This suggests that the growth of wild type pups is not influenced *in utero* by *Grb10* ablation in the mother or by sharing the uterus with *Grb10KO*$^{m/+}$ siblings. Importantly, this implies that neither group has a growth advantage at birth which could be used to explain subsequent differences. In our previous studies, we found that, at e17.5, wild type pups in a mixed wild type and *Grb10KO*$^{m/+}$ litter were ~10 % smaller than wild type pups in a mixed wild type and *Grb10KO*$^{+/p}$ litter (Charalambous *et al* submitted). This difference was not attributed to competition from larger *Grb10KO*$^{m/+}$ sibs but correlated with an increased litter size for *Grb10KO*$^{m/+}$ females. As *Grb10KO*$^{+/p}$ pups do not exhibit a growth phenotype, such a size difference might also have been expected in the present study between wild type pups of a mixed wild type and *Grb10KO*$^{m/+}$ litter and wild type pups of a pure litter. Whilst the original observation of a size difference was made at e17.5, this is late in gestation and might be expected to persist at birth. An unpaired Students' T-test between the two datasets in the current study was performed (not shown) in addition to the one-way ANOVA described, which also failed to detect such a difference. This might be a consequence of using equipment not sensitive enough to detect such a subtle change. If the mean weight of wild type pups born to wild type mothers is ~1.4 g, a 10 % reduction would represent a loss of ~0.14 g. This would be too subtle to detect on the balance used in this study, which displayed weights to only one decimal place. Thus, it is reasonable to assume that this effect may still be apparent at postnatal day 1, and wild type pups in mixed litters therefore exhibit a very small growth disadvantage. However, the influence of litter size was immediately removed at birth by normalising all litters to between 5 and 7 animals.

Secondly, suckling *Grb10KO*$^{m/+}$ pups demanded more nutrients than wild type pups. Evidence for this includes the observation that wild type pups in mixed litters grew more rapidly than wild type pups in pure litters. The implication is that *Grb10KO*$^{m/+}$ pups, which are larger at birth, demand more nutrients, promoting milk supply and thus benefitting wild type siblings. Initially, our prediction was that wild type pups may be disadvantaged by being raised alongside transgenic sibs, as they may be outcompeted in access to a nipple, for example. However, the opposite effect was observed. Indeed, wild type pups were expected to be marginally smaller in mixed litters, due to the effect of an increased litter size *in utero*, as previously discussed. Any such disadvantage was clearly rapidly compensated for by having more demanding *Grb10KO*$^{m/+}$ siblings; a difference in growth became apparent around postnatal days 5-7, and continued to increase to the end of the experimental period.

The third key observation relates to the original goal to identify a phenotype which might be attributed to a perturbation of prolactin action. *Grb10KO*$^{m/+}$ females exhibited a reduced supply of nutrients to suckling offspring relative to wild type female controls. This was

observed regardless of the pup genotype being compared. This implies that the normal *in vivo* role of *Grb10* is to promote mammary gland function in response to prolactin, and fits the prediction that Stat5-dependent genes in the mammary gland are 'survival factors'.

Whilst a separation of the influences of maternal and offspring genotypes revealed phenotypes relating to both lactation and suckling, a combination of the two demonstrated a compound effect. *Grb10KO*$^{m/+}$ mothers were less able to respond than wild type mothers to an increased demand from *Grb10KO*$^{m/+}$ pups. As such, *Grb10KO*$^{m/+}$ pups raised by *Grb10KO*$^{m/+}$ mothers normalised to wild type littermate weight within a few days, whereas those raised by wild type mothers continued to grow significantly larger than their wild type littermates, with the biggest difference observed at the end of the experimental period. *Grb10KO*$^{m/+}$ pups suckling from a *Grb10KO*$^{m/+}$ mother were also indistinguishable from wild type pups in a pure litter raised by a wild type mother at days 8 and 15, demonstrating a compensation effect. These observations suggest that *Grb10* mediates a supply and demand system between lactating mother and suckling pup.

This alone is an intriguing observation, but is perhaps even more so in the knowledge that *Grb10* is an imprinted gene. Can these data say much about why *Grb10* imprinting, and perhaps imprinting more generally, may have evolved? The most widely-accepted explanation for imprinting is the parental conflict hypothesis, discussed in Chapter One. This predicts that maternally-expressed genes will act to suppress growth, whilst paternally-expressed genes have the opposite effect. However, this logic is applicable only up to the point of weaning and cannot explain the existence of imprinting in adult tissues, such as the mammary gland, as discussed in Chapter Five. Indeed, the imprinting profile and function of *Grb10* during embryonic growth fit the hypothesis; *Grb10KO*$^{m/+}$ foetuses are overgrown and have more efficient placentae (Charalambous *et al*, 2003; Charalambous *et al*, submitted). It is therefore possible that imprinting of *Grb10* evolved for this purpose, but an alternative model is required to explain why this should extend to the regulation of nutrient supply from the mammary gland. An attractive alternative is the maternal-offspring coadaptation hypothesis proposed by Wolf and Hager (2006). This model demonstrates that genes with pleiotropy, affecting different maternal and offspring traits, are more likely to be selected for imprinting. Moreover, such selection will favour expression from the maternally-inherited chromosome, as this will increase the adaptive integration between the genomes of mother and offspring. The observed role of *Grb10* in mediating supply and demand is consistent with the model on three levels. Firstly, it is maternally-expressed *Grb10* which is mediating the supply/demand system. Secondly, *Grb10* is pleiotropic, promoting nutrient output from the mother's mammary glands and suppressing nutrient demand in suckling pups. Finally, the integration of these roles controls offspring fitness. Ablation of maternally-expressed *Grb10* in a suckling pup increases demand, but the corresponding ablation of *Grb10* in the lactating mother reduces supply, with the result that *Grb10KO*$^{m/+}$ pups normalise to wild type weight within a few days. A lactating mother with a fully functional *Grb10* allele does not apply such a brake to nutrient output, allowing growth to proceed with a 'check' at a higher threshold. Thus, *Grb10* helps achieve optimal fitness. A larger pup is not necessarily fitter, when one considers the measure of fitness to be the effectiveness of gene propagation. If this was

the case, the wild type weight would simply be larger. Additionally, as discussed in Chapter Four, when considering the likelihood of morbidity, the optimal birth weight is just above the mean for a population (Sansing and Chinnici, 1976).

Coadaptation of an imprinted gene with pleiotropic effects in mother and offspring has previously been described for *Peg3*, but this example exhibits some different properties to those seen for *Grb10*. *Peg3* is a paternally-expressed gene, whose expression is predominantly in the hypothalamus and placenta (Kuroiwa *et al*, 1996; Hiby *et al*, 2001). Because of the direction of the imprint, the effects of *Peg3* mutation in the pup can be separated from the effects of *Peg3* mutation in the mother, without the need for cross-fostering. *Peg3*$^{+/p}$ embryos and placentae were growth retarded, which correlated with a reduced pup size on the day of birth (Curley *et al*, 2004). Wild type females carrying mutant embryos failed to match the weight gain of females carrying wild type embryos at the late stages of pregnancy, which prepares the mother for lactation. Mutant pups failed to gain weight in line with wild type pups through the suckling period, despite suckling from a wild type mother. In the mother, *Peg3* ablation from the paternally-expressed chromosome resulted in a failure to gain weight in the late stages of pregnancy, even though the embryos were all wild type. At birth, wild type pups born to a *Peg3*$^{+/p}$ mother were growth retarded and were restricted in postnatal growth by an impairment of milk letdown. It is intriguing that the outcomes of *Peg3* mutation in mother and pup were essentially complimentary: impaired milk letdown versus impaired suckling; reduced maternal food intake versus a small placenta; the time the mother takes to achieve weaning weight of wild type pups versus impaired postnatal growth. The significance of such coadaptation is that offspring who have extracted 'good' maternal nurturing are well-provisioned and will, themselves, be genetically predisposed towards 'good' mothering (Curley *et al*, 2004; Keverne and Curley, 2008). This complimentarity effect is not the case for *Grb10*. It is not possible to differentiate between the effects of maternal and offspring genotype *in utero*, but the cross-fostering study demonstrates that, postnatally, *Grb10* ablation on the maternally-inherited chromosome increases pup demand whilst limiting maternal supply. The effects of mutation in mother and pup are therefore opposite, producing a compensation effect. In a wild population, it is perhaps more relevant to think of *Grb10* allelic variation, rather than 'wild type' or '*Grb10KO*'. An allelic variant which suppresses nutrient supply is passed to offspring who, as a consequence of that same allelic variant, demand more nutrients in compensation. Expression of this allele from the maternal chromosome ensures that all future generations will continue to compensate a reduced supply with an increased demand. Thus, although *Peg3* and *Grb10* mutations in mother and pup produce complimentary and opposite effects, respectively, the outcome in both cases is increased mother-offspring coadaptation.

Grb10, like *Peg3*, is expressed in the hypothalamus (Smith *et al*, 2007; Garfield *et al*, submitted), and thus it is conceivable that the reduction in nutrient transfer observed in *Grb10KO*$^{m/+}$ mothers is a consequence of perturbed hypothalamic function. However, *Grb10* expression at this site is exclusively from the paternally-derived chromosome, both during development and adulthood (Figure 3.4). Thus, hypothalamic dysfunction is unlikely to be the basis for the observed phenotype.

The mechanism through which *Grb10* mediates nutrient supply via the mammary gland is unclear, but does not seem to be through the regulation of branching morphogenesis. An assessment of milk quality also suggested that this was not the physiological basis for a difference, although the influence of subtle variation, not detected in our approach, cannot be excluded. Many genes encoding milk proteins, including β-*casein* and *WAP*, are direct transcriptional targets of Stat5 (Happ and Groner, 1993; Wakao *et al*, 1994; Li and Rosen, 1995). Although not tested in mammary glands, Stat5 protein levels were unaffected by *Grb10* ablation in the placenta (Figure 5.12), suggesting Grb10 does not feed back to suppress the prolactin-Stat5-*Grb10* pathway. Changes in milk protein levels might not, therefore, have been expected. The result implied that milk letdown might be perturbed, such that the total volume of milk available to suckling offspring was reduced. This was assessed for *Peg3*$^{+/p}$ mutant mothers, by separating mother and pups for a fixed period, then recording weight change in both six hours after being reunited (Curley *et al*, 2004). A similar experiment should be performed for *Grb10KO*$^{m/+}$ mothers to confirm this inference.

We initially hypothesised that lactating *Grb10KO*$^{m/+}$ mothers would exhibit reduced levels of pituitary *Prolactin* expression relative to wild type controls, because of their poor provisioning. However, the opposite result was observed. This apparently paradoxical finding may actually help to pinpoint the physiological basis for the reduced nutrient supply of *Grb10KO*$^{m/+}$ mothers. Pups suckling from transgenic mothers, regardless of their own genotype, are unable to extract the nutrients they demand from the mammary gland. This might promote suckling for longer durations and/or more frequently. The physical act of suckling, through a neurological connection, promotes *Prolactin* expression in the pituitary gland of a lactating female (Callahan *et al*, 1996). The extent of PRL secretion is directly correlated with the intensity of the stimulus, as determined by the assessment of mothers suckling various litter sizes (Mena and Grosvenor, 1968). Thus, the likely increased suckling in pups raised by a *Grb10KO*$^{m/+}$ mother might cause elevated *Prolactin* expression in the mother's pituitary gland, presumably correlating with increased prolactin levels in the blood serum. The observation suggests that this neuroendocrine feedback loop is functioning adequately in *Grb10KO*$^{m/+}$ mothers, but the mammary glands are resistant to the increased levels of prolactin. This effect is not observed in wild type females raising more demanding *Grb10KO*$^{m/+}$ pups, at least at postnatal day 15. The increased demand presumably causes elevated *Prolactin* expression at first, but the wild type mammary gland responds by promoting milk synthesis and release. Pup demand is more closely matched, and thus pituitary *Prolactin* levels normalise again. It would be interesting to examine *Prolactin* expression in the pituitary glands of *Grb10KO*$^{m/+}$ mothers raising mixed litters; levels may be elevated beyond that seen in *Grb10KO*$^{m/+}$ mothers raising wild type pups, because the demand is increased still further. The prediction that pups suckle for longer or more frequently from a *Grb10KO*$^{m/+}$ mother could be tested by behavioural studies. Additionally, prolactin serum levels should be assayed to confirm that this correlates with gene expression.

Expression of *Growth hormone* did not alter between any of the experimental groups. GH is essential for correct pubertal development of the mammary glands, but a role in pregnancy-dependent gland development has not been defined. As such, GH acts as a

suitable control, confirming that the changes in *Prolactin* expression are probably not a consequence of a general hypothalamic or pituitary dysfunction.

Whilst this data suggests a physiological basis for the observed nutrient supply phenotype (i.e. mammary gland resistance to prolactin), the molecular control of this remains unclear. One mechanism for prolactin resistance might be reduced prolactin receptor (PRLR) expression. However, this appears unlikely as *Grb10KO*$^{m/+}$ mammary glands do not exhibit perturbed branching morphogenesis, a process under the influence of pituitary prolactin. Indeed, mice deficient for the prolactin receptor gene are infertile, whilst *Prlr*$^{+/-}$ mice still show an almost complete failure to lactate (Ormandy *et al*, 1997). Additionally, the levels of milk proteins, the expression of which are prolactin- and Stat5-dependent, are unaffected by *Grb10* ablation.

Recently, serotonin (5-HT) has been described as a paracrine/autocrine regulator of mammary gland homeostasis during lactation (Matsuda *et al*, 2004). 5-HT is secreted into milk, and thus the accumulation of milk in the mammary ducts also results in 5-HT accumulation (Stull *et al*, 2007). This molecule suppresses milk protein gene expression in epithelial cells (Matsuda *et al*, 2004). As *Grb10KO*$^{m/+}$ mammary glands are less effective at transferring nutrients to suckling offspring, yet do not exhibit a gross morphological perturbation, one hypothesis might be that 5-HT levels are altered. Indeed, this may even be the mechanism of resistance to prolactin. If *Grb10* ablation causes 5-HT levels to be increased, this would suppress milk production, but the relative levels of milk protein expression might not necessarily change, explaining the consistent levels of whey acidic protein, β-casein and others extracted from wild type and *Grb10KO*$^{m/+}$ milk. Additionally, elevated 5-HT levels would engender more rapid apoptosis, consistent with the observation that *Grb10KO*$^{m/+}$ glands exhibit a trend towards this.

If 5-HT levels are not the molecular basis for prolactin resistance, *Grb10KO*$^{m/+}$ glands might still be expected to display elevated 5-HT levels in response to milk stasis. Thus, examining 5-HT activity would not permit differentiation between the two effects, without further knowledge of the molecular interactions Grb10 is involved in in the mammary gland. Nonetheless, 5-HT levels should be investigated in wild type and *Grb10KO*$^{m/+}$ mammary glands, most easily achieved by assaying for *Tph1* transcript levels as a proxy.

Finally, as previously mentioned, *Grb10KO*$^{m/+}$ mammary glands exhibited a trend towards more rapid involution, although this did not reach statistical significance in the datasets examined. A more comprehensive analysis of involution should be performed, especially in light of the expectation of elevated 5-HT levels in transgenic glands; 5-HT promotes epithelial tight junction disruption, a key event in tissue remodelling (Stull *et al*, 2007; Pai and Horseman, 2008). In the current study, mammary glands were harvested 48 hours after a forced-wean, around the time of the transition from phase I to phase II, and assayed by TUNEL. This should be extended, initially by histological examination of glands at late gestation and at a range of involution stages. Glands isolated from mice deficient for the *Insulin-like growth factor binding protein 5* (*Igfbp5*) gene, for example, showed delayed involution, but a histological difference not observed until 6 days after a forced-wean, which correlated with an increase in TUNEL-positive nuclei (Ning *et al*, 2007).

The observation that *Grb10* is expressed in a pregnancy-dependent manner in the adult mammary gland, and retains its imprinted status, caused us to investigate the function of the gene in this tissue. The study revealed that *Grb10* promotes nutrient transfer from lactating female to offspring, but also that, in a demonstration of coadaptive traits, *Grb10* suppresses nutrient demand in suckling pups. In this manner, *Grb10* is important for the homeostatic control of offspring growth. An analysis of pituitary *Prolactin* expression in *Grb10KO*$^{m/+}$ mothers suggested that the neuroendocrine feedback loop, in response to the suckling stimulus, is functionally intact, but that the mammary gland is resistant to elevated pituitary *Prolactin* expression. The mechanism for the suppression of nutrient supply from *Grb10KO*$^{m/+}$ mammary glands remains elusive. The roles of *Grb10* as a supply promoter and demand suppressor are different to those in the placenta and embryo, in which *Grb10* suppresses supply, as well as demand. These apparently paradoxical observations are discussed with relevance to reproductive strategies in Chapter Seven.

Chapter Seven

Final discussion

Since the demonstration of the requirement for both parental genomes to permit successful embryonic development over 25 years ago (McGrath and Solter, 1983), and the discovery of the first imprinted gene 8 years later (DeChiara *et al*, 1991), the field of genomic imprinting has progressed and diversified rapidly. At the core of this research lie two key questions: 1) why has genomic imprinting evolved; and 2) how is genomic imprinting regulated? In the process of addressing the second of these questions, the new discipline of epigenetics has been spawned. We have subsequently realised that epigenetic modifications are not only important in the regulation of imprinted genes, but are in fact a crucial component of regulating expression throughout the genome. Additionally, epigenetic modifications appear to be fundamental in the regulation of stem cell pluripotency. The significance of these findings is illustrated by the recent drive to 'map' the epigenome, including genome-wide analyses of DNA methylation sites and histone modifications. This has revealed some intriguing global patterns. For example, whilst CpG islands have typically been associated with the control of gene expression and have been identified at many promoter regions, 55 % of CpG islands in the human genome are 'orphans', with no such association (Bird, 2009). Moreover, these orphans are overwhelmingly hypermethylated. That methyl-cytosine can spontaneously deaminate to thymine implies positive selection for the maintenance of these CpG islands, and thus a functional significance. The nature of this role is yet to be defined.

It is becoming increasingly apparent that many cancers arise through aberrant epigenetic regulation, both of imprinted and biallelically-expressed genes. As methylation is typically, although not universally, associated with transcriptional repression, one model is that the *de novo* methylation of CpG islands might silence tumour suppressor genes, and thus contribute to cancer progression (Bestor, 2009). This may provide possibilities for future therapeutic targets, and might aid our identification and staging of cancerous tissues. A study examining the methylation status of CpG islands at four tumour suppressor genes confirmed that 89 % of bladder cancer tumours analysed exhibited at least 20 % methylation at one or more of these loci, relative to almost a complete absence of methylation in control tissues (Salem *et al*, 2000). The stage of the tumour correlated with the number of loci simultaneously methylated, with several highly aggressive cancers demonstrating hypermethylation of all four markers.

Concurrent with this expansion of the epigenetics field has been the drive to understand why imprinted genes have evolved. Key to addressing this question is the elucidation of imprinted gene function. With this knowledge, we can hope to explain why positive selection for functional haploidy should exist. To-date, the most widely-accepted model is the parental conflict hypothesis (Haig and Westoby, 1989; Moore and Haig, 1991), but as discussed in previous chapters, this has some important limitations. There exists a tendency to generalise when discussing imprinted gene function and evolution, but perhaps we cannot account for all imprinted loci with a single explanation. Imprinting at one or two loci may have evolved for the reasons presented in the parental conflict hypothesis, for example, but the mechanism for regulating parent-of-origin specific gene expression might have subsequently been adopted for other roles.

The imprinted gene *Grb10* has some intriguing properties, and provides an excellent model with which to investigate imprinted gene function, and indeed, regulation. The most provocative of these features is the reciprocal imprint apparent between the central nervous system (CNS) and peripheral tissues, a system conserved in both mouse and human (Blagitko *et al*, 2000; Arnaud *et al*, 2003; Monk *et al*, 2009). Sanz *et al* (2008) have described how this reciprocal imprint is achieved at the epigenetic level, but the reasons for this pattern of monoallelic expression are still unclear. Our laboratory aims to address this important question by examining the *in vivo* functions of *Grb10*, by transmitting dysfunctional *Grb10* alleles separately through each parental line.

The first transgenic allele in which *Grb10* was ablated, *Grb10Δ2-4*, identified maternally-expressed *Grb10* as a potent foetal growth inhibitor and attenuator of insulin signalling in adulthood (Charalambous *et al*, 2003; Smith *et al*, 2007). However, the *LacZ* gene-trap introduced at the locus to generate the *Grb10Δ2-4* allele failed to report expression in the CNS of transgenic mice. To address this shortcoming, a second transgenic mouse line, *Grb10KO*, was created. The *LacZ* gene-trap in this allele successfully reported CNS expression, but only when transmitted through the paternal lineage. The function of *Grb10* in this organ was associated with the tempering of social dominance, a role independent of maternally-expressed *Grb10* in peripheral tissues (Garfield, 2007; Garfield *et al*, submitted).

The present study was initiated by characterising the *Grb10KO* allele at the genetic level, and confirming its efficacy in the ablation of full-length *Grb10*. This process identified a phenotypic inconsistency between transgenic mice harbouring the *Grb10KO* and *Grb10Δ2-4* alleles; the former was homozygous lethal during embryonic development, whilst *Grb10Δ2-4*$^{m/p}$ animals were viable. The genetic mapping of *Grb10KO* provided a possible explanation for this effect, although further investigation is required to confirm this.

With a detailed knowledge of the structure of the two transgenic alleles, we were able to hypothesise on why *Grb10Δ2-4*$^{+/p}$ animals failed to report expression in the CNS. This led to the identification of a short conserved sequence at the *Grb10* locus, which exhibited properties of an enhancer element. In an *in vitro* luciferase assay, we demonstrated that this sequence could promote reporter gene expression in the presence of constitutively active Stat5b, consistent with the identification of sequences within the putative enhancer with high similarity to the Stat5 consensus recognition site. The expression profile of *Stat5b* was very similar to that of *Grb10* in the adult mouse brain. That the putative enhancer element is absent from the *Grb10Δ2-4* allele suggested that the failure to detect *LacZ* transcription in the CNS of *Grb10Δ2-4*$^{+/p}$ animals was likely to be a consequence of Stat5b being unable to bind at the locus and promote gene transcription.

Intriguingly, a previous study, working with mammary epithelial cell culture, alluded to an interaction between Stat5 and *Grb10* at the transcriptional level (Clarkson *et al*, 2006). We demonstrated that whilst strong reporter expression was detected in the mammary glands of *Grb10KO*$^{m/+}$ females, no detectable expression was observed in *Grb10Δ2-4*$^{m/+}$ glands, reminiscent of the difference in the CNS, and supportive of a Stat5-*Grb10* interaction in this tissue. Importantly, reporter expression, under the control of the endogenous *Grb10* promoter, was pregnancy-dependent and confined to epithelial cells. This suggested that

Grb10 activation was under the control of prolactin. Whilst the downstream effects of growth hormone can also be transduced through Stat5, the stroma, rather than the epithelium, is the target cell type of this hormone in the mammary gland.

The observation that the imprinted status of *Grb10* expression in the mammary epithelium was retained is particularly intriguing. This is the first description of a tissue in which *Grb10* is activated in adulthood, and is thus inconsistent with conflict theory. With this in mind, we examined the function of the gene in this tissue, using postnatal pup growth as an endpoint measure. To differentiate between the influences of mother and pup genotype, a cross-fostering study was performed, with relevant controls. This extended our understanding of the role of maternally-expressed *Grb10* in the regulation of growth. We clearly demonstrated that *Grb10* ablation enhances postnatal pup nutrient demand and restricts maternal supply, implying that one function of *Grb10* is to mediate a supply/demand system. As such, *Grb10* is a demand suppressor and supply promoter during the suckling period. This contrasts with the role of maternally-expressed *Grb10* in the placenta; work in the present study, as well as studies published previously (Charalambous *et al*, 2003; Charalambous *et al*, submitted), identify *Grb10* as a supply and demand suppressor *in utero*. At first glance, these interpretations might seem paradoxical. However, they hint at a wider role for *Grb10* in the control of reproductive strategy.

Reproductive success can be defined as the number of pregnancies a female can sustain together with successful weaning of those offspring (Keverne and Curley, 2008). A gene, or an allelic variant of a gene, will always be positively-selected if it promotes self-propagation. Thus, the investment of too many resources in a single litter will be to the detriment of the future reproductive success, and therefore gene propagation, of the mother, an assumption upon which conflict theory is based. Whilst it is important to provision offspring adequately to promote gene propagation, there exists a trade-off between resource allocation and litter number. This explains why natural selection does not favour an ever-increasing animal size or maternal investment. Human studies have demonstrated that children with an intermediate birth weight have the highest fitness levels (Sansing and Chinnici, 1976).

Although experimental manipulations show clearly that maternally-expressed *Grb10* restricts foetal growth, it is perhaps more valuable to consider *Grb10* as part of the mechanism maintaining optimal fitness. *Grb10*, expressed from the maternally-inherited chromosome in the placenta and foetus, prevents embryos becoming 'too large' and 'too demanding', promoting their mother's lifetime reproductive success. There is also a risk of death or injury with giving birth to large offspring (Zhang *et al*, 2008), suggesting that natural selection would also favour a reduced embryo size for this reason. The function of *Grb10* as a supply and demand suppressor *in utero* can thus easily be rationalised.

After birth, the role of *Grb10* is to continue to maintain optimal fitness. It prevents pups from demanding 'too much' maternal provisioning, whilst enabling the mother to match supply with demand. This was exquisitely demonstrated by the impaired growth of wild type pups in a pure wild type litter when raised by a *Grb10KO*$^{m/+}$ mother, relative to a wild type mother. As discussed in Chapter Six, *Grb10* demonstrates pleiotropic effects in mother

and offspring, promoting their coadaptation. Whilst the ablation of maternal *Grb10* in both mother and offspring resulted in pup overgrowth on the day of birth, the mother was able to respond by restricting postnatal nutrient supply and normalising pups to wild type weight.

Foetal programming is intimately coupled to optimal fitness. Such programming describes how the conditions to which embryos are exposed *in utero* can influence metabolism in adulthood. This has implications for the understanding of predispositions to human diseases, such as type 2 diabetes and cardiovascular disease (reviewed in Le Clair *et al*, 2009; Jones and Ozanne, 2009). There is also clear evidence that the influence of the postnatal environment is important in future fitness. Lactating female rats receiving diluted ethanol to drink instead of water secrete ethanol in their milk. This has been shown to have dramatic effects on hypothalamic development of suckling offspring, and subsequent hypothalamic function (Klintsova *et al*, 2007), as well as overall growth (Murillo-Fuentes *et al*, 2001). Perinatal undernutrition in humans compromises cognitive development and growth, and increases the risk of chronic adulthood diseases (Prost, 2009). Such effects will ultimately compromise the ability of offspring to breed, and by definition, will decrease their fitness. It would be interesting to examine the body compositions and metabolic states of the pups reared in the cross-fostering study. For example, the *Grb10KO*$^{m/+}$ pups raised by wild type mothers were considerably overgrown at the end of the experimental period; does this overgrowth correlate with an increased fat mass or lean mass? The ratio of fat:lean tissue may influence susceptibility to insulin intolerance, such that a 'fatty' mouse might acquire a diabetic-like state in adulthood. This could be assessed by dual X-ray absorptiometry. Other developmental processes might be perturbed, such as the time at which the pups enter puberty. This would have a considerable effect on the number of litters it may be possible to raise in a lifetime, especially for females, affecting fitness. Wild type pups raised by *Peg3*$^{+/p}$ mothers enter puberty significantly later than controls (Curley *et al*, 2004).

In the case of *Grb10*, its contribution to the maintenance of optimal fitness is achieved by influencing coadaptive traits in mother and offspring. As discussed in Chapter Six, genes with pleiotropic effects, influencing such coadaptive traits, are favoured by selection to become imprinted (Wolf and Hager, 2006). Perhaps imprinting initially arose at the *Grb10* locus for reasons consistent with the conflict theory, regulating embryonic growth. The mechanism might have been adopted for *Grb10* expression in the mammary gland; the consequential increased coadapativeness of mother and offspring would have promoted rapid fixation of the imprinting status in the population. Indeed, the evolution of *Grb10* as a prolactin/Stat5-dependent gene is particularly intriguing, given that the Stat5 binding site is conserved in chicken, an organism which does not demonstrate imprinting nor does it possess mammary glands. Nonetheless, chickens do secrete PRL, which, through Stat5-mediated signalling, is involved in egg production and regulation of the immune system (Skwarlo-Sońta, 1992; Cui *et al*, 2006). PRL involvement in the immune system is conserved in mammals. Whilst it is not clear if *Grb10* is also a downstream target of PRL in lymphocytes, it might explain the evolution of a Stat5 binding site at the *Grb10* locus in chicken, which was retained in mammals and permitted diversification of *Grb10* function.

Perhaps the growth functions of *Grb10* are specific to mammals, and thus correlate with the evolution of imprinting; preliminary data on the functions of the zebrafish *Grb10* orthologs support this hypothesis (Lee, Ward and Kelsh, unpublished data). To help dissect the evolutionary origins of PRL/Stat5-dependent *Grb10* expression, it would be interesting to examine *Grb10* expression and regulation in mouse lymphocytes. Thus, whilst Stat5-mediated *Grb10* expression has been implicated in brain, mammary gland and placenta in the current study, we cannot rule out other tissues in which this system operates.

It is interesting that PRL/Stat5 signalling might represent one of the pathways responsible for *Grb10* expression in the placenta. Unpublished data from our laboratory suggests that much of the foetal growth effects of *Grb10* may be mediated through the *Dlk1* signalling pathway (Madon, Cowley, Garfield and Ward, unpublished data), but this appears not to be the case for the placenta. PRL/Stat5 signalling could account for some of the placental growth effects, perhaps acting in concert with *Dlk1* signalling. The potential for the Grb7 superfamily proteins to mediate cross-talk between signalling pathways has been noted previously (Riedel, 2004). In support of this, deletion of the Stat5 binding site *in vivo*, using the *Grb10Δ2-4* mouse strain, did not abolish *Grb10* expression in the placenta entirely, suggesting the presence of the Stat5 binding site is necessary to achieve correct transcript levels but is not absolutely required for *Grb10* transcription. This is reminiscent of previous observations in the brains of *Grb10Δ2-4*$^{+/p}$ animals (Garfield, 2007).

The *Grb10*-mediated mechanisms maintaining optimal fitness, both *in utero* and postnatally, require further investigation. Previous studies of the placenta had demonstrated that *Grb10* limits labyrinthine volume (Charalambous *et al*, submitted). The present study suggested that this might be a specific restriction of foetal vascularisation, thereby controlling the surface area available for nutrient exchange. Whilst this fits comfortably with the roles of Grb10 as an attenuator of cell proliferation, the molecular pathways through which this is achieved are not clear. Similarly, the mechanism through which *Grb10* regulates nutrient supply in a lactating female is unclear. Perturbed pituitary gland function may be the basis for the reduced provisioning of *Grb10KO*$^{m/+}$ females, but the elevated levels of PRL synthesis in response to pup suckling argues against this, although it would be interesting to examine the levels of PRL synthesis in virgin wild type and *Grb10KO*$^{m/+}$ females as a control. Instead, the data suggests that the provisioning deficiency may be a consequence of mammary gland insensitivity to PRL. No gross morphological perturbations were observed in *Grb10KO*$^{m/+}$ glands, although it is not possible to exclude the influence of subtle effects. Milk quality does not appear to be the physiological basis for the phenotype, inferring that milk letdown may be impaired. Dissecting the molecular mechanism for this effect could begin with an analysis of circulating oxytocin levels in the serum of lactating females, and an assessment of 5-HT accumulation in the glands, as discussed in Chapter Six.

Although there is currently no experimental evidence to support this, it is conceivable that *Grb10* ablation in the placenta affects mammary gland function. As discussed previously, hormone release from the placenta is fundamental for the preparation of the mother for lactation, stimulating mammary gland branching morphogenesis and promoting maternal

care behaviours (Thordarson *et al*, 1986; Bridges *et al*, 1996). Stimulation of these physiological processes might be impaired by the *Grb10KO*$^{m/+}$ placenta, possibly as a mechanism to compensate for increased foetal size, thus normalising postnatal pup weight to that of wild type animals, improving fitness. This argument would be equally applicable to natural allelic variants of the *Grb10* gene. Experimental assessment of this possibility would be challenging, especially in the knowledge that *Grb10KO*$^{m/+}$ mammary gland morphology is not obviously perturbed. Serum levels of placental lactogens in gravid females could be examined as a starting point.

Although the imprinted status of *Grb10* was revealed over ten years ago (Miyoshi *et al*, 1998), the intricacies of its functions and regulation ensure it continues to be a dynamic and exciting gene on which to work. Although not expected at the outset, this study has revealed an important facet to the function of *Grb10* as a growth regulator, which may have implications for understanding why *Grb10*, and perhaps other genes, are imprinted. At present, nothing is known of the imprinted status of other genes in the adult mammary gland, and this may represent an exciting area of future investigation.

References

Aapola, U., Kawasaki, K., Scott, H.S., Ollila, J., Vihinen, M., Heino, M., Shintani, A., Kawasaki, K., Minoshima, S., Krohn, K., Antonarakis, S.E., Shimizu, N., Kudoh, J., Peterson, P. (2000) Isolation and initial characterization of a novel zinc finger gene, DNMT3L, on 21q22.3, related to the cytosine-5-methyltransferase 3 gene family. *Genomics*. 65(3):293-8.

Advani, A.S., Pendergast, A.M. (2002) Bcr-Abl variants: biological and clinical aspects. *Leukemia Research*. 26(8):713-20.

Antonellis, A., Bennett, W.R., Menheniott, T.R., Prasad, A.B., Lee-Lin, S.Q., NISC Comparative Sequencing Program, Green, E.D., Paisley, D., Kelsh, R.N., Pavan, W.J., Ward, A. (2006) Deletion of long-range sequences at Sox10 compromises developmental expression in a mouse model of Waardenburg-Shah (WS4) syndrome. *Human Molecular Genetics*. 15(2):259-71.

Arnaud, P., Hata, K., Kaneda, M., Li, E., Sasaki, H., Feil, R., Kelsey, G. (2006) Stochastic imprinting in the progeny of Dnmt3L$^{-/-}$ females. *Human Molecular Genetics*. 15(4):589-98.

Arnaud, P., Monk, D., Hitchins, M., Gordon, E., Dean, W., Beechey, C.V., Peters, J., Craigen, W., Preece, M., Stanier, P., Moore, G.E., Kelsey, G. (2003) Conserved methylation imprints in the human and mouse GRB10 genes with divergent allelic expression suggests differential reading of the same mark. *Human Molecular Genetics*. 12(9):1005-19.

Arney, K.L. (2003) H19 and Igf2 – enhancing the confusion? *Trends in Genetics*. 19(1):17-23.

Babak, T., DeVeale, B., Armour, C., Raymond, C., Cleary, M.A., van der Kooy, D., Johnson, J.M., Lim, L.P. (2008) Global survey of genomic imprinting by transcriptome sequencing. *Current Biology*. 18:1735-1741.

Bai, R.Y., Jahn, T., Schrem, S., Munzert, G. Weidner, K.M., Wang, J.Y., Duyster, J. (1998) The SH2-containing adapter protein GRB10 interacts with BCR-ABL. *Oncogene*. 17(8):941-8.

Bai, T., Luoh, S.W. (2008) GRB-7 facilitates HER-2/Neu-mediated signal transduction and tumor formation. *Carcinogenesis*. 29(3):473-9.

Bao, L., Tessier, C., Prigent-Tessier, A., Li, F., Buzzio, O.L., Callegari, E.A., Horseman, N.D., Gibori, G. (2007) Decidual prolactin silences the expression of genes detrimental to pregnancy. *Endocrinology*. 148(5):2326-34.

Barlow, D.P., Stöger, R., Herrmann, B.G., Saito, K., Schweifer, N. (1991) The mouse insulin-like growth factor type-2 receptor is imprinted and closely linked to the Tme locus. *Development*. 128(10):1881-7.

Barton, S.C., Surani, M.A., Norris, M.L. (1984) Role of paternal and maternal genomes in mouse development. *Nature*. 311(5984):374-6.

Basham, B., Sathe, M., Grein, J., McClanahan, T., D'Andrea, A., Lees, E., Rascle, A. (2008) In vivo identification of novel STAT5 target genes. *Nucleic Acids Research*. 36(11):3802-18.

Beigneux, A.P., Vergnes, L., Qiao, X., Quatela, S., Davis, R., Watkins, S.M., Coleman, R.A., Walzem, R.L., Philips, M., Reue, K., Young, S.G. (2006) Agpat6 – a novel lipid biosynthetic gene required for triacylglycerol production in mammary epithelium. *Journal of Lipid Research*. 47(4):734-44.

Bell, A.C., Felsenfeld, G. (2000) Methylation of a CTCF-dependent boundary controls imprinted expression of the Igf2 gene. *Nature*. 405(6785):482-5.

Benton, M.J., Donoghue, P.C. (2007) Paleontological evidence to date the tree of life. *Molecular Biology and Evolution*. 24(1):26-53.

Bérézíat, V., Kasus-Jacobi, A., Perdereau, D., Cariou, B., Girard, J., Burnol, A.F. (2002) Inhibition of insulin receptor catalytic activity by the molecular adapter Grb14. *The Journal of Biological Chemistry*. 277(7):4845-52.

Bestor, T. (2009) Cytosine methylation and mammary carcinoma. *Conference abstract, From Imprinting to the Epigenome in 25 Years, Cambridge, UK*.

Bird, A. (2009) Simplifying the genome via DNA methylation and CpG islands. *Conference abstract, From Imprinting to the Epigenome in 25 Years, Cambridge, UK*.

Bischof, J.M., Stewart, C.L., Wevrick, R. (2007) Inactivation of the mouse Magel2 gene results in growth abnormalities similar to Prader-Willi syndrome. *Human Molecular Genetics*. 16:2713-19.

Blagitko, N., Mergenthaler, S., Schulz, U., Wollmann, H.A., Craigen, W., Eggermann, T., Ropers, H.H., Kalscheuer, V.M. (2000) Human GRB10 is imprinted and expressed from the paternal and maternal allele in a highly tissue- and isoform-specific fashion. *Human Molecular Genetics*. 9(11):1587-95.

Blake, J.A., Thomas, M., Thompson, J.A., White, R., Ziman, M. (2008) Perplexing Pax: from puzzle to paradigm. *Developmental Dynamics*. 237:2791-803.

Blanchette, M., Bataille, A.R., Chen, X., Poitras, C., Laganière, J., Lefèbvre, C., Deblois, G., Giguère, V., Ferretti, V., Bergeron, D., Coulombe, B., Robert, F. (2006) Genome-wide computational prediction of transcriptional regulatory modules reveals new insights into human gene expression. *Genome Research*. 16(5):656-68.

Blum, D., Dorchy, H., Mouraux, T., Vamos, E., Mardens, Y., Kumps, A., De Prez, C., Heimann, P., Fowler, B., Baumgartner, R. (1993) Congenital absence of insulin cells in a neonate with diabetes mellitus and mutase-deficient methylmalonic acidaemia. *Diabetologia*. 36(4):352-7.

Bonnette, S.G., Hadsell, D.L. (2001) Targeted disruption of the IGF-I receptor gene decreases cellular proliferation in mammary terminal end buds. *Endocrinology*. 142(11):4937-45.

Bourc'his, D., Xu, G.L., Lin, C.S., Bollman, B., Bestor, T.H. (2001) Dnmt3L and the establishment of maternal genomic imprints. *Science*. 294(5551):2536-9.

Bridges, R.S., Robertson, M.C, Shiu, R.P., Friesen, H.G., Stuer, A.M., Mann, P.E. (1996) Endocrine communication between conceptus and mother: placental lactogen stimulation of maternal behaviour. *Neuroendocrinology.* 64(1):57-64.

Brisken, C., Park, S., Vass, T., Lydon, J.P., O'Malley, B.W., Weinberg, R.A. (1998) A paracrine role for the epithelial progesterone receptor in mammary gland development. *Proceedings of the National Academy of Sciences of the United States of America*. 95(9):5076-81.

Brown, K.W., Villar, A.J., Bickmore, W., Clayton-Smith, J., Catchpoole, D., Maher, E.R., Reik, W. (1996) Imprinting mutation in the Beckwith-Wiedemann syndrome leads to biallelic IGF2 expression through an H19-independent pathway. *Human Molecular Genetics*. 5(12):2027-32.

Butler, M.G., Bittel, D.C. (2007) Plasma obestatin and ghrelin levels in subjects with Prader-Willi syndrome. *American Journal of Medical Genetics*. 143A:415-21.

Callahan, P., Baumann, M.H., Rabii, J. (1996) Inhibition of tuberoinfundibular dopaminergic neural activity during suckling: involvement of mu and kappa opiate receptor subtypes. *Journal of Neuroendocrinology*. 8(10):771-6.

Cao, X.R., Lill, N.L., Boase, N., Shi, P.P., Croucher, D.R., Shan, H., Qu, J., Sweezer, E.M., Place, T., Kirby, P.A., Daly, R.J., Kumar, S., Yang, B. (2008) Nedd4 controls animal growth y regulating IGF-1 signalling. *Science Signalling*. 1(38):ra5.

Carlson, L.L., Page, A.W., Bestor, T.H. (1992) Properties and localization of DNA methyltransferase in preimplantation mouse embryos: implications for genomic imprinting. *Genes & Development*. 6(12B):2536-41.

Caron, M.G., Beaulieu, M., Raymond, V., Gagné, B., Drouin, J., Lefkowitz, R.J., Labrie, F. (1978) Dopaminergic receptors in the anterior pituitary gland. Correlation of [3H]dihydroergocryptine binding with the dopaminergic control of prolactin release. *The Journal of Biological Chemistry*. 253(7):2244-53.

Cassidy, S.B., Driscoll, D.J. (2009) Prader-Willi syndrome. *European Journal of Human Genetics*. 17(1):3-13.

Caterina, J.J., Donze, D., Sun, C.W., Ciavatta, D.J., Townes, T.M. (1994) Cloning and functional characterisation of LCR-F1: a bZIP transcriptional factor that activates erythroid-specific, human globin gene expression. *Nucleic Acids Research*. 22(12):2383-91.

Cattanach, B.M. (1986) Parental origin effects in mice. *Journal of Embryology and Experimental Morphology.* 97 suppl:137-50.

Cattanach, B.M., Beechey, C.V., Rasberry, R., Jones, J., Papworth, D. (1996) Time of initiation and site of action of the mouse chromosome 11 imprinting effects. *Genetical Research*. 68(1):35-44.

Cattanach, B.M., Kirk, M. (1985) Differential activity of maternally and paternally derived regions in mice. *Nature*. 315:496-498.

Cattanach, B.M., Moseley, H. (1973) Nondisjunction and reduced fertility caused by the tobacco mouse metacentric chromosomes. *Cytogenetics and Cell Genetics*. 12(4):264-87.

Chamberlain, S.J., Johnstone, K.A., DuBose, A.J., Simon, T.A., Bartolomei, M.S., Resnick, J.L., Brannan, C.I. (2004) Evidence for genetic modifiers of postnatal lethality in PWS-IC deletion mice. *Human Molecular Genetics*. 13:2971-77.

Chan, L.C., Karhi, K.K., Rayter, S.I., Heisterkamp, N., Eridani, S., Powles, R., Lawler, S.D., Groffen, J., Foulkes, J.G., Greaves, M.F. (1987) A novel abl protein expressed in Philadelphia chromosome positive acute lymphoblastic leukaemia. *Nature*. 325(6105):635-7.

Charalambous, M., Cowley, M., Geoghegan, F., Smith, F.M., Radford, E.J., Marlow, B.P., Graham, C.F., Hurst, L.D., Ward, A. Maternally-inherited Grb10 reduces placental size and efficiency. *Submitted*.

Charalambous, M., Menheniott, T.R., Bennett, W.R., Kelly, S.M., Dell, G., Dandolo, L., Ward, A. (2004) An enhancer element at the Igf2/H19 locus drives gene expression in both imprinted and non-imprinted tissues. *Developmental Biology*. 271(2):488-97.

Charalambous, M., Smith, F.M., Bennett, W.R., Crew, T.E., Mackenzie, F., Ward, A. (2003) Disruption of the imprinted Grb10 gene leads to disproportionate overgrowth by an Igf2-independent mechanism. *Proceedings of the National Academy of Sciences of the United States of America*. 100(14):8292-7.

Chen, J., Sadowski, H.B., Kohanski, R.A., Wang, L.H. (1997) Stat5 is a physiological substrate of the insulin receptor. *Proceedings of the National Academy of Sciences of the United States of America*. 94(6):2295-300.

Chen, M., Gavrilova, O., Liu, J., Xie, T., Deng, C., Nguyen, A.T., Nackers, L.M., Lorenzo, J., Shen, L., Weinstein, L.S. (2005) Alternative Gnas gene products have opposite effects on glucose and lipid metabolism. *Proceedings of the National Academy of Sciences of the United States of America*. 102:7386-7391.

Cheutin, T., McNairn, A.J., Jenuwein, T., Gilbert, D.M., Singh, P.B., Misteli, T. (2003) Maintenance of stable heterochromatin domains by dynamic HP1 binding. *Science*. 299(5607):721-5.

Choi, Y.S., Chakrabarti, R., Escamilla-Hernandez, R., Sinha, S. (2009) Elf5 conditional knockout mice reveal its role as a master regulator in mammary alveolar development: failure of Stat5 activation and functional differentiation in the absence of Elf5. *Developmental Biology*. 329(2):227-41.

Chow, J., Heard, E. (2009) X inactivation and the complexities of silencing a sex chromosome. *Current Opinion in Cell Biology*. 21(3):359-66.

Chu, P.Y., Huang, L.Y., Hsu, C.H., Liang, C.C., Guan, J.L., Hung, T.H., Shen, T.L. (2009) Tyrosine phosphorylation of growth factor receptor-bound protein-7 by focal adhesion kinase in the regulation of cell migration, proliferation, and tumorigenesis. *The Journal of Biological Chemistry*. 284(30):20215-26.

Chuang, L.S., Ian, H.I., Koh, T.W., Ng, H.H., Xu, G., Li, B.F. (1997) Human DNA-(cytosine-5) methyltransferase-PCNA complex as a target for p21WAF1. *Science*. 277(5334):1996-2000.

Ciani, E., Hoffmann, A., Schmidt, P., Journot, L., Spengler, D. (1999) Induction of the PAC1-R (PACAP-type I receptor) gene by p53 and Zac. *Brain Research: Molecular Brain Research*. 69(2):290-4.

Clarkson, R.W., Boland, M.P., Kritikou, E.A., Lee, J.M., Freeman, T.C., Tiffen, P.G., Watson, C.J. (2006) The genes induced by signal transducer and activators of transcription (STAT)3 and STAT5 in mammary epithelial cells define the roles of these STATs in mammary development. *Molecular Endocrinology*. 20(3):675-85.

Clarkson, R.W., Watson, C.J. (2003) Microarray analysis of the involution switch. *Journal of Mammary Gland Biology and Neoplasia*. 8(3):309-19.

Coan, P.M., Angiolini, E., Sandovici, I., Burton, G.J., Constância, M., Fowden, A.L. (2008) Adaptations in placental nutrient transfer capacity to meet fetal growth demands depend on placental size in mice. *The Journal of Physiology*. 586(18):4567-76.

Coan, P.M., Ferguson-Smith, A.C., Burton, G.J. (2004) Developmental dynamics of the definitive mouse placenta assessed by stereology. *Biology of Reproduction*. 70(6):1806-13.

Constância, M., Angiolini, E., Sandovici, I., Smith, P., Smith, R., Kelsey, G., Dean, W., Ferguson-Smith, A., Sibley, C.P., Reik, W., Fowden, A. (2005) Adaptation of nutrient supply to fetal demand in the mouse involves interaction between the Igf2 gene and placental transporter systems. *Proceedings of the National Academy of Sciences of the United States of America*. 102(52):19219-24.

Constância, M., Dean, W., Lopes, S., Moore, T., Kelsey, G., Reik, W. (2000) Deletion of a silencer element in Igf2 results in loss of imprinting independent of H19. *Nature Genetics*. 26(2):203-6.

Constância, M., Hemberger, M., Hughes, J., Dean, W., Ferguson-Smith, A., Fundele, R., Stewart, F., Kelsey, G., Fowden, A., Sibley, C., Reik, W. (2002) Placental-specific IGF-II is a major modulator of placental and fetal growth. *Nature*. 417(6892):945-8.

Cooney, G.J., Lyons, R.J., Crew, A.J., Jensen, T.E., Molero, J.C., Mitchell, C.J., Biden, T.J., Ormandy, C.J., James, D.E., Daly, R.J. (2004) Improved glucose homeostasis and enhanced insulin signalling in Grb14-deficient mice. *The EMBO Journal*. 23(3):582-93.

Crick, F. (1958) On protein synthesis. *Symposia for the Society of Experimental Biology: The Biological Replication of Macromolecules*. 12:152-3.

Cross, J.C., Baczyk, D., Dobric, N., Hemberger, M., Hughes, M., Simmons, D.G., Yamamoto, H., Kingdom, J.C.P. (2003) Genes, development and evolution of the placenta. *Placenta*. 24:123-130.

Crossland, J., Lewandowski, A. (2006) *Peromyscus* – a fascinating laboratory animal model. *Techtalk*. 11:1-2.

Crouse, H.V. (1971) Chromosome inheritance and the problem of chromosome 'imprinting' in *Sciara* (*Sciaridea diptera*). *Chromosoma*. 34:324-338.

Cui, J.X., Du, H.L., Liang, Y., Deng, X.M., Li, N., Zhang, X.Q. (2006) Association of polymorphisms in the promoter region of chicken prolactin with egg production. *Poultry Science*. 85(1):26-31.

Cunha, G.R., Young, P., Christov, K., Guzman, R., Nandi, S., Talamantes, F., Thordarson, G. (1995) Mammary phenotypic expression induced in epidermal cells by embryonic mammary mesenchyme. *Acta Anatomica*. 152(3):195-204.

Curley, J.P., Barton, S., Surani, A., Keverne, E.B. (2004) Coadaptation in mother and infant regulated by a paternally expressed imprinted gene. *Proceedings of the National Academy of Sciences of the United States of America*. 271(1545):1303-9.

Daly, R.J., Sanderson, G.M., Janes, P.W., Sutherland, R.L. (1996) Cloning and characterization of GRB14, a novel member of the GRB7 gene family. *The Journal of Biological Chemistry.*271(21):12502-10.

da Rocha, S.T., Charalambous, M., Lin, S.P., Gutteridge, I., Ito, Y., Gray, D., Dean, W., Ferguson-Smith, A.C. (2009) Gene dosage effects of the imprinted delta-like homologue 1 (dlk1/pref1) in development: implications for the evolution of imprinting. *PLoS Genetics*. 5(2):e1000392.

Davies, S.J., Hughes, H.E. (1993) Imprinting in Albright's hereditary osteodystrophy. *Journal of Medical Genetics*. 30:101-3.

Davies, W., Lynn, P.M.Y., Relkovic, D., Wilkinson, L.S. (2008) Imprinted genes and neuroendocrine function. *Frontiers in Neuroendocrinology*. 29:413-427.

DeChiara, T.M., Robertson, E.J., Efstratiadis, A. (1991) Parental imprinting of the mouse insulin-like growth factor II gene. *Cell*. 64:49-59.

Deng, Y., Bhattacharya, S., Swamy, O.R., Tandon, R., Wang, Y., Janda, R., Riedel, H. (2003) Growth factor receptor-binding protein 10 (Grb10) as a partner of phosphatidylinositol 3-kinase in metabolic insulin action. *The Journal of Biological Chemistry*. 278(41):39311-22.

Depetris, R.S., Wu, J., Hubbard, S.R. (2009) Structural and functional studies of the Ras-associating and pleckstrin-homology domains of Grb10 and Grb14. *Nature Structural & Molecular Biology*. 16(8):833-9.

Doe, C.M., Relkovic, D., Garfield, A.S., Dalley, J.W., Theobald, D.E., Humby, T., Wilkinson, L.S., Isles, A. (2009) Loss of the imprinted snoRNA mbii-52 leads to increased 5htr2c pre-RNA editing and altered 5HT2CR-mediated behaviour. *Human Molecular Genetics*. 18(12):2140-8.

Dong, L.Q., Du, H., Porter, S.G., Kolakowski, L.F. Jr., Lee, A.V., Mandarino, L.J., Fan, J., Yee, D., Liu, F. (1997a) Cloning, chromosome localization, expression and characterization of an Src homology 2 and pleckstrin homology domain-containing insulin receptor binding protein hGrb10gamma. *The Journal of Biological Chemistry*. 272(46):29104-12.

Dong, L.Q., Farris, S., Christal, J., Liu, F. (1997b) Site-directed mutagenesis and yeast two-hybrid studies of the insulin and insulin-like growth factor-1 receptors: the Src homology-2 domain-containing protein hGrb10 binds to the autophosphorylated tyrosine residues in the kinase domain of the insulin receptor. *Molecular Endocrinology*. 11(12):1757-65.

Drew, H.R., Travers, A.A. (1985) DNA bending and its relation to nucleosome positioning. *Journal of Molecular Biology*. 186(4):773-90.

Drewell, R.A., Brenton, J.D., Ainscough, J.F., Barton, S.C., Hilton, K.J., Arney, K.L., Dandolo, L., Surani, M.A. (2000) Deletion of a silencer element disrupts H19 imprinting independently of a DNA methylation epigenetic switch. *Development*. 127(16):3419-28.

Eblaghie, M.C., Song, S.J., Kim, J.Y., Akita, K., Tickle, C., Jung, H.S. (2004) Interactions between FGF and Wnt signals and Tbx3 gene expression in mammary gland initiation in mouse embryos. *Journal of Anatomy*. 205(1):1-13.

Eggenschwiler, J., Ludwig, T., Fisher, P., Leighton, P.A., Tilghman, S.M., Efstratiadis, A. (1997) Mouse mutant embryos overexpressing IGF-II exhibit phenotypic features of the Beckwith-Wiedemann and Simpson-Golabi-Behmel syndromes. *Genes & Development*. 11(23):3128-42.

Farris, S.D., Rubio, E.D., Moon, J.J., Gombert, W.M., Nelson, B.H., Krumm, A. (2005) Transcription-induced chromatin remodelling at the c-myc gene involves the local exchange of histone H2A.Z. *The Journal of Biological Chemistry*. 280(26):25298-303.

Feil, R., Berger, F. (2007) Convergent evolution of genomic imprinting in plants and mammals. *Trends in Genetics*. 23(4):192-9.

Festenstein, R., Pagakis, S.N., Hiragami, K., Lyon, D., Verreault, A., Sekkali, B., Kioussis, D. (2003) Modulation of heterochromatin protein 1 dynamics in primary mammalian cells. *Science*. 299(5607):719-21.

Fisher, M.E., Clelland, A.K., Bain, A., Baldock, R.A., Murphy, P., Downie, H., Tickle, C., Davidson, D.R., Buckland, R.A. (2008) Integrating technologies for comparing 3D gene expression domains in the developing chick limb. *Developmental Biology*. 317(1):13-23.

Foltz, D.W. (1981) Genetic evidence for long-term monogamy in a small rodent, *Peromyscus polionotus*. *American Naturalist*. 117:665-75.

Fowden, A.L. (1997) Comparative aspects of fetal carbohydrate metabolism. *Equine Veterinary Journal*. 24(Supplement):19-25.

Fowden, A.L., Ward, J.W., Wooding, F.P.B., Forhead, A.J., Constância, M. (2006) Programming placental nutrient transport capacity. *Journal of Physiology*. 572(1):5-15.

Frank, D., Fortino, W., Clark, L., Musalo, R., Wang, W., Saxena, A., Li, C.M., Reik, W., Ludwig, T., Tycko, B. (2002) Placental overgrowth in mice lacking the imprinted gene Ipl. *Proceedings of the National Academy of Sciences of the United States of America*. 99(11):7490-5.

Frantz, J.D., Giorgetti-Peraldi, S., Ottinger, E.A., Shoelson, S.E. (1997) Human GRB10-IRbeta/GRB10: splice variants of an insulin and growth factor receptor-binding protein with PH and SH2 domains. *The Journal of Biological Chemistry*. 272(5):2659-67.

Freeman, M.E., Kanyicska, B., Lerant, A., Nagy, G. (2000) Prolactin: structure, function, and regulation of secretion. *Physiological Reviews*. 80(4):1523-631.

Freemark, M. (2006) Regulation of maternal metabolism by pituitary and placental hormones: roles in fetal development and metabolic programming. *Hormone Research*. 65(Supplement 3):41-49.

Gallego, M.I., Binart, N., Robinson, G.W., Okagaki, R., Coschigano, K.T., Perry, J., Kopchick, J.J., Oka, T., Kelly, P.A., Hennighausen, L. (2001) Prolactin, growth hormone, and epidermal growth factor activate Stat5 in different compartments of mammary tissue and exert different and overlapping developmental effects. *Developmental Biology*. 229(1):163-75.

Garfield, A.S. (2007) Investigating the roles of mouse Grb10 in the regulation of growth and behaviour. *PhD Thesis, University of Bath*.

Garfield, A.S., Cowley, M., Smith, F.M., Stewart-Cox, J.E., Moorwood, K., Ward, A. Brain-specific expression from the paternal Grb10 allele influences social dominance whereas the maternal allele regulates fetal growth. *Submitted*.

Gehring, M., Huh, J.H., Hsieh, T.F., Penterman, J., Choi, Y., Harada, J.J., Goldberg, R.B., Fischer, R.L. (2006) DEMETER DNA glycosylase establishes MEDEA polycomb gene self-imprinting by allele-specific demethylation. *Cell*. 124(3):495-506.

Germain-Lee, E.L., Ding, C.L., Deng, Z., Crane, J.L., Saji, M., Ringel, M.D., Levine, M.A. (2002) Paternal imprinting of Galpha(s) in the human thyroid as the basis of TSH resistance in pseudohypoparathyroidism type 1a. *Biochemical and Biophysical Research Communications*. 296(1):67-72.

Giorgetti-Peraldi, S., Murdaca, J., Mas, J.C., Van Obberghen, E. (2001) The adapter protein, Grb10, is a positive regulator of vascular endothelial growth factor signalling. *Oncogene*. 20(30):3959-68.

Giovannone, B., Lee, E., Lavoila, L., Giorgino, F., Cleveland, K.A., Smith, R.J. (2003) Two novel proteins that are linked to insulin-like growth factor (IGF-I) receptors by the Grb10 adapter and modulate IGF-I signalling. *The Journal of Biological Chemistry*. 278(34):31564-73.

Goday, C., Esteban, M.R. (2001) Chromosome elimination in sciarid flies. *Bioessays*. 23(3):242-50.

Gordon, K.E., Binas, B., Chapman, R.S., Kurian, K.M., Clarkson, R.W., Clark, A.J., Lane, E.B., Watson, C.J. (2000) A novel cell culture model for studying differentiation and apoptosis in the mouse mammary gland. *Breast Cancer Research*. 2(3):222-35.

Gouilleux, F., Pallard, C., Dusanter-Fourt, I., Wakao, H., Haldosen, L.A., Norstedt, G., Levy, D., Groner, B. (1995) Prolactin, growth hormone, erythropoietin and granulocyte-macrophage colony stimulating factor induce MGF-Stat5 DNA binding activity. *The EMBO Journal*. 14(9):2005-13.

Grandjean, V., Smith, J., Schofield, P.N., Ferguson-Smith, A.C. (2000) Increased IGF-II protein affects p57kip2 expression in vivo and in vitro: implications for Beckwith-Wiedemann syndrome. *Proceedings of the National Academy of Sciences of the United States of America*. 97(10):5279-84.

Grattan, D.R., Xu, J., McLachlan, M.J., Kokay, I.C., Bunn, S.J., Hovey, R.C., Davey, H.W. (2001) Feedback regulation of PRL secretion is mediated by the transcription factor, signal transducer and activator of transcription 5b. *Endocrinology*. 142(9):3935-40.

Grueso, E., Rocha, M., Puerta, M. (2001) Plasma and cerebrospinal fluid leptin levels are maintained despite enhanced food intake in progesterone-treated rats. *European Journal of Endocrinology*. 144(6):659-65.

Guo, Y., Jankovic, J., Zhu, S., Le, W., Song, Z., Xie, W., Liao, D., Yang, H., Deng, H. (2009) GIGYF2 Asn56Ser and Asn457Thr mutations in Parkinson disease patients. *Neuroscience Letters*. 454(3):209-11.

Haig, D. (1994) Refusing the ovarian time bomb – 3 viewpoints and a reply. *Trends in Genetics*. 10:346-7.

Haig, D. (1999) Genetic conflicts and the private life of *Peromyscus polionotus*. *Nature Genetics*. 22(2):131.

Haig, D., Westoby, M. (1989) Parent specific gene expression and the triploid endosperm. *American Naturalist*. 134:147-55.

Hamilton-Shield, J.P. (2007) Overview of neonatal diabetes. *Endocrine Development*. 12:12-23.

Han, D.C., Guan, J.L. (1999) Association of focal adhesion kinase with Grb7 and its role in cell migration. *The Journal of Biological Chemistry*. 274(34):24425-30.

Happ, B., Groner, B. (1993) The activated mammary gland specific nuclear factor (MGF) enhances in vitro transcription of the beta-casein gene promoter. *The Journal of Steroid Biochemistry and Molecular Biology*. 47(1-6):21-30.

Harris, J., Stanford, P.M., Sutherland, K., Oakes, S.R., Naylor, M.J., Robertson, F.G., Blazek, K.D., Kazlauskas, M., Hilton, H.N., Wittlin, S., Alexander, W.S., Lindeman, G.J., Visvader, J.E., Ormandy, C.J. (2006) Socs2 and elf5 mediate prolactin-induced mammary gland development. *Molecular Endocrinology*. 20(5):1177-87.

Haslam, R.J., Koide, H.B., Hemmings, B.A. (1993) Pleckstrin domain homology. *Nature*. 363(6427):309-10.

Hayward, B.E., Barlier, A., Korbonits, M., Grossman, A.B., Jacquet, P., Enjalbert, A., Bonthron, D.T. (2001) Imprinting of the G(s)alpha gene GNAS1 in the pathogenesis of acromegaly. *The Journal of Clinical Investigation*. 107(6):R31-6.

He, W., Rose, D.W., Olefsky, J.M., Gustafson, T.A. (1998) Grb10 interacts differentially with the insulin receptor, insulin-like growth factor I receptor, and epidermal growth factor receptor via the Grb10 Src homology 2 (SH2) domain and a second novel domain located between the pleckstrin homology and SH2 domains. *The Journal of Biological Chemistry*. 273(12):6860-7.

He, X., Treacy, M.N., Simmons, D.M., Ingraham, H.A., Swanson, L.W., Rosenfeld, M.G. (1989) Expression of a large family of POU-domain regulatory genes in mammalian brain development. *Nature*. 340(6228):35-41.

Henikoff, S. (2007) Nucleosome destabilization in the epigenetic regulation of gene expression. *Nature Reviews: Genetics*. 9(1):15-26.

Hennighausen, L., Robinson, G.W. (2008) Interpretation of cytokine signaling through the transcription factors STAT5A and STAT5B. *Genes & Development*. 22(6):711-21.

Hens, J.R., Dann, P., Zhang, J.P., Harris, S., Robinson, G.W., Wysolmerski, J. (2007) BMP4 and PTHrP interact to stimulate ductal outgrowth during embryonic mammary development and to inhibit hair follicle induction. *Development*. 134(6):1221-30.

Hiby, S.E., Lough, M., Keverne, E.B., Surani, M.A., Loke, Y.W., King, A. (2001) Paternal monoallelic expression of PEG3 in the human placenta. *Human Molecular Genetics*. 10(10):1093-100.

Hikichi, T., Kohda, T., Kaneko-Ishino, T., Ishino, F. (2003) Imprinting regulation of the murine Meg1/Grb10 and human GRB10 genes; roles of brain-specific promoters and mouse-specific CTCF binding sites. *Nucleic Acids Research*. 31(5):1398-406.

Hiremath, M., Lydon, J.P., Cowin, P. (2007) The pattern of beta-catenin responsiveness within the mammary gland is regulated by progesterone receptor. *Development*. 134(20):3703-12.

Holt, L.J., Lyons, R.J., Ryan, A.S., Beale, S.M., Ward, A., Cooney, G.J., Daly, R.J. (2009) Dual ablation of Grb10 and Grb14 in mice reveals their combined role in regulation of insulin signalling and glucose homeostasis. *Molecular Endocrinology*. Jun 18 e-pub ahead of print.

Holt, L.J., Siddle, K. (2005) Grb10 and Grb14: enigmatic regulators of insulin action – and more? *The Biochemical Journal*. 388(pt 2):393-406.

Howie, P.W., Forsyth, J.S., Ogston, S.A., Clark, A., Florey, C.D. (1990) Protective effect of breast feeding against infection. *BMJ*. 300(6716):11-6.

Humphreys, R.C., Krajewska, M., Krnacik, S., Jaeger, R., Weiher, H., Krajewski, S., Reed, J.C., Rosen, J.M. (1996) Apoptosis in the terminal endbud of the murine mammary gland: a mechanism of ductal morphogenesis. *Development*. 122(12):4013-22.

Hurst, L.D. (1997) Evolutionary theories of genomic imprinting, pp 211-237 in *Genomic Imprinting: Frontiers in Molecular Biology*, edited by W. Reik and A. Surani. Oxford University Press, Oxford.

Hurst, L.D. (1998) *Peromysci*, promiscuity and imprinting. *Nature Genetics*. 20(4):315-6.

Hurst, L.D., Pomiankowski, A., McVean, G. (2000) Peg3 and the conflict hypothesis. *Science*. 287:1167.

Hutt, J.A., O'Rourke, J.P., DeWille, J. (2000) Signal transducer and activator of transcription 3 activates CCAAT enhancer-binding protein delta gene transcription in G0 growth-arrested mouse mammary epithelial cells and in involuting mouse mammary gland. *The Journal of Biological Chemistry*. 275(37):29123-31.

Iavnilovitch, E., Groner, B., Barash, I. (2002) Overexpression and forced activation of stat5 in mammary gland of transgenic mice promotes cellular proliferation, enhances differentiation, and delays postlactational apoptosis. *Molecular Cancer Research*. 1(1):32-47.

Jackson, D., Volpert, O.V., Bouck, N., Linzer, D.I. (1994) Stimulation and inhibition of angiogenesis by placental proliferin and proliferin-related protein. *Science*. 266(5190):1581-4.

Jacobs, S.A., Khorasanizadeh, S. (2002) Structure of HP1 chromodomain bound to a lysine 9-methylated histone H3 tail. *Science*. 295(5562):2080-3.

Jiang, Y., Tsai, T.F., Bressler, J., Beaudet, A.L. (1998) Imprinting in Angelman and Prader-Willi syndromes. *Current Opinion in Genetics & Development*. 8(3):334-42.

Jones, R.H., Ozanne, S.E. (2009) Fetal programming of insulin-glucose metabolism. *Molecular and Cellular Endocrinology*. 297(1-2):4-9.

Kagitani, F., Kuroiwa, Y., Wakana, S., Shiroishi, T., Miyoshi, N., Kobayashi, S., Nishida, M., Kohda, T., Kaneko-Ishino, T., Ishino, F. (1997) Peg5/Neuronatin is an imprinted gene located on sub-distal chromosome 2 in the mouse. *Nucleic Acids Research*. 25(17):3428-32.

Kaneko-Ishino, T., Kuroiwa, Y., Miyoshi, N., Kohda, T., Suzuki, R., Yokoyama, M., Viville, S., Barton, S.C., Ishino, F., Surani, M.A. (1995) Peg1/Mest imprinted gene on chromosome 6 identified by cDNA subtraction hybridization. *Nature Genetics*. 11(1):52-9.

Karl, P.I. (1995) Insulin-like growth factor-I stimulates amino acid uptake by the cultured human placental trophoblast. *Journal of Cellular Physiology*. 165(1):83-8.

Kas, K., Voz, M.L., Hensen, K., Meyen, E., Van de Ven, W.J. (1998) Transcriptional activation capacity of the novel PLAG family of zinc finger proteins. *The Journal of Biological Chemistry*. 273(36):23026-32.

Kasus-Jacobi, A., Bérézíat, V., Perdereau, D., Girard, J., Burnol, A.F. (2000) Evidence for an interaction between the insulin receptor and Grb7. A role for two of its binding domains, PIR and SH2. *Oncogene*. 19(16):2052-9.

Kaufman, M.H., Robertson, E.J., Handyside, A.H., Evans, M.J. (1983) Establishment of pluripotential cell lines from haploid mouse embryos. *Journal of Embryology and Experimental Morphology*. 73:249-61.

Kehrer-Sawatzki, H., Cooper, D.N. (2007) Understanding the recent evolution of the human genome: insights from human-chimpanzee genome comparisons. *Human Mutation*. 28(2):99-130.

Kelsey, G., Bodle, D., Miller, H.J., Beechey, C.V., Coombes, C., Peters, J., Williamson, C.M. (1999) Identification of imprinted loci by methylation-sensitive representational difference analysis: application to mouse distal chromosome 2. *Genomics*. 62(2):129-38.

Kermicle, J.L. (1970) Dependence of the R-mottle aleurone phenotype in maize on mode of sexual transmission. *Genetics*. 66:69-85.

Keverne, E.B., Curley, J.P. (2008) Epigenetics, brain evolution and behaviour. *Frontiers in Neuroendocrinology*. 29(3):398-412.

Killian, J.K., Byrd, J.C., Jirtle, J.V., Munday, B.L., Stoskopf, M.K., MacDonald, R.G., Jirtle, R.L. (2000) M6P/IGF2R imprinting evolution in mammals. *Molecular Cell*. 5(4):707-16.

Kinoshita, T., Yadegari, R., Harada, J.J., Goldberg, R.B., Fischer, R.L. (1999) Imprinting of the MEDEA polycomb gene in the *Arabidopsis* endosperm. *The Plant Cell*. 11(10):1945-52.

Kitsberg, D., Selig, S., Brandeis, M., Simon, I., Keshet, I., Driscoll, D.J., Nicholls, R.D., Cedar, H. (1993) Allele-specific replication timing of imprinted gene regions. *Nature*. 364(6436):459-63.

Kiyosue, T., Ohad, N., Yadegari, R., Hannon, M., Dinneny, J., Wells, D., Katz, A., Margossian, L., Harada, J.J., Goldberg, R.B., Fischer, R.L. (1999) Control of fertilization-independent endosperm development by the MEDEA polycomb gene in *Arabidopsis*. *Proceedings of the National Academy of Sciences of the United States of America*. 96(7):4186-91.

Kleinberg, D.L., Feldman, M., Ruan, W. (2000) IGF-I: an essential factor in terminal end bud formation and ductal morphogenesis. *Journal of Mammary Gland Biology and Neoplasia*. 5(1):7-17.

Klintsova, A.Y., Helfer, J.L., Calizo, L.H., Dong, W.K., Goodlett, C.R., Greenough, W.T. (2007) Persistent impairment of hippocampal neurogenesis in young adult rats following early postnatal alcohol exposure. *Alcoholism, Clinical and Experimental Research*. 31(12):2073-82.

Kölliker, M., Brinkhof, M.W., Heeb, P., Fitze, P.S., Richner, H. (2000) The quantitative genetic basis of offspring solicitation and parental response in a passerine bird with biparental care. *Proceedings of the Royal Society: Biological Sciences*. 267(1457):2127-32.

Komuro, I., Izumo, S. (1993) Csx: a murine homeobox-containing gene specifically expressed in the developing heart. *Proceedings of the National Academy of Sciences of the United States of America*. 90(17):8145-9.

Kratochwil, K., Schwartz, P. (1976) Tissue interaction in androgen response of embryonic mammary rudiment of mouse: identification of target tissue for testosterone. *Proceedings of the National Academy of Sciences of the United States of America*. 73(11):4041-4.

Kritikou, E.A., Sharkey, A., Abell, K., Came, P.J., Anderson, E., Clarkson, R.W., Watson, C.J. (2003) A dual, non-redundant, role for LIF as a regulator of development and STAT3-mediated cell death in mammary gland. *Development*. 130(15):3459-68.

Kullander, K., Klein, R. (2002) Mechanisms and functions of Eph and ephrin signalling. *Nature Reviews Molecular Cell Biology*. 3(7):475-86.

Kumar, S., Clarke, A.R., Hooper, M.L., Horne, D.S., Law, A.J.R., Leaver, J., Springbett, A., Stevenson, E., Simons, J.P. (1994) Milk composition and lactation of beta-casein deficient mice. *Proceedings of the National Academy of Sciences of the United States of America*. 91:6138-42.

Kuroiwa, Y., Kaneko-Ishino, T., Kagitani, F., Kohda, T., Li, L.L., Tada, M., Suzuki, R., Yokoyama, M., Shiroishi, T., Wakana, S., Barton, S.C., Ishino, F., Surani, M.A. (1996) Peg3 imprinted gene on proximal chromosome 7 encodes for a zinc finger protein. *Nature Genetics*. 12(2):186-90.

Lampert, K.P. (2008) Facultative parthenogenesis in vertebrates: reproductive error or chance? *Sexual Development*. 2(6):290-301.

Latinkić, B.V., Cooper, B., Smith, S., Kotecha, S., Towers, N., Sparrow, D., Mohun, T.J. (2004) Transcriptional regulation of the cardiac-specific MLC2 gene during Xenopus embryonic development. *Development*. 131(3):669-79.

Lau, M.M., Stewart, C.E., Liu, Z., Bhatt, H., Rotwein, P., Stewart, C.L. (1994) Loss of the imprinted IGF2/cation-independent mannose 6-phosphate receptor results in fetal overgrowth and perinatal lethality. *Genes & Development*. 8(24):2953-63.

Lautier, C., Goldwurm, S., Dürr, A., Giovannone, B., Tsiaras, W.G., Pezzoli, G., Brice, A., Smith, R.J. (2008) Mutations in the GIGYF2 (TNRC15) gene at the PARK11 locus in familial Parkinson disease. *American Journal of Human Genetics*. 82(4):822-33.

Laviola, L., Giorgino, F., Chow, J.C., Baquero, J.A., Hansen, H., Ooi, J., Zhu, J., Riedel, H., Smith, R.J. (1997) The adapter protein Grb10 associates preferentially with the insulin receptor as compared with the IGF-I receptor in mouse fibroblasts. *The Journal of Clinical Investigation*. 99(5):830-7.

Leavey, S.F., Arend, L.J., Dare, H., Dressler, G.R., Briggs, J.P., Margolis, B. (1998) Expression of Grb7 growth factor receptor signaling protein in kidney development and in adult kidney. *The American Journal of Physiology*. 275(5 Pt 2):F770-6.

Le Clair, C., Abbi, T., Sandhu, H., Tappia, P.S. (2009) Impact of maternal undernutrition on diabetes and cardiovascular disease risk in adult offspring. *Canadian Journal of Physiology and Pharmacology*. 87(3):161-79.

Lee, H., Volonte, D., Galbiati, F., Iyengar, P., Lublin, D.M., Bregman, D.B., Wilson, M.T., Campos-Gonzalez, R., Bouzahzah, B., Pestell, R.G., Scherer, P.E., Lisanti, M.P. (2000) Constitutive and growth factor-regulated phosphorylation of caveolin-1 occurs at the same site (Tyr-14) in vivo: identification of a c-Src/Cav-1/Grb7 signaling cassette. *Molecular Endocrinology*. 14(11):1750-75.

Lemmon, M.A. (2007) Pleckstrin homology (PH) domains and phosphoinositides. *Biochemical Society Symposium*. 74:81-93.

Li, E., Beard, C., Jaenisch, R. (1993) Role for DNA methylation in genomic imprinting. *Nature*. 366(6453):362-5.

Li, L., Keverne, E.B., Aparicio, S.A., Ishino, F., Barton, S.C., Surani, M.A. (1999) Regulation of maternal behaviour and offspring growth by paternally expressed Peg3. *Science*. 284(5412):330-3.

Li, S., Rosen, J.M. (1995) Nuclear factor I and mammary gland factor (STAT5) play a critical role in regulating rat whey acidic protein gene expression in transgenic mice. *Molecular and Cellular Biology*. 15(4):2063-70.

Lichanska, A.M., Waters, M.J. (2008) How growth hormone controls growth, obesity and sexual dimorphism. *Trends in Genetics*. 24(1):41-7.

Lim, M.A., Riedel, H., Liu, F. (2004) Grb10: more than a simple adaptor protein. *Frontiers in Bioscience*. 9:387-403.

Ling, J.Q., Li, T., Hu, J.F., Vu, T.H., Chen, H.L., Qiu, X.W., Cherry, A.M., Hoffman, A.R. (2006) CTCF mediates interchromosomal colocalization between Igf2/H19 and Wsb1/Nf1. *Science*. 312(5771):269-72.

Liu, F., Roth, R.A. (1995) Grb-IR: a SH2-domain-containing protein that binds to the insulin receptor and inhibits its function. *Proceedings of the National Academy of Sciences of the United States of America*. 92(22):10287-91.

Liu, J.P., Baker, J., Perkins, L.S., Robertson, E.J., Efstratiadis, A. (1993) Mice carrying null mutations of the genes encoding insulin-like growth factor 1 (Igf-1) and type 1 IGF receptor (Igf1r). *Cell*. 75:59-72.

Liu, X., Robinson, G.W., Wagner, K.U., Garrett, L., Wynshaw-Boris, A., Hennighausen, L. (1997) Stat5a is mandatory for adult mammary gland development and lactogenesis. *Genes & Development*. 11(2):179-86.

Liu, Z.J., Zhuge, Y., Velazquez, O.C. (2009) Trafficking and differentiation of mesenchymal stem cells. *Journal of Cellular Biochemistry*. 106(6):984-91.

Ludwig, T., Eggenschwiler, J., Fisher, P., D'Ercole, A.J., Davenport, M.L., Efstratiadis, A. (1996) Mouse mutants lacking the type 2 IGF receptor (IGF2R) are rescued from perinatal lethality in Igf2 and Igf1r null backgrounds. *Developmental Biology*. 177(2):517-35.

Luedi, P.P., Hartemink, A.J., Jirtle, R.L. (2005) Genome-wide prediction of murine imprinted genes. *Genome Research*. 15(6):875-84.

Lyle, R., Watanabe, D., te Vruchte, D., Lerchner, W., Smrzka, O.W., Wutz, A., Schageman, J., Hahner, L., Davies, C., Barlow, D.P. (2000) The imprinted antisense RNA at the Igf2r locus overlaps but does not imprint Mas1. *Nature Genetics*. 25(1):19-21.

Lyons, I., Parsons, L.M., Hartley, L., Li, R., Andrews, J.E., Robb, L., Harvey, R.P. (1995) Myogenic and morphogenetic defects in the heart tubes of murine embryos lacking the homeo box gene Nkx2.5. *Genes & Development*. 9(13):1654-66.

Ma, D., Shield, J.P.H., Dean, W., Leclerc, I., Knauf, C. Burcelin, R. Rutter, G.A., Kelsey, G. (2004) Impaired glucose homeostasis in transgenic mice expressing the human transient neonatal diabetes mellitus locus, TNDM. *The Journal of Clinical Investigation*. 114(3):339-48.

MacLeod, R.M., Lehmeyer, J.E. (1974) Studies on the mechanism of the dopamine-mediated inhibition of prolactin secretion. *Endocrinology*. 94(4):1077-85.

Mager, J., Montgomery, N.D., de Villena, F.P., Magnuson, T. (2003) Genome imprinting regulated by the mouse Polycomb group protein Eed. *Nature Genetics*. 33(4):502-7.

Maher, E.R., Reik, W. (2000) Beckwith-Wiedemann syndrome: imprinting in clusters revisited. *The Journal of Clinical Investigation*. 105(3):247-52.

Mailleux, A.A., Spencer-Dene, B., Dillon, C., Ndiaye, D., Savona-Baron, C., Itoh, N., Kato, S., Dickson, C., Thiery, J.P., Bellusci, S. (2002) Role of FGF10/FGFR2b signaling during mammary gland development in the mouse embryo. *Development*. 129(1):53-60.

Mallepell, S., Krust, A., Chambon, P., Brisken, C. (2006) Paracrine signaling through the epithelial estrogen receptor alpha is required for proliferation and morphogenesis in the mammary gland. *Proceedings of the National Academy of Sciences of the United States of America*. 103(7):2196-201.

Manhès, C., Kayser, C., Bertheau, P., Kelder, B., Kopchick, J.J., Kelly, P.A., Touraine, P., Goffin, V. (2006) Local over-expression of prolactin in differentiating mouse mammary gland induces functional defects and benign lesions, but no carcinoma. *Journal of Endocrinology*. 190:271-85.

Mano, H., Ohya, K., Miyazato, A., Yamashita, Y., Ogawa, W., Inazawa, J., Ikeda, U., Shimada, K., Hatake, K., Kasuga, M., Ozawa K., Kajigaya, S. (1998) Grb10/GrbIR as an in vivo substrate of Tec tyrosine kinase. *Genes to Cells*. 3(7):431-41.

Manser, J., Roonprapunt, C., Margolis, B. (1997) C. elegans cell migration gene mig-10 shares similarities with a family of SH2 domain proteins and acts cell nonautonomously in excretory canal development. *Developmental Biology*. 184(1):150-64.

Mantovani, G., Ballare, E., Giammona, E., Beck-Peccoz, P., Spada, A. (2002) The gsalpha gene: predominant maternal origin of transcription in human thyroid gland and gonads. *The Journal of Clinical Endocrinology and Metabolism*. 87(10):4736-40.

Matsuda, M., Imaoka, T., Vomachka, A.J., Gudelsky, G.A., Hou, Z., Mistry, M., Bailey, J.P., Nieport, K.M., Walther, D.J., Bader, M., Horseman, N.D. (2004) Serotonin regulates mammary gland development via an autocrine-paracrine loop. *Developmental Cell*. 6(2):193-203.

McGrath, J., Solter, D. (1983) Nuclear transplantation in the mouse embryo by microsurgery and cell fusion. *Science*. 220(4603):1300-2.

McGrath, J., Solter, D. (1984) Completion of mouse embryogenesis requires both the maternal and paternal genomes. *Cell*. 37(1):179-83.

McWilliams, D., Boime, I. (1980) Cytological localization of placental lactogen messenger ribonucleic acid in syncytiotrophoblast layers of human placenta. *Endocrinology*. 107(3):761-5.

Meadows, K.N., Bryant, P., Pumiglia, K. (2001) Vascular endothelial growth factor induction of the angiogenic phenotype requires Ras activation. *The Journal of Biological Chemistry*. 276(52):49289-98.

Meeus, B., Nuytemans, K., Crosiers, D., Engelborghs, S., Pals, P., Pickut, B., Peeters, K., Mattheijssens, M., Corsmit, E., Cras, P., De Deyn, P.P., Theuns, J., Van Broeckhoven, C. (2009) GIGYF2 has no major role in Parkinson genetic etiology in a Belgian population. *Neurobiology of Ageing*. E-publication ahead of print.

Mena, F., Grosvenor, C.E. (1968) Effect of number of pups upon suckling-induced fall in pituitary prolactin concentration and milk ejection in the rat. *Endocrinology*. 82(3):623-6.

Menheniott, T.R., Cowley, M., Charalambous, M., Tosh, D., Ward, A. Igf2 escapes imprinted regulation in choroid plexus epithelial cells by uncoupling regional DNA methylation marks. *Submitted*.

Menheniott, T.R., Woodfine, K., Schulz, R., Wood, A.J., Monk, D., Giraud, A.S., Baldwin, H.S., Moore, G.E., Oakey, R.J. (2008) Genomic imprinting of Dopa decarboxylase in heart and reciprocal allelic expression with neighbouring Grb10. *Molecular and Cellular Biology*. 28(1):286-96.

Miller, J.L., Goldstone, A.P., Couch, J.A., Shuster, G., He, G., Driscoll, D.J., Liu, Y., Schmalfuss, I.M. (2007) Pituitary abnormalities in Prader-Willi syndrome and early onset morbid obesity. *American Journal of Medical Genetics*. 146A(5):570-7.

Miquerol, L., Gertsenstein, M., Harpal, K., Rossant, J., Nagy, A. (1999) Multiple developmental roles of VEGF suggested by a LacZ-tagged allele. *Developmental Biology*. 212(2):307-22.

Miyoshi, N., Kuroiwa, Y., Kohda, T., Shitara, H., Yonekawa, H., Kawabe, T., Hasegawa, H., Barton, S.C., Surani, M.A., Kaneko-Ishino, T., Ishino, F. (1998) Identification of the Meg1/Grb10 imprinted gene on mouse proximal chromosome 11, a candidate for the Silver-Russell syndrome gene. *Proceedings of the National Academy of Sciences of the United States of America*. 95(3):1102-7.

Monami, G., Emiliozzi, V., Morrione, A. (2008) Grb10/Nedd4-mediated multiubiquitination of the insulin-like growth factor receptor regulates receptor internalization. *Journal of Cellular Physiology*. 216(2):426-37.

Monk, D., Arnaud, P., Frost, J., Hills, F.A., Stanier, P., Feil, R., Moore, G.E. (2009) Reciprocal imprinting of human GRB10 in placental trophoblast and brain: evolutionary conservation of reversed allelic expression. *Human Molecular Genetics*. 18(16):3066-74.

Monk, D., Wakeling, E.L., Proud, V., Hitchins, M., Abu-Amero, S.N., Stanier, P., Preece, M.A., Moore, G.E. (2000) Duplication of 7p11.2-p13, including GRB10, in Silver-Russell syndrome. *American Journal of Human Genetics*. 66(1):36-46.

Monks, J., Rosner, D., Geske, F.J., Lehman, L., Hanson, L., Neville, M.C., Fadok, V.A. (2005) Epithelial cells as phagocytes: apoptotic epithelial cells are engulfed by mammary alveolar epithelial cells and repress inflammatory mediator release. *Cell Death and Differentiation*. 12(2):107-14.

Moore, T. (1994) Refusing the ovarian time bomb – 3 viewpoints and a reply. *Trends in Genetics*. 10:347-8.

Moore, T., Haig, D. (1991) Genomic imprinting in mammalian development: a parental tug-of-war. *Trends in Genetics*. 7(2):45-9.

Moore, T., Mills, W. (1999) Imprinting and monogamy. *Nature Genetics*. 22(2):130-1.

Morrione, A. (2003) Grb10 adapter protein as regulator of insulin-like growth factor signalling. *Journal of Cellular Physiology*. 197(3):307-11.

Morrione, A., Plant, P., Valentinis, B., Staub, O., Kumar, S., Rotin, D., Baserga, R. (1999) mGrb10 interacts with Nedd4. *The Journal of Biological Chemistry*. 275(34):24094-9.

Motamedi, M.R., Hong, E.J., Li, X., Gerber, S., Denison, C., Gygi, S., Moazed, D. (2008) HP1 proteins form distinct complexes and mediate heterochromatic gene silencing by nonoverlapping mechanisms. *Molecular Cell*. 32(6):778-90.

Moucadel, V., Constantinescu, S.N. (2005) Differential Stat5 signalling by ligand-dependent and constitutively active cytokine receptors. *The Journal of Biological Chemistry*. 280(14):13364-73.

Moutoussamy, S., Renaudie, F., Lago, F., Kelly, P.A., Finidori, J. (1998) Grb10 identified as a potential regulator of growth hormone (GH) signaling by cloning of GH receptor target proteins. *The Journal of Biological Chemistry*. 273(26):15906-12.

Murillo-Fuentes, L., Artillo, R., Carreras, O., Murillo, L. (2001) Effects of maternal chronic alcohol administration in the rat: lactation performance and pup's growth. *European Journal of Nutrition*. 40(4):147-54.

Murrell, A., Heeson, S., Bowden, L., Constância, M., Dean, W., Kelsey, G., Reik, W. (2001) An intragenic methylated region in the imprinted Igf2 gene augments transcription. *EMBO Reports*. 2(12):1101-6.

Murrell, A., Heeson, S., Reik, W. (2004) Interaction between differentially methylated regions partitions the imprinted genes Igf2 and H19 into parent-specific chromatin loops. *Nature Genetics*. 36(8):889-93.

Muscatelli, F., Abrous, D.N., Massacrier, A., Boccaccio, I., Le Moal, M., Cau, P., Cremer, H. (2000) Disruption of the mouse Necdin gene results in hypothalamic and behavioural alterations reminiscent of the human Prader-Willi syndrome. *Human Molecular Genetics*. 9:3101-3110.

Nagano, T., Mitchell, J.A., Sanz, L.A., Pauler, F.M., Ferguson-Smith, A.C., Feil, R., Fraser, P. (2008) The Air non-coding RNA epigenetically silences transcription by targeting G9a to chromatin. *Science*. 322(5908):1717-20.

Nagy, A., Rossant, J. (1993) Production of completely ES cell-derived fetuses, pp 147-49 in *Gene Targeting: a practical approach*, edited by A. Joyner. Oxford University Press, Oxford.

Nantel, A., Huber, M., Thomas, D.Y. (1999) Localization of endogenous Grb10 to the mitochondria and its interaction with the mitochondrial-associated Raf-1 pool. *The Journal of Biological Chemistry*. 274(50):35719-24.

Nantel, A., Mohammad-Ali, K., Sherk, J., Posner, B.I., Thomas, D.Y. (1998) Interaction of the Grb10 adapter protein with the Raf1 and MEK1 kinases. *The Journal of Biological Chemistry*. 273(17):10475-84.

Nguyen, A.V., Pollard, J.W. (2000) Transforming growth factor beta3 induces cell death during the first stage of mammary gland involution. *Development*. 127(14):3107-18.

Ning, Y., Hoang, B., Schuller, A.G., Cominski, T.P., Hsu, M.S., Wood, T.L., Pintar, J.E. (2007) Delayed mammary gland involution in mice with mutation of the insulin-like growth factor binding protein 5 gene. *Endocrinology*. 148(5):2138-47.

Nishizawa, K., Freund, C., Li, J., Wagner, G., Reinherz, E.L. (1998) Identification of a proline-binding motif regulating CD2-triggered T lymphocyte activation. *Proceedings of the National Academy of Sciences of the United States of America*. 95(25):14897-902.

Oakey, R.J., Beechey, C.V. (2002) Imprinted genes: identification by chromosome rearrangements and post-genomic strategies. *Trends in Genetics*. 18(7):359-66.

Obata, Y., Kaneko-Ishino, T., Koide, T., Takai, Y., Ueda, T., Domeki, I., Shiroishi, T., Ishino, F., Kono, T. (1998) Disruption of primary imprinting during oocyte growth leads to the modified expression of imprinted genes during embryogenesis. *Development*. 125(8):1553-60.

Okano, M., Bell, D.W., Haber, D.A., Li, E. (1999) DNA methyltransferases Dnmt3a and Dnmt3b are essential for de novo methylation and mammalian development. *Cell*. 99(3):247-57.

Oliver, M.H., Hawkins, P., Harding, J.E. (2005) Periconceptional undernutrition alters growth trajectory and metabolic and endocrine responses to fasting in late-gestation fetal sheep. *Pediatric Research*. 57(4):591-8.

Onishi, M., Nosaka, T., Misawa, K., Mui, A.L., Gorman, D., McMahon, M., Miyajima, A., Kitamura, T. (1998) Identification and characterisation of a constitutively active STAT5 mutant that promotes cell proliferation. *Molecular and Cellular Biology*. 18(7):3871-9.

Ooi, J., Yajnik, V., Immanuel, D., Gordon, M., Moskow, J.J., Buchberg, A.M., Margolis, B. (1995) The cloning of Grb10 reveals a new family of SH2 domain proteins. *Oncogene*. 10(8):1621-30.

Opgaard, O.S., Wang, P.H. (2005) IGF-I is a matter of heart. *Growth Hormone and IGF Research*. 15:89-94.

Ormandy, C.J., Camus, A., Barra, J., Damotte, D., Lucas, B., Buteau, H., Edery, M., Brousse, N., Babinet, C., Binart, N., Kelly, P.A. (1997) Null mutation of the prolactin receptor gene produces multiple reproductive defects in the mouse. *Genes & Development*. 11(2):167-78.

Oswald, J., Engemann, S., Lane, N., Mayer, W., Olek, A., Fundele, R., Dean, W., Reik, W., Walter, J. (2000) Active demethylation of the paternal genome in the mouse zygote. *Current Biology*. 10(8):475-8.

Pai, V.P., Horseman, N.D. (2008) Biphasic regulation of mammary epithelial resistance by serotonin through activation of multiple pathways. *The Journal of Biological Chemistry*. 283(45):30901-10.

Pandey, A., Duan, H., Di Fiore, P.P., Dixit, V.M. (1995) The Ret receptor protein tyrosine kinase associates with the SH2-containing adapter protein Grb10. *The Journal of Biological Chemistry*. 270(37):21461-3.

Pandey, A., Liu, X., Dixon, J.E., Di Fiore, P.P., Dixit, V.M. (1996) Direct association between the Ret receptor tyrosine kinase and the Src homology 2-containing adapter protein Grb7. *The Journal of Biological Chemistry*. 271(18):10607-10.

Park, D.S., Lee, H., Frank, P.G., Razani, B., Nguyen, A.V., Parlow, A.F., Russell, R.G., Hulit, J., Pestell, R.G., Lisanti, M.P. (2002) Caveolin-1-deficient mice show accelerated mammary gland development during pregnancy, premature lactation, and hyperactivation of the Jak-2/STAT5a signaling cascade. *Molecular Biology of the Cell*. 13(10):3416-30.

Peaker, M. (2002) The mammary gland in mammalian evolution: a brief commentary on some of the concepts. *Journal of Mammary Gland Biology and Neoplasia*. 7(3):347-53.

Peters, J., Wroe, S.F., Wells, C.A., Miller, H.J., Bodle, D., Beechey, C.V., Williamson, C.M., Kelsey, G. (1999) A cluster of oppositely imprinted transcripts at the Gnas locus in the distal imprinting region of mouse chromosome 2. *Proceedings of the National Academy of Sciences of the United States of America*. 96(7):3830-5.

Pfaffl, M.W. (2001) A new mathematical model for relative quantification in real-time RT-PCR. *Nucleic Acids Research*. 29(9):e45.

Plagge, A., Gordon, E., Dean, W., Boiani, R., Cinti, S., Peters, J., Kelsey, G. (2004) The imprinted signaling protein XL alpha s is required for postnatal adaptation to feeding. *Nature Genetics*. 36(8):818-26.

Plagge, A., Isles, A.R., Gordon, E., Humby, T., Dean, W., Gritsch, S., Fischer-Colbrie, R., Wilkinson, L.S., Kelsey, G. (2005) Imprinted Nesp55 influences behavioural reactivity to novel environments. *Molecular and Cellular Biology*. 25(8):3019-26.

Plagge, A., Kelsey, G., Germain-Lee, E.L. (2008) Physiological functions of the imprinted Gnas locus and its protein variants Galpha(s) and XLalpha(s) in human and mouse. *The Journal of Endocrinology*. 196(2):193-214.

Preece, M.A. (2002) The genetics of Silver-Russell syndrome. *Reviews in Endocrine & Metabolic Disorders*. 3(4):369-79.

Propper, A., Gomot, L. (1973) Control of chick epidermis differentiation by rabbit mammary mesenchyme. *Experientia*. 29(12):1543-4.

Prost, M.A. (2009) Postnatal origins of undernutrition. *Nestlé Nutrition Workshop Series; Paediatric Programme*. 63:79-92.

Pullan, S., Wilson, J., Metcalfe, A., Edwards, G.M., Goberdhan, N., Tilly, J., Hickman, J.A., Dive, C., Streuli, C.H. (1996) Requirement of basement membrane for the suppression of programmed cell death in mammary epithelium. *Journal of Cell Science*. 109(Pt3):631-42.

Ramos, F.J., Langlais, P.R., Hu, D., Dong, L.Q., Liu, F. (2006) Grb10 mediates insulin-stimulated degradation of the insulin receptor: a mechanism of negative regulation. *American Journal of Physiology: Endocrinology and Metabolism*. 290(6):E1262-6.

Reed, R. (1996) Initial splice-site recognition and pairing during pre-mRNA splicing. *Current Opinion in Genetics & Development*. 6(2):215-20.

Reik, W., Constância, M., Fowden, A., Anderson, N., Dean, W., Ferguson-Smith, A., Tycko, B., Sibley, C. (2003) Regulation of supply and demand for maternal nutrients in mammals by imprinted genes. *Journal of Physiology*. 547(1):35-44.

Reik, W., Lewis, A. (2005) Co-evolution of X-chromosome inactivation and imprinting in mammals. *Nature Reviews: Genetics*. 6(5):403-10.

Reik, W., Walter, J. (2001) Genomic imprinting: parental influence on the genome. *Nature Reviews Genetics*. 2:21-32.

Renfree, M., Shaw, G., Pask, A. (2008) The evolution of genomic imprinting in marsupials. *Conference abstract, EMBO Workshop on Genomic Imprinting, Singapore*.

Richards, R.G., Klotz, D.M., Walker, M.P., Diaugustine, R.P. (2004) Mammary gland branching morphogenesis is diminished in mice with a deficiency of insulin-like growth factor-I (IGF-I), but not in mice with a liver-specific deletion of IGF-I. *Endocrinology*. 145(7):3106-10.

Riedel, H. (2004) GRB10 exceeding the boundaries of a common signalling adapter. *Frontiers in Bioscience*. 9:603-18.

Rodríguez-Henche, N., Jamen, F., Leroy, C., Bockaert, J., Brabet, P. (2002) Trancription of the mouse PAC1 receptor gene: cell-specific expression and regulation by Zac1. *Biochimica et Biophysica Acta*. 1576(1-2):157-62.

Rougier, N., Bourc'his, D., Gomes, D., Niveleau, A., Plachot, M. Pàldi, A., Viegas-Péguignot, E. (1998) Chromosome methylation patterns during mammalian preimplantation development. *Genes & Development.* 12(14):2108-13.

Sakakura, T., Nishizuka, Y., Dawe, C.J. (1976) Mesenchyme-dependent morphogenesis and epithelium-specific cytodifferentiation in mouse mammary gland. *Science*. 194(4272):1439-41.

Salem, C., Liang, G., Tsai, Y.C., Coulter, J., Knowles, M.A., Feng, A.C., Groshen, S., Nichols, P.W., Jones, P.A. (2000) Progressive increases in de novo methylation of CpG islands in bladder cancer. *Cancer Research*. 60(9):2473-6.

Sambrook, J., Russell, D.W. (2001) Molecular cloning; a laboratory manual. Cold Spring Harbour Laboratory Press, Cold Spring Harbour, New York, United States of America.

Sansing, R.C., Chinnici, J.P. (1976) Optimal and discriminating birth weights in human populations. *Annals of Human Genetics*. 40(1):123-31.

Sanz, L.A., Chamberlain, S., Sabourin, J.C., Henckel, A., Magnuson, T., Hugnot, J.P., Feil, R., Arnaud, P. (2008) A mono-allelic bivalent chromatin domain controls tissue-specific imprinting at Grb10. *The EMBO Journal*. 27(19):2523-32.

Sawka-Verhelle, D., Filloux, C., Tartare-Deckert, S., Mothe, I., Van Obberghen, E. (1997) Identification of Stat5b as a substrate on the insulin receptor. *European Journal of Biochemistry*. 250(2):411-7.

Saxonov, S., Berg, P., Brutlag, D.L. (2006) A genome-wide analysis of CpG dinucleotides in the human genome distinguishes two distinct classes of promoters. *Proceedings of the National Academy of Sciences of the United States of America*. 103(5):1412-7.

Schulz, R., McCole, R.B., Woodfine, K., Wood, A.J., Chahal, M., Monk, D., Moore, G.E., Oakey, R.J. (2009) Transcript- and tissue-specific imprinting of a tumour suppressor gene. *Human Molecular Genetics*. 18(1):118-27.

Schulz, R., Menheniott, T.R., Woodfine, K., Wood, A.J., Choi, J.D., Oakey, R.J. (2006) Chromosome-wide identification of novel imprinted genes using microarrays and uniparental disomies. *Nucleic Acids Research*. 34(12):e88.

Schwertfeger, K.L., Richert, M.M., Anderson, S.M. (2001) Mammary gland involution is delayed by activated Akt in transgenic mice. *Molecular Endocrinology*. 15(6):867-81.

Scott, R.J., Spielman, M., Bailey, J., Dickinson, H.G. (1998) Parent-of-origin effects on seed development in *Arabidopsis thaliana*. *Development*. 125(17):3329-41.

Shalaby, F., Rossant, J., Yamaguchi, T.P., Gertsenstein, M., Wu, X.F., Breitman, M.L., Schuh, A.C. (1995) Failure of blood-island formation and vasculogenesis in Flk-1-deficient mice. *Nature*. 376(6535):62-6.

Shaywitz, A.J., Greenberg, M.E. (1999) CREB: a stimulus-induced transcription factor activated by a diverse array of extracellular signals. *Annual Review of Biochemistry*. 68:821-61.

Shingo, T., Gregg, C., Enwere, E., Fujikawa, H., Hassam, R., Geary, C., Cross, J.C., Weiss, S. (2003) Pregnancy-stimulated neurogenesis in the adult female forebrain mediated by prolactin. *Science*. 299(5603):117-20.

Shiura, H., Miyoshi, N., Konishi, A., Wakisaka-Saito, N., Suzuki, R., Muguruma, K., Kohda, T., Wakana, S., Yokoyama, M., Ishino, F., Kaneko-Ishino, T. (2005) Meg1/Grb10 overexpression causes postnatal growth retardation and insulin resistance via negative modulation of the IGF1R and IR cascades. *Biochemical and Biophysical Research Communications*. 329(3):909-16.

Shiura, H., Nakamura, K., Hikichi, T., Hino, T., Oda, K., Suzuki-Migishima, R., Kohda, T., Kaneko-Ishino, T., Ishino, F. (2009) Paternal deletion of Meg1/Grb10 DMR causes maternalisation of the Meg1/Grb10 cluster in mouse proximal chromosome 11 leading to severe pre- and postnatal growth retardation. *Human Molecular Genetics*. 18(8):1424-38.

Sibley, C.P., Boyd, R.D. (1988) Control of transfer across the mature placenta. *Oxford Reviews of Reproductive Biology*. 10:382-435.

Sibley, C., Glazier, J., D'Souza, S. (1997) Placental transporter activity and expression in relation to fetal growth. *Experimental Physiology*. 82(2):389-402.

Simon, I., Tenzen, T., Reubinoff, B.E., Hillman, D., McCarrey, J.R., Cedar, H. (1999) Asynchronous replication of imprinted genes is established in the gametes and maintained during development. *Nature*. 401(6756):929-32.

Skwarlo-Sońta, K. (1992) Prolactin as an immunoregulatory hormone in mammals and birds. *Immunology Letters*. 33(2):105-21.

Sleutels, F., Tjon, G., Ludwig, T., Barlow, D.P. (2003) Imprinted silencing of Slc22a2 and Slc22a3 does not need transcriptional overlap between Igf2r and Air. *The EMBO Journal*. 22(14):3696-704.

Sleutels, F., Zwart, R., Barlow, D.P. (2002) The non-coding Air RNA is required for silencing autosomal imprinted genes. *Nature*. 415(6873):810-3.

Smith, F.M. (2004) An investigation of mouse Grb10, an imprinted gene that links foetal growth and insulin-regulated metabolism. *PhD Thesis, University of Bath*.

Smith, F.M., Garfield, A.S., Ward, A. (2006) Regulation of growth and metabolism by imprinted genes. *Cytogenetic and Genome Research*. 113(1-4):279-91.

Smith, F.M., Holt, L.J., Garfield, A.S., Charalambous, M., Koumanov, F., Perry, M., Bazzani, R., Sheardown, S.A., Hegarty, B.D., Lyons, R.J., Cooney, G.J., Daly, R.J., Ward, A. (2007) Mice with a disruption of the imprinted Grb10 gene exhibit altered body composition, glucose homeostasis, and insulin signalling during postnatal life. *Molecular and Cellular Biology*. 27(16):5871-86.

Smith, R.J., Dean, W., Konfortova, G., Kelsey, G. (2003) Identification of novel imprinted genes in a genome-wide screen for maternal methylation. *Genome Research*. 13(4):558-69.

Soares, M.J., Schaberg, K.D., Pinal, C.S., De, S.K., Bhatia, P., Andrews, G.K. (1987) Establishment of a rat placental cell line expressing characteristics of extraembryonic membranes. *Developmental Biology*. 124(1):134-44.

Solter, D. (1994) Refusing the ovarian time bomb – 3 viewpoints and a reply. *Trends in Genetics*. 10:346.

Songyang, Z., Shoelson, S.E., Chaudhuri, M., Gish, G., Roberts, T., Ratnofsky, S., Lechleider, R.J., Neel, B.G., Birge, R.B., Fajardo, J.E., Chou, M.M., Hanafusa, H., Schaffhausen, B., Cantley, L. (1993) SH2 domain recognize specific phosphopeptide sequences. *Cell*. 72:767-78.

Stedman, W., Kang, H., Lin, S., Kissil, J.L., Bartolomei, M.S., Lieberman, P.M. (2008) Cohesins localise with CTCF at the KSHV latency control region and at cellular c-myc and H19/Igf2 insulators. *The EMBO Journal*. 27(4):654-66.

Steenman, M.J., Rainier, S., Dobry, C.J., Grundy, P., Horon, I.L., Feinberg, A.P. (1994) Loss of imprinting of IGF2 is linked to reduced expression and abnormal methylation of H19 in Wilms' tumour. *Nature Genetics*. 7(3):433-9.

Stein, D., Wu, J., Fuqua, S.A., Roonprapunt, C., Yajnik, V., D'Eustachio, P., Moskow, J.J., Buchberg, A.M., Osborne, C.K., Margolis, B. (1994) The SH2 domain protein GRB-7 is co-amplified, overexpressed and in a tight complex with HER2 in breast cancer. *The EMBO Journal*. 13(6):1331-40.

Stein, E., Cerretti, D.P., Daniel, T.O. (1996) Ligand activation of ELK receptor tyrosine kinase promotes its association with Grb10 and Grb2 in vascular endothelial cells. *The Journal of Biological Chemistry*. 271(38):23588-93.

Stein, E.G., Ghirlando, R., Hubbard, S.R. (2003) Structural basis for dimerization of the Grb10 Src homology 2 domain: implications for ligand specificity. *The Journal of Biological Chemistry*. 278(15):13257-64.

Stein, E.G., Gustafson, T.A., Hubbard, S.R. (2001) The BPS domain of Grb10 inhibits the catalytic activity of the insulin and IGF1 receptors. *FEBS Letters*. 493(2-3):106-11.

Stein, T., Morris, J.S., Davies, C.R., Weber-Hall, S.J., Duffy, M.A., Heath, V.J., Bell, A.K., Ferrier, R.K., Sandilands, G.P., Gusterson, B.A. (2004) Involution of the mouse mammary gland is associated with an immune cascade and an acute-phase response, involving LBP, CD14 and STAT3. *Breast Cancer Research*. 6(2):R75-91.

Sternlicht, M.D., Kouros-Mehr, H., Lu, P, Werb, Z. (2006) Hormonal and local control of mammary branching morphogenesis. *Differentiation*. 74:365-81.

Stockdale, C., Bruno, M., Ferreira, H., Garcia-Wilson, E., Wiechens, N., Engeholm, M., Flaus, A., Owen-Hughes, T. (2006) Nuclesome dynamics. *Biochemical Society Symposium*. 73:109-19.

Stull, M.A., Pai, V., Vomachka, A.J., Marshall, A.M., Jacob, G.A., Horseman, N.D. (2007) Mammary gland homeostasis employs serotonergic regulation of epithelial tight junctions. *Proceedings of the National Academy of Sciences of the United States of America*. 104(42):16708-13.

Stryke, D., Kawamoto, M., Huang, C.C., Johns, S.J., King, L.A., Harper, C.A., Meng, E.C., Lee, R.E., Yee, A., L'Italien, L., Chuang, P.T., Young, S.G., Skarnes, W.C., Babbitt, P.C., Ferrin, T.E. (2003) BayGenomics: a resource of insertional mutations in mouse embryonic stem cells. *Nucleic Acids Research*. 31(1):278-81.

Surani, M.A., Barton, S.C., Norris, M.L. (1984) Development of reconstituted mouse eggs suggests imprinting of the genome during gametogenesis. *Nature*. 308(5959):548-50.

Suzuki, S., Ono, R., Narita, T., Pask, A.J., Shaw, G., Wang, C., Kohda, T., Alsop, A.E., Graves, J.A.M., Kohara, Y., Ishino, F., Renfree, M.B., Kaneko-Ishino, T. (2007) Retrotransposon silencing by DNA methylation can drive mammalian genomic imprinting. *PLoS Genetics*. 3(4):e55.

Tada, M., Tada, T., Lefebvre, L., Barton, S.C., Surani, M.A. (1997) Embryonic germ cells induce epigenetic reprogramming of somatic nucleus in hybrid cells. *The EMBO Journal*. 16(21):6510-20.

Tada, T., Tada, M., Hilton, K., Barton, S.C., Sado, T., Takagi, N., Surani, M.A. (1998) Epigenotype switching of imprintable loci in embryonic germ cells. *Development, Genes and Evolution.* 207(8):551-61.

Takahashi, K., Kobayashi, T., Kanayama, N. (2000) p57(Kip2) regulates the proper development of labyrinthine and spongiotrophoblasts. *Molecular Human Reproduction*. 6(11):1019-25.

Tanaka, S., Mori, M., Akiyoshi, T., Tanaka, Y., Mafune, K., Wands, J.R., Sugimachi, K. (1997) Coexpression of Grb7 with epidermal growth factor receptor or Her2/erbB2 in human advanced esophageal carcinoma. *Cancer Research*. 57(1):28-31.

Teglund, S., McKay, C., Schuetz, E., van Deursen, J.M., Stravopodis, D., Wang, D., Brown, M., Bodner, S., Grosveld, G., Ihle, J.N. (1998) Stat5a and Stat5b proteins have essential and nonessential, or redundant, roles in cytokine responses. *Cell*. 93(5):841-50.

Temple, I.K., Gardner, R.J., Mackay, D.J., Barber, J.C., Robinson, D.O., Shield, J.P. (2000) Transient neonatal diabetes: widening the understanding of the etiopathogenesis of diabetes. *Diabetes*. 49(8):1359-66.

Thomas, M.C., Chiang, C.M. (2006) The general transcription machinery and general cofactors. *Critical Reviews in Biochemistry and Molecular Biology*. 41(3):105-78.

Thomas, P., Beddington, R. (1996) Anterior primitive endoderm may be responsible for patterning the anterior neural plate in the mouse embryo. *Current Biology*. 6(11):1487-96.

Thordarson, G., Villalobos, R., Colosi, P., Southard, J., Ogren, L., Talamantes, F. (1986) Lactogenic response of cultured mouse mammary epithelial cells to mouse placental lactogen. *The Journal of Endocrinology*. 109(2):263-74.

Tveden-Nyborg, P.Y., Alexopoulos, N.I., Cooney, M.A., French, A.J., Tecirlioglu, R.T., Holland, M.K., Thomsen, P.D., D'Cruz, N.T. (2008) Analysis of the expression of putatively imprinted genes in bovine per-implantation embryos. *Theriogenology*. 70(7):1119-28.

Udy, G.B., Towers, R.P., Snell, R.G., Wilkins, R.J., Park, S.H., Ram, P.A., Waxman, D.J., Davey, H.W. (1997) Requirement of Stat5b for sexual dimorphism of body growth rates and liver gene expression. *Proceedings of the National Academy of Sciences of the United States of America*. 94(14):7239-44.

Ueda, T., Abe, K., Miura, A., Yuzuriha, M., Zubair, M., Noguchi, M., Niwa, K., Kawase, Y., Kono, T., Matsuda, Y., Fujimoto, H., Shibata, H., Hayashizaki, Y., Sasaki, H. (2000) The paternal methylation imprint of the mouse *H19* locus is acquired in the gonocyte stage during foetal testis development. *Genes to Cells*. 5(8):649-59.

Varmuza, S., Mann, M. (1994) Genomic imprinting – defusing the ovarian time bomb. *Trends in Genetics*. 10:118-23.

Vecchione, A., Marchese, A., Henry, P., Rotin, D., Morrione, A. (2003) The Grb10/Nedd4 complex regulates ligand-induced ubiquitination and stability of the insulin-like growth factor I receptor. *Molecular and Cellular Biology*. 23(9):3363-72.

Veltmaat, J.M., Mailleux, A.A., Thiery, J.P., Bellusci, S. (2003) Mouse embryonic mammogenesis as a model for the molecular regulation of pattern formation. *Differentiation*. 71(1):1-17.

Vidal, K., Labéta, M.O., Schiffrin, E.J., Donnet-Hughes, A. (2001) Soluble CD14 in human breast milk and its role in innate immune responses. *Acta Odontologica Scandinavica*. 59(5):330-4.

Vrana, P.B., Guan, X.J., Ingram, R.S., Tilghman, S.M. (1998) Genomic imprinting is disrupted in interspecific *Peromyscus* hybrids. *Nature Genetics*. 20(4):362-5.

Wagschal, A., Sutherland, H.G., Woodfine, K., Henckel, A., Chebli, K., Schulz, R., Oakey, R.J., Bickmore, W.A., Feil, R. (2008) G9a histone methyltransferase contributes to imprinting in the mouse placenta. *Molecular and Cellular Biology*. 28(3):1104-13.

Wakao, H., Gouilleux, F., Groner, B. (1994) Mammary gland factor (MGF) is a novel member of the cytokine regulated transcription factor gene family and confers the prolactin response. *The EMBO Journal*. 13(9):2182-91.

Wang, J., Dai, H., Yousaf, N., Moussaif, M., Deng, Y., Boufelliga, A., Swamy, O.R., Leone, M.E., Riedel, H. (1999) Grb10, a positive, stimulatory signalling adapter in platelet-derived growth factor BB-, insulin-like growth factor I-, and insulin-mediated mitogenesis. *Molecular and Cellular Biology*. 19(9):6217-28.

Wang, J., Mager, J., Chen, Y., Schneider, E., Cross, J.C., Nagy, A., Magnuson, T. (2001) Imprinted X inactivation maintained by a mouse Polycomb group gene. *Nature Genetics*. 28(4):371-5.

Wang, L., Balas, B., Christ-Roberts, C.Y., Kim, R.Y., Ramos, F.J., Kikani, C.K., Li, C., Deng, C., Reyna, S., Musi, N., Dong, L.Q., DeFronzo, R.A., Liu, F. (2007) Peripheral disruption of the Grb10 gene enhances insulin signalling and sensitivity in vivo. *Molecular and Cellular Biology*. 27(18):6497-505.

Wang, L., Ma, W., Markovich, R., Chen, J.W., Wang, P.H. (1998) Regulation of cardiomyocyte apoptotic signalling by insulin-like growth factor I. *Circulation Research*. 83(5):516-22.

Waterland, R.A., Jirtle, R.L. (2004) Early nutrition, epigenetic changes at transposons and imprinted genes, and enhanced susceptibility to adult chronic diseases. *Nutrition*. 20(1):63-8.

Watson, C.J. (2006) Involution: apoptosis and tissue remodelling that convert the mammary gland from milk factory to a quiescent organ. *Breast Cancer Research*. 8(2):203-8.

Weinstein, L.S., Yu, S., Warner, D.R., Liu, J. (2001) Endocrine manifestations of stimulatory G protein alpha-subunit mutations and the role of genomic imprinting. *Endocrine Reviews*. 22:675-705.

Weisstein, A.E., Feldman, M.W., Spencer, H.G. (2002) Evolutionary genetic models for the ovarian time bomb hypothesis for the evolution of genomic imprinting. *Genetics*. 162:425-39.

Weksberg, R., Shen, D.R., Fei, Y.L., Song, Q.L., Squire, J. (1993) Disruption of insulin-like growth factor 2 imprinting in Beckwith-Wiedemann syndrome. *Nature Genetics*. 5:143-150.

Whitehouse, I., Tsukiyama, T. (2006) Antagonistic forces that position nucleosomes in vivo. *Nature Structural & Molecular Biology*. 13(7):633-40.

Wick, K.R., Werner, E.D., Langlais, P., Ramos, F.J., Dong, L.Q., Shoelson, S.E., Liu, F. (2003) Grb10 inhibits insulin-stimulated insulin receptor substrate (IRS)-phosphatidylinositol 3-kinase/Akt signaling pathway by disrupting the association of IRS-1/IRS-2 with the insulin receptor. *The Journal of Biological Chemistry*. 278(10):8460-7.

Wlodek, M.E., Westcott, K.T., Serruto, A., O'Dowd, R., Wassef, L., Ho, P.W.M., Moseley, J.M. (2003) Impaired mammary function and parathyroid hormone-related protein during lactation in growth-restricted spontaneously hypertensive rats. *Journal of Endocrinology*. 178:233-45.

Wojcik, J., Girault, J.A., Labesse, G., Chomilier, J., Mornon, J.P., Callebaut, I. (1999) Sequence analysis identifies a Ras-associating (RA)-like domain in the N-termini of band 4.1/JEF domains and in the Grb7/10/14 adapter family. *Biochemical and Biophysical Research Communications*. 259(1):113-20.

Wolf, J.B., Hager, R. (2006) A maternal-offspring coadaptation theory for the evolution of genomic imprinting. *PLoS Biology*. 4(12):e380.

Wroe, S.F., Kelsey, G., Skinner, J.A., Bodle, D., Ball, S.T., Beechey, C.V., Peters, J., Williamson, C.M. (2000) An imprinted transcript, antisense to Nesp, adds complexity to the cluster of imprinted genes at the mouse Gnas locus. *Proceedings of the National Academy of Sciences of the United States of America*. 97(7):3342-6.

Yamaguchi, T.P., Dumont, D.J., Conlon, R.A., Breitman, M.L., Rossant, J. (1993) Flk-1, a flt-related receptor tyrosine kinase is an early marker for endothelial cell precursors. *Development*. 118(2):489-98.

Yamasaki, K., Joh, K., Ohta, T., Masuzaki, H., Ishimaru, T., Mukai, T., Niikawa, N., Ogawa, M., Wagstaff, J., Kishino, T. (2003) Neurons but not glial cells show reciprocal imprinting of sense and antisense transcripts of Ube3a. *Human Molecular Genetics*. 12(8):837-47.

Yevtodiyenko, A., Schmidt, J.V. (2006) Dlk1 expression marks developing endothelium and sites of branching morphogenesis in the mouse embryo and placenta. *Developmental Dynamics*. 235:1115-23.

Yoshihashi, H., Maeyama, K., Kosaki, R., Ogata, T., Tsukahara, M., Goto, Y., Hata, J., Matsuo, N., Smith, R.J., Kosaki, K. (2000) Imprinting of human GRB10 and its mutations in two patients with Russell-Silver syndrome. *American Journal of Human Genetics*. 67(2):476-82.

Yu, S., Yu, D., Lee, E., Eckhaus, M., Lee, R., Corria, Z., Accili, D., Westphal, H., Weinstein, L.S. (1998) Variable and tissue-specific hormone resistance in heterotrimeric Gs protein alpha-subunit (Gsalpha) knockout mice is due to tissue-specific imprinting of the gsalpha gene. *Proceedings of the National Academy of Sciences of the United States of America*. 95(15):8715-20.

Zhang, C., Xuan, Z., Otto, S., Hover, J.R., McCorkle, S.R., Mandel, G., Zhang, M.Q. (2006) A clustering property of highly-degenerate transcription factor binding sites in the mammalian genome. *Nucleic Acids Research*. 34(8):2238-46.

Zhang, X., Decker, A., Platt, R.W., Kramer, M.S. (2008) How big is too big? The perinatal consequences of fetal macrosomia. *American Journal of Obstetrics and Gynecology*. 198(5):517.e1-6.

Zhu, X., Zhang, J., Tollkuhn, J., Ohsawa, R., Bresnick, E.H., Guillemot, F., Kageyama, R., Rosenfeld, M.G. (2006) Sustained Notch signalling in progenitors is required for sequential emergence of distinct cell lineages during organogenesis. *Genes & Development*. 20:2739-53.

Zucker, K.E., Riggs, A.D., Smith, S.S. (1985) Purification of human DNA (cytosine-5)-methyltransferase. *Journal of Cellular Biochemistry*. 29(4):337-49.